Microbial activity in marine sediment constrained via lipid-based stable isotope probing

Dissertation for the Doctoral Degree in Natural Sciences
Dr. rer. nat
in the Faculty of Geosciences
at the University of Bremen

submitted by

Weichao Wu

Bremen, November, 2017

Universität Bremen

Versicherung an Eides Statt

gem.§ 5 Abs. 5 der Promotionsordnung vom 15.07.2015

Ich, **Weichao Wu**

Anschrift: Carl-Severing-Str. 40, 28329 Bremen

Matr.-Nr.: 2972267

Versichere an Eides Statt durch meine Unterschrift, dass ich die vorstehende Arbeit selbständig und ohne fremde Hilfe angefertigt und alle Stellen, die ich wörtlich dem Sinne nach aus Veröffentlichungen entnommen habe, als solche kenntlich gemacht habe, mich auch keiner anderen als der angegebenen Literatur oder sonstiger Hilfsmittel bedient habe, und die zu Prüfungszwecken beigelegte elektronische Version der Dissertation mit der abgegebenen gedruckten Version identisch ist. / *With my signature I affirm in lieu of an oath that I prepared the submitted dissertation independently and without illicit assistance from third parties, that I appropriately referenced any text or content from other sources, that I used only literature and resources listed in the dissertation, and that the electronic (PDF) and printed versions of the dissertation are identical.*

Ich versichere an Eides Statt, dass ich die vorgenannten Angaben nach besten Wissen und Gewissen gemacht habe und dass die Angaben der Wahrheit entsprechen und ich nichts verschwiegen habe. / *I affirm in lieu of an oath that the information provided herein to the best of my knowledge is true and complete*.

Die Strafbarkeit einer falschen eidesstattlichen Versicherung ist mir bekannt, namentlich die Strafandrohung gemäß § 156 StGB bis zu drei Jahren Freiheitsstrafe oder Geldstrafe bei vorsätzlicher Begehung der Tat bzw. gemäß § 161 Abs. 1 StGB bis zu einem Jahr Freiheitsstrafe oder Geldstrafe bei fahrlässiger Begehung. / *I am aware that a false affidavit is a criminal offence which is punishable by law in accordance with § 156 of the German Criminal Code (StGB) with up to three years imprisonment or a fine in case of intention, or in accordance with § 161 (1) of the German Criminal Code with up to one year imprisonment or a fine in case of negligence.*

_____ _____

Ort, Datum Unterschrift

1. Gutachter:

Prof. Dr. Kai-Uwe Hinrichs, Universität Bremen

2. Gutachter:

Prof. Dr. Volker Thiel, Universität Göttingen

Tag des Promotionskolloquiums:

30 Jan 2018

Mitglieder der Kommission

Herr Prof. Dr. Kai-Uwe Hinrichs

Herr Prof. Dr. Volker Thiel

Frau Prof. Dr. Gesine Mollenhauer

Herr PD. Dr. Matthias Zabel

Frau Dr. Florence Schubotz

Herr Stanislav Jabinski

Contents

Abstract I

Zusammenfassung III

Chapter I Introduction 1
- I.1. Microbes in marine sediment 1
- I.2. Microbial metabolism 3
- I.3. Hydrogen isotope chemistry of microbial lipids 9
- I.4. Calculation of growth rates of microbial community based on D_2O labelling 13
- I.5. Structure and scientific objectives 16

Chapter II

Substrate-dependent utilization of carbon and hydrogen for lipid biosynthesis by *Methanosarcina barkeri* 19
- Abstract 20
- II. 1. Introduction 21
- II. 2. Materials and Methods 23
- II. 3. Results 28
- II. 4. Discussion 35
- II. 5. Conclusion 40
- Acknowledgements 41

Chapter III

Production and turnover of microbial organic matter in surface sandy sediments 42
- Abstract 43
- III.1. Introduction 44
- III.2. Sampling and Methods 45
- III.3. Results and Discussion 48
- III.4. Conclusions 56
- Acknowledgements 57

Chapter IV

Microbial activity in marine surface sediment controlled by the proportion of terrestrial organic matter 58
- Abstract 59
- IV.1. Introduction 60
- IV.2. Samples and Methods 62
- IV.3. Results 68
- IV.4. Discussion 75
- IV.5. Conclusion 84
- Acknowledgements 84

Chapter V

Growth of abundant sedimentary Bathyarchaeota on lignin as an energy source 85
- Abstract 86
- Significance 87
- V.1. Introduction 88
- V.2. Results 89
- V.3. Discussion 93
- V.4. Methods 96

Acknowledgements 100
Chapter VI 101
Conclusion & Outlook 101
References 104
Author contributions 119
Supplementary materials 120
Acknowledgments 146

Abstract

Microbial-driven organic matter mineralization in marine sediment plays a vital role in the global carbon cycle. However, microbial activities and metabolisms in this environment are poorly constrained. This thesis aimed to quantitatively assess microbial activity by using a lipid-based stable isotope probing (SIP) method. Compared with ^{13}C- or ^{15}N-labelled organic substrates, dual labelling with D_2O and ^{13}C-inorganic carbon (IC) substrates serves to estimate in situ microbial activity with minimal distortion of in situ nutrient conditions. This approach provides an estimate of total microbial activity and can distinguish microbial metabolisms based on the ratio of incorporation of ^{13}C-IC vs D_2O ($R^{13}C/D$) into microbial lipids (cf. Wegener et al., 2012). However, the current working hypothesis is based solely on the cultivation of the Deltaproteobacterium *Desulfosarcina variabilis* and thus poorly constrained. Therefore, additional empirical evidence is required for broad scale application of this proxy, e.g., to archaea. To extend the application of this dual SIP method, the methanogen archaeon *Methanosarcina barkeri* was incubated with D_2O and ^{13}C-IC under different conditions (H_2/CO_2, acetate and methanol; **Chapter II**). Incorporation of IC and water-derived H were dependent on the carbon substrates used for growth. The relatively low water H contribution (< 40%) to lipids yielded an increased $R^{13}C/D$ ratio that exceeded the assumed upper limit of 1 (cf. Wegener et al., 2012). This finding invokes more investigation of water H contribution to microbial lipids in order to quantitatively estimate microbial activity in environmental settings.

By using the dual SIP method, this thesis further investigated the microbial activities and metabolisms in surface costal sediments under in situ sulfate-reducing conditions including an intertidal sediment from Janssand (Wadden Sea, Germany; **Chapter III**) and estuarine sediment from the Rhône River prodelta (Gulf of Lions, France; **Chapter IV**). Average turnover times of bacteria and archaea populations were 7.4 and 110 years, respectively. Compared with archaea, IC was significantly incorporated into bacterial fatty acids in surface sediments, with the assimilation rates ranging from 0.15 to 1.3 μg g_{dw}^{-1} yr^{-1}. Furthermore, $R^{13}C/D$ of bacterial fatty acids ranged from 0.07 to 0.23, indicating that heterotrophic bacteria were dominant and measured inorganic carbon fixation rates likely resulted from their anapleurotic reactions.

To further explore the potential for IC assimilation among Archaea, a surface estuarine sediment (upper 10 cm) from Hangzhou Bay (East China Sea, China; **Chapter V**) was incubated anaerobically with different organic substrates (i.e., casein, oleic acids, cellulose, phenol and lignin) and ^{13}C-IC. Only the addition of lignin stimulated the growth of

Bathyarchaeota (formerly referred as Miscellaneous Crenarchaeotal Group, MCG) and resulted in ^{13}C-labelling of their putative lipids. Together, these results suggest that Bathyarchaeota can use lignin as an energy source and IC as a carbon source. The demonstration of Bathyarchaeota metabolism of lignin sheds new light into microbial carbon cycling and important energy substrates for microbial populations in marine sediments.

This thesis quantitatively assessed microbial activity and compared the difference between bacterial and archaeal activity in surface marine sediment via lipid-based SIP method. The findings suggest that dark inorganic carbon fixation may be an important consequence of heterotrophic microbial activity in marine sediment and should be considered as important role for constraining sedimentary C fluxes in the biogeochemical carbon cycle.

Zusammenfassung

Die Mineralisierung von organischem Material in marinen Sedimenten durch Mikroorganismen spielt eine wesentliche Rolle im globalen Kohlenstoffkreislauf. Allerdings sind die Aktivität und Stoffwechselwege der Mikroorganismen in dieser Umgebung noch nicht ausreichend untersucht. Diese Arbeit hat die quantitative Erfassung der mikrobiellen Aktivität durch den Einsatz einer lipidbasierten Markierungsmethode mit stabilen Isotopen (SIP, stable isotope probing) zum Ziel. Im Gegensatz zur Verwendung von ^{13}C- oder ^{15}N-markierten organischen Substanzen kann durch duale Markierung mit D_2O und ^{13}C in anorganischem Kohlenstoffsubstrat (IC, inorganic carbon) die mikrobielle Aktivität in situ mit einer minimalen Störung der Nährstoffbedingungen abgeschätzt werden. Der duale Ansatz ermöglicht weiterhin die Einschätzung der gesamten mikrobiellen Aktivität und kann aufgrund des Aufnahmeverhältnisses von ^{13}C-IC zu D_2O ($R^{13}C/D$) beim Einbau in mikrobielle Lipide (vgl. Wegener et al., 2012) zwischen unterschiedlichen mikrobiellen Stoffwechselwegen unterscheiden. Die derzeitige Arbeitshypothese beim Einsatz dieses Verfahrens basiert jedoch ausschließlich auf Ergebnissen aus der Kultivierung des Deltaproteobakteriums *Desulfosarcina variabilis* und ist entsprechend stark eingeschränkt. Um das Verhältnis ($R^{13}C/D$) auch für andere Kulturen und Umweltproben als Proxy anwenden zu können, z.B. für Archaeen, sind daher zusätzliche empirische Nachweise erforderlich. Zur Erweiterung des Anwendungsbereichs der dualen SIP-Methode wurde daher das methanogene Archaeon *Methanosarcina barkeri* mit D_2O und ^{13}C-IC unter unterschiedlichen Bedingungen inkubiert (H_2/CO_2, Acetat und Methanol; **Chapter II**). Die Aufnahmeraten von anorganischem Kohlenstoff und wasserbürtigem Wasserstoff in die Lipide waren von den jeweiligen Kohlenstoffsubstraten abhängig welche für das Wachstum verwendet wurden. Der relativ geringe Anteil von Wasser-Wasserstoff in den Lipiden (< 40%) führte zu einem erhöhten $R^{13}C/D$-Verhältnis welches den bisher angenommenen oberen Grenzwert von eins überstieg (vgl. Wegener et al., 2012). Dieses Ergebnis erfordert weitere Nachforschungen über den Anteil von Wasser-Wasserstoff in mikrobiellen Lipiden, um die mikrobielle Aktivität unter verschiedenen natürlichen Umweltbedingungen quantitativ zu erfassen.

Außerdem wurde in dieser Arbeit die duale SIP-Methode zur Erforschung der mikrobiellen Aktivität und von mikrobiellen Stoffwechselwegen in Sedimentproben eingesetzt. Untersucht wurden hierbei Oberflächensedimente aus dem Küstenbereich unter in-situ sulfatreduzierenden Bedingungen sowie Sedimente im Gezeitenbereich aus dem Wattenmeer der Nordsee (Janssand, Deutschland; **Chapter III)** und ästuarines Sediment aus dem Rhône Prodelta (Golfe du Lion, Frankreich; **Chapter IV**). Die berechnete

durchschnittliche Umsatzdauer der Bakterien- und Archaeenpopulationen lag bei 7,4 bzw. 110 Jahren. Im Gegensatz zu den Archaeen wurde ein signifikanter Einbau des anorganischen Kohlenstoffes in den bakteriellen Fettsäuren beobachtet, wobei für die Assimilationsraten in den Oberflächensedimenten Werte zwischen 0,15 bis 1,3 µg g_{dw}^{-1} yr^{-1} ermittelt wurden. Darüber hinaus deutet das $R^{13}C/D$-Verhältnis der bakteriellen Fettsäuren mit Werten zwischen 0,07 und 0,23 darauf hin, dass heterotrophe Bakterien dominieren und die gemessenen Fixierungsraten des anorganischen Kohlenstoffes vorrangig aus deren anaplerotischen Reaktionen resultierten.

Um das Potential der Assimilation von anorganischem Kohlenstoff durch Archaeen näher zu untersuchen, wurde ein ästuarines Oberflächensediment (bis 10 cm Tiefe) aus der Bucht von Hangzhou (Ostchinesisches Meer, China; **Chapter V**) mit ^{13}C-IC und unterschiedlichen organischen Substraten (u.a. Kasein, Oleinsäure, Zellulose, Phenol, Lignin) unter anaeroben Bedingungen inkubiert. Einzig die Zugabe von Lignin stimulierte das Wachstum von Bathyarchaeota (früher als MCG, Miscellaneous Crenarchaeotal Group, bezeichnet) und resultierte in einer Markierung von ^{13}C in den mutmaßlich für diese Gruppe typischen Lipiden. Diese Ergebnisse deuten darauf hin, dass Bathyarchaeota Lignin als Energiequelle und anorganischen Kohlenstoff als Kohlenstoffquelle verwenden können. Die Aufdeckung des Ligninstoffwechsels bei Bathyarchaeota bringt neue Aspekte des mikrobiellen Kohlenstoffkreislaufs und relevanter Energiequellen für mikrobielle Populationen in marinen Sedimenten ans Licht.

In der vorliegenden Dissertation wurde die mikrobielle Aktivität in marinen Oberflächensedimenten mithilfe einer lipid-basierten SIP-Methode quantitativ erfasst und im Hinblick auf bakterielle und archaeelle Anteile differenziert. Die Ergebnisse lassen darauf schließen, dass die Kohlenstofffixierung ohne Photosynthese einen bedeutenden Anteil der heterotrophen mikrobiellen Aktivität in marinen Sedimenten darstellen kann und als ein wichtiger Faktor bei der Aufklärung von Kohlenstoffflüssen in Sedimenten durch den biogeochemischen Kohlenstoffkreislauf berücksichtigt werden sollt

Chapter I Introduction

I.1. Microbes in marine sediment

The ocean accounts for 70% of the Earth's surface. The subseafloor is the largest sedimentary setting that harbors the greatest reservoir of organic carbon (OC) on Earth (Hedges and Keil, 1995), and at the same time it is the largest microbial habitat where more than half of all microbial cells in the ocean live (Whitman, 1998; Kallmeyer et al., 2012; Parkes et al., 2014). The microorganisms in marine sediments are metabolically active to as deep as ~2.5 km below seafloor (Inagaki et al., 2015) and can survive for several million years owing to an extremely low energy requirement (Hoehler and Jørgensen, 2013). The deep biosphere plays an important role in regulating the biogeochemical cycles of elements and energy; however, little is known regarding the microbial abundance, composition and metabolic activity in subseafloor sedimentary environments (D'Hondt et al., 2004; Lipp et al., 2008; Parkes et al., 2014).

Biogeochemists are intrigued by the low energy supply and long residence times of microbial life in the deep biosphere (Parkes et al., 2014). In 1998, a first survey by Whitman et al. proposed that prokaryotic biomass residing in the subseafloor sediment amounted to about 3.55×10^{30} cells, which would comprise 55-86% of the total prokaryotic biomass and 27-33% of the total living biomass on the Earth. Lipp et al. (2008) reached a similar estimate of about 5×10^{30} living cells inhabiting deep sediments, based on the distribution and concentration of "live" intact polar membrane lipids. Kallmeyer et al. (2012) reduced the estimated global sediment inventory to roughly 2.9×10^{29} cells, corresponding to about 0.6% of the living biomass on the Earth, which is much lower than previous estimates largely due to the consideration of several orders of magnitude lower cell numbers in oceanic gyres (D'Hondt et al., 2009) than in ocean margins and upwelling regions. Recently, Parkes et al. (2014) included more study sites and updated the estimates about 5.4×10^{29} cells. However, the estimates will probably be updated due to new discoveries such as the presence of active microbes even ~2,5 km below seafloor during the IODP Expedition 337 (Inagaki et al., 2015). The cell numbers in marine sediments generally decrease with increasing depth (or ages) of sediments and the empirical relationship is: Log cells = 8.5 – 0.68 × Log depth (2037 cell counts; Parkes et al., 2014). So far, these global estimates of microbial biomass in marine sediments include only the prokaryotic populations i.e., bacteria and archaea; however, recent studies show the significance of viruses (Middelboe et al., 2011; Engelhardt et al., 2013) and fungi (Damare et

al., 2006; Edgcomb et al., 2011). Their global presence in deep marine sediments implies that previous estimates might have underestimated the global sedimentary microbial biomass.

Microbial activities and metabolisms depend on the availability of electron acceptors (O_2, NO_3^-, Mn^{4+}, Fe^{3+}, SO_4^{2-} and CO_2; Fig. I.1), organic substrates (labile vs refractory), and the energy yield of redox reactions, such that microbial community compositions and biogeochemical processes are stratified in marine sediment according to the sequential redox cascade (Fig. I.1; Canfield and Thamdrup, 2009). For example, depending on the availability of organic matter, dissolved oxygen typically penetrates only a few millimeters to several decimeters into the sediment, resulting in an anoxic environment below this zone. Subsequent electron acceptors that yield the greatest energy are preferentially and sequentially used, as manifested by sequential changes in the dominant microbial mineralization pathway (Fig. I.1). Sulfate-reduction and methanogenesis are important OM mineralization pathways in marine sediment (Jørgensen, 1982; Canfield et al., 1993; Mitterer, 2010), and they can contribute >30% of OM mineralization in anoxic marine sediment. The upper anoxic sediment zone repleted with sulfate is often called sulfate-reducing zone, where sulfate-reducing bacteria outcompete methanogenic archaea and oxidize OM to CO_2. With the depletion of sulfate, methanogenic archaea take over and oxidize organic matter to CH_4 (Fig. I.1).

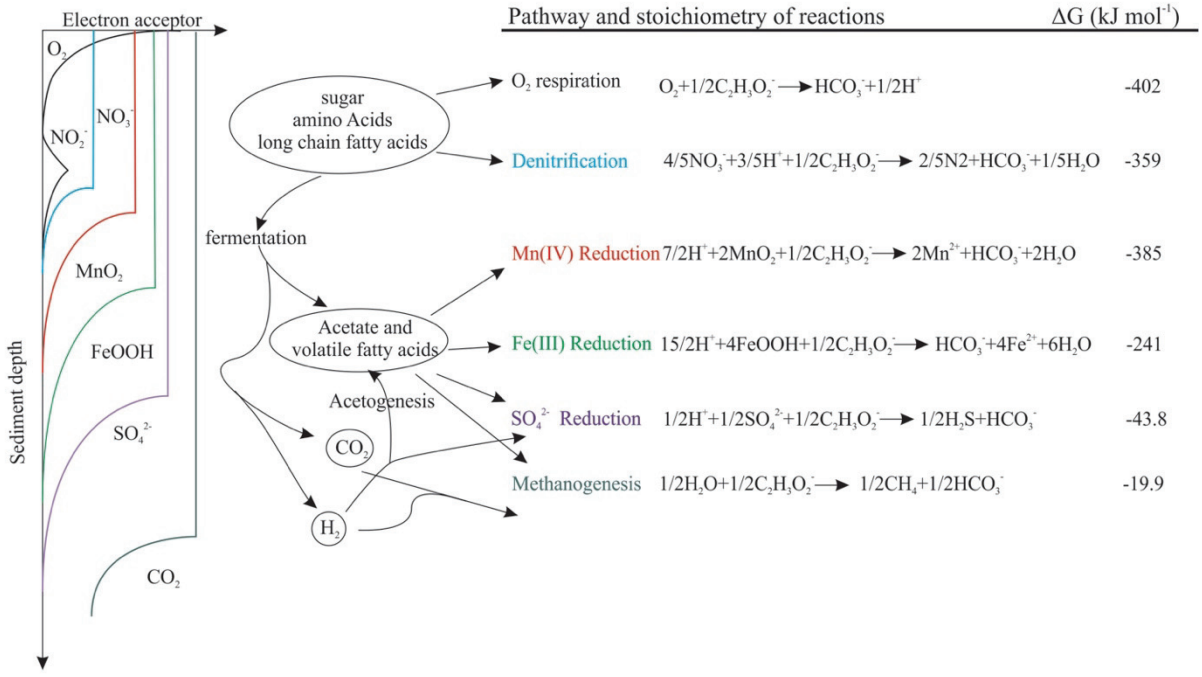

Fig. I.1. Schematic pathways of organic matter degradation and the related redox-active compounds in marine sediments (modified after Canfield and Thamdrup, 2009; Parkes et al., 2014). The standard Gibbs free energy and stoichiometry of reactions are based on acetate as organic matter and electron donor (modified from Canfield and Thamdrup, 2009).

The quantification of microbial activity is generally based on metabolic and enzymatic assays (Jørgensen 1978; D'Hondt et al., 2009; Adhikari and Kallmeyer, 2010). Metabolic assay measures changes in the concentration of either substrates and/or products over time. Isotope labelling methods, in particular those based on radioactive isotopes, are very sensitive to trace microbial activity. Nevertheless, accurate estimates of total activity and turnover times of microbial communities in deeply buried sediments remain very challenging, partly due to the extremely low concentrations of microbial cells and extremely low activity (Inagaki et al., 2015; Jørgensen and Marshall, 2016). The activity of sulfate-reducing bacteria is generally quantified by measuring the rate of ^{35}S-sulfate reduction to ^{35}S-sulfide during incubation (Jørgensen, 1978). Assuming a C_{org} (organic carbon): SO_4^{2-} stoichiometry of 2:1, the mineralization rate of organic carbon can also be estimated. Beside the radioisotope labelling approaches, geochemical models have been applied to estimate turnover in the deep biosphere. Jørgensen and Marshall (2016) modelled the depth (z) distribution of sulfate reduction rates from the sulfate concentration in porewater and proposed the following function:

$$\text{Sulfate reduction rate} = 5.4 \times z^{-1.5} \text{ nmol } SO_4^{2-} \text{ cm}^{-3} \text{ year}^{-1}$$

I.2. Microbial metabolism

Microorganisms utilize a wide variety of electron donors, energy and carbon sources (cf. Table I.1). Autotrophs use inorganic carbon (IC) as the carbon source to build biomass, whereas heterotrophs incorporate organic carbon. According to the electron donor, autotrophy includes chemolithotrophy and photoautotrophy, whereas heterotrophy include chemoorganotrophy and photoheterotrophy. For autotrophic growth, there are six main pathways to fix IC into microbial biomass (details see I.2.1). In contrast, heterotrophs use organic carbon to obtaining energy and build biomass. Mixotrophy describes organisms who oxidize inorganic compounds to gain energy, but require organic matter as a carbon source (Madigan et al., 2015).

Table I.1. The metabolic types in microorganisms (Modified from Madigan et al., 2015).

Types	Electron donor	Energy Source	Carbon source	Examples
Chemolithotrophy	Inorganic chemicals (e.g., H_2S, H_2, Fe^{2+}, NH_3)	Oxidation of Inorganic chemicals	CO_2	Thaumarchaeota
Chemoorganotrophy	Organic matter	Organic matter	Organic matter	Sulfate-reducing bacteria
Photoautotrophy	Inorganic chemicals (i.e., H_2O)	Sunlight	CO_2	Cyanobacteria
Photoheterotrophy	Organic matter	Sunlight	Organic matter	Purple nonsulfur bacteria
Mixotrophy	Inorganic chemicals	Oxidation of inorganic chemicals	Organic matter	*Beggiatoa*

I.2.1. Pathways of autotrophic inorganic carbon fixation

The main pathways for autotrophic carbon fixation include: 1) Calvin-Benson-Bassham cycle (CBB), 2) reductive tricarboxylic acid cycle (rTCA); 3) reductive acetyl-CoA pathway, or Wood-Ljungdahl (WL) pathway; 4) 3-hydroxypropinate (3-HP) bicycle, 5) 3-hydroxypropionate/4-hydroxybutyrate cycle (3-HP/4-HB) and 6) dicarboxylate/4-hydroxybutyrate cycle (DC/4-HB), of which the rTCA pathway is known to be used by both bacteria and archaea (cf. Hügler and Sievert, 2011).

CBB cycle

The Calvin-Benson-Bassham cycle (CBB), also called reductive pentose phosphate cycle, is the most widespread carbon fixation pathway. It has been known to exist in green plants, purple bacteria, cyanobacteria and algae as well as in most chemolithotrophic bacteria and even in some Archaea. In the CBB cycle, the first step of CO_2 reduction is catalyzed by the enzyme ribulose bisphosphate carboxylase (RubisCO; Table I.2), and finally CO_2 is converted to glucose (Eq I.1). Assays of RubisCO enzymatic activity in the environment are thus important tools to characterize the autotrophic carbon fixation.

$$6CO_2 + 12NADPH + 18ATP \rightarrow C_6H_{12}O_6(PO_3H_2) + 12NADP^+ + 18ADP + 17Pi \quad (1)$$

rTCA cycle

The reductive tricarboxylic acid cycle (rTCA) is also called the reverse citric acid cycle or Arnon-Buchanan cycle. The citric acid cycle is the main way by which heterotrophic organisms oxidize organic matter to CO_2, vice versa, the rTCA is an alternative mechanism for autotrophic CO_2 fixation (Eq I.2). This pathway is present in green sulfur bacteria (e.g., *Chlorobium*), and it is also found in some nonphototrophic hyperthermophiles including Bacteria *Aquifex* and Archaea *Sulfolobus* and *Thermoproteus*.

$$3CO_2 + 12H + 5ATP \rightarrow C_3H_6O_3PO_3^{2-} + 3H_2O \quad (2)$$

Reductive acetyl-CoA pathway

The reductive acetyl-CoA pathway is also called Wood-Ljungdahl (WL) pathway, and was discovered in the laboratories of Harland G. Wood and Lars G. Ljungdahl (Hügler and Sievert, 2011). Unlike other autotrophic pathways, it is not a cycle. It is mainly found in anaerobic acetogenic bacteria, which can form acetate from H_2 and CO_2 (Ragsdale and Pierce, 2008; Reaction I.3). It is a relatively simple pathway in which two molecules of CO_2 are directly converted to acetyl-CoA (Reaction I.3). This pathway is present in both Bacteria and Archaea such as autotrophic sulfate-reducing bacteria and methanogenic archaea. Acetogenic bacteria may exhibit diverse metabolisms, as they can also grow heterotrophically. For instance, sulfate-reducing bacteria, the most widespread microbes in marine sediments can

grow on H_2/CO_2 plus sulfate for autotrophic growth as well as on acetate plus sulfate for heterotrophic growth (Widdel and Pfennig, 1981). Carbon monoxide dehydrogenase (CODH) and Acetyl-CoA Synthase are the key enzymes of this pathway (CODH/ACS; Table I.2).

$$4H_2 + 2HCO_3^- + 2H^+ \rightarrow CH_3COOH + 4H_2O \quad (3)$$

3-Hydroxypropionate bicycle

The 3-hydroxypropionate bicycle (3-HP) is present in green nonsulfur bacteria (e.g., *Chloroflexus*), and forms hydroxypropionate as a key intermediate. This carbon fixation pathway mainly includes two main cycles: in the first cycle, two bicarbonate molecules are fixed to form glyoxylate acid (Reaction I.4); in the second cycle, glyoxylate and propionyl-CoA are disproportionated to pyruvate and acetyl-CoA (Hügler and Sievert, 2011).

$$2HCO_3^- + 2H^+ + 3ATP \rightarrow C_2H_2O_3 + H_2O \quad (4)$$

3-hydroxypropionate/4-hydroxybutyrate cycle

The 3-hydroxypropionate/4-hydroxybutyrate (3-HP/4-HB) cycle, as a novel autotrophic pathway, was discovered in autotrophic members of the hyperthermophile archaeal *Sulfolobales*, *Metallosphaera sedula* by Berg et al., (2007; 2010a; 2010b). In this cycle, two HCO_3^- and one acetyl-CoA are reductively converted via 3-hydroxypropionate to succinyl-CoA, and subsequently reduced to 4-hydrobutyrate (Berg et al., 2007). This autotrophic fixation way is also present in the mesophilic Archaea Thaumarchaeota (previously “marine group-1” Crenarchaea; Brochier-Armanet et al., 2008), as confirmed by Könneke et al. (2014). This pathway is likely ubiquitous in microorganisms which can survive in energy-limited environment (Könneke et al., 2014), and it may be of similar importance as the CBB cycle in global carbon cycling (Berg et al., 2007).

Dicarboxylate/4-hydroxybutyrate cycle

The dicarboxylate/4-hydroxybutyrate cycle (DC/4-HB) was firstly described for anerobic and hyperthermophilic Crenarchaeota *Ignicoccus hospitalis* by Huber et al. (2008), and it was also found in other Crenarchaeota such as *Thermoproteales* (Ramos-Vera et al., 2009; Berg et al., 2010a). Within the DC/4-HB cycle, CO_2 is fixed by pyruvate synthase and phosphoenolpyruvate carboxylase. Some enzymes involved in this cycle are partly redundant with those in the rTCA cycle (enzymes transforming oxaloacetate to succinyl-CoA) as well as in the 3-HP/4-HB cycle (the enzymes transforming succinyl-CoA to acetyl-CoA; Ramos-Vera et al., 2009; Hügler and Sievert, 2011).

I.2.2 Heterotrophic metabolism

A heterotroph is defined as an organism that cannot directly fix carbon from inorganic carbon, but can obtain energy or carbon from organic substrates, such as carbohydrates, sugars and proteins. Based on their energy acquisition, heterotrophs can be divided into photoheterotrophs and chemoheterotrophs. Photoheterotrophs use light as an energy source but organic matter as a carbon source, e.g., purple nonsulfur bacteria. Chemoheterotrophs (also known as chemoorganotrophs) are heterotrophs who generate energy via oxidation of organic matter, e.g., sulfate-reducing and denitrifying bacteria. According to the electron acceptors, heterotrophic metabolism can be divided into aerobic respiration, fermentation, and anaerobic respiration. During aerobic respiration of organic matter, O_2 serves as the final electron acceptor; whereas, in the absence of O_2, if the electron acceptor and donor are organic matters themselves, it is fermentation; if the electron acceptor is an inorganic ion or metal, e.g., sulfate, nitrate or Fe^{3+}, it is anaerobic respiration.

.

Table I.2. Pathways for autotrophic carbon fixation (cited from Berg et al., 2010)

Pathways	ATP*	Reductants for synthesis of one pyruvate (10[H])	CO_2-fixing enzymes	Active CO_2 species	Intermediates that can be used for biosynthesis	Carbon isotope fractionation	Key enzymes
CBB	7	5 NADH or NADPH	RubisCO	CO_2	3-Phosphoglycerate, triose phosphates and sugar phosphates	-20 to -30 ‰	RubisCO and phosphoribulokinase
rTCA	2[§]	2 NADH or NADPH, 1 unknown donor[#] and 2 ferredoxin[¶]	2-oxoglutarate synthase	CO_2	Acetyl-CoA, pyruvate, PEP, oxaloacetate, succinyl-CoA and 2-oxoglutarate	-2 to -12‰	2-Oxoglutarate synthase and ATP-citrate lyase
			Isocitrate dehydrogenase	CO_2[§]			
			Pyruvate synthase	CO_2			
			PEP carboxylase	HCO_3^-			
Wood-Ljungdahl	Approx. 1	3 ferredoxin[¶] and two $F_{420}H_2$ (in methanogens)	Acetyl-CoA synthase-CO dehydrogenase	CO_2	Acetyl-CoA and pyruvate	< -30‰	Acetyl-CoA synthase-CO dehydrogenase and enzymes reducing CO_2 to methyltet-rahydropterin
			Formylmethanofuran dehydrogenase	CO_2			
			Pyruvate synthase	HCO_2			
3-HP	7	Six NADH or NADPH, but 1 FAD is reduced	Acetyl-CoA and propionyl-CoA carboxylase	HCO_3^-	Acetyl-CoA, pyruvate and succinyl-CoA	-12.5 to -13.7‰	Malonyl-CoA reductase, propionyl-CoA synthase and malyl-CoA lyase
3-HP/4-HB	9	6 NADH or NADPH, but one FAD is reduced	Acetyl-CoA and propionyl-CoA carboxylase	HCO_3^-	Acetyl-CoA and succinyl-CoA	-0.2 to -3.8‰	Acetyl-CoA-propionyl-CoA carboxylase, enzymes reducing malonyl-CoA, methylmalonyl-CoA mutase and 4-hydroxybutyryl-CoA dehydratase
DC/4-HB	5	2 or 3 ferredoxin[¶], 1 or 2 NADH or NADPH and 1 unknown donor	p	CO_2	Acetyl-CoA, pyruvate, PEP, oxaloacetate and succinyl-CoA	-0.2 to -3.8	4-hydroxybutyryl-CoA dehydratase
			PEP carboxylase	HCO_3^-			

*Equivalents for synthesis of one pyruvate; F420, deazaflavin factor 420; FAD, Flavin adenine dinucleotide; PEP, phosphoenolpyruvate; RubisCO, ribulose 1, 5-bisphosphate carboxylase-oxygenase.

[§]The presence of biotin-dependent 2-oxoglutarate carboxylase in, for example, *Hydrogenbacter thermophilus*, can increase the energy requirements of the cycle.

[#]NADH in *Hydrogenobacter thermophilus*.

[¶]Note that reduction of ferredoxin may be energy driven, which would increase the energy demands of the ferredoxin-dependent pathways.

During the utilization of OM, heterotrophic microbes degrade or breakdown big or complex molecues to small molecules (e.g., acetyl-CoA or pyruvate) via different pathways, which is called catabolism. Subsequently, these small molecules are further synthesized to big molecules, e.g., proteins and nucleic acids, which is also called anabolism. The citric acid cycle is a very common and important pathway to gain energy during heterotrophic growth in which pyruvate is oxidized to CO_2, NADPH, and the energy-rich substance acetyl-CoA (Fig. I.2). The citric acid cycle plays two major roles in the cell: energy conservation and biosynthesis (i.e., acetyl-CoA as precursor for lipid biosynthesis). During the metabolism of organic substrates (e.g., carbohydrates, proteins and lipids), they are firstly converted to pyruvate via diverse pathways before entering the citric acid cycle. For instance, glucose is firstly converted to pyruvate via glycolysis process, and then pyruvate enters the citric acid cycle to be oxidized to CO_2. In the presence of O_2, glucose is completely oxidized to CO_2 with a high energy yield (32 ATP per glucose; cited from Madigan et al., 2015). However, in the absence of O_2, glucose is partially oxidized to CO_2 plus ethanol or organic acids, and the energy yield (2 ATP per glucose) is lower than that for aerobic respiration.

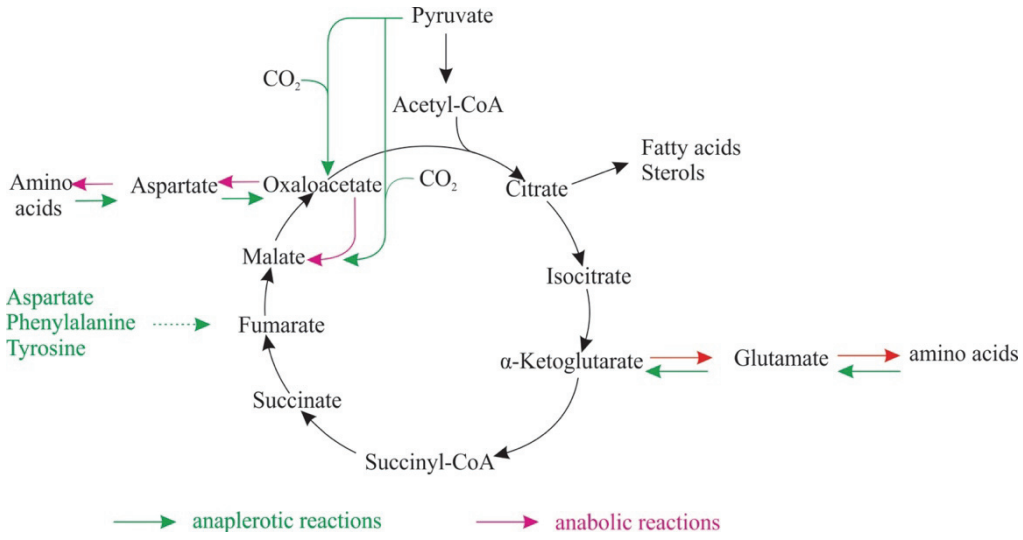

Fig. I.2. The anapleurotic and anabolic reactions in the citric acid cycle (modified from Owen et al., 2002).

I.2.3. Heterotrophic inorganic carbon assimilation

Inorganic carbon can also be fixed during heterotrophic growth, as shown by previous studies on pure cultures (Sorokin, 1966; Roslev et al., 2004; Feisthauer et al., 2008) and environmental communities (Yakimov et al., 2014). However, the significance of this process and the underlying mechanisms still remain to be explored. For instance, *Escherichia coli*, a widespread chemoheterotrophic bacterium, was recently observed to directly synthesize sugar from CO_2 rather than consuming sugar for growth (Antonovsky et al., 2016). The main pathway of IC fixation during heterotrophic growth is called anaplerosis, i.e., anapleurotic or

replenishing reactions, which occurs as a part of the citric acid cycle (Kornberg, 1965). In anaplerosis, intermediates used for biosynthesis are replenished in order to further fuel the citric acid cycle. That is, the flux of precursor molecules used for anabolic (synthesis) pathways is dependent on those derived from catabolism (breakdown), and microbial growth may be maintained if some intermediates can be replenished

Pyruvate + HCO_3^-+ATP → oxaloacetate + ADP + Pi + H_2O (5)

Phosphoenolpyruvate + CO_2 + GDP→ oxaloacetate + GTP (6)

Phosphoenolpyruvate + HCO_3^-→ oxaloacetate + Pi (7)

Pyruvate+HCO_3^- + NAD(P)H→ malate + $NAD(P)^+$ (8)

Reversible enzymatic reactions are another possible route for the uptake of CO_2 during heterotrophic growth. For instance, carbon monoxide dehydrogenase (CODH) is an important enzyme in both acetate oxidation and acetate formation for some sulfate-reducing bacteria and methanogenic archaea. As a result, when organic substrates are oxidized to CO_2, some portion of CO_2 can flow back into the pathway for biosynthesis. However, the magnitude of the proportion of backflow in enzymatic reactions remains to be explored due to the different functional capabilities of the enzymes (Holler et al., 2011).

Furthermore, the exchange of CO_2 and acetate might be another important process for heterotrophic carbon fixation. Eikmanns and Thauer (1984) found that the carboxyl group of acetate can exchange carbon with CO_2 during acetoclastic methanogenesis, but this exchange was not observed between formate and acetate. Thus, this exchange between CO_2 and acetate was a partial reaction in acetoclastic methanogenesis. This exchange is possible to exist in sulfate-reducing bacteria when grown on acetate (Thauer, 1988).

I.3. Hydrogen isotope chemistry of microbial lipids

The strong correlation between the stable hydrogen isotopic composition of microbial lipids and water suggests that the δ^2H value of water is the main factor controlling the δ^2H value of lipids (Zhang et al., 2009a). Hence, D_2O labelling method can thus be used to trace the total microbial lipid production. In order to apply this method, the following factors that may determine microbial lipid H isotope composition must be considered: 1) the δ^2H value of environmental water, which serves as the ultimate H source for lipid biosynthesis; 2) growth conditions (e.g., temperatures, salinity and light) or growth stage (exponential or stationary phase); 3) physiological and metabolic processes during the biosynthesis of lipids (e.g., the biosynthesis of the reducing agent NADPH), and 4) kinetic isotope effects during enzymatic

reactions (e.g., hydrogenation and dehydrogenation; Schimmelmann et al., 2006; Zhang et al., 2009a; Sachse et al., 2012; Session et al., 2016). The last two factors are related, as H fractionation imparted by enzymes favoring light isotopes depends on the size of the internal H pools. Zhang et al., (2009a) hypothesized that the central metabolic pathway yielding NADPH controls the hydrogen isotopic composition of microbial lipids because most biosynthetic reactions generally require NADPH as a reducing agent and it is typically directly involved in H-transfer during the lipid biosynthesis. This notion was supported by the observation that $\varepsilon_{l/w}$ (fractionation factor between lipid hydrogen isotope on water; Eq. 11) was generally most depleted during chemoautotrophic growth (approx. -200 to -400‰) followed by photoautotrophic growth (-150 to -250‰), heterotrophic growth on sugars (0 to -150‰) and heterotrophic growth on TCA-cycle precursors and intermediates (-50 to +200‰) in Fig. I.3.

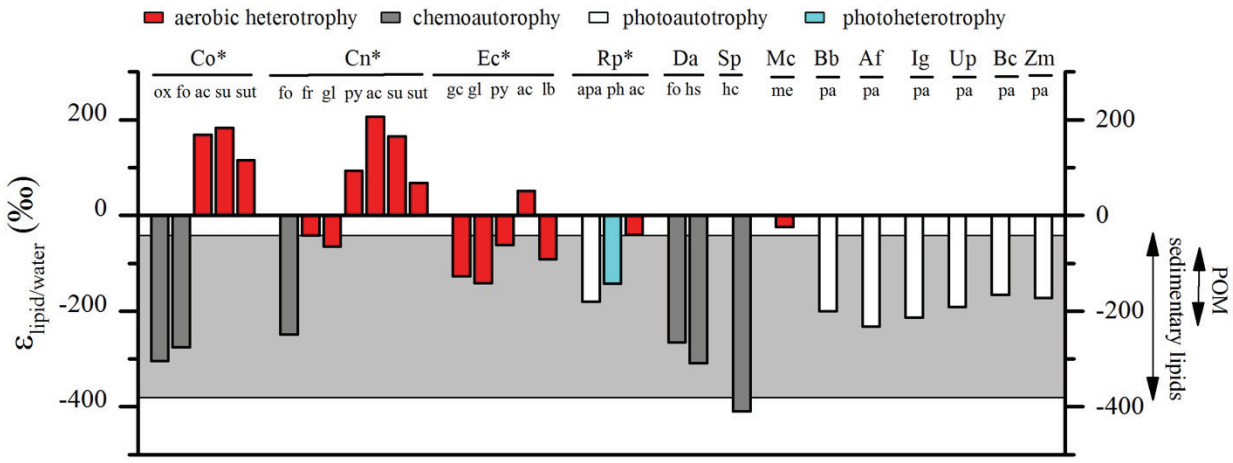

Fig. I.3. Summary of hydrogen isotope fractionations between fatty acids and water observed in culture experiments, native specimens, and marine organic matter fractions (modified from Zhang et al., 2009a). Plotted fractionations are based on the average δD value of palmitic acid, or the fatty acid/alkane of nearest chain length, in the culture with water δD closest to 0‰. Bacterial cultures include *C. oxalaticus* (Co), *C. necator* (Cn), *E. coli* (Ec), *R. palustris* (Rp), D. autotrophicum (*Da*), *Sporumusa* sp. (Sp), *M. capsulatus* (Mc), *B. braunii* (Bb), *Alexandrium fundyense* (Af), *Isochrysis galbana* (Ig), and natural specimens of brown alga *Undaris pinnatifida* (Up), red alga *Binghamia californica* (Bc) and seagrass *Zostera marina* (Zm). The gray box covers the ranges of fractionations observed in marine POM and sediments. Growth substrates are oxalate (ox), formate (fo), fructose (fr), glucose (gc), gluconate (gl), pyruvate (py), acetate (ac), succinate (su, sut), LB (lb), H_2+CO_2 (hc), H_2+SO_4^{2-} (hs), methane (me), acetate+light (ph), CO_2+light (pa), $S_2O_3^{2-}$+CO_2+light (apa).

However, the different δ^2H values between intracellular and extracellular water, observed by Kreuzer-Martin et al., 2006, suggests that water transport into the cells is another important factor that controls the lipid H isotopic composition. Recently Li et al., (2016) observed that metabolic water can contribute up to 70% of intracellular water, based on the isotopic composition of oxygen in the phosphate groups of DNA, probably suggesting that metabolic water can affect the lipid H composition. Nevertheless, the strong correlation ($R^2 \approx 1$) of δ^2H values of lipids and extracellular water reported by many studies (Sessions et al., 2002;

Englebrecht et al., 2005; Zhang et al., 2009a; Zhang et al., 2009b; Osburn et al., 2016) suggests that water H is the ultimate controlling factor of lipid hydrogen isotopic compositions. Furthermore, the coefficients for the regressions of δ^2H values of lipid and water (a_w; Eq. 9) are generally < 1 (Zhang et al., 2009a), suggesting that external water H are not sole H source to lipid biosynthesis. Considering the large variation of δ^2H of microbial lipids (Fig. I.3), Sessions and Hayes (2005) proposed a two-member model (Eq. 9) to estimate $\varepsilon_{l/w}$ (Eq. 11). Thus, the regressions of lipid H isotope on that of water (a_w; Eq. 10) reveal the "gross" isotope fractionation between lipid and external water without considering the mole contribution of water H (X_w) to lipid synthesis (Zhang et al., 2009a). Because X_w is not resolved, $\alpha_{l/w}$ as the "net" fractionation factor between lipid and water is likely to vary.

$$R_l = X_w\, \alpha_{l/w}\, R_w + (1\text{-}X_w)\, \alpha_{l/s}\, R_s \quad (9)$$

$$a_w = X_w\, \alpha_{l/w} \quad (10)$$

$$\varepsilon_{l/w} = (\alpha_{l/w}\text{-}1) * 1000‰ \quad (11)$$

where, X_w is the contribution of lipid H from external water, and $1\text{-}X_w$ is the contribution from substrates. $\alpha_{l/w}$ and $\alpha_{l/s}$ are the net fractionation factor between lipid and water, and lipid and substrates, respectively. $a_w = X_w\alpha_{l/}w$ is the coefficient of the regressions of lipid H isotope on water.

The coefficient a_w for regressions is considered as a physiological parameter (Kreuzer-Martin et al., 2006) and has also been defined as the water hydrogen assimilation constant (Kopf et al., 2015; 2016). The variation of a_w for lipids might depend on the lipid types (Zhang et al., 2009a), growth conditions (Kreuzer-Martin et al., 2006; Kopf et al., 2015), temperature (Zhang et al., 2009b) and different species (Zhang et al., 2009a). Furthermore, when not considering the difference of lipid components and growth conditions, a_w for microbial lipids is ordered as follows: unicellular Eukaryotes > Bacteria > Archaea (Fig. I.4). In particular, the investigation of hydrogen isotope composition of archaeal lipids is relatively sparse and it is not clear yet, which factors drive the lower a_w values of archaeal lipids (Fig. I.4).

In this thesis, I hypothesize that the different a_w values of archaeal and bacteria lipids arise from the structural differences of the cell membrane. Most unicellular Eukaryotes and Bacteria have a membrane consisting of a lipid bilayer and ester-bound phosphate lipid fatty acids, but Archaea have a membrane of a glycosidic or phosphate tetraether monolayer (e.g., Thaumarchaeota) or a diether bilayer (e.g., *Methanosarcina acetivorans*). The archaeal cell membrane is less permeable than eukaryotic and bacterial membranes because the former has di- or tetraether lipids with two hydrophobic ends spanning the half and entire membrane, respectively, while Eukaryotes and Bacteria have the phospholipid-fatty acids with one

hydrophobic end (Valentine, 2007). The higher a_w observed in Bacteria and Eukaryotes compared to Archaea may thus result from such differences in permeability. Furthermore, eukaryotic fatty acids generally have more unsaturated bonds than bacterial fatty acids (Chan et al., 1971; Gill and Valivety, 1997), which imparts higher permeability of the membranes of unicellular eukaryotes.

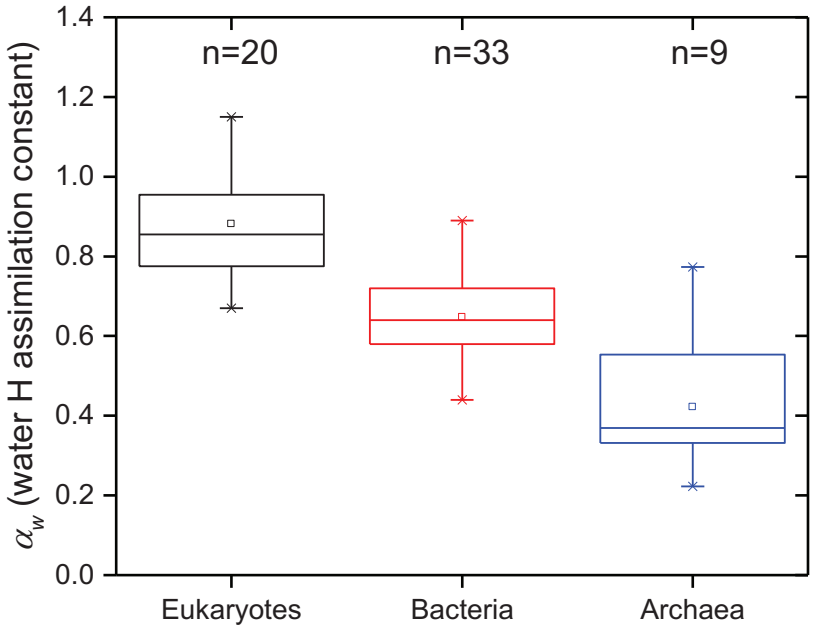

Fig. I.4. The water H assimilation factor (a_w) for lipids of different microbial domains. It is obtained from the regression of hydrogen isotope composition of lipids and different external water sources. The detailed data see supplementary Table S.I.1.

I.4. Calculation of growth rates of microbial community based on D_2O labelling

The strong relationship between microbial lipids and water establishes a solid foundation that the D_2O labelling method can trace the total activity of a microbial community (Kellermann et al., 2012; Wegener et al., 2012; Berry et al., 2015; Kopf et al., 2015; 2016) without characterizing some specific subgroups, like the case for ^{13}C and ^{15}N labelling method (Boschker et al., 1998; 2002; Kreuzer-Martin, 2007) because water is required by all microbes. For instance, ^{13}C or ^{15}N labelled organic substrates only trace the activity of heterotrophic microorganisms, whereas ^{13}C-IC trace autotrophs. The estimation of growth rates or turnover times of the microbial community based on hydrogen isotope incorporation into lipids has been described by Kopf et al. (2015; 2016), based on the assumption that: *a*) all isotopically analyzed lipids are representative of the bulk biomass; *b*) the rate of isotope incorporation rate into biomass (lipids) is well correlated with growth rate; *c*) incubation times are shorter than the turnover time of the community and *d*) there is fast diffusion and no loss of label tracer during incubation. Due to the high porosity of sediment, D_2O would diffuse very quickly and equilibrate with artificial sea water before incubation. In addition, the ratio of D_2O (1%) in water likely remains constant because contributions from metabolic water can be assumed to be negligible during incubation.

In pure cultures, the production and death of biomass from a microbial population (***B***) is controlled by the specific growth rate ***μ*** (which signifies cellular replication, hour^{-1}, day^{-1} or year^{-1}), turnover rate ***ω*** (which describes biosynthesis in excess of growth to compensate for degradation and turnover of macromolecules; day^{-1} or year^{-1}), and the death/degradation rate ***d***. The biomass B is thus the difference between synthesis (***μ + ω***) and removal fluxes (***ω + d***). The differential equation is:

$$\frac{dB}{dt} = (\mu + \omega - \omega - d) \cdot B = (\mu - d) \cdot B \quad \text{(S1)}$$

$$\frac{dB_{new}}{dt} = (\mu + \omega) \cdot B - (d + \omega) \cdot B_{new} \quad \text{(S2)}$$

The fraction of new vs. total biomass ($f_{B_{new}} = (B_{new}/B)$) can be obtained according to the quotient rule

$$\begin{aligned} \frac{df_{B_{new}}}{dt} &= \frac{\partial}{\partial t}\left(\frac{B_{new}}{B}\right) = \frac{1}{B}\frac{dB_{new}}{dt} - \frac{B_{new}}{B^2}\frac{dB}{dt} \\ &= \frac{1}{B}\left(\frac{dB_{new}}{dt} - f_{B_{new}}\frac{dB}{dt}\right) \\ &= (\mu + \omega) - f_{B_{new}}(d + \omega) - f_{B_{new}}(\mu - d) \\ &= (1 - f_{B_{new}}) \cdot (\mu + \omega) \end{aligned} \quad \text{(S3)}$$

When integration was used for $f_{B_{new}}(t)$, the derivative is,

$$f'_{B_{new}}(t) = (\mu + \omega) \cdot e^{-(\mu+\omega)\cdot t}$$

$$f_{B_{new}}(t) = 1 - e^{-(\mu+\omega)\cdot t} \quad \text{(S4)}$$

The observed or apparent growth rate $\boldsymbol{\mu_{act}}$ actually includes the specific growth rate $\boldsymbol{\mu}$ and turnover rate $\boldsymbol{\omega}$ ($\boldsymbol{\mu_{act} = \mu+\omega}$; Kopf et al., 2016). Furthermore, the relationship between $\boldsymbol{\mu}$ and $\boldsymbol{\omega}$ of microbial communities in marine sediment remains unclear. In order to simplify the equations, $\boldsymbol{\mu_{act}}$ is used to characterize the apparent growth rate. After the addition of an isotope tracer (e.g., D_2O), the overall H isotopic compositions of bulk microbial lipids include the newly produced lipids (${}^2F_{B_{new}}$) and the original (${}^2F_{B_{original}}$).

Based on mass balance,

$${}^2F_B(t) = \frac{B_{new}}{B} \cdot {}^2F_{B_{new}} + \frac{B_{original}}{B} \cdot {}^2F_{B_{original}} \quad \text{(S5)}$$

where $\frac{B_{original}}{B} = 1 - \frac{B_{new}}{B} = 1 - f_{B_{new}}(t)$, when Eq. S4 is combined with Eq. S5, we can obtain the overall hydrogen isotope composition of microbial lipids,

$${}^2F_B(t) = {}^2F_{B_{new}} \cdot (1 - e^{-\mu_{act}\cdot t}) + {}^2F_{B_{original}} \cdot e^{-\mu_{act}\cdot t} \quad \text{(S6)}$$

The hydrogen isotopic composition of microbial lipids ($^2F_{lipid}$) is generally determined by the source water or medium involved in their biosynthesis (for sediment incubation, it refers to the spiked water or medium water after addition of D_2O, ${}^2F_{w_{med}}$) and other substrates including organic matter or metabolic water (${}^2F_{sub}$; Sessions and Hayes, 2005; Zhang et al., 2009a). For instance, the hydrogen isotopic composition of microbial fatty acids (${}^2F_{fa_{new}}$) is described in terms of the mole fraction contribution of spiked water (x_w) and associated net hydrogen isotope fraction between lipids and water ($\alpha_{l/w}$), and the residual contribution from substrates (1- x_w) and associated net H isotope fraction between lipids and substrates ($\alpha_{l/s}$).

$${}^2F_{lipid_{new}}(t) = x_w \cdot \alpha_{l/w} \cdot {}^2F_{w_{med}} + (1 - x_w) \cdot \alpha_{l/s} \cdot {}^2F_{sub} \quad \text{(S7)}$$

$a_w = x_w \cdot \alpha_{l/w}$ is defined as water assimilation constant, and it can be obtained from the regressions of $^2F_{lipid}$ and $^2F_{water}$ (Zhang et al., 2009; Kopf et al., 2016). a_w is used to describe the physiological relationship of hydrogen isotopic fractionation between lipids and water. In natural environments, it is difficult to resolve $\alpha_{l/w}$, $\alpha_{l/s}$ and $^2F_{sub}$. However, it is not necessary to know every parameter because the H composition of the original lipids (${}^2F_{lipid_{original}}$) is related to the H isotopic composition of natural water (${}^2F_{w_{nat}}$) and substrates ($^2F_{sub}$) according to Eq. S7,

$$(1 - x_w) \cdot \alpha_{l/s} \cdot {}^2F_{sub} = {}^2F_{lipid_{original}} - a_w \cdot {}^2F_{w_{nat}} \quad \text{(S8)}$$

When Eq. S8 is combined with Eq. S7, we obtain

$${}^2F_{lipid_{new}}(t) = a_w \cdot {}^2F_{w_{med}} + {}^2F_{lipid_{original}} - a_w \cdot {}^2F_{w_{nat}} \quad \text{(S9)}$$

When Eq. S9 is applied to Eq. S7, the overall H isotopic composition of lipids after incubation ($^2F_{lipid}$) is

$$^2F_{lipid}(t) = a_w \cdot (1 - e^{-\mu_{act} \cdot t}) \cdot (\ ^2F_{w_{med}} - \ ^2F_{w_{nat}}) + \ ^2F_{lipid_{original}} \quad \text{(S10)}$$

When Eq. S10 is resolved, the estimates of μ_{act} is

$$\mu_{act} = -\frac{1}{t} \ln \left[1 - \frac{^2F_{lipid}(t) - \ ^2F_{lipid_{original}}}{a_w(\ ^2F_{w_{med}} - \ ^2F_{w_{nat}})}\right] \quad \text{(S11)}$$

In incubation experiments, the $^2F_{w_{med}}$ after the spiking with D_2O (e.g., about 0.01 of the final D concentration in water) is much higher than that of the natural water (~ 0.00015575), thus $^2F_{w_{med}} - \ ^2F_{w_{nat}} \approx \ ^2F_{w_{med}}$. In addition, the difference $\Delta\ ^2F_{lipid}$ after a certain incubation time ***t*** (e.g., 50 days) incubation is $^2F_{lipid}(t) - \ ^2F_{lipid_{original}}$.

The turnover time of a microbial community (***τ*; day or year**) is determined from the reciprocal of the apparent growth rate (Eq. S12).

$$\tau = \frac{1}{\mu_{act}} = -t \cdot [\ln(1 - \frac{\Delta\ ^2F_{lipid}}{a_w \cdot\ ^2F_{w_{med}}})]^{-1} \quad \text{(S12)}$$

I.5. Structure and scientific objectives

The relatively high microbial activity in surface coastal sediment directly affects the nutrient cycle and the degradation and burial of sedimentary OM. However, the assessments of microbial activity and their metabolisms are poorly understood. Traditional molecular biochemical methods can reveal microbial community compositions, abundance and potential metabolisms, but most of the estimates of microbial activity are based on the consumption or production of electron acceptors or electron donors (e.g., sulfate or acetate). Direct estimates of the turnover times of total biomass or specific components (DNA, proteins or lipids) are relatively scarce. Wegener et al. (2012) established the lipid-based dual stable isotope probing method to estimate the total microbial activity in marine sediment. This method utilizes the dual isotopically labeled substrates [i.e., deuterated water (D_2O) and ^{13}C-bicarbonate] to characterize the total activity of microbial communities. In addition, this approach can distinguish the potential microbial metabolisms in marine sediments based on the ratio of ^{13}C-IC vs D_2O incorporation into microbial lipids. In contrast to the metabolic potentials revealed by biological molecular methods (e.g., metagenomics and metatranscriptomics), this method can directly reveal the mode of carbon utilization.

This thesis aims to quantify microbial activity in marine sediments via lipid-based stable isotope probing to better understand the role of microbes in the biogeochemical C cycle in marine sediment. Specifically, it aims to answer the following overarching questions:

1) **How do archaea utilize carbon substrates and water hydrogen for lipid biosynthesis?**
2) **Is the dual SIP method with ^{13}C-IC and D_2O applicable to study archaeal activity and metabolisms?**
3) **How different are bacterial and archaeal lipid biosynthesis rates in marine sediment?**
4) **How are rates of microbial lipid biosynthesis in shallow subseafloor sediments linked to quantity and quality of organic matter and the oceanographic settings?**

This thesis is organized around four manuscript chapters (Chapter II to V)

[Chapter II] Substrate-dependent utilization of carbon and hydrogen for lipid biosynthesis by *Methanosarcina barkeri.* This study investigated the extent of assimilation by *M. barkeri* when grown heterotrophically (i.e., on acetate or methanol) or autotrophically (i.e., on H_2/CO_2) by tracing the incorporation of ^{13}C-DIC and D_2O into cell membrane lipids. This work demonstrates that the ratio of the incorporation of ^{13}C-DIC vs D_2O ($R^{13}C/D$) into archaeal lipids, as measures of autotrophic vs. total activity, respectively, may exceed the previously assumed upper limit of 1. This finding invokes the cycling of internal, metabolic

pools of water as a control of the δD value of microbial lipids and thus has important implications for the use of this ratio as a proxy to distinguish microbial metabolism. This study is conducive to broaden the application of the dual stable isotope labelling method on assessing of microbial activity and metabolisms. **(Addressing Questions 1 and 2)**

[Chapter III] Production and turnover of microbial organic matter in surface sandy sediments. This study measured the incorporation rates of ^{13}C-IC and D_2O into microbial fatty acids and the total organic carbon (TOC) pool in order to determine bacterial lipid production rates and their turnover times in an intertidal sediment core (22 cm) collected from the Janssand tidal flat (Wadden Sea, Germany). The measured rates of microbial fatty acids production corresponded to microbial biomass production rates that were high enough to replenish the entire TOC pool on the order of a few decades. (**Addressing Questions 3 and 4**)

[Chapter IV] Microbial activity in marine surface sediment controlled by the proportion of terrestrial organic matter. In order to further understand the effect of organic matter sources and qualities on microbial activity in surface sediment, microbial activities were quantified by incubating the surface sediment (0-6 cm) collected along a transect of the Rhône prodelta in the Gulf of Lions (Northwestern Mediterranean Sea) with ^{13}C-IC and D_2O under sulfate-reducing and H_2/CO_2 conditions. This study shows that the sources of sedimentary organic matter are the main factor controlling microbial activity, in particular with regard to the bacterial community composition. Based on the hypothesis of $R^{13}C/D$ into lipids (i.e., ~1 and < 0.3 for autotrophy and heterotrophy, respectively), $R^{13}C/D$ of < 0.3 for bacterial FAs in this study suggests that dark IC fixation into bacterial lipids and even sedimentary TOC may be an important component in the mineralization of organic matter in marine sediments. (**Addressing Questions 1, 2, 3 and 4**)

[Chapter V] Growth of abundant sedimentary Bathyarchaeota on lignin as an energy source. This study is the first to demonstrate that the refractory biopolymer lignin may stimulate the growth of Bathyarchaeota, a globally widespread archaeal phylum. The incorporation pattern of ^{13}C-labelled bicarbonate into putative bathyarchaeotal tetraether lipids was indicative of organoautotrophic growth of a bathyarchaeotal group that utilizes lignin as an energy source and bicarbonate as a carbon source, which is consistent with the main finding presented in Chapters III and IV that heterotrophic microbes can also fix IC for growth. The study sheds new light onto the cycling of one of Earth's most abundant biopolymers in anoxic marine sediments and may even provide new strategies and enzymes for the biotechnological utilization of plant materials. (**Addressing Questions 1 and 4**).

Chapter II

Substrate-dependent utilization of carbon and hydrogen for lipid biosynthesis by *Methanosarcina barkeri*

Weichao Wu[1*], Travis Meador[1], Marcus Elvert[1], Gunter Wegener[2], Martin Könneke[1], Kai-Uwe Hinrichs[1]

1 Organic Geochemistry Group, MARUM-Center for Marine Environmental Sciences & Department of Geosciences, University of Bremen, 28359 Bremen, Germany.
2 Max-Planck institute for Marine Microbiology, 28359 Bremen, Germany.
* Corresponding author: wwu@marum.de

(***In preparation for Geochimica et Cosmochimica Acta***)

Abstract

The distribution and isotopic compositions (C and H) of lipids produced by sedimentary microorganisms provide information on microbial carbon cycling. Stable isotope probing with the combination of heavy water (D_2O) and ^{13}C-Dissolved Inorganic Carbon (^{13}C-DIC) can be employed to infer production rates and carbon metabolisms of microorganisms, respectively, based on the ratios of assimilation of water-derived protons and DIC (Wegener, G., Bausch, M., Holler, T., Thang, N.M., Mollar, X.P., Kellermann, M.Y., Hinrichs, K.-U., Boetius, A., 2012. Assessing sub-seafloor microbial activity by combined stable isotope probing with deuterated water and ^{13}C-bicarbonate). The dual labelling method is considered to differentiate the carbon metabolism on the basis of the ratio of ^{13}C-DIC versus D_2O incorporation into lipids ($R^{13}C/D$) (autotrophy ~1 vs. heterotrophy < 0.3); the underlying assumptions are that heterotrophs shuttle only small fractions of IC into microbial lipid biosynthesis (< 30%), and that most of the lipid hydrogen comes from water. However, this approach has not been experimentally verified for archaeal lipid biosynthesis. In order to test the validity of this method to further study archaeal activity in marine sediment, the methanogenic archaeon, *Methanosarcina barkeri*, was grown under chemolithotrophic (H_2/CO_2) and chemoorganotrophic conditions (acetate or methanol) with D_2O and ^{13}C-DIC labelling substrates. The results revealed that a relatively low proportion of lipid hydrogen was derived from water with 35.7±4.2%, 22.6±2.3% and 39.3±2.9% for growth on H_2/CO_2, acetate and methanol, respectively. This is substantially below the previously reported values for sulfate reducing bacterium under both autotrophic and heterotrophic conditions. This difference of water H assimilation into lipids by *M. barkeri* for growth on different substrates is possibly attributed to different energy yield during exponential growth with a high energy yield accelerating the exchange between NADPH and water. In addition, IC plays an important role in lipid biosynthesis by *M. barkeri,* accounting for 86.8±7.4%, 19.6±2.2% and 41.2±6.7% for growth on H_2/CO_2, acetate or methanol, respectively. The low water D incorporation into lipids by *M. barkeri* may bias the application of $R^{13}C/D$ to distinguish the archaeal activity and carbon metabolism in marine sediment (e.g. 2.4 for autotroph vs. 1.0 for heterotroph in our study) if other archaea show similar behavior. Thus, further validation with diverse archaeal strains is required to establish dual isotope labelling as technique for confidently estimating archaeal lipid production and discern archaeal metabolism.

Keywords: lipid biosynthesis; *Methanosarcina barkeri*; carbon and hydrogen isotopes; metabolisms

II. 1. Introduction

The stable isotope composition (C and H) of specific microbial lipids in environments provides important taxonomic and metabolic information that helps to decipher the role of microorganisms in biogeochemical cycles (Hayes et al., 1993, and references therein). The stable carbon isotopic composition of microbial lipids is primarily determined by the carbon isotopic composition of carbon substrates, fixation pathway and physiological conditions (e.g., Hinrichs et al., 1999; Hayes et al., 2001; Boschker and Middelburg, 2002; Londry et al., 2008; Blaser et al., 2015), whereas the stable hydrogen isotopic composition, δD of microbial lipids is rather related to the central metabolic pathways (Zhang et al., 2009a). The fractionation factors between δD lipids vs. water varied systematically with metabolism: heterotrophic growth on TCA-cycle precursors and intermediates > heterotrophic growth on sugars > photoautotrophy > chemoautotrophy (Valentine et al., 2004a; Sessions and Hayes, 2005; Zhang et al., 2009a). Hydrogen isotopic compositions of microbial lipids are thus a good tool to decipher the central metabolic pathways.

In order to understand the functional activity of microorganisms in their natural environment, stable isotope probing (SIP) approaches targeting diagnostic molecules (lipids or nucleic acids) have been widely used because they can trace the activity of microbial community and estimate metabolic processes (Boschker et al., 1998; Kreuzer-Martin, 2007). The widely used ^{13}C-labelled substrates are like ^{13}C-inorganic carbon (IC) and organic substrates such as glucose, amino acids and biomass (Wegener et al., 2016). However, the utilization of organic substrates probably distorts the in situ nutrition conditions, particularly for organic matter-lean microbial habitats, and it selects for a subpopulation of the microbial community, which utilizes a specific metabolic process (Kopf et al., 2015).

The recently developed heavy water labelling (D_2O) method can trace the total activity of microbial community, independent of the carbon substrates utilized, and can even be used for sorting and identifying active single cells (Berry et al., 2015; Kopf et al., 2016) because water is utilized by all microorganisms (Wegener et al., 2012, 2016; Kopf et al., 2015). Furthermore, the approach involving combined amendment of ^{13}C-labelled dissolved inorganic carbon (DIC) and D_2O labelling, also called dual-SIP, can even reveal the information on the metabolism of microorganisms without changing availability of reduced substrates (Kellermann et al., 2012, 2016; Wegener et al., 2012; Huguet et al., 2017). This approach is based on the observation from *Desulfosarcina variabilis* and assumed that: 1) independent of the utilized carbon substrates, most of microbial lipid hydrogen derives from water (> 80%) so that D_2O incorporation rate into lipids can be used to estimate the total lipid production rate; 2) minor

IC (< 30%) is assimilated into lipids when microorganisms are grown heterotrophically; 3) the ratio of ^{13}C (from DIC) versus D (from water) into lipids ($R^{13}C/D$) can be used to distinguish microbial metabolism (~1 for autotroph vs. < 0.3 for heterotroph). However, it remains unknown if this approach is valid to trace archaeal metabolism in environment due to the lack of the cultivation of archaeal isolates with the dual SIP approach.

Isotopic labelling studies of fatty acid biosynthesis indicate that NADPH is the most important cellular H source and can directly provide ~50% H, and water is less of importance (Valentine, 2009; Zhang et al., 2009a). Despite this relatively low fraction, the δD of lipids is correlated well with that of water (Valentine et al., 2004a, 2004b; Zhang et al., 2009a; Zhang et al., 2009b; Dirghangi and Pagani, 2013a, 2013b). In fact, the fractionation factor between water and lipids ($\alpha_{l/w}$) and water-derived hydrogen contribution (X_w) are not well resolved (Sessions and Hayes, 2005; Zhang et al., 2009a), resulting that the factors controlling hydrogen isotope fractionation between lipids and water is not well constrained. In order to better understand this relationship, a physiological parameter "water hydrogen assimilation constant (a_w)" was defined by Kopf et al. (2015), which was obtained from the regression of lipid hydrogen isotopic composition vs. water. Thus, a_w includes two factors: X_w and $\alpha_{l/w}$, and it appears to be "gross" hydrogen isotope fractionation factor between lipids and water (Sessions and Hayes, 2005; Zhang et al., 2009a; Kopf et al., 2015; 2016). Most studies about the hydrogen isotopic compositions of microbial lipids are focused on bacterial or eukaryotic fatty acids (Zhang and Sachs, 2007; Zhang et al., 2009a; Heinzelmann et al., 2015), alkenones (Englebrecht and Sachs, 2005; Schouten et al., 2006; van der Meer et al., 2015) and sterols (Sessions et al., 2002; Sachs and Schwab, 2011; Sachs and Kawka, 2015), and a_w for those lipids ranges from 0.6 to 0.9 (Zhang et al., 2009a; Zhang et al., 2007; 2009b; Kopf et al., 2015; 2016). The diverse a_w values found among different microorganisms indicate that a correction factor is required to further assess specific microbial lipid production via D_2O labelling method despite water being used by all microbes (Kopf et al., 2015; 2016; Wegener et al., 2016). However, the hydrogen isotopic compositions of archaeal lipids have been rarely constrained (Kaneko et al., 2011; Dirghangi and Pagani, 2013a) as well as a_w factor for archaeal lipids, probably due to the measurement challenge of archaeal biomarker di- or tetraether on GC-IRMS (Kaneko et al., 2011).

In analogy to hydrogen, the carbon utilization for lipid biosynthesis by archaea is also poorly known (Takano et al., 2010; Könneke et al., 2012; Lin et al., 2012; Villanueva et al., 2014). If facultative archaea can also assimilate IC when grown heterotrophically, as hypothesized from the incubation of *Desulfosarcina variabilis* (cf. Wegener et al., 2012), it is necessary to investigate the contribution of IC for archaeal lipid biosynthesis during heterotrophic growth. Methanogenic archaea are a widespread group of strictly anaerobic Euryarchaeota and can

utilize diverse carbon substrates for energy metabolism like CO/CO_2 and H_2, formate, acetate and methanol or methylamines (Thauer, 2008). Archaeal lipids are often used to reveal the biogeochemical cycle of methane in environments (Hinrichs et al., 1999; Elvert et al., 2000). The biosynthesis pathway of methanogenic archaeal lipids indicates the possibility of IC requirement not only for autotrophic but for heterotrophic growth, i.e., IC is fixed into intermediate acetyl-CoA catalyzed by carbon monoxide dehydrogenase (CODH), and further utilized for lipid biosynthesis (cf. Thauer, 1998). However, it is not clear about how much IC is flowing into lipid biosynthesis of methanogenic archaea during heterotrophic growth (Londry et al., 2008), and it thus hinders the application of dual stable isotope probing method and the elucidation of the carbon isotope variability of archaeal lipids.

In this study, we grew the methanogenic archaeon *Methanosarcina barkeri* under conditions of the dual SIP approach (Wegener et al., 2012) to better understand the underlying mechanisms on carbon and hydrogen isotopic compositions of archaeal lipids. *Methanosarcina barkeri* inhabits freshwater and marine ecosystem, and can use diverse substrates for growth. This study also aims to extend utilization of the dual SIP method to study microbial activity of archaeal community members in natural settings. Specifically, we (1) quantify the contribution of IC in lipid biosynthesis of *M. barkeri* growing under different conditions (H_2/CO_2, acetate or methanol); (2) follow the assimilation of water derived protons into archaeal lipids produced during under these conditions; (3) evaluate the ratios of ^{13}C-DIC and D_2O derived carbon assimilation and lipid production rates.

II. 2. Materials and Methods

II.2.1. Culturing conditions

M. barkeri (DSM 800) was purchased from the German Collection of Microorganisms and Cell Cultures (DSMZ, Braunschweig, Germany) and grown on medium modified from Penger et al. (2014) with the following composition (in g L^{-1}): K_2HPO_4, 0.25; KH_2PO_4, 0.23; $MgSO_4 \cdot 7H_2O$, 0.5; $CaCl_2 \cdot 2H_2O$, 0.25; NaCl, 2.25; $NaHCO_3$, 2.25; yeast extracts, 1.0; casitone, 1.0; cysteine-$HCl \cdot H_2O$, 0.3; $Na_2S \cdot 9H_2O$, 0.24, 1 mL trace element solution SL-10, 1 mL vitamin solution. The pH of medium was adjusted with sterile HCl to 6.7 and the headspace was filled with H_2/CO_2 (80:20; 200 kPa), N_2 or N_2/CO_2 (90:10).

Cultures (ca. 100 mL) were grown in 250 mL serum vials. The carbon substrates included H_2/CO_2, acetate, methanol, yeast extracts, casitone and cysteine, and cultures for labelling experiment were grown separately on H_2/CO_2 (80:20; 2 bar), acetate (30 mM), or methanol

(30 mM). Isotope labelling incubations were inoculated with 5 mL of *M. barkeri* inoculum (5%, v/v) at exponential phase. Before inoculation, the labelled substrates were added independently such as $NaH^{13}CO_3$ (99 atom % ^{13}C, Sigma Aldrich), D_2O (99.9 atom % D, Sigma Aldrich), 2-^{13}C-sodium acetate (99 atom % ^{13}C, Campro Scientific GmbH) and ^{13}C-methanol (99 atom % ^{13}C, Sigma Aldrich). The labelling strength of C substrates (ca. 5%) and D_2O (ca. 0.2%, 0.5% and 1%) in each incubation was measured as described below (Table II.1; *Section II.2.5*).

Table II.1. The labelling strategy for the incubation of *M. barkeri* on different substrates

No.	energy source	labelled substrates
1	H_2/CO_2	$NaH^{13}CO_3$ (5%), D_2O (1%)
2	H_2/CO_2	D_2O (0.2% or 0.5%)
3	acetate	$NaH^{13}CO_3$ (5%), D_2O (1%)
4	acetate	2-^{13}C-acetate (5%), D_2O (1%)
5	acetate	D_2O (0.2% or 0.5%)
6	methanol	$NaH^{13}CO_3$ (5%), D_2O (1%)
7	methanol	^{13}C-methanol (5%), D_2O (1%)
8	methanol	D_2O (0.2% or 0.5%)

The labelling strength (i.e., 0.2%, 0.5%, 1% or 5%) refers to the ratio of labelled substrates to bulk substrates, such that a labelling strength of 5% of $NaH^{13}CO_3$ means that the concentration of $NaH^{13}CO_3$ is about 5% of the bulk $NaHCO_3$ in medium. 0.2%, 0.5% and 1% D_2O are the volume ratios of D_2O used to water medium. In this text, ^{13}C-DIC refers to $NaH^{13}CO_3$ if no other explanation is provided.

II.2.2. Methane analysis

Growth of *M. barkeri* was monitored by measuring methane mixing ratios in headspace. Briefly, 100 µL gas samples from headspace of incubation bottles at room temperature and pressure were injected on a gas chromatograph with a flame ionization detector (GC-FID, Thermo Scientific, Germany) equipped with an Alltech Heliflex AT-Q column (30 m×0.32 mm) and held at a constant temperature of 60°C, and methane was quantified relative to an external methane standard.

The $\delta^{13}C$-methane was measured using a Thermo Finnigan Trace GC coupled to a DELTA Plus XP isotope ratio mass spectrometry via a GC combustion III interface (Thermo Scientific, Germany). The gas samples in the headspace were separated isothermally at 60°C on a Carboxen-1006 PLOT column (30 m×0.32 mm) for 8 minutes with a constant carrier gas flow of 3 mL min^{-1}. The $\delta^{13}C$-methane was calibrated with CO_2 reference gas.

II.2.3. Acetate and methanol analysis

The concentrations and stable carbon isotopic compositions of acetate and methanol were analyzed on a Thermo Finnigan Surveyor HPLC combined with Thermo Finnigan DELTA Plus XP isotope ratio mass spectrometer (IRMS) via LC Isolink interface (Heuer et al., 2006; Krummen et al., 2004). The volatile organic intermediates were separated on a VA 300/7.8 Nucleogel Sugar 810-H column (300 mm × 7.8 mm; Macherey-Nagel) with a guard column (CC30/4 Nucleogel Sugar 810H) at room temperature. The mobile phase was 5 mM phosphoric acid in water and the flow rate was 300 μL min^{-1}. The effluents were chemically oxidized by sodium peroxodisulfate at 100°C. The yielded CO_2 was transferred to the IRMS with a helium stream. The concentrations of volatile organic intermediates were quantified based on the external calibration that the linear correlation between peak area on IRMS and the concentration of the corresponding standards. The $\delta^{13}C$ values of acetate and methanol were calibrated based on the CO_2 reference gas. For the methanol analysis, the co-eluting IC was removed via acidification with phosphoric acid (85%). The detection limits for $\delta^{13}C$ of acetate and methanol were 10 μM and 20 μM, respectively.

II.2.4. DIC analysis

The $\delta^{13}C$-dissolved inorganic carbon (DIC) in medium water was measured on the Delta Ray Isotope Ratio Infrared Spectrometer (IRIS, Thermo Scientific, Germany) with GasBench II on-line gas preparation and introduction system (Thermo Scientific, Germany). Before measurement, the water samples were acidified with phosphoric acid (85%, H_3PO_4) overnight at room temperature and then CO_2 was introduced to the IRIS system. Briefly, the 10 mL crimp top vials were filled with 0.1 mL of 85% H_3PO_4 and flushed with CO_2-free synthetic air for 10 min on GasBench II in order to remove the headspace CO_2. Then water samples collected from culture media (1 mL) were injected into the vials and left overnight at room temperature to achieve equilibrium of CO_2 between water and the headspace. All CO_2 in headspace was transferred to the IRIS system with CO_2-free synthetic air. The CO_2 concentration was shown as ppm in headspace according to as external calibration with CO_2 reference gas and then converted to mM in water samples. In order to eliminate the memory effect due to the high ^{13}C, the system was flushed with CO_2-free synthetic air and monitored with reference gas. The $\delta^{13}C$ value was calibrated by reference CO_2 gas with a $\delta^{13}C$ value of -35.4‰ relative the Vienna Pee Dee Belemnite standard (VPDB) and the precision was 0.05‰.

II.2.5. Water hydrogen isotope analysis

The deuterium-enriched medium was measured on Picarro L-2130i Cavity Ring Down Spectrometer (Picarro, USA). Before measurement, the medium was filtered and diluted 100 times with MilliQ water of known D content. The δD values of medium water were calibrated

according to the mass balance. For samples highly enriched in D, the δD values of calibration standard ranges from +10‰ to +1000‰ by mixing MilliQ water with D_2O volumetrically.

II.2.6. Lipid analysis

The lyophilized *M. barkeri* was extracted using the modified Bligh and Dyer method (Sturt et al., 2004). After drying under nitrogen, total lipid extracts (TLEs) were separated into apolar and polar fractions on silica gel column using hexane, DCM and MeOH, and then DCM and MeOH fractions were combined into one polar fractions. The apolar fraction containing 2, 6, 10, 15, 19-pentamethylicosane (PMI) and unsaturated PMI (unsPMIs) was directly measured for quantitative and isotopic analysis. Archaeol (AR) and hydroxyarchaeol (OH-AR) in the polar fractions were derivatized with a 1:1 mixture (v/v) of pyridine and BSTFA/TMCS (99:1) at 70°C for 2h before measurement.

The $\delta^{13}C$ and δD values of lipids were measured on a Thermo Finnigan Trace GC connected to a DELTA Plus XP isotope ratio mass spectrometry via GC combustion III interface (Thermo Scientific, Germany). Lipids were introduced to injector set at 310°C and separated on a Rix-5ms column (30 m × 0.25 mm, 0.25 μm film thickness; Restek GmbH, Germany) with a constant helium flow of 1.2 mL/min. The temperature program of the oven was from 60°C to 150°C at 10°C/min, and then ramped to 320°C at 4°C/min with holding for 22.5 min. The combustion and pyrolysis temperatures for carbon and hydrogen isotope analysis were 940°C and 1420°C, respectively. Carbon and hydrogen isotope ratios were determined using ISODAT NT 3.0 software, and were reported using standard δ notation. For highly labelled samples, the carbon and hydrogen isotopes of co-injected standard squalane were off its known value, likely due to serious memory effect (Wang and Sessions, 2008). In this case, $\delta^{13}C$ and δD of highly labelled samples were directly calibrated compared with reference CO_2 or H_2 gas, respectively. For natural samples, the $\delta^{13}C$ values of lipids were also calibrated with reference CO_2 gas, and the internal squalane standard was used to monitor the stability of machine. For δD measurement, the external alkane standards (δD from -270‰ to -30‰; Mixed A, Indiana University Biogeochemical Laboratory) were used to monitor the stability and precision of instrument. The H_3 factor (correction for abundance of the trihydrogen ion H_3^+) was measured daily based on reference hydrogen gas. The δD values of lipids by *M. barkeri* grown on natural water were re-calibrated with external Mixed A standard. The $\delta^{13}C$ and δD values of AR and OH-AR were corrected for the additional carbon and hydrogen of *N*,*O*-bis(trimethylsilyl)trifloroacetamide (BSTFA). The $\delta^{13}C$-BSTFA ($\delta^{13}C$ = -40.3‰) was obtained via derivatization with di-O-hexadecyl-*rac*-glycerol with known value ($\delta^{13}C$ = -26.43‰). The

δD values of BSTFA/TMCS (δD = -119‰) was obtained via direct measurement on TC/EA connected to isotope mass spectrometry.

II.2.7. Calculation of ^{13}C and D contribution to lipid biosynthesis

For carbon isotope, a two-end member model (Hayes, 2001; Sessions and Hayes, 2005) was employed to estimate the net contribution of inorganic or organic carbon, and water hydrogen to lipid biosynthesis.

$$^{13C}F_{lipid} = X_{TIC}\ ^{13C}F_{TIC} + (1\text{-}X_{TIC})\ ^{13C}F_{S} \quad (1)$$

where $^{13C}F_{lipid,}$ $^{13C}F_{TIC}$ and $^{13C}F_{S}$ denote the ^{13}C fractional abundance in lipids, total inorganic carbon (TIC) and organic substrates (i.e., acetate and methanol), respectively. X_{TIC} is the mole fraction of TIC, which is the initial total inorganic carbon pool including dissolved inorganic carbon (DIC) and CO_2 gas in headspace, and $^{13C}F_{TIC}$ is weighted average ^{13}C fractional abundance of TIC, and (1-X_{TIC}) is the mole fraction of organic substrates. When grown on H_2/CO_2 with ^{13}C-DIC, the contribution of organic substrates was assumed as zero.

When 2-^{13}C-acetate was used, X_{TIC} cannot be solved based on the above equation (Eq. 1) because the methyl group (C2) of acetate is preferentially used to produce methane (Weimer and Zeikus, 1978). Considering that acetate was only labelled at C2, the ^{13C}F value of entire acetate was replaced by that of acetate-C2, which was calculated assuming that the $\delta^{13}C$ of carboxyl group of acetate (acetate-C1) was -34.2‰ (non-labelled acetate in our study). Thus, the three carbon sources (i.e., TIC, C2 and C1 of acetate) were considered for growth on ^{13}C-acetate:

$$^{13C}F_{lipid} = X_{TIC}\ ^{13C}F_{TIC} + X_{C1}\ ^{13C}F_{C1} + X_{C2}\ ^{13C}F_{C2} \quad (2)$$

$$X_{TIC} + X_{C1} + X_{C2} = 1 \quad (3)$$

where $^{13C}F_{lipid}$, $^{13C}F_{TIC,}$ $^{13C}F_{C1}$ and $^{13C}F_{C2}$ are the ^{13}C fractional abundance of lipid, TIC, and carboxyl (C1) and methyl group (C2) of acetate, respectively. X_{TIC}, X_{C1} and X_{C2} are the relative contributions of TIC, methyl group and carboxyl group of acetate to lipid contribution, respectively. X_{TIC} was assumed to be the value determined for *M. barkeri* grown on acetate and ^{13}C-DIC, as above Eq. 1.

For hydrogen isotope, a similar two-end member model was used to estimate the contributions of hydrogen derived from medium water or substrates during lipid biosynthesis (Sessions and Hayes, 2005; Zhang et al., 2009a):

$$^{D}F_l = X_w\ \alpha_{l/w}\ ^{D}F_w + (1-X_w)\ \alpha_{l/s}\ ^{D}F_s \quad (4)$$

$$a_w = X_w\ \alpha_{l/w} \quad (5)$$

where $^{D}F_l$, $^{D}F_w$ and $^{D}F_s$ denote the deuterium fractional abundance of lipids, water and substrates, respectively. X_w is the mole fraction of lipid hydrogen from external water, and $1-X_{water}$ is the mole fraction from other substrates (i.e., H_2, acetate or methanol). $\alpha_{l/w}$ and $\alpha_{l/s}$ are the net fractionation factor of hydrogen isotope between lipids and water, and lipids and substrates, respectively. $X_w\ \alpha_{l/w}$ is defined as "water hydrogen assimilation factor" (a_w; Kopf et al., 2015), which is a physiological factor and indicates the ultimate water hydrogen contribution to lipids without considering the net isotope fractionation factor. The a_w can be obtained from the slope of regression of lipid δD vs. water δD (Sessions and Hayes, 2005; Zhang et al., 2009a).

II. 3. Results

II.3.1. CH_4 production and $\delta^{13}C$-CH_4

When grown on methanol, methanol was completely consumed by *M. barkeri* in 4 days and was associated with rapid production of methane, which increased up to ~20% of the headspace (Fig. II.1). Methane mix ratios increased more slowly when grown on acetate and H_2/CO_2 (Fig. II.1a). Methane production lagged several days (~4 days) to produce methane when grown on acetate.

When grown on H_2/CO_2 with ^{13}C-DIC (+2500 < $\delta^{13}C$-TIC < +2740‰; Table II.2), the $\delta^{13}C$ values of CH_4 at harvest was close to that of TIC, however, when grown on acetate or methanol with ^{13}C-DIC (+3200 < $\delta^{13}C$-TIC < +8743‰; Table II.2), the $\delta^{13}C$ value of CH_4 was smaller than that of TIC (+38 < $\delta^{13}C$-CH4 < +215‰; Table II.2), suggesting a minor contribution of IC to methane production.

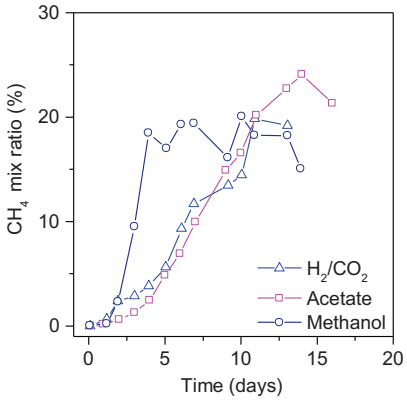

Fig. II.1. The mixing ratio of CH_4 (v/v; %) in headspace in cultures of *M. barkeri* for growth on different substrates

II.3.2. Variable PMI for different methanogenesis

The most abundant lipids of *M. barkeri* during stationary phase growth, as determined by the CH_4 production (cf. Fig. II.1), included PMI, unsPMIs, AR and OH-AR. For cells grown on methanol, unsPMIs with 1-3 double bonds accounted for 73-96% (avg. 85%) of the apolar fraction, whereas growth on H_2/CO_2 yielded only minor amounts of unsPMIs (~10%) and no unsPMIs were detected in acetoclastic methanogenesis incubations (Fig. II.2). Summons et al. (1998) reported that the relative proportion of unsPMIs was related to growth phase. While we only harvested in stationary growth phase, our data suggest that the carbon substrate plays an important role for the biosynthesis of unsPMI.

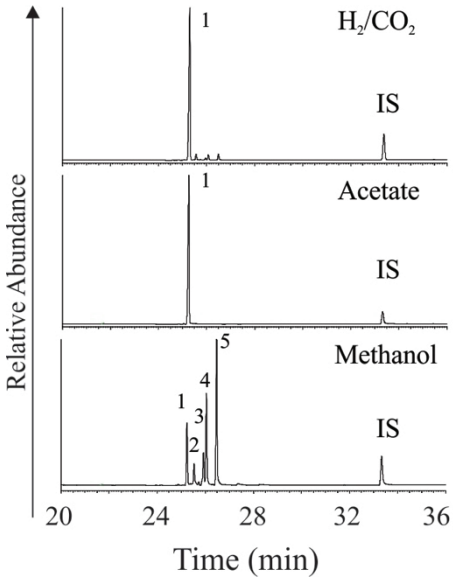

Fig. II.2. Gas chromatograms of the apolar fraction of lipids extracted from *M. barkeri* grown on different substrates i.e., H_2/CO_2, acetate and methanol. Peak 1 indicates 2, 6, 10, 15, 19-pentamethylicosane (PMI) and peaks 2–5 are pentamethylicosenes with 1–3 double bonds (unsPMIs). IS: the internal standard squalane.

II.3.3. Carbon isotopic composition of archaeal lipids

II.3.3.1. H_2/CO_2

When grown on H_2/CO_2 ($\delta^{13}C$-TIC ranging from = -18.0 to -20.0‰), AR ($\delta^{13}C$ = -39.7‰) was slightly enriched in ^{13}C relative to PMI ($\delta^{13}C$ = -43.4‰), OH-AR (-44.5‰) and unsPMIs (-45.9‰; Fig. S.II.1). The $\delta^{13}C$ difference between lipids and TIC ($\Delta\delta^{13}C = \delta^{13}C_{product} - \delta^{13}C_{substrate}$) varied from -27.5‰ to -19.0‰. When grown on H_2/CO_2 with ^{13}C-DIC, $\delta^{13}C$-lipids (+1590‰ to +2290‰) was slightly lower than $\delta^{13}C$-TIC (+2410‰ to +2740‰), and the $\delta^{13}C$ values were unsPMIs > AR > PMI > OH-AR (Table II.2).

II.3.3.2. Acetate

When grown on non-labelled acetate ($\delta^{13}C$ = -34.2‰), all lipids were more enriched in ^{13}C than acetate, which was consistent with the growth on limited acetate as reported by Londry et al. (2008). When ^{13}C-DIC was used for growth on acetate ($\delta^{13}C$-TIC was between +3239‰ and +4368‰ and $\delta^{13}C$-acetate = -34.2‰), $\delta^{13}C$-lipids ranged from +670‰ to +730‰ (Table II.2), indicating that IC was also used for lipid biosynthesis. When 2-^{13}C-acetate was amended for growth (+1330‰ < $\delta^{13}C$-acetate < +1830‰; Table II.2), the $\delta^{13}C$ values of PMI, AR and OH-AR (+1539‰ to +2180‰; Table II.2) were on average 14% higher than $\delta^{13}C$-acetate, but it was lower than $\delta^{13}C$-acetate-C2 with the $\delta^{13}C$ values being PMI > AR ≈ OH-AR (Table II.2).

II.3.3.3. Methanol

When grown on non-labelled methanol ($\delta^{13}C$ = -49.2‰), the $\Delta\delta^{13}C$ between methanol and lipids was smaller than that of the growth on H_2/CO_2 or acetate (Table II.2; Fig. S.II.1), and the $\delta^{13}C$ values were AR > OH-AR > PMI > unsPMIs (Table II.2; Fig. S.II.1). When ^{13}C-DIC was used for growth on methanol (+4255‰ < $\delta^{13}C$-TIC< +8743‰; Table II.2), the $\delta^{13}C$ values of unsPMIs, AR and OH-AR ranged from +1438‰ to +2593‰ (Table II.2) with the $\delta^{13}C$ values being unsPMIs > AR ≈ OH-AR. When grown on ^{13}C-methanol (+4370‰ < $\delta^{13}C$-methanol < +5560‰; Table II.2), the $\delta^{13}C$ values of unsPMIs, AR and OH-AR were much lower than that of methanol. Notably, when ^{13}C-DIC or ^{13}C-methanol was used, $\delta^{13}C$-PMI was positive but always much smaller (+7‰ to +1112‰; Table II.2) than that of other lipids, and even not related with $\delta^{13}C$-TIC or $\delta^{13}C$-methanol.

Table II.2. $\delta^{13}C$ values of methane and acetate at harvest (stationary phase), and $\delta^{13}C$ and δD values of lipids produced by *M. barkeri* during growth on labelled substrates and deuterated water (D_2O, 1%). n.d. = not detected. n.a. = not analyzed.

Conditions	Labelled substrates	Sample No.	$\delta^{13}C$initial (‰; VPDB)		$\delta^{13}C$final (‰; VPDB)						δD (‰; VSMOW)			
			TIC	organic substrates	Acetate	CH4	PMI	unsPMIs[e]	AR	OH-AR	PMI	unsPMIs	AR	OH-AR
H_2/CO_2	^{13}C-DIC	1	2416	n.a.	2634	2409	1919	2068	2031	1767	20579	n.d.	15247	15494
		3	2740	n.a.	2975	2618	1850	2108	1967	1592	14303	n.d.	12837	11907
		26	2493	n.a.	2323	2493	2275	n.d.	2290	2276	24860	n.d.	22180	22453
	no	2	-18.0	n.a.	0.1	-54.3	-45.5	-45.9	-39.6	-43.9	-336	n.d.	-258	-263
		24	-20.0	n.a.	-7.7	-63.8	-42.3	n.d.	-39.0	-44.4	-341	n.d.	-305	-334
		25	-20.0	n.a.	-8.3	-63.6	-42.5	n.d.	-40.5	-45.1	-357	n.d.	-312	-338
Acetate	^{13}C-DIC	18	3888	-34.2[a]	946	189	671	n.d.	718	690	13431	n.d.	12565	12590
		19	3239	-34.2[a]	934	198	676	n.d.	716	695	13157	n.d.	12893	12840
		31	4368	-34.2[a]	936	215	675	n.d.	729	702	15027	n.d.	14200	14099
		36	n.a.	-34.2[a]	1046	208	752	n.d.	876	712	16892	n.d.	12554c	13646d
		37	n.a.	-34.2[a]	1137	164	823	n.d.	935	758	14699	n.d.	13599	13164
	2-^{13}C-acetate	20	-10.6	1409	1145	2617	1674	n.d.	1595	1606	13717	n.d.	12808	12824
		21	-10.6	1409	1144	2506	1618	n.d.	1539	1547	13746	n.d.	13027	13072
		32	-10.6	1339	1084	2460	1543	n.d.	1473	1477	14173	n.d.	13059	13008
		38	n.a.	1814	1483	3437	2174	n.d.	2127	2071	13231	n.d.	14722	14505
		39	n.a.	1826	1555	3435	2181	n.d.	2105	2068	15939	n.d.	16180	15782
	no	22	-10.6	-34.2[a]	7.3	-56.4	-30.7	n.d.	-31.1	-32.2	-244	n.d.	-234.9	-248.5
		23	-10.6	-34.2[a]	7.6	-55.9	-32.1	n.d.	-31.1	-33.4	-254	n.d.	-251.3	-261.3
Methanol	^{13}C-DIC	11	8743	-49.2[b]	2577	120	109	2593	2533	2499	1204	23390	23033	23196
		12	4582	-49.2[b]	1814	143	75	1704	1603	1591	1934	29080	22667	24094
		28	4255	-49.2[b]	1164	71	901	1494	1438	1472	14547	23945	21104	22158
		41	n.a.	-49.2[b]	1668	38	156	1550	1626	1484	n.d.	22339	23221[c]	21987[d]
		42	n.a.	-49.2[b]	1797	43	186	1665	1709	1654	n.d.	25601	25114	24159

Methanol	^{13}C-methanol	13	-5.4	4373	1941	4415	7	2514	2332	2262	607	30611	27085	27864
		14	-5.4	4593	2030	5069	89	2875	2524	2483	1431	27781	24144	25089
		29	-10.6	4585	976	4532	1122	2080	1919	1964	13479	23185	21022	22176
		43	n.a.	5556	2254	5492	205	2955	2848	2685	n.d.	24370	23903[c]	27297[d]
		44	n.a.	4869	2012	4858	362	2593	2514	2459	n.d.	27043	24856	25599
	no	15	-5.4	-49.2[b]	-33.7	-64.8	-69.3	-75.4	-65.6	-68.7	-250	-285	-239	-223
		16	-5.4	-49.2[b]	-46.0	-67.2	-66.2	-67.5	-60.8	-62.3	-252	-281	-185	-200
		30	-10.6	-49.2[bc]	-29.4	-66.6	-53.7	-71.0	-63.5	-67.6	-248	-292	-234	-257

(a) δ^{13}C of non-labelled acetate =-34.2‰; (b) δ^{13}C of non-labelled methanol =-49.2‰; (c, d) data reported for ether cleavage products of phytane and unsaturated phytenes, respectively.

(e) δ^{13}C and δD of unsPMIs are weighted average δ^{13}C and δD of all unsPMIs

II.3.4. The estimates of inorganic carbon contribution (X_{TIC}) to lipid biosynthesis

II. 3.4.1. H_2/CO_2

X_{TIC} for the biosynthesis of PMI, unsPMIs, AR and OH-AR were 85.6±8.5%, 89.3±4.7%, 87.8±7.3% and 81.9±11.9%, respectively with an average of X_{TIC} = 86.8±7.4% during growth on H_2/CO_2 (Fig. II.3).

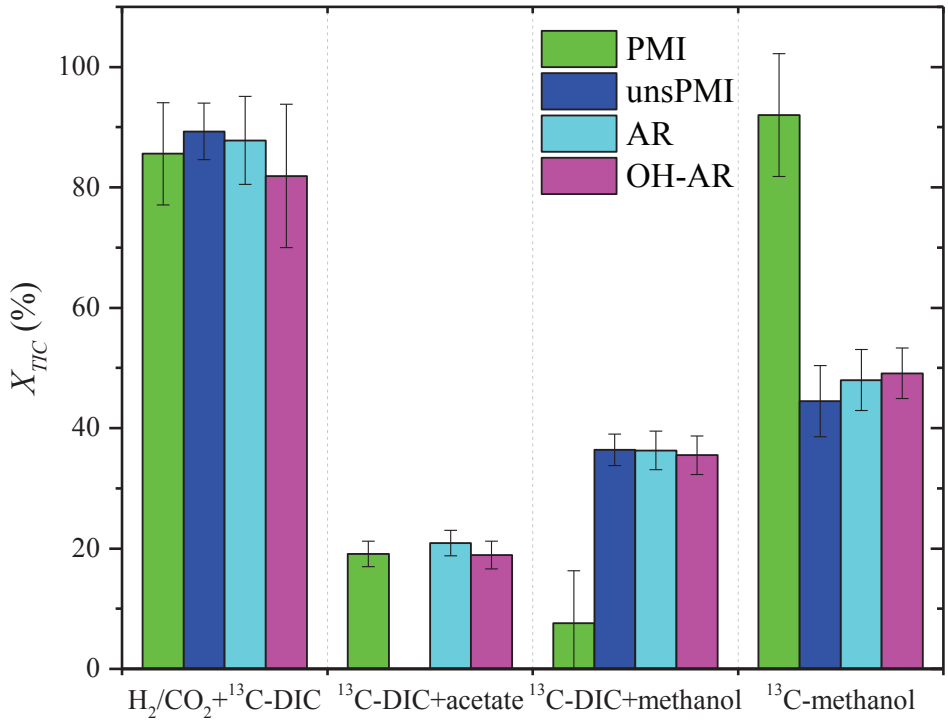

Fig. II.3. The molar fraction of inorganic carbon (X_{TIC}; %) to lipid carbon produced during growth on H_2/CO_2, acetate or methanol. Values determined by ^{13}C-substrate labelling according to Eq. 1-3.
(1) X_{TIC} for PMI (green) estimated from both ^{13}C-DIC+methanol (X_{TIC} = 7.6±8.7%) and ^{13}C-methanol (X_{TIC} = 92.0±10.2%) experiments shows large difference.
(2) X_{TIC} for lipids estimated from 2-^{13}C-acetate experiment is not listed because X_{TIC} was not derived independently.

II. 3.4.2. Acetate

X_{TIC} for the biosynthesis of PMI, AR and OH-AR was 19.1±2.1%, 20.9±2.1% and 18.9±2.3%, respectively (Fig. II.3), with an average of 19.6±2.2% during acetoclastic methanogenesis, as determined for the incubation with ^{13}C-DIC (Eq. 1). Because only the C2 (methyl group) of acetate was labelled, a three-end member model (Eq. 2 and 3) was used to estimate the contribution of C2 (methyl) and C1 (carboxyl) of acetate, assuming that X_{TIC} was 19.6±2.2%. Thus, X_{C2} and X_{C1} for the biosynthesis of PMI, AR and OH-AR were on average 56.7±1.7% and 23.7±1.7%, respectively.

II. 3.4.3. Methanol

During methylotrophic methanogenesis, X_{TIC} for the biosynthesis of unsPMIs, AR and OH-AR was 36.4±2.6%, 36.3±3.2%, 35.5±3.3%, respectively (Fig. II.3) with an average of 36.2±3.3%, as determined from the incubation with ^{13}C-DIC, which was significantly lower than the value determined from the incubation with ^{13}C-methanol (X_{TIC} was 44.5±5.9%, 48.0±5.1% and 49.1±4.2% for unsPMIs, AR and OH-AR, respectively with an average of 46.2±5.7%; Fig. II.3). In comparison to the other lipids, PMI was not strongly labelled during growth on methanol (Table II.2). This led to inconsistent mass balance calculations of X_{TIC}, to the effect that experiments with ^{13}C-DIC yielded low values of X_{TIC} (7.6±8.7%; Fig. II.3) and those with ^{13}C-methanol yielded high values (92.0±10.2%; Fig. II.3). Because neither bicarbonate nor methanol were apparent substrates for PMI during growth on methanol, the weighted average X_{TIC} for lipid biosynthesis (41.2±6.7%) considered only the values determined for unsPMIs, AR and OH-AR via the two labelling strategies (i.e., ^{13}C-DIC and ^{13}C-methanol).

II.3.5. hydrogen isotopic composition of lipids

The δD values of lipids varied with substrates when grown in unlabelled water medium (δD = -50.6‰). Lipids produced during growth on H_2/CO_2 had lower δD (avg. δD = -345‰; Table II.2; Fig. S.II.2) compared to growth on acetate (avg. δD = -278‰; Table II.2; Table S.II.2) or methanol (avg. δD = -266‰; Table II.2; Table S.II.2), which is consistent with the generally larger lipid biosynthetic isotopic fractionation during autotrophic versus heterotrophic growth (Zhang et al., 2009a; Osburn et al., 2011). Furthermore, when grown on H_2/CO_2, the δD values of PMI and OH-AR were similar, but lower than AR by ~28‰. However, when grown on acetate, δD-PMI was similar to δD-AR, but larger than δD-OH-AR by ~14‰. When grown on methanol, unsPMIs were more depleted in D than PMI, AR and OH-AR. To summarize, AR exhibited the highest δD, followed by OH-AR, and then unsPMIs, but the difference of δD between PMI and other lipids appeared to vary with carbon substrate.

Higher discrimination against D was apparent for lipids produced in labelled medium (1%D_2O with δD ≈ +63,850‰; $\Delta\delta D_{lipid\text{-}medium}$ ≈ -46,700‰; Table II.2), compared to that observed in unlabelled water medium ($\Delta\delta D_{lipid\text{-}medium}$ ≈ -250‰; Table S.II.2). When grown on H_2/CO_2 or acetate spiked with 1% D_2O, the δD values of PMI, AR and OH-AR were similar, but δD-PMI was significantly lower and more variable (δD= 607 to 14507‰; Table II.2) than that for unsPMIs, AR and OH-AR when grown on methanol, suggesting that PMI probably had a different pathway from other lipids for growth on methanol.

II.3.6. The estimates of water hydrogen to lipid biosynthesis

During growth on H_2/CO_2, acetate or methanol, the D fractional abundance (^DF) of lipids correlated well with that of water in medium (Fig. II.4), where $^DF_{water}$ ranged from 148 ppm (unlabelled water) to ~10000 ppm (1% D_2O). The slope of regression was defined as the water hydrogen assimilation factor α_w, which represents the contribution of water hydrogen to lipid biosynthesis (Kopf et al., 2015; 2016). The average α_w value for PMI, AR and OH-AR during the growth on H_2/CO_2 and acetate was 35.7±4.2% and 22.6±0.3%, respectively (Table S.II.1). However, when grown on methanol, the $^DF_{PMI}$ was not strongly correlated well with water (R^2 = 0.35; Fig. II.4; Table S.II.1) and α_w for PMI was lower (avg. 6.5±6.5%) than that for unsPMIs, AR and OH-AR (avg. 39.3±2.9%; Table S1). The large deviations of α_w for PMI is consistent with the questionable estimates of X_{TIC} for PMI during growth on methanol

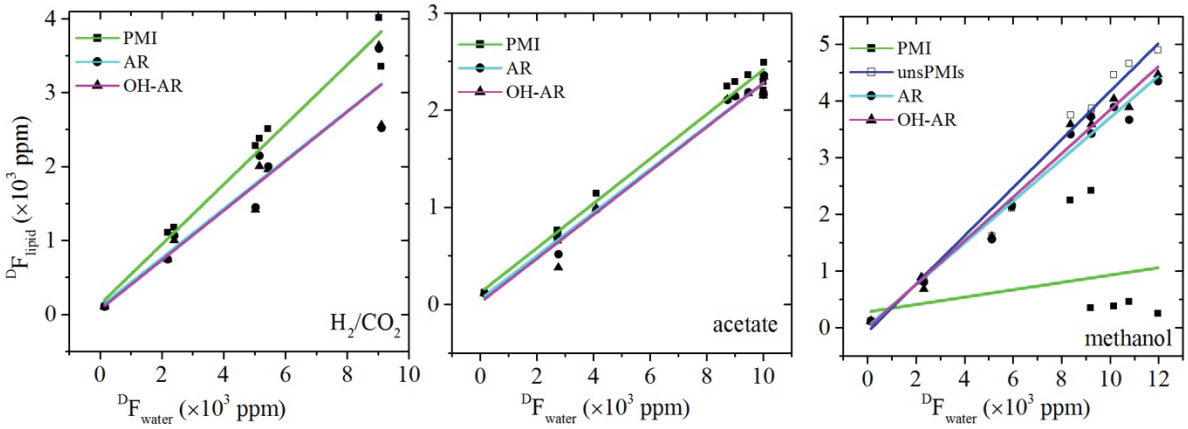

Fig. II.4. Regressions of D fractional abundance (^DF, ×10^3 ppm) in lipids versus water for *M. barkeri* grown on H_2/CO_2, acetate or methanol. The coefficients for the regressions are listed in Table S.II.1.

II. 4. Discussion

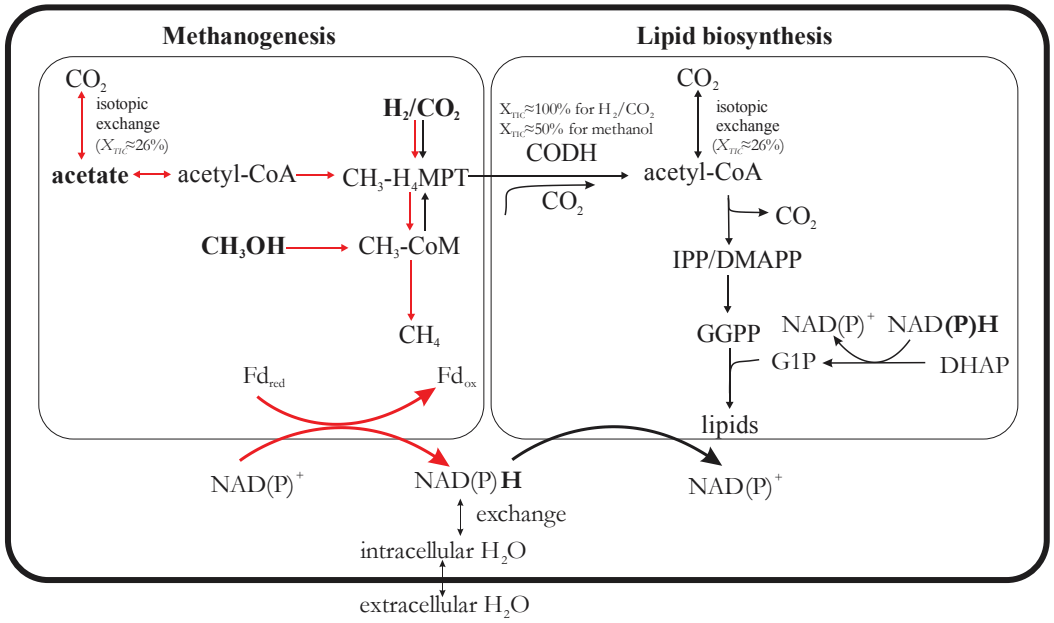

Fig. II.5. Schematic of methane production and lipid synthesis in methanogens (modified from Thauer, 1998; Koga and Morii, 2007; Londry et al., 2008; Jain et al., 2014). The black and red lines are lipid biosynthesis and methanogenesis pathways, respectively. CH_3-H_4MPT: methyl-tetrahydromethanopterin; CH_3-CoM: methyl-coenzyme M; Fd_{ox}/Fd_{red}: oxidized and reduced ferredoxin; NADP/NADPH: nicotinamide adenine dinucleotide phosphate/ reducing NADP; NAD/NADH: nicotinamide adenine dinucleotide/ reducing NAD; IPP: isopentenylpyrophosphate; DMAPP: dimethylallylpyrophosphate; GGPP: geranylgeranylpyrophosphate; G1P: *sn*-glycerol-1-phosphate; DHAP: dihydroxyacetonephosphate.
For hydrogenotrophic and methylotrophic methanogenesis, CO_2 is fixed from CH_3-H_4MPT catalyzed by carbon monoxide dehydrogenase (CODH). The carbon isotopic exchange between CO_2 and acetate-C1 is partial reaction of methanogenesis from acetate (Eikmanns and Thauer, 1984). NAD(P)H can directly provide hydride (H^-) for lipid biosynthesis (Zhang et al., 2009a), and a possible production during from methanogenesis is transfer of reducing equivalents between carrier ferredoxin (Fd) and NADP(H) by ferredoxin: NADP+ oxidoreductases (NfnAB; Spaan et al., 2015): $2Fd_{red} + NADP^+ + H^+ \leftrightarrow 2Fd_{ox} + NADPH$. The carbon flow in figure is explained as below:
(1) $X_{TIC} \approx 100\%$ and 50% were the IC contributions for acetate biosyntheis for growth on H_2/CO_2 and methanol, respectively, determined from the growth on H_2/CO_2 plus ^{13}C-DIC, and methanol plus ^{13}C-DIC or ^{13}C-methanol (cf. Eq. 1).
(2) $X_{TIC} \approx 26\%$ is IC contribution to acetate-C1 due to isotopic exchange between $^{13}CO_2$ and aceate-C1, determined from the growth on acetate plus ^{13}C-DIC (cf. Eq.1).

II.4.1. The role of inorganic carbon in lipid biosynthesis by *M. barkeri*

Except during growth on acetate, methanogens require CO_2 to synthesize acetyl-CoA as precursor for isoprenoid moieties of diether lipids (Fig. II.5; Koga and Morii, 2007; Jain et al., 2014). The intermediate methyl-tetrahydrosarcinapterin (CH_3-H_4MPT) during methanogenesis is converted to acetyl-CoA by carbon monoxide dehydrogenase (CODH) and acetyl-CoA synthase (Fig. II.5; Thauer, 1998), which is consistent with the high labelling of acetate observed during growth on methanol with ^{13}C-methanol or ^{13}C-DIC, or H_2/CO_2 with ^{13}C-DIC (Table II.2). Based on a two-end member model (Eq. 1), the contribution of IC (i.e., X_{TIC}) to acetate biosynthesis was 102±6% and 48.5±14.6% for growth on H_2/CO_2 and methanol, respectively. It is plausible that methanol and CO_2 would form methyl and carboxyl groups of acetate, respectively (Kenealy and Zeikus, 1982). Furthermore, ^{13}C-DIC was incorporated into acetate during growth on methanol, indicating that *M. barkeri* utilized external IC for acetate production although CO_2 can be derived from methanol catabolically.

For growth on H_2/CO_2, X_{TIC} for lipid biosynthesis was 86.8±7.4% (Fig. II.3), which was lower than X_{TIC} for acetate synthesis (102±6%). The difference may be explained by biosynthetic isotopic fractionation against ^{13}C and/or could have derived from organic substrates that are essential components of the growth medium (e.g., yeast extract, casitone and cysteine) or those recycled from the inoculum. Several lines of evidence suggest that PMI that accumulated during methylotrophic methanogenesis incubations was not produced from methanol or IC. Firstly, the relative abundance of PMI in the apolar fraction was much lower (4-22%) than that observed in hydrogenotrophic or acetoclastic incubations (> 90%; Fig. II.2). Also, neither ^{13}C-DIC nor ^{13}C-methanol was strongly incorporated into PMI (Fig. II.3; Section 3.4). Lastly, the δD value of PMI was much lower than that of unsPMIs, AR and OH-AR as well as δD-water in the medium (Table II.2). Together, these observations suggest that *M.*

barkeri performing methylotrophic methanogenesis preferentially produced unsPMIs instead of PMI. Therefore, unsPMIs, which are frequently observed in cold seep environments (Elvert et al., 2000; Pancost et al., 2001), might bear some potential as an indicator for the utilization of methanol or potentially other methyl substrates.

For acetoclastic methanogenesis, the contributions of IC, acetate-C1 and acetate-C2 to total lipid biosynthesis (i.e., average of PMI, AR and OH-AR) were 19.6±2.2%, 23.7±1.7% and 56.7±1.7%, respectively. The higher incorporation of acetate-C2 into PMI, AR and OH-AR suggests that methanogenic lipids were predominantly synthesized via the classic mevalonate (MVA) pathway, where acetate-C2 and acetate-C1 are incorporated via acetyl-CoA into the five-carbon isoprenoid unit at a ratio of 3:2 (Koga and Morii, 2007). However, a much higher ratio 2.4 of acetate-C2 to C1 in our study suggests the continuous loss of acetate-C1 during the biosynthesis of GGPP from acetyl-CoA (Fig. 5). Preferential incorporation of acetate-C2 into membrane lipids has been also reported in *Methanospirillum hungatei* (Ekiel et al., 1983) and *Sulfolobus solfataricus* (Rosa and Gambacorta, 1986). Because acetate can be directly converted to acetyl-CoA by acetate kinase and phosphotransacetylase (Fig. II.5), IC is not required to form acetyl-CoA. However, IC may have been introduced into isoprenoid lipids via exchange between CO_2 and acetate-C1 (Eq.7), which is an important partial reaction in acetoclastic methanogenesis (Eikmanns and Thauer, 1984). A simple mass balance (e.g., Eq. 1) of the isotopic enrichment of acetate (Table II.2) suggests that, on average, X_{TIC} of acetate is 26.1±2.8% by the end of the growth phase. The lower X_{TIC} value for lipid biosynthesis (19.6±2.2%) may result from the loss of acetate-C1 as CO_2 during lipid biosynthesis via the MVA pathway; such loss is also implied by X_{TIC} values of acetate and lipids for growth on H_2/CO_2 and methanol (Fig. II.5).

$$H^{13}CO_3^- + CO_2 \rightarrow {}^{13}CO_2 + HCO_3^- \quad (6)$$

$$^{13}CO_2 + CH_3COO^- \rightarrow CO_2 + CH_3{}^{13}COO^- \quad (7)$$

II.4.2. The contribution of water-derived hydrogen to lipid biosynthesis

The contribution of water-derived H to lipid biosynthesis (water hydrogen assimilation constant a_w) by *M. barkeri* varied with carbon sources, i.e., H_2/CO_2 (35.7%), acetate (22.6%), and methanol (39.4%; Fig. II.4; Table S.II.1). The relatively low water-derived H contribution (<40%) may mean that the residual H of lipids was derived from other substrates (e.g., H_2, acetate and methanol). The dependency of water uptake for lipid biosynthesis on substrates indicates the substrates utilized for energy metabolism may likewise influence the water H contribution to lipid biosynthesis because variable substrates will introduce the different central metabolic

pathways and further introduce different NADPH pools, which can directly provide hydride (H^-; ≈ 50%) for lipid synthesis (Zhang et al. 2009a; Valentine, 2009). Acetyl-CoA is a common precursor for the biosynthesis of isoprenoidal lipids during growth on all three different substrates (i.e., H_2/CO_2, methanol and acetate), the hydrogen isotopic fractionation factor between lipids and water ($\alpha_{l/w}$) should not differ significantly for each pathway (Fig. II.5). Therefore, the different a_w values of the three growth conditions are probably a direct reflection of the difference in the water-derived H contribution to lipid biosynthesis. The degree at which NADPH incorporates H from water is probably linked to the variability of a_w for *M. barkeri* in our study. The production of NADPH is mainly related to the central carbon metabolism (Zhang et al., 2009a). However, the central pathway leading to acetyl-CoA for lipid biosynthesis by *M. barkeri* appears unrelated to the production of NADPH (Fig. II.5). For acetoclastic methanogenesis, acetate can be directly converted to acetyl-CoA with phosphotransacetylase without NADPH production, whereas, for hydrogenotrophic and methylotrophic methanogenesis, the intermediate methyl-H_4MPT produced from methanogenesis pathway is converted to acetyl-CoA by CODH enzyme without obvious NADHP production as well (Fig. II.5). The most important sources of NADPH include the glycolysis, oxidative pentose phosphate pathway (oxPPP) and the tricarboxylic acid (TCA) cycle (Zhang et al., 2009a; Spaans et al., 2015). Based on genome analysis, it is unlikely that *M. barkeri* or other methanogens utilize these pathways for biomass synthesis (Allen et al., 2009; Sakai et al., 2011). Instead, the exergonic reduction of $NADP^+$ to NADPH coupled with ferredoxin by transhydrogenase NADH-dependent ferredoxin:NADP oxidoreductase (NfnAB) seems the main pathway for NADPH, which is present in all three domains of life (Huang et al., 2012; Spaans et al., 2015). In particular, NfnAB plays an important role in energy conservation for anaerobic bacteria and archaea (Buckel and Thauer, 2013; Spaans et al., 2015), and is hypothesized to have significant effect on hydrogen isotopic compositions of lipids from anaerobic bacteria (e.g., sulfate reducing bacteria; Leavitt et al., 2016; Osburn et al., 2016). During the production of NADPH, an electron is transferred from ferredoxin (Fd; Fig. II.5), which is widespread in methanogens with cytochromes (e.g., *Methanosarcina* species) and plays an important role in energy metabolism (Thauer, 2008). Thus, NADPH production in *M. barkeri* is likely related to the energy yield during methanogenesis process. Indeed, energy yield (J/day) during exponential phase was correlated well with a_w (Fig. II.6), suggesting that incorporation of D into lipids was correlated with high energy yield (and possibly growth rate). A possibility is that a higher energy yield can accelerate the proton exchange between NADPH and water. For acetoclastic methanogenesis, growth rate of *M. barkeri* was much lower than that for hydrogenotrophic and methylotrophic methanogenesis. As a result, the lower a_w is observed for growth on acetate versus H_2/CO_2 or methanol (Table S.II.1).

In summary, our parallel data for hydrogenotrophic, acetoclastic, and methylotrophic methanogenesis suggest that proton exchange between extracellular water and intracellular NADPH may determine the assimilation of H derived from extracellular water into membrane lipids.

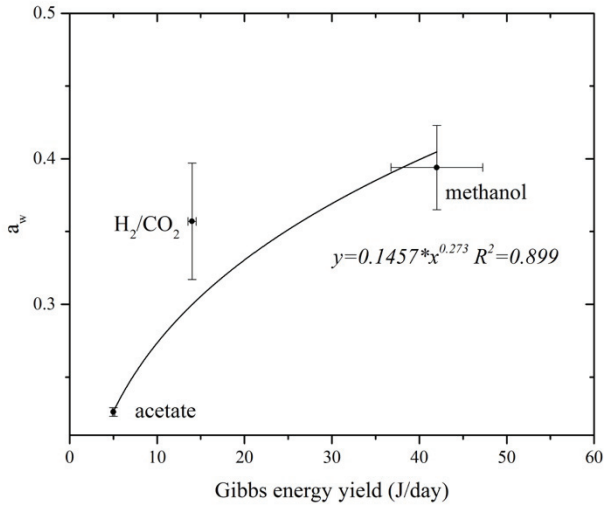

Fig. II.6. The relationship of Gibbs energy yield during exponential growth (J/day) and water hydrogen assimilation factor a_w. The energy yield is calculated based on the methane production rate (mmol CH_4 /day) and standard Gibbs energy equation (kJ/mmol CH_4; Eq. 8, 9 and 10) during exponential phase.

$CO_2+4H_2 \rightarrow CH_4+2H_2O$ $\Delta G^{o'}$=-130 kJ/mol CH_4 (8)

$CH_3COOH \rightarrow CH_4+CO_2$ $\Delta G^{o'}$=-36 kJ/mol CH_4 (9)

$4CH_3OH \rightarrow 3CH_4+CO_2+2H_2O$ $\Delta G^{o'}$=-106 kJ/mol CH_4 (10)

II.4.3. The implication of D_2O and ^{13}C-DIC labelling approach to study microbial activity in marine sediment

When use the dual stable isotope probing method with D_2O and ^{13}C-DIC, the ratio of ^{13}C versus D incorporation into lipids ($R^{13}C/D$) can distinguish autotrophic versus heterotrophic modes of carbon assimilation (cf. Wegener et al., 2012). For example, sulfate-reducing bacteria *D. variabilis* exhibited an $R^{13}C/D$ was 1 and 0.3 during autotrophic and heterotrophic growth, respectively (Wegener et al., 2012). Thus, $R^{13}C/D$ 0.3 as a "cut-off" value was used to distinguish microbial metabolism (autotroph vs. heterotroph) at least for bacteria. In comparison, *M. barkeri* exhibited a very different pattern of ^{13}C and D assimilation with $R^{13}C/D$ = 2.4, 0.9 and 1.1 for growth on H_2/CO_2, acetate and methanol, respectively (Fig. II.7). We attribute the relatively higher values of $R^{13}C/D$ to low incorporation of water-derived D (Table S.II.1). If a corrected factor 0.33 (the average of a_w for three growth conditions) is applied to calibrate D incorporation to about 1, $R^{13}C/D$ would be down to 0.78, 0.28 and 0.30. It indicates that the estimates of microbial lipid production based on D incorporation should consider the

water H assimilation factor (a_w) in the future study due to diverse water H contribution (Kopf et al., 2016; Wegener et al., 2016). If corrected with a_w, it seems that 0.3 of $R^{13}C/D$ can still be used the "cut-off" value to distinguish archaeal metabolisms (i.e., auto- or heterotroph). Due to the limited investigation of a_w for microbial lipids, we suggest the corrected factor a_w 0.67 (Wegener et al., 2012) and 0.33 (this study) for estimating bacterial and archaeal lipid production in environmental samples, respectively, until more data on diverse archaea and bacteria available.

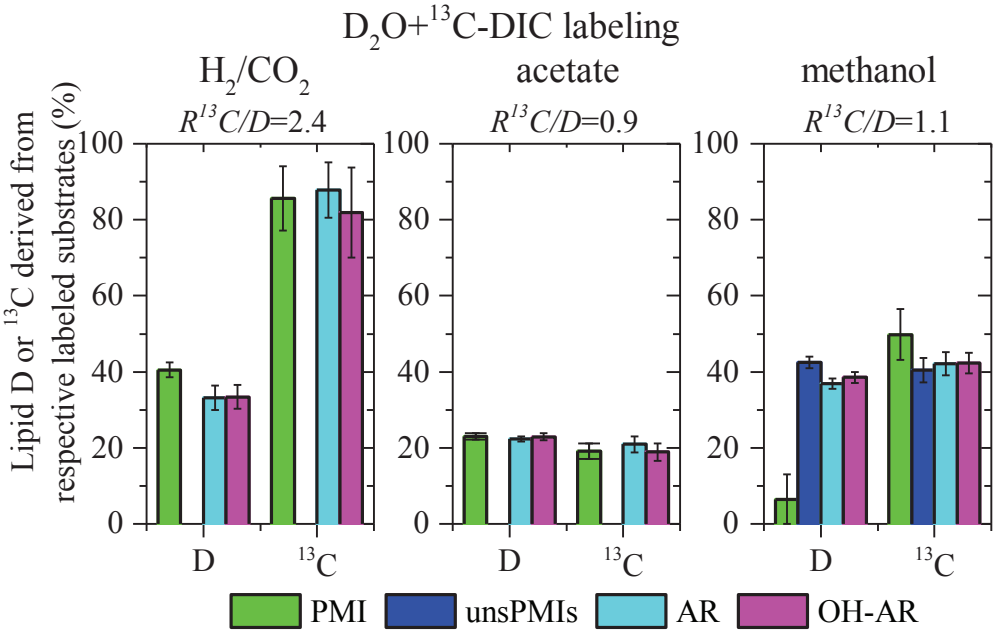

Fig. II.7. The incorporation of ^{13}C-DIC and D_2O into lipids ($R^{13}C/D$) by M. barkeri grown on different substrates. $R^{13}C/D$ above the figure is the average for all lipids. Due to the disparity of PMI for growth on methanol, $R^{13}C/D$ is from the average value for unsPMIs, AR and OH-AR.

II. 5. Conclusion

This study investigated the utilization of carbon and hydrogen for lipid biosynthesis by *M. barkeri* incubated with D_2O and different ^{13}C-labelled substrates (^{13}C-DIC, 2-^{13}C-acetate and ^{13}C-methanol). During both autotrophic and heterotrophic growth, inorganic carbon was utilized for lipid biosynthesis by *M. barkeri*, which occurred via a combination of production H_2 as an intermediate, biosynthesis of acetyl-CoA, and exchange between CO_2 and acetate-C1. The incorporation of water-derived hydrogen into *M. barkeri* lipids varied between the different substrates used for methane production (avg. 0.33), and was low compared to that determined for bacterial and eukaryotic lipids. These differences may be associated with energy yield, growth rate, and their effects on NADPH/NADP$^+$ turnover. Therefore, the application of dual stable isotope probing with D_2O and ^{13}C-DIC to study microbial activity and metabolism in

environmental settings should consider that D discrimination varies both between both organisms as wells as C substrates, which complicates the $R^{13}C/D$ as proxy for heterotrophy vs. autotrophy. However, based on all available evidence to data, an $R^{13}C/D$ value of < 0.3 remains as a conservative cutoff that distinguishes the dominance of heterotrophic over autotrophic metabolism.

Acknowledgements

This work was primarily funded by the Deutsch Forschungsgemeinschaft through the Gottfried Wihelm Leibniz Price to KUH (HI 616-14-1). W. Wu was funded by the scholarship from China Scholarship Council (CSC). We also thank X. P. Mollar, J. Wendt, H. Taubner, E. Schefuß and M. Kölling for their support of $\delta^{13}C$ and δD measurements.

Chapter III

Production and turnover of microbial organic matter in surface sandy sediments

Weichao Wu*, Travis Meador, Kai-Uwe Hinrichs

Organic Geochemistry Group, MARUM-Center for Marine Environmental Sciences & Department of Geosciences, University of Bremen, 28359 Bremen, Germany

* Corresponding author: wwu@marum.de

(***In revision for Organic Geochemistry***)

Abstract

Benthic microorganisms play a significant role in the remineralization of sedimentary organic carbon (OC). In order to constrain the growth rate, turnover and carbon metabolism of microbial communities in sandy sediments, we quantified the rates of inorganic carbon (IC) assimilation and lipid production via a recently developed dual isotope-probing assay that enables the differentiation of biosynthesis by autotrophic and heterotrophic metabolism in a 22 cm deep sediment core collected from the Janssand tidal flat (Wadden Sea, Germany). Despite an extremely low concentration of total OC (TOC) in the majority of samples (< 0.1%), the concentration of total fatty acids (TFAs) was in the range 4.5 to 20.1 µg/mg TOC, suggestive of an extraordinarily high contribution of fresh microbial and algal biomass to the TOC pool. This notion was corroborated by a high production rate of microbial fatty acids (FAs), which declined from the surface (3.58 µg TFAs/g_{dw}/yr, where dw = dry wt) to the deepest horizon (1.43 µg TFAs g_{dw}/yr) and the mean turnover time of bacterial lipids was 6 ± 5 yr. The enhanced production rate of *iso*- and *anteiso*-branched FAs strongly suggested an active population of sulfate reducing *Deltaproteobacteria*. The assimilation rate of IC into bacterial lipids was relatively low (0.16 ± 0.07 µg C/g_{dw}/yr) in organic matter (OM)-lean sandy sediments (i.e. upper 17 cm), such that the IC assimilation to lipid production ratio values were typically < 0.3, indicating that heterotrophic bacteria were dominant and dark IC fixation played a minor role at the study site. The measured rate values of FA production corresponded to microbial biomass production rate values that were high enough to replenish the entire TOC pool on the order of a few decades. Such high biomass production rate suggests that dissolved OM must play a vital role in sustaining the active heterotrophic microbial populations in these sandy sediments.

Keywords: stable isotope probing; intertidal flat; microbial production; microbial fatty acids; heterotrophic inorganic carbon assimilation

III.1. Introduction

Marine sediments harbour diverse microorganisms that catalyse biogeochemical reactions of major importance to the global C cycle such as the degradation of organic matter (OM) to CO_2 or CH_4 (Jørgensen, 1982; Middelburg et al., 1993). Many studies have assessed the composition of the microbial community and possible metabolism based on genomic analyses (Mußmann et al., 2005; Wilms et al., 2006a) or biomarker analysis (Lipp et al., 2008; Seidel et al., 2012). However, estimates of bulk microbial community growth rate and carbon metabolism in sediments are not well constrained.

Experimental approaches to determine microbial activity in sediments have applied stable isotope probing (SIP; Boschker et al., 1998), radiotracer probing (Moeslundi et al., 1994; Dumont and Murrell, 2005) and D/L-amino acid modelling (Lomstein et al., 2012). In principle, SIP and radiotracer techniques measure the uptake of specific stable isotope (e.g. ^{13}C-acetate, glucose or ^{15}N-amino acids) or radioisotope labelled substrates (e.g. ^{14}C-thymidine) into biomolecules via analysis of nucleic acids or microbial lipids as informative taxonomic biomarkers. However, conventional stable isotope or radioisotope labelling methods based on the uptake of carbon substrates are selective and thus target only a subset of the microbial community. Recently, D_2O labelling incubation methods have become a powerful tool for studying the activity of the bulk microbial community (Kellermann et al., 2012; Wegener et al., 2012) and even single cells (Berry et al., 2015; Kopf et al., 2015) in different environmental settings as well as human sputum (Kopf et al., 2016). This relies on the passive uptake of isotopic label, as water is utilized for biosynthesis by all organisms, independent of the carbon substrate (cf. Zhang et al., 2009). In addition, the coupled applications of ^{13}C-bicarbonate with D_2O labelling provides information about whether the targeted biomarkers originate from autotrophic or heterotrophic metabolism (Wegener et al., 2012). The assimilation of IC into biomass is a hallmark of autotrophic microorganisms, although microbial heterotrophs also incorporate a small fraction of IC via anaplerotic reactions (Roslev et al., 2004; Feisthauer et al., 2008).

Intertidal sediment is characterized by a high nutrient supply from terrestrial and marine OM (Volkman et al., 2000; Rütters et al., 2002), both of which can stimulate benthic microbial community activity. In tidal flats, these inputs enhance microbial activity to depths of several m as a result of pore-water advection and diffusion (Billerbeck et al., 2006a,b; Røy et al., 2008; Beck et al., 2009). In coastal sediments, OM mineralization by sulfate-reducing bacteria is often thought to dominate the sedimentary biogeochemical C cycle. However, Boschker et al.

(2014) reported that the rate of dark IC assimilation in coastal sediments was similar to that of C mineralization, and other studies likewise suggested the potential importance of IC fixation in benthic C cycling (Thomsen and Kristensen, 1997; Lenk et al., 2011; Dyksma et al., 2016). *Gammaprotebacteria* were proposed as a main player in the assimilation of IC via sulfur oxidation to gain energy (Lenk et al., 2011; Boschker et al., 2014; Dyksma et al., 2016). However, the heterotrophic members of the dominant sulfate-reducing *Deltaproteobacteria* in sediments also have the potential to fix IC (Sorokin, 1966; Wegener et al., 2012).

Microbial activity and community composition in the backbarrier tidal flat of the island of Spiekeroog in the German North Sea have been well studied and appear to be controlled by OM source and availability (e.g. marine vs. terrestrial OM; Rütters et al., 2002; Seidel et al., 2012), hydrogeological conditions (e.g. advection vs. diffusion; Beck and Brumsack, 2012) and redox conditions (e.g. aerobic vs. anaerobic respiration; Billerbeck et al., 2006a,b; Beck et al., 2017). The upper sandy layers (shallower than 75 cm) are characterized by rapid burial of fresh marine OM and strong pore-water advection (Seidel et al., 2012), which can sustain the growth of heterotrophic microbes in marine sediment and the nutrients released as products of remineralization can even stimulate high primary production in the Wadden Sea (Beck and Brumsack, 2012). *Gamma- and Deltaproteobacteria* dominated the bacterial community (> 60%) in the upper layer and even down to 2 m (Wilms et al., 2006a,b). In this study, we applied a lipid-based ^{13}C-bicarbonate and D_2O labelling approach to quantitatively assess the microbial activity and mode of carbon metabolism in surface (0-22 cm) Janssand tidal flat sediment (Wadden Sea, Germany).

III.2. Sampling and Methods

III.2.1. Sediment slurry preparation

The core (22 cm) was retrieved by manual push coring during low tide from the Janssand intertidal flat in the northeastern Wadden Sea, Germany. The core was closed with a rubber stopper and then transported in a cooling box at 4°C to the lab for further treatment. Sediment was sliced to five horizons (0–2, 2–7, 7–12, 12–17 and 17–22 cm) and transferred to Schott glass bottles under N_2 as soon as possible. Anoxic sediment slurries were prepared in a glove box (3% H_2 in N_2) by adding an equal volume of sterilized artificial seawater with the following composition (g/l) modified from Xie et al. (2013): NaCl, 26; $MgCl_2.6H_2O$, 5.0; $MgSO_4$, 5.0; $CaCl_2.2H_2O$, 1.5; KBr, 0.1; KH_2PO_4, 0.014; NH_4Cl, 0.053; $NaHCO_3$, 1.26; $Na_2S.9H_2O$, 0.24. Stock solutions of $NaH^{13}CO_3$ and D_2O were then added to the slurries to achieve final ^{13}C and ^{2}H enrichments of ca. 5%. An aliquot of sample collected from the 17–22 cm horizon was

autoclaved at 120 °C for 30 min to serve as a sterilised control, and $NaH^{13}CO_3$ and D_2O solutions were added after cooling to room temperature, to avoid chemical isotope exchange triggered by the high temperature. The sediment slurries were flushed with N_2 and incubated in the dark for 21 days at 12 °C (in situ temperature in October) and room temperature (roughly summer temperature of ca. 20°C), respectively.

III.2.2. Lipid analysis

The total lipid extract (TLE) was obtained after modified Bligh and Dyer extraction (Sturt et al., 2004). Briefly, each freeze-dried sample was extracted 2x in an ultrasonic bath with 2:1:0.8 (v/v/v) of MeOH/dichloromethane (DCM)/phosphate buffer (pH 7.4) and then 2x with MeOH/DCM/trichloroacetic acid (pH 2.0). The organic fractions were combined, then DCM and water were added to a final ratio of MeOH/DCM/water 1:1:0.9 to separate the organic phase. The organic extract was then washed 3x with Milli-Q water. The TLE was dried under N_2 and stored at -20 °C until further processing.

Total microbial FAs were retrieved via saponification of the TLE with 5% KOH in MeOH at 80 °C for 2 h (Elvert et al., 2003). An equal volume of water was then added and neutral lipids removed by extracting 3x with hexane. The basic aqueous solution was then acidified with 25% HCl to pH 1. The FA fraction was extracted 3x with hexane, dried under N_2, and esterified with 20% BF_3 in MeOH at 70 °C for 1 h to form the FA methyl esters (FAMEs), which were subsequently extracted with hexane. The double bound positions in FAMEs were identified using the dimethyl disulfide (DMDS) adduction method (Nichols et al., 1986).

III.2.3. Molecular and isotopic analyses

FAMEs were quantified relative to the internal standard (2-methyloctadecanoic acid) and identified via gas chromatography with flame ionisation detection (GC-FID) and GC-mass spectrometry (GC-MS; Trace GC and Trace DSQ II MS, Thermo Scientific, Germany). Compound specific carbon and hydrogen isotopes of FAMEs were determined using GC-isotope ratio monitoring-MS (GC-IRMS) with a Trace GC Ultra connected to a Delta V Plus isotope ratio mass spectrometer (Thermo Scientific, Germany) via Thermo GC IsoLink and ConFlo IV interfaces and are expressed using the delta notation ($\delta^{13}C$ and δD, respectively; Eq. 1). The combustion and pyrolysis temperatures were 940 °C and 1420 °C for C and H isotope measurement, respectively. The columns for all GC instruments were Rxi-5ms (30 m × 0.25 mm, 0.25 µm film thickness; Restek GmbH, Germany). The injector temperature was 310 °C and the oven temperature ramped from 60 °C to 150 °C at 10 °C/min, and then to 320 °C (held 22.5 min) at 4 °C/min.

$\delta^{13}C$ values of TOC and TOC (%, w/w) were determined with a Flash 2000 CHNS/O Analyzer connected to a Delta V Plus isotope ratio mass spectrometer (Thermo Scientific, Germany). Prior to analysis, IC in the sediment was removed by incubation in a 10% HCl solution (2 ml) overnight, followed by rinsing with Milli Q water to pH 5. The residual sample was lyophilized and measured via flash EA-IRMS. TOC, as well as $\delta^{13}C$ and δD of FAMEs were measured at least in duplicate. $\delta^{13}C$ and δD values of FAs were not corrected for the Me added during derivatization, which represented only a minor contribution of C and H in comparison vs. the highly labelled alkyl chain.

III.2.4. Data manipulation

The measured rate of microbial lipid production ($prod_{Lipid}$; µg lipids/$g_{dw\ (dry\ weight)}$/yr) and assimilation of IC ($assim_{IC}$; µg C/g_{dw}/yr), as well as the turnover time of bacterial lipids (τ_{Lipid}; yr), were estimated from the fractional abundance enrichment of ^{13}C and D of FAMEs and the lipid pool size. The main calculation equations are:

$$\delta = \left(\frac{R_{sample}}{R_{std}} - 1\right) \times 1000‰ \quad (1)$$

$$F = \frac{R}{R+1} \quad (2)$$

R_{sample} is the C or H isotope ratio of samples ($^{13}C/^{12}C$ and D/H), and R_{std} that of the standard 0.011180 for $^{13}C/^{12}C$ of Vienna Pee Dee Belemnite (VPDB), and 0.0001557 for D/H of Vienna Standard Mean Oceanic Water (VSMOW). F is the fractional abundance of ^{13}C and D.

$$prod_{Lipid} = conc_{Lipid} \times \frac{\Delta FD_{Lipid}}{FD_{med} \times time} \quad (3)$$

$$assim_{IC} = conc_{Lipid} \times \frac{\Delta F^{13}C_{Lipid}}{F^{13}C_{med} \times time} \quad (4)$$

ΔFD_{Lipid} and $\Delta F^{13}C_{Lipid}$ ($\Delta F = \Delta F_{t21} - \Delta F_{kc}$; kc is "killed" control) represent the increased proportion of fractional abundance of D and ^{13}C after 21 days incubation, compared with that of the killed control, and FD_{med} and $F^{13}C_{med}$ are the fractional abundance of D and ^{13}C of water and dissolved IC in the incubation medium, respectively. Because $\delta^{13}C$-TOC also increased after incubation, $assim_{IC}$ into TOC was similarly estimated using TOC % and $\Delta F^{13}C_{TOC}$ data. For the calculation of $assim_{IC}$, the lipid concentrations were assumed to be equal to that of lipid carbon in order to further compare $assim_{IC}$ with $prod_{Lipid}$.

$$\tau_{Lipid} = \frac{conc_{Lipid}}{prod_{Lipid}} \quad (5)$$

τ_{lipid} represents the turnover time of microbial lipids in marine sediments.

III.2.5. The propagation of error

The Gaussian error of variables in the above equations (e.g., $prod_{Lipid}$ and $assim_{IC}$) was calculated via:

$$\sigma_y=\sqrt{\left(\frac{\partial y}{\partial x_1}\right)^2\sigma_{x_1}^2+\left(\frac{\partial y}{\partial x_2}\right)^2\sigma_{x_2}^2+\ldots+\left(\frac{\partial y}{\partial x_n}\right)^2\sigma_n^2} \quad (6)$$

where σ is the standard deviation of the variable, and $\left(\frac{\partial y}{\partial x_n}\right)^2\sigma_n^2$ is the squared partial derivative deviation of each variable. In the case that only single measurements were available (i.e., for some FAMEs), the coefficient of variation (CV) of other lipids was applied. In addition, the concentrations of FAMEs were determined from a single measurement and isotope composition of medium was calculated theoretically, based on the known volume additions. CV of 5% was assumed for FAME concentration and isotope composition of medium.

III.3. Results and Discussion

III.3.1. Abundances and stable isotopic compositions of microbial fatty acids

TOC was typically < 0.1%, but increased to > 0.2% in the 17–22 cm horizon. (Fig. III.1A). The deep horizon was darker than shallower depths, suggesting that OM and/or iron sulfides were possibly deposited and/or better preserved during a period of anoxia. The terrestrially-derived long chain (> C_{20}) and algal-derived polyunsaturated FAs (e.g. $C_{20:4}$ and $C_{20:5}$), accounted for < 10% of the total FAs, whereas short chain FAs (e.g. C_{14}, C_{15} and C_{17}) ranged up to 23%, suggesting that the microbial source was more strongly imprinted the FA profile. C_{16} and C_{18} were dominant, accounting for > 75% at all depths, and were probably contributed from both algal and bacterial sources. Total microbial FA (C_{14} to C_{18}; TFA) concentration generally decreased with depth, from > 12 $\mu g/g_{dw}$ at the surface 2 cm to as low as 2.8 $\mu g/g_{dw}$ at 7–12 cm (Fig. III.1B); however, TFAs increased in the 17–22 cm horizon (10.5 and 12.7 $\mu g/g_{dw}$ for the incubation at 12 °C and 20 °C, respectively; Fig. V.1B).

After incubation for 21 days in the dark at 12 °C and 20 °C, all microbial FAs (C_{14}–C_{18}) had incorporated ^{13}C and D (Fig. III.2). Relative to the killed control, the *iso*- and *anteiso*-branched C_{14} and C_{15} FAs typically exhibited the greatest increases in ^{13}C and D (Fig. III.2). No significant ^{13}C and D were incorporated into long chain FAs (> C_{20}) as well as algal polyunsaturated FAs (data not shown). The greatest ^{13}C enrichment of a TFA, expressed as the change in weighted average $\delta^{13}C$ relative to the killed control ($\Delta\delta^{13}C_{TFAs} = \delta^{13}C_{TFAs\text{-}t21} - \delta^{13}C_{TFAs\text{-}kc}$; Hayes, 2001), was observed in the 12–17 cm horizon (Fig. III.2A). Throughout the depth profile, $\Delta\delta^{13}C_{TFAs}$ was slightly higher in the 20 °C treatment (7.2–12.7‰) than at 12 °C (5.5–10.8‰).

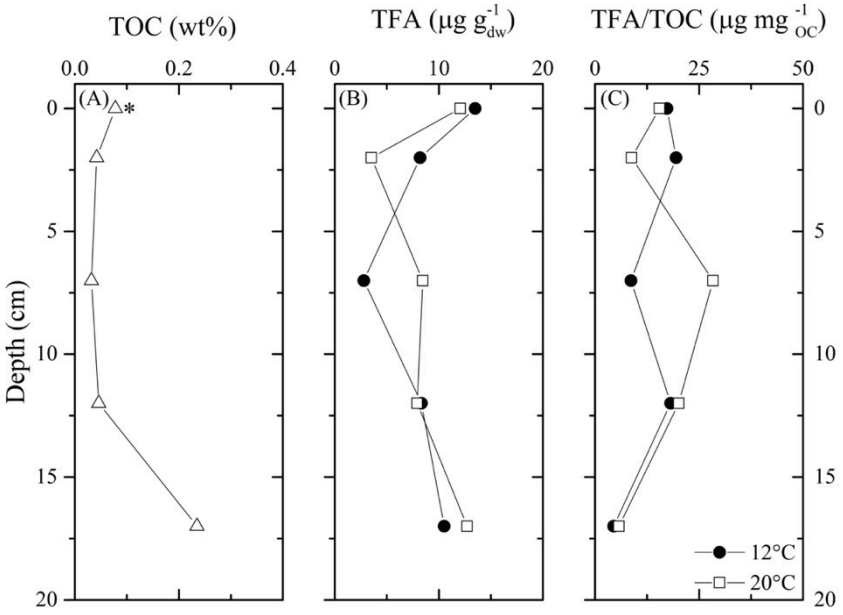

Fig. III.1. Concentrations of TOC and total fatty acids (TFA) in Janssand sediment after incubation for 21 days. A: the amount of TOC (wt%); B: total fatty acids (TFA, µg g_{dw}^{-1}); C: TOC-normalized TFA concentrations (µg $mg_{oc\ (organic\ carbon)}^{-1}$). *: The TOC concentration for the 0–2 cm sample was obtained from the extracted sample residue and may therefore slightly underestimate the actual concentration.

Label incorporation was also evident in the bulk TOC pool, consistent with a notable contribution of microbial biomass to the sedimentary OM, as implied by the TFA concentration. $\Delta\delta^{13}C_{TOC}$ typically decreased with increasing depth (Fig. III.2A). In the upper 12 cm, $\Delta\delta^{13}C_{TOC}$ (e.g. 11.2‰ at 20 °C) was higher than $\Delta\delta^{13}C_{TFAs}$ (e.g. 8.3‰ at 20°C; Fig. III.2A). The similar ^{13}C enrichment in both pools (TFA and TOC) suggested that the TOC pool in these sandy sediments is composed largely of freshly produced benthic bacterial biomass. Accordingly, the slightly higher enrichment in the TOC pool relative to TFAs may have resulted from greater uptake of label into other biomolecules (e.g. protein) relative to lipids (Feisthauer et al., 2008). Previous studies have demonstrated that bacteria dominated the microbial communities in Janssand sediment (Seidel et al., 2012), which is consistent with the low concentrations of archaeal lipids (data not shown). Considering the low TOC values in the upper 17 cm sandy sediment (< 0.1wt%), the decreasing trend of $\Delta\delta^{13}C_{TOC}$ with depth likely resulted from the reduced proportion of microbial biomass in the deeper horizons, as also indicated by TFAs/TOC (Fig. III.1C). The TOC-normalized TFA concentration in the OM-rich depth of 17–22 cm (0.23%) was 4.5 µg/mg_{oc}, which was much lower than that in the OM-lean (0.04%) shallower sediment (28 µg/mg_{oc}).

The weighted average D enrichment of TFAs relative to the killed control ($\Delta\delta D_{TFAs}$) was higher in the 20 °C incubations (3600‰ to 9420‰) than those kept at 12 °C (2010‰ to 4340‰; Fig.

III.2B). In addition, the 50–60% decrease in $\Delta\delta D_{TFAs}$ with depth was inconsistent with $\Delta\delta^{13}C_{TFAs}$, which had no uniform depth-related pattern (Fig. III.2A).

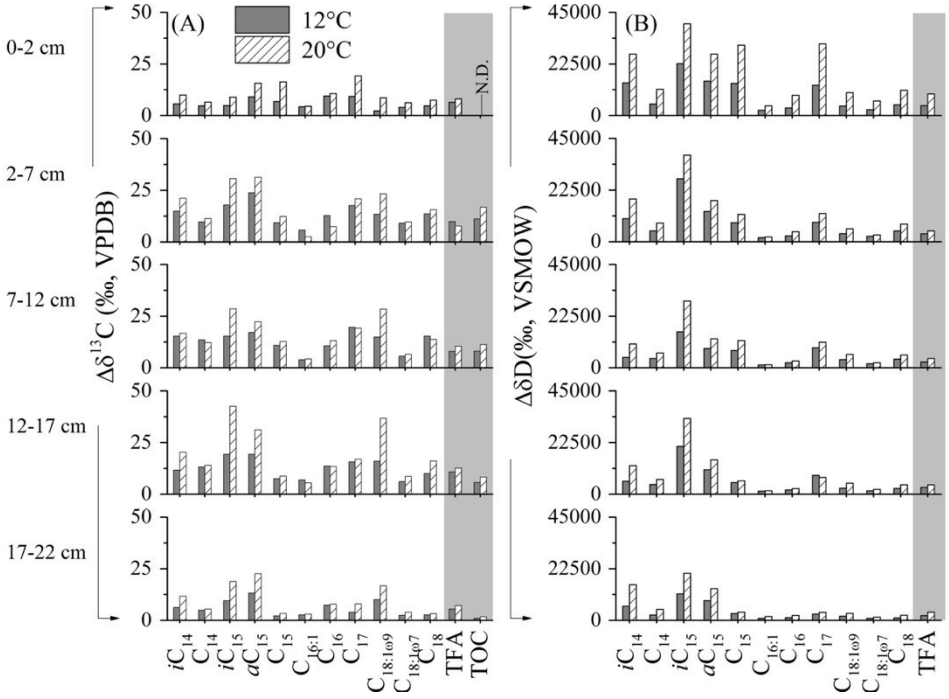

Fig. III.2. The increase of $\delta^{13}C$ (‰, A) and δD (‰, B) of fatty acids in Janssand sediment core after incubation at 12°C (grey) and 20°C (striped). The increase of $\delta^{13}C$ and δD are expressed as $\Delta\delta^{13}C$ and ΔδD, respectively, and $\Delta\delta=\delta t_{21}-\delta_{kc}$ (killed control). The sample at the depth of 17-22 cm was treated as killed control with autoclave treatment, and also incubated for 21 days. TFA is the total fatty acids (grey area), and $\delta^{13}C$ or δD-TFA is the weighted average $\delta^{13}C$ or δD of TFA.

III.3.2. Rates of lipid production and inorganic carbon assimilation

Because water is the main hydrogen source for the lipid biosynthesis for both auto- and heterotrophs (Sessions et al., 1999; Zhang et al., 2009), D incorporation may serve as a proxy for the production rate of microbial acyl lipids, which we consider to be directly related to new production of microbial cells and inversely to the lipid turnover time (τ_{lipid}). The production rate of C_{16} and its unsaturated analogues was highest among all FAs in the upper 2 cm; below the surface they decreased five-fold (Fig. III.3A) and were exceeded by the production of C_{15}, in particular *i*C_{15} and *a*C_{15} in deeper depth (e.g. 12-17 and 17-22 cm; Fig. III.3A). The *i*C_{15} and *a*C_{15} could originate from the gram-negative *Deltaproteobacterium Desulfovibrio* (Taylor and Parkes, 1983; Kaneda, 1991; Seidel et al., 2013), which can perform various metabolisms (Taylor and Parkes, 1983) and even survive under oxic conditions (Johnson et al., 1997). The production rate of C_{17} and C_{18} FAs was consistently lower than those of other FAs.

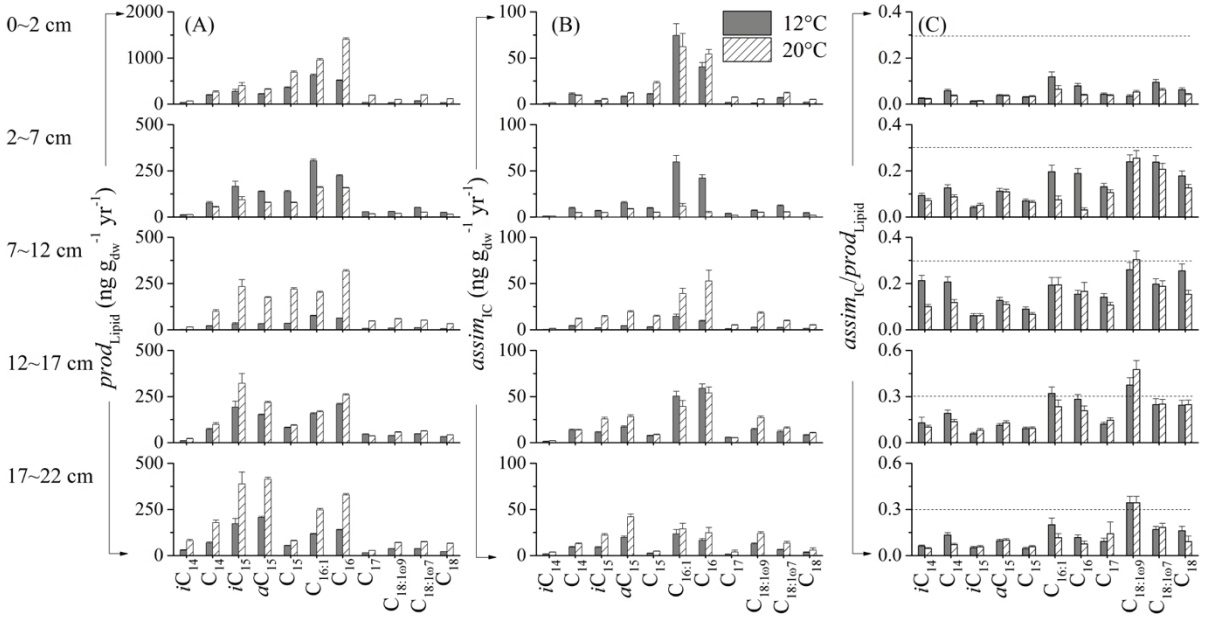

Fig. III.3. The $prod_{Lipid}$ (A, ng g_{dw}^{-1} yr^{-1}) and $assim_{IC}$ (B, ng g_{dw}^{-1} yr^{-1}) of individual fatty acids, and their *Ra/p* (C) in different horizons. The dashed line at *Ra/p* of 0.3 designates the putative border between autotrophy or heterotrophy (cf. Wegener et al. 2012).

Except for 2-7 cm, bulk microbial acyl lipid production rate ($prod_{Lipid}$) at different depths was higher in the 20 °C treatment than in the 12 °C treatment (Fig. III.4A), suggesting that the higher temperature stimulated microbial activity. Values of $prod_{Lipid}$ were highest in the top 2 cm and reached 4.7 ± 0.1 µg lipids/g_{dw}/yr (Fig. III.4A) at 20 °C, similar to values measured in fjord surface sediment in Himmersfjärden, Sweden (6.4 µg lipids/g_{dw}/yr, Wegener et al., 2012). Production rate in subsurface samples was relatively uniform with a minimum of 0.88 ± 0.81 µg lipids/g_{dw}/yr at 7–12 cm (Fig. III.4A). The deep OM-rich horizon at 17–22 cm exhibited slightly higher production rate (1.43 ± 0.75 µg lipids/g_{dw}/yr, Fig. III.4A) vs. the shallower sediment.

Patterns of assimilation of IC ($assim_{IC}$) into individual FAs differed from their $prod_{Lipid}$ pattern. In particular, $assim_{IC}$ for C_{16} was highest among all FAs (Fig. III.3B). $Assim_{IC}$ for C_{15} including branched isomers, were second to that of C_{16} and increased with depth, particularly for the 20 °C treatment (Fig. III.3B). Although $assim_{IC}$ for $C_{18:1\omega9}$ was relatively minor (e.g. < 5% of TFAs in the top 2 cm; Fig. III.3B), it increased with depth, possibly indicating that autotrophic sources of it were more active in the deeper horizon (Fig. III.3B).

$Assim_{IC}$ for TFAs ($assim_{IC}$-*TFAs*) in different horizons ranged from 0.05 to 0.16 µg C/g_{dw}/yr at 12 °C, and from 0.05 to 0.23 µg C/g_{dw}/yr at 20 °C (Fig. III.4B). There was no significant difference between the temperature treatments (p > 0.05), indicating that temperature had little influence on rate of IC fixation into lipids. The average $assim_{IC}$-*TFAs* in the upper 7 cm

(0.15 µg C/g_{dw}/yr) was lower than values reported for surface sediments (1-6 cm) in Himmersfjärden, Sweden (1.3 µg C/g_{dw}/yr; Wegener et al., 2012), and much lower than that in the OM-rich estuarine surface sediments incubated under oxic conditions (12–167 µg C/g_{dw}/yr; converted from 2.6–36.3 mmol C/m^2/d reported by Boschker et al., 2014 by assuming a sediment density of 1.5 g dry sediment/cm^3 and an integrated depth of 0–5 cm). The difference in IC fixation rate between oxic and anoxic conditions may be due to higher yield of metabolic energy and thus increased production during oxic respiration (Harvey et al., 1986; Sun et al., 1997).

Interestingly, $assim_{IC}$ into TOC ($assim_{IC}$-*TOC*) at each depth horizon was always lower at 12 °C (12.4 to 6.0 µg C/g_{dw}/yr) than that at 20 °C (17.6 to 8.6 µg C/g_{dw}/yr; Fig. III.4B), suggesting that temperature influences IC assimilation in bacterial biomass. The lower $assim_{IC}$-*TOC* in the subsurface relative to the surface samples is consistent with reduced activity (i.e. $prod_{Lipid}$) in deeper sediments. The estimates of $assim_{IC}$-*TOC* in the TOC-rich horizon at 17–22 cm were based on a $\Delta\delta^{13}C_{TOC}$ value of only 1.0–1.7‰ (Fig. III.2A), which significantly exceeds the analytical precision of the instrument (0.2‰), but should be regarded with greater caution than the overlying horizons. In contrast to shallower samples, $\Delta\delta^{13}C_{TOC}$ in the 17–22 cm horizon was lower than that of $\Delta\delta^{13}C_{TFAs}$ (up to 5.5‰ at 20 °C; Fig. III.2A), further suggesting that the deepest relatively TOC-rich horizon contained a greater fraction of fossil OM. Values of $assim_{IC}$-*TFAs* throughout the depth profile accounted for 0.3 to 2.9% of that into TOC (1.7% on average), which is close to the proportion of lipids in anaerobic bacterial biomass (ca. 5.6% FAs of anaerobic bacterial biomass C; Brinch-Iversen and King, 1990; Middelburg et al., 2000). This higher flux of HCO_3^--derived ^{13}C into TOC relative to acyl lipids may have multiple explanations. Firstly, it is conceivable that non-lipid pools of biomass were more highly labelled than lipids. For example, Feisthauer et al. (2008) showed in experiments with the heterotrophs *Pseudomonas knackmussii* and *Rhodococcus opacus*, both supplied with non-labelled glucose and $^{13}CO_2$, that bulk biomass was much more strongly labelled than the FA pool. Secondly, ^{13}C-labelled metabolites may have accumulated in the TOC pool over the course of the experiment.

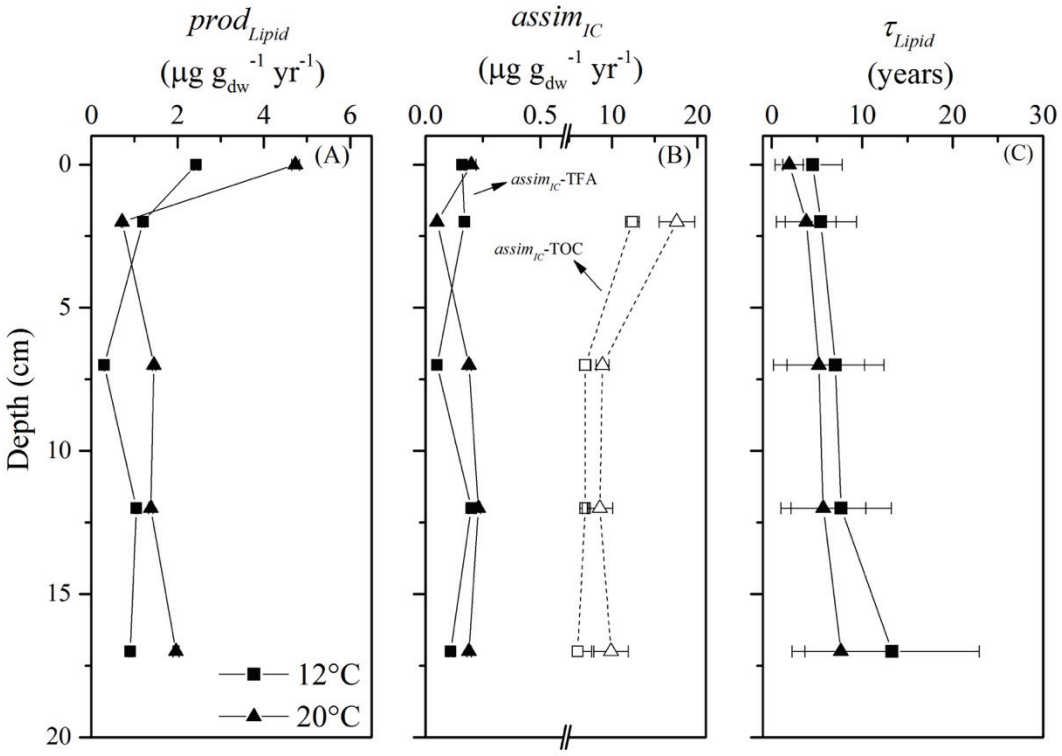

Fig. III.4. Summary of microbial activity in different horizons after incubation at 12°C (square) and 20°C (triangle). A: Microbial lipid production rates ($prod_{Lipid}$, µg g_{dw}^{-1} yr^{-1}). B: Assimilation rates of inorganic carbon ($assim_{IC}$, µg g_{dw}^{-1} yr^{-1}) into total microbial fatty acids ($assim_{IC}$-*TFA*, solid) or TOC ($assim_{IC}$-*TOC*, open). C: Turnover times of microbial lipids (τ_{lipid}, years).

III.3.3. Bacterial lipid turnover times (τ_{lipid})

In the 20 °C treatment, τ_{Lipid} ranged from 1.9 ± 1.6 yr in the top 2 cm to 7.6 ± 5.4 in the 17–22 cm horizon; this range was 4.5 ± 3.3 to 13.3 ± 9.6 yr in the 12 °C treatment (Fig. III.4C). τ_{Lipid} was slightly shorter than independent estimates previously reported by Xie et al. (2013) (several decades) who applied a reverse fitting model that incorporated degradation rate data of intact bacterial acyl lipids from the same study site (Logemann et al., 2011). Assuming that τ_{Lipid} is similar, if not longer than that of the bacterial community (Wegener et al., 2012), the estimated turnover time of the bacterial community in the Janssand surface intertidal sediment (0–2 cm) is far shorter than reported based on D/L-amino acid modelling in surface sediments (several hundred yr) from Aarhus Bay (Langerhuus et al., 2012) and the Peruvian continental shelf (Lomstein et al., 2012).

III.3.4. The contribution of active bacterial biomass to the TOC pool

The first hint on a relatively high contribution of fresh sedimentary microbial biomass to the TOC pool comes from the TFA concentration. Based on the assumption that microbial biomass comprises ca. 5.6% lipids (w/w; Middelburg et al., 2000), our data suggest that up to

one third (34%) at 12-17 cm and 9% at 17–22 cm of TOC could be comprised of recently produced microbial biomass (Table III.1). This value is an upper boundary because the TFA pool contains a fraction derived from non-sedimentary algae as well as remnants of decayed biomass. For similar sandy intertidal flat sediments near Sylt Island, Rusch et al. (2001) estimated a microbial biomass C contribution of 2 to 9% to the TOC pool. Such high proportions are in stark contrast to habitable subsurface sediments in the deep sea, for which Lipp et al. (2008) have estimated a global average microbial biomass contribution to the TOC pool of ~0.02%.

Table III.1. Estimated microbial biomass production rate and its turnover times. Values of experiments conducted at 12°C and 20°C are reported as averages.

Depth (cm)	TOC (wt%)	TFA (μg g_{dw}^{-1})	Biomass C[a]/TOC	$prod_{Biomass}$ (μg C g_{dw}^{-1} yr^{-1})[b]	τ_{TOC}[c] *(years)*
0-2	0.078	12.8	30%	64	13.6
2-7	0.041	5.85	26%	17	25.5
7-12	0.031	5.65	33%	16	36.2
12-17	0.042	8.10	34%	22	20.3
17-22	0.228	11.60	9%	26	104.6

a: Biomass C is estimated from the total microbial fatty acids (TFA) divided by 0.056 g fatty acids per gram biomass-C.

b: calculated from the lipid production rate (μg lipid g_{dw}^{-1} yr^{-1}) divided by 0.056 g fatty acids per gram biomass-C.

c: τ_{TOC} signifies the turnover time of TOC pool, and is calculated as the ratio of TOC versus $prod_{Biomass}$.

The determined lipid production rates enable us to estimate microbial biomass production rates. These can be related to the TOC pool size and converted into TOC turnover time, if we assume that the flux of TOC in the sandy sediment is dominated by sedimentary microbial biomass production under steady state conditions. For example, we estimate microbial biomass production rate of 16 to 64 μg $C/g_{dw}/yr$ (Table III.1). Considering the sedimentary TOC pool size, the values translate into turnover time values of the TOC pool on the order of a few decades (Table III.1). In concert with the high proportion of microbial biomass, the estimates are consistent with a vigorously active microbial ecosystem sustained in extremely organic-lean sandy sediments. In contrast to deep sea sediments, where relatively degraded, pre-aged OM is incorporated into the seabed, the availability of fresh algal particulate OM, in combination with high advective flux of dissolved OM and presumed recycling of a substantial fraction of fresh microbial metabolites can explain the sustenance of a relatively active bacterial community (Beck et al., 2009, 2017; Seidel et al., 2012).

III.3.5. Implications of inorganic carbon fixation and carbon cycle in sedimentary system

The ratio of $assim_{IC}/prod_{Lipid}$ (*Ra/p*) can distinguish the prevalence of autotrophic vs. heterotrophic production (cf. Wegener et al., 2012) and provide a detailed glimpse of carbon metabolism by different members of the sedimentary bacterial community (Fig. III.3C). Throughout the depth profile, values of *Ra/p* for C_{16} and C_{18} FAs were generally higher than C_{14}, C_{15} and C_{17} FAs (Fig. III.5), suggesting a co-occurrence of both heterotrophic and autotrophic community members in the sediments. In the upper 2 cm, values of *Ra/p* for TFAs were < 0.3 (Fig. III.3 and 5). In the sandy Janssand intertidal sediment, the maximum O_2 penetration depth ranges from 2.4 to 2.8 cm in the lower sand flat (Billerbeck et al., 2006b). Its presence therefore likely selected for a dominant heterotrophic community in the upper 0–2 cm. In the subsurface horizons, the weighted average *Ra/p* ratio values of TFAs slightly increased, but never > 0.3 (Fig. III.5), suggesting that the bulk community was predominantly heterotrophic throughout the depth profile, with the potential of an increased contribution of FAs from autotrophic community members in deeper horizons (Fig. III.5).

Concentrations of C_{14}, C_{15} and C_{17} fatty acids accounted for < 20% of TFAs, but exhibited production rate values similar to those of C_{16} and C_{18} (Fig. III.5). The relatively high production rates of C_{14}, C_{15} and C_{17} exhibiting low *Ra/p* values (Fig. III.5) is consistent with a high activity of heterotrophic *Deltaproteobacteria* (cf. Wegener et al., 2012), which have been shown to produce C_{14}, C_{15} and C_{17} FAs (Kaneda 1991; Londry et al., 2004). The small flux of IC fixed during heterotrophy was probably due to anaplerotic or replenishing reactions (Roslev et al., 2004). For example, during OM degradation, IC is assimilated by phosphoenolpyruvate carboxylase in order to replenish oxaloacetate and maintain the citric acid cycle during degradation of OM (Kornberg, 1965; Thauer, 1988). This heterotrophic IC fixation was also observed in the cultivation of pure sulfate-reducing bacteria (Wegener et al., 2012), and can account for up to 30% of CO_2 for cell carbon synthesis (Sorokin, 1966).

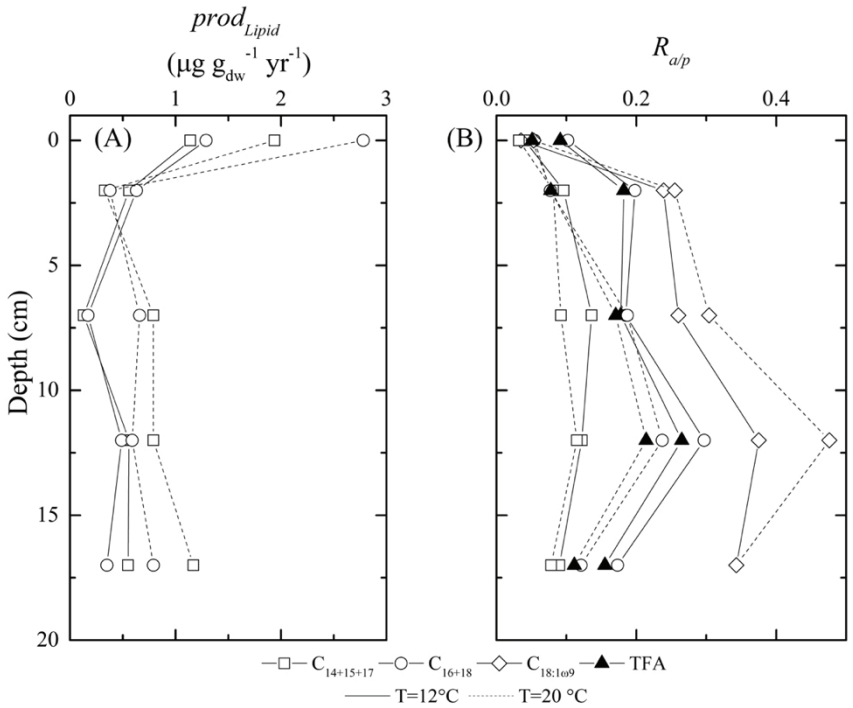

Fig. III.5. Ratio of $assim_{IC}$ to $prod_{lipid}$ (*Ra/p*) and $prod_{lipid}$ for different fatty acid groups after incubating at 12°C and 20°C.

(1) *Ra/p* for $C_{14+15+17}$ refers the weighted average *Ra/p* of C_{14}, C_{15} and C_{17} fatty acids including their analogues, same treatment for C_{16} and C_{18} fatty acids (C_{16+18}).

(2) $prod_{lipid}$ for $C_{14+15+17}$ refers the sum production rate of C_{14}, C_{15} and C_{17} fatty acids including their analogues, same treatment for C_{16} and C_{18} fatty acids (C_{16+18})

However, with increasing depth, *Ra/p* for C_{16} and C_{18} increased to ca. 0.3 (Fig. III.5), much higher than those for C_{14}, C_{15} and C_{17} (Fig. III.5). The higher values of the relatively generic C_{16} and C_{18} may be a mixed signal derived from heterotrophic bacteria and a smaller admixture from autotrophs. In particular, *Ra/p* for $C_{18:1\omega9}$ was highest and > 0.3 at 7-22 cm (Fig. III.3C and 5), indicative of a notable admixture produced by autotrophic bacteria. $C_{18:1\omega9}$ is a major FA of the cell membrane of *Gammaproteobacteria*, particularly the genus *Psychrobacter* (> 60%; Freese et al., 2008; Baik et al., 2010; Matsuyama et al., 2015), which fixes IC in combination with sulfur oxidation (Lenk et al., 2011; Boschker et al., 2014; Vasquez-Cardenas et al., 2015; Dyksma et al., 2016). Although it seems that O_2 is required for sulfur oxidation by *Gammaproteobacteria* (Vasquez-Cardenas et al., 2015; Dyksma et al., 2016), their presence and high activity in anoxic surface and even deep subseafloor sediments (Vasquez-Cardenas et al., 2015; Dyksma et al., 2016) may indicate that they can also use other electron acceptors.

III.4. Conclusions

The activity of the bacterial community in the sandy sediment was quantitatively estimated via ^{13}C-bicarbonate and D_2O incorporation rate into microbial FAs. The turnover time of FAs in these permeable sandy intertidal sediments ranged on the scale of decades. The dark IC fixation during mineralization of OM plays only a minor role in the biogeochemical carbon cycle at our study site, where it appears to be predominantly related to CO_2 uptake during heterotrophic metabolism. Despite very low concentration of particulate OC, the sandy intertidal sediment hosts a relatively active community that contributes substantially to the sedimentary OC pool.

Acknowledgements

We thank M. Elvert, X. Prieto Mollar and J. Wendt for isotope measurement support. We also thank M. Könneke, R. Adhikari, F. Schmidt and N. Goldenstein for collecting samples. The study was funded by the ERC Grant Project No. 247153 (DARCLIFE; PI, K.-U.H.). W. Wu was funded by a scholarship from the China Scholarship Council (CSC). Further support was from the Bremen International Graduate School for Marine Sciences (GLOMAR) funded by the German Research Foundation (DFG). We thank J. Maxwell for constructive comments and suggestions.

Chapter IV

Microbial activity in marine surface sediment controlled by the proportion of terrestrial organic matter

Weichao Wu, Travis B. Meador, Julius Lipp, Marcus Elvert, Verena B. Heuer, Kai-Uwe Hinrichs

Organic Geochemistry Group, MARUM-Center for Marine Environmental Sciences & Department of Geosciences, University of Bremen, 28359 Bremen, Germany

* Corresponding author: wwu@marum.de

(***In preparation for Geochimica et Cosmochimica Acta***)

Abstract

In marine sediments, microbial life is widespread and largely depends on the availability of organic substrates and electron acceptors. While the redox reactions associated with the remineralization of organic matter have been studied in great detail, only little is known about the microbial utilization of organic substrates and inorganic carbon (IC) for biomass production. In particular potential relations between organic matter quality (e.g., terrestrial vs marine sources) and production rates of membrane lipids remain to be explored. To better understand this relationship, we quantitatively assessed microbial production of membrane lipids and the dominant metabolisms in surface sediments (0-6 cm) collected along a transect of four sites off the Rhône delta in the Gulf of Lions (North Western Mediterranean Sea), which receives various amounts of terrestrial organic matter from the River Rhône. The sediment samples were amended with D_2O and ^{13}C-bicarbonate (^{13}C-IC) containing artificial seawater, incubated for 50 days under sulfate-reducing (SR) conditions to stimulate bacteria, and subsequently for another 50 days under H_2/CO_2 atmosphere to promote archaea. Independent of SR or H_2/CO_2 conditions, the incorporation rates of D_2O and ^{13}C-IC into bacterial fatty acids (FAs) were faster than that into intact polar archaeal di- and tetraether lipid-derived hydrocarbons, which suggests that the bacterial activity was higher than the archaeal community. Under in situ SR conditions, the turnover times of the bacterial FAs were significantly shorter (7.5–21.3 yr with avg. 12.7 yr) than those of archaeal lipids (88–136 yr with avg. 110 yr). Furthermore, bacterial lipid production decreased with increasing distance from the river mouth from 3.0 μg g_{dw}^{-1} yr^{-1} in the prodelta area to 0.8 μg g_{dw}^{-1} yr^{-1} 11.7 km off the river mouth, but it increased again to 2.3 μg lipids g_{dw}^{-1} yr^{-1} 29.7 km off the river mouth, where organic matter derives mainly from marine sources. The assimilation of ^{13}C-IC into both bacterial FAs and TOC under in situ SR conditions indicates substantial assimilation of IC not only into bacterial biomass but also into the sedimentary OM pool. The average ratio of bacterial IC assimilation to lipid production is below 0.3 and points to heterotrophic bacteria carrying out dark IC fixation. Our findings suggest that dark IC fixation by benthic bacteria may attenuate the emission of IC from organic matter degradation in anaerobic marine sediments.

Key words: lipid production, terrigenous organic matter, stable isotope probing, bioavailability of OM.

IV.1. Introduction

Microbial-driven organic matter (OM) degradation (e.g., aerobic respiration, sulfate reduction and methanogenesis) is a keystone for benthic microorganisms in marine sediments, and plays an important role in the biogeochemical carbon cycle in marine sediments (Jørgensen, 1982; Canfield, 1989; Parkes et al., 2014). Microbial metabolic activity in marine sediments is generally controlled by bioavailability of OM (Koho et al., 2013) as well as by the availability of electron acceptors (e.g., O_2, Fe^{3+} and SO_4^{2-}; Froelich et al., 1979). Sulfate reduction and methanogenesis are two major terminal steps in the degradation of OM in anoxic marine sediment, and the former typically controls the early diagenesis of OM in surface marine sediment (Jørgensen, 1982; Canfield, 1989).

River-dominated ocean margins as a convergence area linking land and sea provide a favorable environment for benthic microorganisms, as they receive large amounts of terrestrial OM and sustain high marine primary production (Hedges et al., 1997; Bianchi, 2011). Sedimentary OM contains both autochthonous marine and allochthonous terrigenous origins. The terrestrially-derived OM is predominated by highly degraded soil OM (Bianchi, 2011), and it is generally thought to be more recalcitrant to degradation than marine plankton-derived OM (Hedges et al., 1997). Prior to its settling on the seafloor, particulate OM has been experiencing aerobic mineralization in the water column and at the sediment/water interface as well as flocculation, sedimentation and resuspension (Pruski et al., 2015). The aerobic OM mineralization can be characterized by the in situ oxygen uptake in the upper several millimeters of sediment (D'Hondt et al., 2004; Lansard et al., 2008; 2009). Below the oxic surface layer, the further anaerobic degradation of sedimentary OM was facilitated by sulfate reducing bacteria and methanogenic archaea, which can contribute > 30% of global OM mineralization in marine sediment (Jørgensen 1982; Bowles et al., 2014). Therefore, the activity of benthic microorganisms is generally constrained by the investigation of electron acceptor reduction rates (e.g., O_2, Fe^{3+} and SO_4^{2-}; Jørgensen, 1978; D'Hondt et al., 2004) or terminal metabolic products (e.g., CO_2, NH_4^+ and CH_4; Ferry and Lessner, 2008). However, these methods can only reveal the rates of bulk carbon oxidation based on stoichiometry (D'Hondt et al., 2004; Bowles et al., 2014) and do not provide insights into the manifold potential ways of carbon utilization by benthic microbial communities. Stable isotope probing (SIP) targeted with microbial components (e.g., nucleic acids, proteins and lipids) is a widely used method to track microbial activity, composition and metabolism in environmental settings (Kreuzer-Martin; 2007; Wegener et al., 2012; 2016; Jehmlich et al., 2016). Particularly, a recently developed D_2O labelling method can trace total microbial activity without distortion of

in situ nutrient conditions (Wegener et al., 2012; 2016), and even reveal the microbial metabolism when coupled with ^{13}C-inorganic carbon labelling (Wegener et al., 2012; Kellermann et al., 2012).

The Rhône River as the major river flowing directly to the Mediterranean Sea contributes 80% of the terrestrially-derived sediment into the Gulf of Lions (Ludwig et al., 2003), and is of crucial importance in the carbon cycle in the Gulf of Lions and even the entire Mediterranean Sea. The Rhône prodelta provides a natural platform to study the fate of terrestrial OM in marine sediments and the physical and biogeochemical aspects of OM mineralization rate. Most of the riverine materials (~80%) are settled in the vicinity of the river mouth (Lansard et al., 2008; 2009; Cathlot et al., 2010). The bulk- (e.g., total organic carbon and total nitrogen) and molecular-level (e.g., lignin-phenols, *n*-alkanes and fatty acids) analyses of particulate and sedimentary OM as well as their stable and radio-carbon isotopic compositions reveal that terrestrial vascular C3 plant detritus predominates in the composition of sedimentary OM in the prodelta and the age of OM increases on the adjacent shelf (Harmelin-Vivien et al., 2008; 2010; Cathalot et al., 2013; Pruski et al., 2015). The analyses of amino acids and pigments, which is used to characterize the degradation or bioavailability of OM (Bourgeois et al., 2011; Pastor et al., 2011), indicate that the prodelta contains more labile OM than the adjacent shelf. Concurrently, OM mineralization rates (microbial activity) are highest at the river mouth and decrease with increasing distance from river mouth, as seen in in-situ oxygen uptake rates (Lansard et al., 2008; 2009; Cathalot et al., 2010). The oxygen penetration depth is generally restricted to a few millimeters (Lansard et al., 2008; 2009), and anaerobic processes (e.g., sulfate reduction) contribute to most of the total OM mineralization in surface sediment (Pastor et al., 2011).

The different OM sources and qualities (i.e., composition and bioavailability) potentially affect the composition of microbial communities in marine sediments (Heuer et al., 2014). Thus, they could also influence the residing microbial activity and further OM mineralization. However, the effect of OM source and quantity on microbial activity is poorly constrained. To better understand this effect on microbial activity, this study aims to quantitatively investigate the microbial activity in the context of different sedimentary OM sources.and compare the difference of C utilization when external energy was provided. Surface sediments (0-6 cm) were sampled at four sites (GeoB17305 - 17308) along a southwestward transect from river outlet to continental shelf during RV Poseidon cruise POS450 in April 2013 (Heuer et al., 2014). Site GeoB17306 and 17307 are the terrestrial end members in the prodelta area, Site GeoB17305 represents the marine end member in the distal domain of the shelf, and Site 17308 was located half-way between the two end members. The sediments were incubated

under anaerobic conditions with D_2O and ^{13}C-bicarbonate to track bacterial and archaeal lipid production. In order to support sulfate reducing bacteria, sulfate was added and sulfate reducing (SR) conditions were maintained for 50 days. Subsequently, H_2 was provided for 50 days to promote archaeal activity.

IV.2. Samples and Methods

IV.2.1. Incubation preparation

Four live surface sediments (0-6 cm) were collected during RV Poseidon cruise POS450 along a transect of four sites (GeoB17305 – 17308; Table IV.1) off the Rhône River, Gulf of Lions, Northwestern Mediterranean Sea, in April 2013. The samples were stored under nitrogen atmosphere in Schott glass bottles at + 4°C until incubation experiments were conducted in 2015. The sediment slurries were prepared in an anoxic chamber with N_2/H_2 (99:1) by mixing sediment and the artificial seawater (ASW; 1: 1) with replete sulfate (~30 mM) modified from Xie et al. (2013). The ASW composition (g/L) was: NaCl, 26; $MgCl_2.6H_2O$, 5.0; $MgSO_4$, 3.6; $CaCl_2.2H_2O$, 1.5; KBr, 0.1; KH_2PO_4, 0.014; NH_4Cl, 0.053; $NaHCO_3$, 0.84; $Na_2S.9H_2O$, 0.24. The slurries were dispensed into three identical Schott glass bottles with two as parallel samples and one as killed control, and the headspace was subsequently purged with N_2. Afterwards, stock solutions of $NaH^{13}CO_3$ in water (98atom% ^{13}C, Sigma-Aldrich) and D_2O (99.9 atom% D, Sigma-Aldrich) were added to the slurries, yielding final isotopic enrichments of about 5% ^{13}C-$NaHCO_3$ and 1% D_2O relative to non-labelled $NaHCO_3$ and natural water in the slurries. Finally, the fractional abundance of ^{13}C of DIC and D of water in the slurries was determined as described below (see *Section IV.2.2*). The killed controls were prepared by addition of 5% $ZnCl_2$ (w/w, final concentration) and were incubated under the same conditions as normal incubation. After incubation at 12°C in dark for 50 days (t_{50}), about half of the slurry in each bottle was harvested with sterile syringes in the glovebox, and the headspace of residual samples was then refilled with 1 bar of H_2/CO_2 (80:20) followed by incubation for an additional 50 days (t_{100}). During the incubation, the concentration of methane in the headspace of the incubation vials was monitored regularly. Finally, the slurries were centrifuged at 3000rpm for 10 min, the supernatant were filtered through 0.2 µm nylon filters, and the harvested water and sediment samples were then stored at -20°C until further treatment.

Table IV.1. Sample information for incubation.

Cruise	Site	Sediment depth (cm)	Position	Water Depth (m)	Setting	Distance to river mouth (km)*	TOC (wt%)	δ^{13}C-TOC (‰;VPDB)
POS450	GeoB17306	0-6	43°18'57.60"N /4°52'10.20"E	30	prodelta	2.8	1.50	-26.2
POS450	GeoB17307	0-6	43°18'14.40"N /4°51'31.80"E	52	prodelta	3.5	1.13	-26.2
POS450	GeoB17308	0-6	43°16'12.00"N /4°43'47.40"E	62	transition	11.7	0.95	-24.8
POS450	GeoB17305	0-6	43°13'48.00"N /4°30'36.60"E	61	shelf	29.7	0.78	-23.9

*calculated using http://www.movable-type.co.uk/scripts/latlong.html

IV.2.2. Biogeochemical analyses

CH_4

Concentrations of headspace CH_4 were analysed by gas chromatography with flame ionization detector (GC-FID; Thermo Finnigan Trace GC). Prior to sampling, the stopper was sterilized via ethanol burning method. Afterwards, 100 µL gas was taken with gas-tight syringe, and then directly injected on an Alltech Heliflex AT-Q column (30 m×0.32 mm) with 1.0 mL min^{-1} of helium as carrier gas at 60°C. The injector was operated with 1:10 split ratio, and the oven temperature was held constant at 60°C. Since methane concentrations were initially below the detection limit of isotopic analyses, only samples incubated under H_2/CO_2 at t_{100} were sampled for δ^{13}C-CH_4 analyses. δ^{13}C-CH_4 was measured on a Thermo Finnigan Trace GC connected to a DELTA Plus XP isotope ratio mass spectrometer via GC combustion III interface (GC-C-IRMS). 500 µL gas sample from the headspace was injected on a Carboxen-1006 PLOT column (30 m×0.32 mm) with 1:3 split ratio. Helium was used as carrier gas with a flow rate of 3 mL min^{-1}. The temperature program was: 60°C (1min) increase to 240°C at 40°C/min and hold for 7 min.

Sulfate

For the measurement of sulfate concentrations, water samples were diluted 50 times with MilliQ water, filtered (0.2 µm nylon filters), and analyzed on an ion chromatography with conductivity detector after chemical suppression (Metrohm 861 Advanced Compact IC, Metrohm) as described previously (Goldhammer et al., 2011).

Acetate

Concentrations of acetate and δ^{13}C-acetate in the slurries were determined by isotope-ratio-monitoring liquid chromatograph/mass spectrometry (irm-LC/MS) using a Thermo Finnigan Surveyor HPLC combined with DELTA Plus XP isotope ratio spectrometry via LC Isolink interface (Krummen et al., 2004; Heuer et al., 2006; 2009). 100 µL water sample was injected on a VA 200/7.8 Nucleogel Sugar 810-H column (300 mm × 7.8 mm; Macherey-Nagel) with a guard column (CC30/4 Nucleogel Sugar 810H) at room temperature. The eluent was 5 mM phosphoric acids in water with a flow rate of 300 µL min^{-1}, and the online wet chemical oxidation of eluting compounds to CO_2 was performed with sodium peroxodisulfate at 100°C. Acetate was quantified according to the linear correlation between the signal area of m/z 44 and the amount of external acetate standard. Standard deviation for δ^{13}C-acetate analysis was < 0.6‰, and the detection limit for quantitative analysis of acetate was 5 µM.

δD-water analysis

The *δD* values of water at t_0 was analyzed by Cavity Ring Down Spectrometer (Picarro L-2130i, USA). Because 1% D_2O (δD = ~63,850‰, VSMOW) wasn't suitable for direct measurement and would bring about a severe memory effect, the filtered water samples were diluted 200 times with MilliQ water of δD= -48.9‰. To test the precision of positive δD-water, the external calibration standard water ranging from +10‰ to +1000‰ was employed by mixing MilliQ water with D_2O volumetrically. The analyzed results of external water samples were close to the theoretical prediction and showed a good precision (root-mean-square error = 1.8‰) and show a good relationship (R^2 = 0.999). Afterwards, the δD values of the undiluted slurry water were calculated based on mass-balance considerations.

δ^{13}C-DIC analysis

δ^{13}C-dissolved inorganic carbon (DIC) in slurry water was measured on a Thermo Finnigan Trace GC connected to a DELTA Plus XP isotope ratio mass spectrometer via GC combustion III interface. The instrument and conditions were the same as those used for δ^{13}C-CH_4 measurement. Prior to analysis, 1 mL water samples were acidified with 100 µL phosphoric acid (85%, H_3PO_4) overnight at room temperature in Exetainer vials (12 mL), which were fluxed with CO_2-free synthetic air until no CO_2, and the purity was checked by Thermo Scientific Delta Ray IRIS with URI connect. Then, 100 µL headspace gas was introduced to GC-C-IRMS and separated on a Carboxen-1006 PLOT column (30 m × 0.32 mm) with 1:3 split ratio.

TOC analysis

Contents and δ^{13}C values of total organic carbon (TOC) were determined on a Flash 2000 elemental analyzer coupled with DELTA V Plus IRMS via a ConFlow II interface (Thermo

Scientific). Prior to TOC analysis, IC was removed from the sediment samples by acidification. The samples were allowed to react overnight with 10% in a glass vial and subsequently washed with MilliQ water until pH 5. The TOC quantification was based on the calibration of the instrument with an internal laboratory standard (TOC = 4.6 wt%, δ^{13}C-TOC = -24.1‰), sediments from the White Oak River (NC, USA). Each sample was measured at least in duplicate.

IV.2.3. Lipids and isotope analyses

Lipids were extracted from dried sediments, which were amended with 2-methyloctadecanoic acid as internal standard, by modified Bligh and Dyer protocol (Sturt et al., 2014). Briefly, the samples were extracted ultrasonically twice for 15 mins with 2:1:0.8 of methanol/DCM/phosphate buffer (pH 7.4), followed by two extractions with 2:1:0.8 of methanol/DCM/trichloroacetic acid (TCA, pH 2.0). The organic fractions were combined, and then DCM and water were added to adjust the ratio of methanol/DCM/water to 1:1:0.9. The bottom organic phase was collected, and the residual water phase was extracted two times with DCM. The combined organic extracts were washed three times with MilliQ water to remove TCA. The total lipid extracts (TLEs) were dried under N_2 and stored at -20°C until further processing.

An aliquot of TLEs (30%) was used for fatty acid methyl ester (FAME) preparation via saponification and esterification (Elvert et al., 2003). The TLEs were saponified with 2 mL of 6% KOH in methanol at 80°C for 3h. After cooling down, 2 mL of 0.05M KCl solution was added, and the neutral fraction was extracted three times with 4 mL of hexane. The residual basic solution was adjusted to pH 1 with 25% HCl, and the fatty acid fraction was extracted at least 3 times with 4 mL of hexane. The fatty acid fraction was dried under N_2, followed by esterification reaction with 500 µL of 20% BF_3 in methanol at 80°C for 1h. After cooling down, 500 µL of water was added, and then the solution was extracted 4 times with 1 mL of hexane. The FAME fraction was dried under N_2 and stored at -20°C for further processing. The position of double bonds of FAMEs was determined as the dimethyl disulfide (DMDS) adduction (Nichols et al., 1986).

In our study, only intact archaeal lipids were used for carbon and hydrogen analysis. They were purified on preparative HPLC for further quantification, and carbon and hydrogen isotope analyses. Briefly, an aliquot of TLEs (60%) was separated on an Inertsil Diol column (150×10 mm, 5µm particle size; GL Sciences Inc., Tokyo, Japan) on an Agilent 1200 HPLC system connected to a fraction collector. The eluents A and B were n-hexane/isopropanol (85:15, v/v)

and isopropanol/water (90:10), respectively. The eluent flow rate was 3 mL min^{-1} and the gradient program was: 0%B to 10%B at 5 min, and then to 100%B at 6 min, and held for 10 min. Afterwards, the HPLC system was equilibrated with 100% A for 10 min prior to the next injection. The core and intact lipid fractions were collected in the windows 0.0-5.0 min and 5.1-15.0 min, respectively. The carryover rate of core lipids into intact lipids was checked on UPLC-qTOF-MS as described in Zhu et al. (2013), and the carryover was < 5% (Elling et al., 2014). Intact archaeal lipids were liberated to the hydrocarbon cores via BBr_3 ether-cleavage and superhydride (LiEt3BH, Aldrich) reduction treatment (Jahn et al., 2004; Liu et al., 2012.)

FAMEs and intact archaeal lipid-derived hydrocarbons (ALDs) were quantified on a Thermo Finnigan Trace GC connected to FID by injection on a Rix-5ms column (30 m × 0.25 mm × 0.25 μm; Restek GmbH, Germany) with a constant helium flow of 1 mL min^{-1}. The injector temperature was 310°C, and the oven temperature increased from 60°C to 150°C at 10°C min^{-1}, and then ramped to 320°C at 4°C min^{-1} and held for another 22.5 min. FAMEs were quantified with the internal standard 2-methyloctadecanoic acid methyl ester and intact archaeal lipid derivatives were based on the co-injected C_{40} *n*-alkane.

The C and H isotopic compositions of lipids were analyzed on a Thermo Finnigan Trace GC connected to a DELTA Plus XP isotope ratio mass spectrometer via GC combustion III interface. The lipids were oxidized to CO_2 via CuO/NiO column at 940°C for $\delta^{13}C$ analysis, and pyrolyzed to H_2 via High Temperature Conversion (HTC) column at 1420°C for δD analysis. The oven program and GC column was identical to the one used for GC-FID analysis. The C and H isotopic compositions of lipids were determined by ISODAT NT 3.0 software, and reported in standard δ notion. The stability and precision were checked with mixed *n*-alkane standards (from Indiana University Biogeochemical Laboratory) every day with mean deviation of $\delta^{13}C$ and δD values of <1 and 5‰, respectively.

IV.2.4. Calculation of microbial activity

The estimates for microbial activity are based on the D and ^{13}C incorporation rates into lipids (Wegener et al., 2012) including lipid production rate ($prod_{lipid}$; μg g_{dw}^{-1} yr^{-1}), and assimilation rates of inorganic carbon into both individual lipids ($assim_{IC\text{-}lipid}$; μg g_{dw}^{-1} yr^{-1}) and TOC pool ($assim_{IC\text{-}TOC}$; μg g_{dw}^{-1} yr^{-1}):

$$prod_{lipid} = conc_{lipid} \times \frac{\Delta\, {}^{2}F_{lipid}}{{}^{2}F_{med} \times t} \times \frac{1}{a_w} \quad (1)$$

$$assim_{IC\text{-}lipid} = conc_{lipid} \times \frac{\Delta^{13}F_{lipid}}{^{13}F_{med} \times t} \quad (2)$$

$$assim_{IC\text{-}TOC} = TOC \times \frac{\Delta F^{13}C_{TOC}}{F^{13}C_{med} \times t} \quad (3)$$

^{2}F and ^{13}F refer the fractional abundances of D and ^{13}C in lipids or medium. They are obtained from the measured isotope ratios according to $F = R/(1+R)$ and $R = (\delta/1000+1) \times R_{standard}$, where $R_{standard}$ is 0.0001575 (VMSOW) and 0.011180 (VDPB) for H and C isotope analysis, respectively. $Conc_{lipid}$ is the concentration of microbial lipids at harvest without considering the change of lipid concentration during incubation. Due to no significant ^{13}C and D incorporation into polyunsaturated fatty acids (e.g., $C_{20:4}$ and $C_{20:5}$) and long-chain FAs (e.g., C > 20), all common bacterial fatty acids (C_{14} to C_{18}) were used for calculating bacterial activity rather than specific fatty acids. For archaeal lipids, the lipids used for estimation included archaeol or hydroxyarchaeol-derived phytane, and tetraether-derived biphytanes with 0-3 cycloalkyl rings. $\Delta^{2}F_{lipid}$, $\Delta^{13}F_{lipid}$ and $\Delta^{13}F_{TOC}$ signify the change in the fractional D abundance in lipids, and ^{13}C abundance in lipids and TOC after incubation, respectively. Since the slurries were firstly incubated under sulfate-reducing (SR) condition for 50 days, followed by H_2/CO_2 spiking and incubation for additional 50 days, microbial activity for two conditions would be estimated independently, i.e., $\Delta F_1 = F_{t_{50}} - F_{t_0}$ and $\Delta F_2 = F_{t_{100}} - F_{t_{50}}$. t is incubation time, i.e., 50 days. Considering the change in $\delta^{13}C$-DIC during incubation, $^{13}F_{med}$ for growth on SR condition is the ^{13}C abundance of DIC in the slurries at t_0 assuming that $\delta^{13}C$-DIC didn't change. For growth on H_2/CO_2, $^{13}F_{med}$ in the slurries at t_{100} is used for the calculation due to the dilution of non-labelled CO_2 in the headspace. Notably, the lipid carbon amount (μg C g_{dw}^{-1}) is assumed to be equal to its total lipid amount (μg lipids g_{dw}^{-1}) in order to further compare the ratio of $assim_{IC}$ to $prod_{lipid}$ (*Ra/p*) because *Ra/p* is used to distinguish microbial metabolisms, i.e., < 0.3 and ~1 for heterotrophy and autotrophy, respectively (cf. Wegener et al., 2012).

$$R_{a/p} = \frac{assim_{IC\text{-}lipid}}{prod_{lipid}} \quad (4)$$

Due to the large H isotope fractionation effect between lipid and medium water, a factor a_w, which is the water-hydrogen assimilation factor into microbial lipids (Kopf et al., 2015; 2016; Wegener et al., 2016), is used to calibrate the lipid production. In pure cultivation, a_w is obtained from the regression of lipid D composition on water D when grown on water with different D (Sessions and Hayes, 2005; Zhang et al., 2009a). Here, α_w = 0.77 from the incubation of *Desulfosarcina variabilis* (Wegener et al., 2012) is applied for the estimation of bacterial lipid production in marine sediment, and α_w = 0.33 from the incubation of

Methanosarcina barkeri (*M. barkeri;* Chapter II) for that of archaeal lipid production in marine sediment. We don't take into consideration diverse α_w because α_w is diverse among different species (Zhang et al., 2009a), and moreover it is variable for growth conditions (*Chapter II*). In addition, our knowledge of α_w values for archaeal lipids is limited, and we have to note that archaeal lipid production might be overestimated because a relatively large $1/a_w$ is used for archaea compared to bacteria.

Turnover times of microbial lipids (τ_{lipid}; year or day) are also estimated to directly compare the heterogeneity of microbial communities. In most cases, the newly synthesized microbial biomass reflects the isotopic composition of the isotopic tracer, and the lipid production rate is correlated with the apparent biomass growth rate without considering the maintenance rate (Kopf et al., 2016). According to this rule, we provide the below equation to estimate the turnover time of microbial lipids (Eq. 4; full derivation in Chapter I.4)

$$\tau_{lipid} = -t \cdot [\ln(1-\frac{\Delta\ ^2F_{lipid}}{a_w \cdot\ ^2F_{w_{med}}})]^{-1} \quad (5)$$

IV.2.5. Principal component analysis (PCA)

The parameters of $assim_{IC}$ and $prod_{lipid}$ were performed via PCA by CANOCO software (Canonical Community Ordination; version 5; Ter Braak and Šmilauer, 2012) to investigate the potential dominant microbial community in our incubation experiment. Because only microbial FAs obtained high ^{13}C and D label, the data of $assim_{IC}$ and $prod_{lipid}$ for individual microbial fatty acids other than archaeal lipids was used for analysis. Prior to analysis, $assim_{IC}$ and $prod_{lipid}$ for fatty acids in each incubation sample were first normalized to total $assim_{IC}$ and $prod_{lipid}$, and then was transformed with log (x+1). The relative abundance of FAs from reference bacteria were also utilized in PCA using the same log (x+1) transformation. The reference bacteria include: γ-proteobacteria *Beggiatoa*, *Pseudomonas* sp. *Psychrobacter* sp. and *Shewanella sp*. (Zhang et al., 2005; Freese et al., 2008); δ-proteobacteria *Desulfobulbus sp*. grown on H_2 or propionate (Desu-H_2 and Desu-P; Taylor and Parkes, 1983), *Desulfobacter* sp. grown on acetate (Desu-ace; Taylor and Parkes, 1983); ε-protebacteria *Arcobacter sp.* (Freese et al., 2008). For detailed values see Table S.IV.5.

IV.3. Results

IV.3.1. Geochemical investigation

During the 50-day incubation replete with sulfate (~30 mM; Fig. IV.1), no methane was detected and sulfate concentration did not decrease significantly in the four samples (Fig. IV.1). After the addition of H_2/CO_2 at t_{50}, sulfate concentrations rapidly decreased to 0.1~3.4 mM (Fig. IV.1) at t_{98} and methane concentrations noticeably increased in the headspace of incubation bottles, particularly in GeoB17306 (1375 ppm at t_{98}) and GeoB17307 (295 ppm at t_{98}; Fig. IV.1). At t_{98}, a positive δ^{13}C-methane value was observed, particularly in GeoB17306 (345±39‰) and 17307 (416±82‰) (Table S.IV.1). Distinctly ^{13}C-enriched acetate was detected at t_{98} with δ^{13}C values ranging from +366 to +483‰ (Table S.IV.1). The corresponding acetate accumulation varied distinctly along the transect of sites, with concentrations being 36.0±4.1, 16.4±2.7, 1.5±0.0, 9.1±0.4 mM at sites GeoB17306, 17307, 17308 and 17305, respectively.

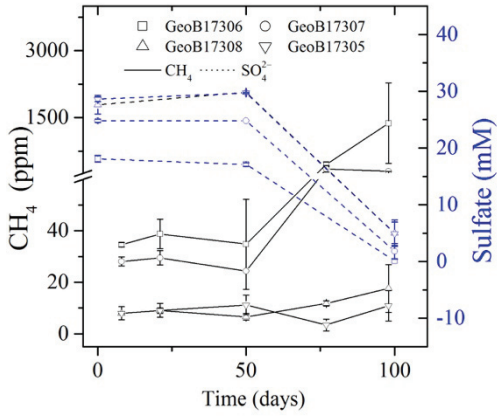

Fig. IV.1. Concentrations of methane in headspace and sulfate in the slurries during incubation. After 50 days, the headspace was changed from N_2 to 1 bar of H_2/CO_2 and incubation continued for additional 50 days. The error bar was calculated from the standard deviation of duplicate samples, and the large deviation for methane concentration might be due to different methane production rate between two samples.

IV.3.2. The abundance and isotope change of microbial lipids

Microbial FAs were dominated by C16 and C18 chains (>60%, Fig. IV.2). In the original samples (t_0), the concentration of total microbial FAs (TFAs) decreased with increasing distance from the river mouth (from 32.9 μg g_{dw}^{-1} to 14.2 μg g_{dw}^{-1}; Table S.IV.1). After incubation under SR conditions, the concentrations of TFAs didn't change significantly relative to those at t_0 (i.e., 5%). However, under H_2/CO_2 atmosphere, the concentrations of TFAs in sediments increased significantly by an average of 26% compared with those at t_{50}; this increase was driven by changes in unsaturated fatty acids, e.g., C15:1, C16:1ω7, and C17:1ω6 (Fig. IV.2). Compared to microbial FAs, the total amount of intact archaeal lipid derivatives (ALDs, e.g., phytane, biphytanes with 0-3 rings) was much lower (0.39, 0.32, 0.37

and 0.40 µg g^{-1}_{dw} for GeoB17306, 17307, 17308 and 17305, respectively; Fig. IV.2), and did not significantly change during incubation.

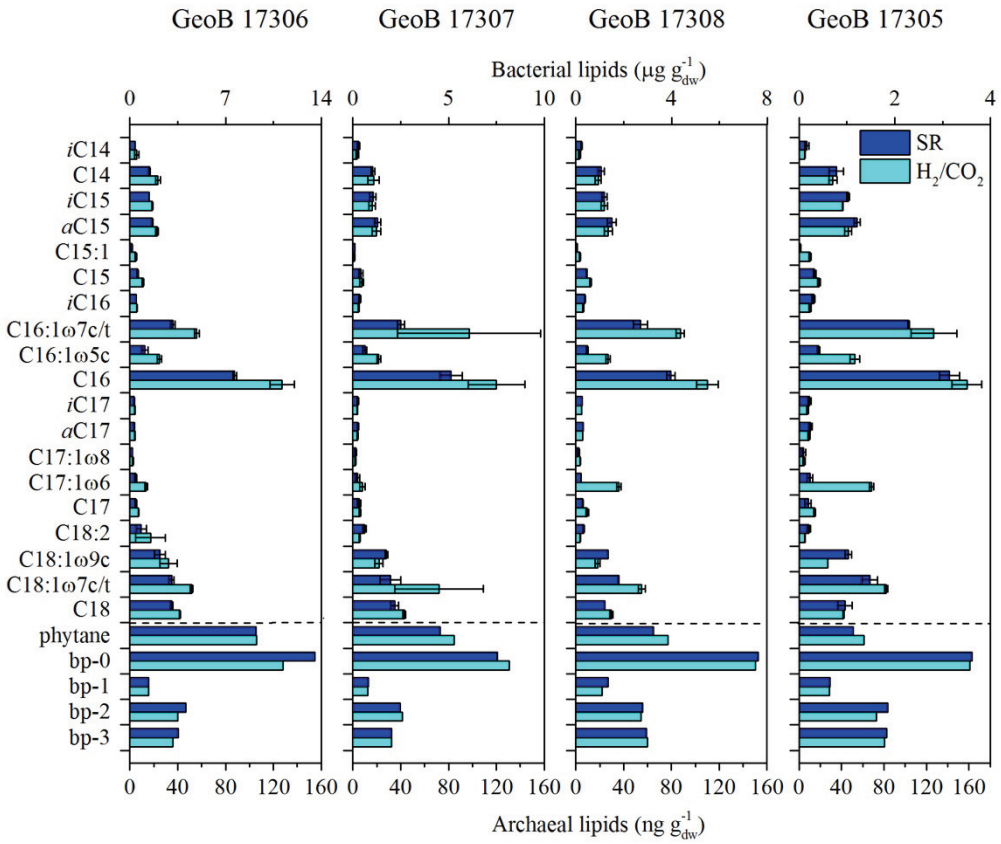

Fig. IV.2. Concentrations of microbial FAs (C14-C18; µg g_{dw}^{-1}; upper dash) and archaeal lipid derivatives (ALDs) including phytane and biphytanes (bp) with 0-3 rings (ng g_{dw}^{-1}; below dash) during incubation under sulfate (t_{50}) and H_2/CO_2 (t_{98}). The sediments (GeoB17306, 17307, 17308 and 17305) were incubated under SR conditions for 50 days. Afterwards, the headspace was changed from N_2 to 1 bar of H_2/CO_2 and incubation continued for another 50 days.

IV.3.3. Change in C and H isotopic compositions of microbial lipids

$\delta^{13}C$

The $\delta^{13}C$ values of FAs and ALDs in original samples show an increasing trend from prodelta (GeoB17306) to shelf sediment (GeoB17305; Table S.IV.2). For instance, the weighted average $\delta^{13}C$ of FAs shifted from -31.1‰ to -25.8‰; whereas $\delta^{13}C$-bp-0 presumably derived from GDGT-0 shifted from -28.6‰ to -24.9‰ (Table S.IV.2). In addition, ALDs were slightly enriched in ^{13}C compared to FAs (Table S.IV.2).

Independent of SR or H_2/CO_2 incubation conditions, the $\delta^{13}C$ and δD values of microbial FAs from all sites significantly increased during the incubation period (Fig. IV.3; Fig. IV.4); whereas

those of archaeal lipids increased significantly only under incubated H_2/CO_2 conditions (Fig. IV.3; Fig. IV.4). When incubated under SR conditions (δ^{13}C-DIC ≈ 5,700‰), the change in the weighted average δ^{13}C of bacterial lipids (expressed as $\Delta\delta^{13}C=\delta^{13}C_{t_{50}}-\delta^{13}C_{t_0}$) was +6.2‰, +12.8‰, +14.6‰ and +29.7‰ for GeoB17306, 17307, 17308 and 17305, respectively. After the addition of H_2/CO_2, the $\Delta\delta^{13}$C values of TFAs ($\Delta\delta^{13}C = \delta^{13}C_{t_{100}}-\delta^{13}C_{t_{50}}$) were much higher than those under SR conditions, i.e., $\Delta\delta^{13}$C = +43.9‰, +59.4‰, +98.1‰ and +75.3‰ for GeoB17306, 17307, 17308 and 17305, respectively. Compared to bacterial FAs, the δ^{13}C values of biphytanes did not significantly increase ($\Delta\delta^{13}C$ < +2‰; Fig. IV.3) under SR or H_2/CO_2 conditions. However, the δ^{13}C value of phytane increased significantly at GeoB17306 under H_2/CO_2 condition with a $\Delta\delta^{13}$C value of phytane of +7.4‰.

The δ^{13}C value of TOC increased under SR conditions (from $\Delta\delta^{13}$C-TOC +0.35‰ at GeoB17306 to +1.46‰ at GeoB17305) considering the analytical precision (0.2‰). In particular, it increased much higher when H_2/CO_2 was provided, and the $\Delta\delta^{13}$C-TOC values for GeoB17306, 17307, 17308 and 17305 were +2.93‰, +6.96‰, +5.57‰, and +5.00‰, respectively.

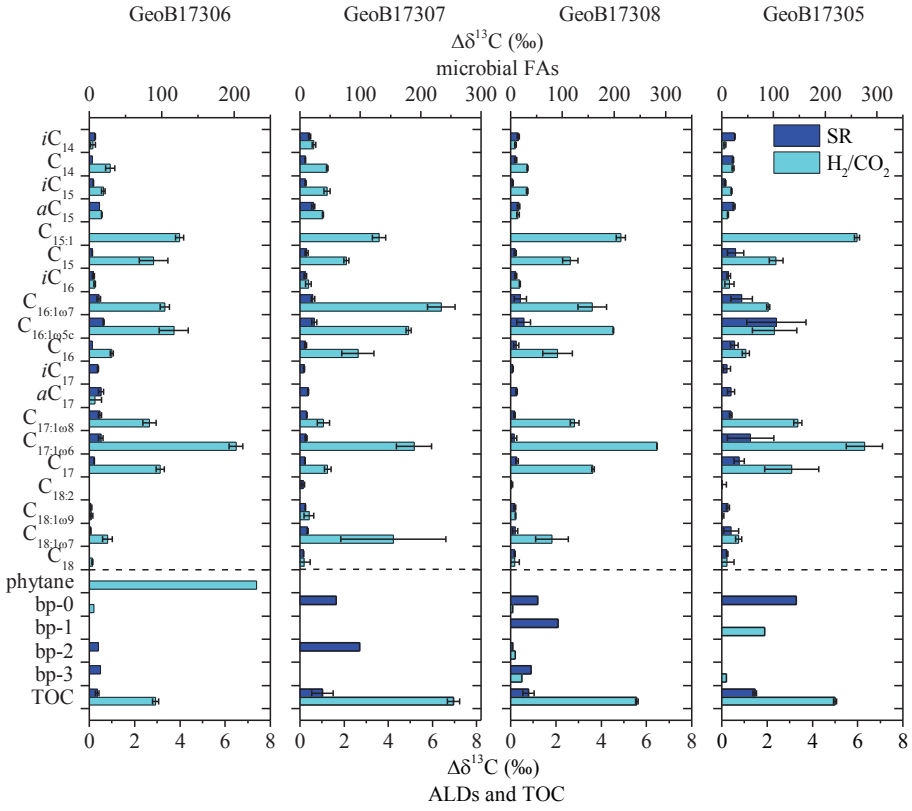

Fig. IV.3. The increase in δ^{13}C ($\Delta\delta^{13}$C; ‰, VPDB) of individual microbial FAs (above dashed line), intact polar archaeal lipids, and TOC (below dashed line) after incubation under two conditions. For SR conditions, $\Delta\delta^{13}C=\delta^{13}C_{t_{50}}-\delta^{13}C_{t_0}$, whereas $\Delta\delta^{13}C=\delta^{13}C_{t_{100}}-\delta^{13}C_{t_{50}}$ for H_2/CO_2 conditions.

δD

When incubated under SR conditions with ~1% D_2O (δD = 63,850‰), the change of weighted average δD of TFAs ($\Delta\delta D = \delta D_{t_{50}} - \delta D_{t_0}$) was +1150‰, +955‰, +520‰ and +1170‰ for GeoB17306, 17307, 17308 and 17305, respectively (Fig. IV.4; Table S.IV.3). After the addition of H_2/CO_2, the δD values of TFAs increased to much higher values with ΔδD (= $\delta D_{t_{100}} - \delta D_{t_{50}}$) of +8,120‰, 19,170‰, 12,120‰ and 5,600‰ for GeoB17306, 17307, 17308 and 17305, respectively (Fig. IV.4; Table S.IV.3). However, the ΔδD values of ALDs were much lower than those for microbial FAs when incubated under both conditions (Fig. IV.4). For example, when incubated under SR conditions, the ΔδD values of ALDs was less than +100‰ (Fig. IV.4). When incubated under H_2/CO_2 conditions, ΔδD-phytane was much higher (about +1200‰), but those of biphytanes were still less than +100‰ (Fig. IV.4).

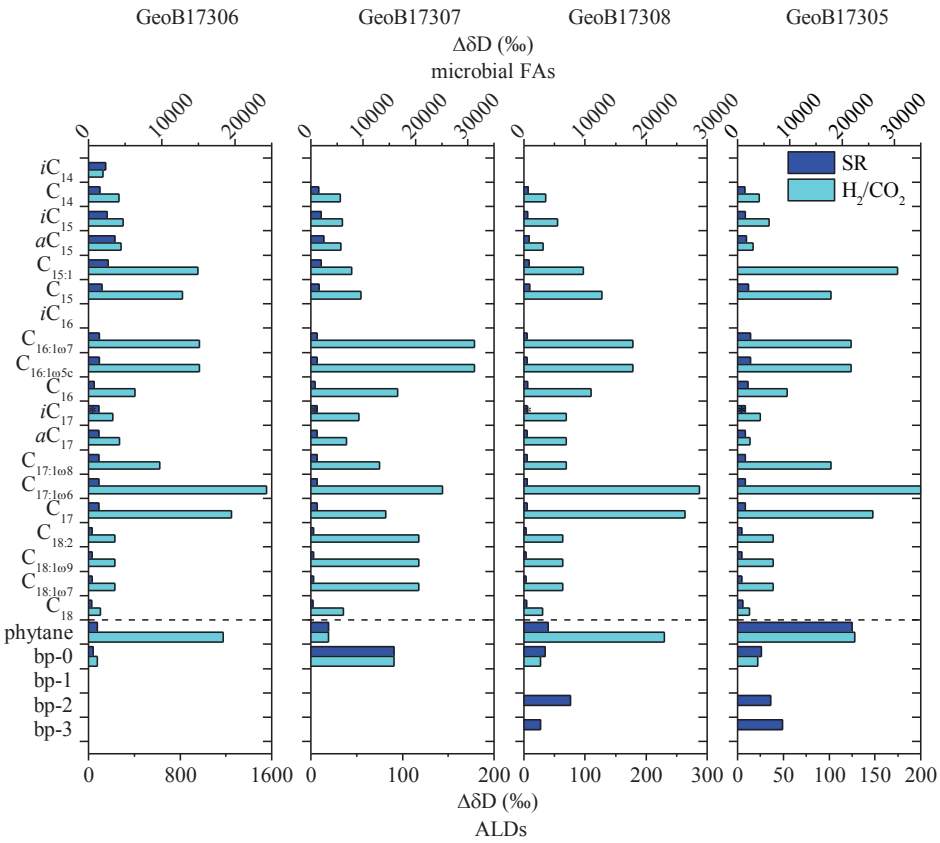

Fig. IV.4. Increase in δD (ΔδD; ‰, VMSOW) of microbial FAs (above dashed line), and ALDs (below dashed line) after incubation under two conditions (i.e., SR and H_2/CO_2). The calculation method is similar to that for $\delta^{13}C$ (see Fig. IV.3). Some individual fatty acids (e.g., C16:1ω7c/t and C16:1ω5c) share the same ΔδD values because their peaks were not separated well by chromatography, and therefore their peaks were integrated together, but δD is still shown separately for further comparison.

IV.3.4. Microbial lipid production rates

When surface sediments were incubated under in SR conditions, the total bacterial lipid production (bacterial $prod_{lipid}$) in the surface sediments decreased with increasing distance

from river mouth (3.0, 2.0, and 0.8 lipids g_{dw}^{-1} yr^{-1} for GeoB17306, 17307, 17308; Fig. IV.5), but increased again in the shelf area (2.3 µg lipids g_{dw}^{-1} yr^{-1} at GeoB17305; Table IV.1). Under H_2/CO_2 conditions, bacterial $prod_{lipid}$ increased by an order of magnitude in the river prodelta incubations (27.0, 63.8, 26.0 µg lipids g_{dw}^{-1} yr^{-1} for GeoB17306, 17307 and 17308, respectively) and up to 15.5 µg lipids g_{dw}^{-1} yr^{-1} for the shelf sediment (i.e., GeoB17305, Fig. IV.5). The *i*C15, *a*C15, C16:1ω7c/t and C16 FAs contributed more than 50% of the total bacterial $prod_{lipid}$ (Fig. IV.5) under SR conditions. In addition, both the production rate and the relative contribution of C17:1ω6, C18:1ω9 and C18:1ω7 FAs to total bacterial production significantly increased in H_2/CO_2 incubations, with C17:1ω6 accounting for ca. 20% of bacterial $prod_{lipid}$ for GeoB17308 (Fig. IV.5)

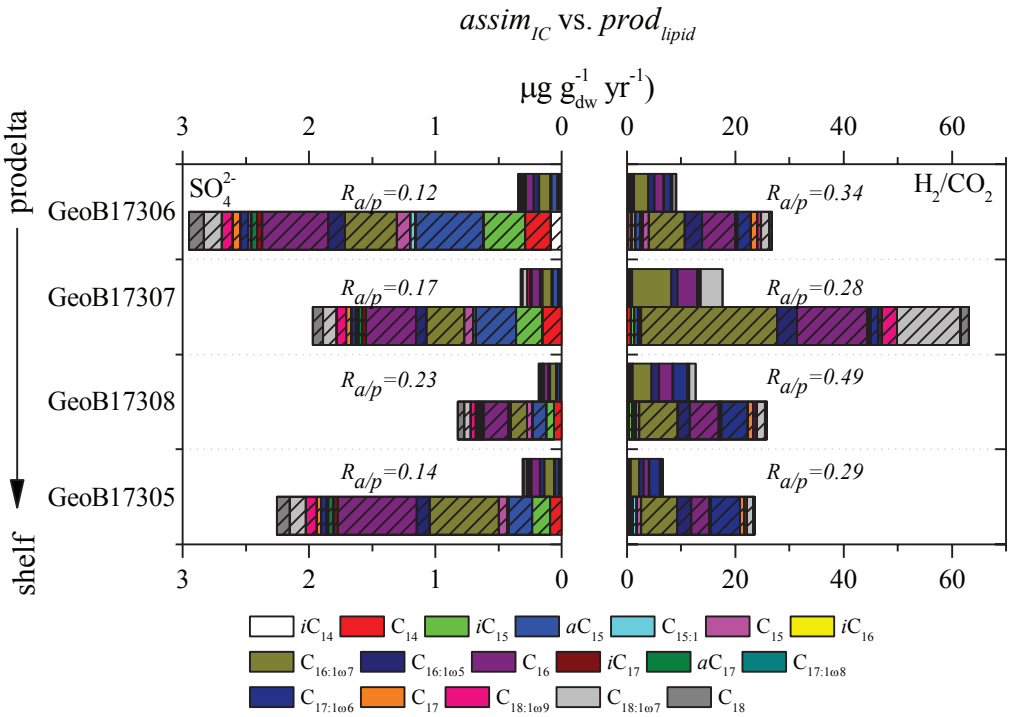

Fig. IV.5. Assimilation rates of IC ($assim_{IC}$; solid; µg C g_{dw}^{-1} yr^{-1}) into individual FAs and their lipid production rates ($prod_{lipid}$; striped; µg lipids g_{dw}^{-1} yr^{-1}) after incubation under SR conditions (left), and the following H_2/CO_2 conditions (right). $R_{a/p}$ refers the ratio of $assim_{IC}$ to $prod_{lipid}$, which is relevant to infer the dominant metabolism of microbial community (i.e., <0.3 and ~1 for heterotrophy and autotrophy, respectively; Wegener et al., 2012).

Archaeal $prod_{lipid}$ was much less (three orders of magnitude lower) than that of bacterial lipids when incubated under both conditions. When incubated under SR conditions, archaeal lipid production was 0.47, 2.87, 2.11 and 4.40 ng lipids g_{dw}^{-1} yr^{-1} for GeoB17306, 17307, 17308 and 17305, respectively. However, it is difficult to conclude that archaeal $prod_{lipid}$ increased with increasing distance from the river mouth because the δD signals for all polar archaeal lipid-derived biphytanes were below the detection limit (Table IV.2 and Table S.IV.3). When incubated under H_2/CO_2 conditions, archaeal lipid production only for GeoB17306 and 17307 sites significantly increased to 10.6 and 4.89 ng lipids g_{dw}^{-1} yr^{-1}, respectively, whereas it

decreased to 1.21 and 2.81 ng lipids g_{dw}^{-1} yr^{-1} for GeoB17308 and 17305, respectively. Phytane production accounted for the most of the archaeal *$prod_{lipid}$* (Table IV.2).

Table IV.2. *$Prod_{lipid}$* (ng lipids g_{dw}^{-1} yr^{-1}) and *$assim_{IC}$* (ng g_{dw}^{-1} yr^{-1}) of individual ALDs incubated under SR and H_2/CO_2 conditions A, B, C and D refer the sites GeoB17306, 17307, 17308 and 17305. (n.d.: not determined because of no significant increase in $\delta^{13}C$ and δD).

	$prod_{lipid}$								***$assim_{IC}$***							
	SR				**H_2/CO_2**				**SR**				**H_2/CO_2**			
	A	B	C	D	A	B	C	D	A	B	C	D	A	B	C	D
phytane	0.47	0.33	0.15	1.58	10.6	4.89	1.21	1.94	n.d.	n.d.	n.d.	n.d.	3.89	0.04	0.04	0.04
bp-0	n.d.	2.54	n.d.	1.06	n.d.	n.d.	n.d.	0.86	n.d.	0.27	0.16	0.44	0.15	0.17	0.17	0.17
bp-1	n.d.	n.d.	n.d.	n.d.	n.d.	n.d.	n.d.	n.d.	n.d.	n.d.	0.05	n.d.	n.d.	n.d.	n.d.	n.d.
bp-2	n.d.	n.d.	1.06	0.74	n.d.	n.d.	n.d.	n.d.	n.d.	0.14	n.d.	n.d.	n.d.	0.04	0.04	0.04
bp-3	n.d.	n.d.	0.89	1.02	n.d.	n.d.	n.d.	n.d.	n.d.	n.d.	0.05	n.d.	n.d.	n.d.	n.d.	n.d.

IV.3.5. Assimilation rates of IC

When incubated under SR conditions, *$assim_{IC}$* into total microbial FAs (*$assim_{IC}$-TFAs*) was 0.35, 0.33, 0.19 and 0.29 µg C g_{dw}^{-1} yr^{-1} for GeoB17306, 17307, 17308 and 17305, respectively (Fig. IV.5). Among those microbial FAs, *$assim_{IC}$* into aC15, C16:1ω7c/t, C16:1ω5 and C16 accounted for more than 50% of *$assim_{IC}$-TFAs* (Fig. IV.5). When incubated under H_2/CO_2, *$assim_{IC}$-TFAs* significantly increased by > 20-fold, i.e., 9.1, 17.7, 12.7 and 6.7 µg C g_{dw}^{-1} yr^{-1} for GeoB17306, 17307, 17308 and 17305, respectively (Fig. IV.5). The contributions of $C_{15:1}$, $C_{17:1\omega6}$ and C_{17} FAs, which were minor (<5%; Fig. IV.2), also significantly increased after addition of H_2/CO_2. For instance, when incubated under SR conditions, *$assim_{IC}$* into $C_{15:1}$ and $C_{17:1\omega6}$ for GeoB17305 accounted for 0% and 4% of *$assim_{IC}$-TFAs*, respectively (Fig. IV.5); however, these values increased to 4% and 27% (Fig. IV.5), respectively, when incubated under H_2/CO_2 conditions.

For reliable estimation of ^{13}C uptake into lipids, the change of $\delta^{13}C$ of phytane and biphytanes needs to exceed the analytical uncertainty (>2‰). *$Assim_{IC}$* into archaeal lipid derivatives (*$assim_{IC}$-ALDs*) ranged from 0.05 to 0.44 ng C g_{dw}^{-1} yr^{-1} under SR conditions (Table IV.2), which was much lower than that into *$assim_{IC}$-TFAs* (Fig. 5). When incubated with H_2/CO_2, *$assim_{IC}$-ALDs* did not increase significantly except at GeoB17306 (Table IV.2), where *$assim_{IC}$* into phytane was 3.89 ng C g_{dw}^{-1} yr^{-1}.

Furthermore, the significant increase in $\delta^{13}C$-TOC incubated under both conditions (Fig. IV.3) indicates that IC was fixed into microbial biomass and/or released as intermediates consequently changing $\delta^{13}C$-TOC. It is noticeable that $\Delta\delta^{13}C$-TOC of 0.35‰ for GeoB17306 under SR conditions (Fig. IV.3) barely exceeds variability related to analytical precision of the

instrument (0.2‰), bringing about relatively high propagated error. By adopting the same estimation method (Eq.3), $assim_{IC}$ into TOC ($assim_{IC}$-TOC) in surface sediment from the Rhône prodelta ranged from 6.8 to 15.5 µg C g_{dw}^{-1} yr^{-1} under SR conditions vs. from 204 to 380 µg C g_{dw}^{-1} yr^{-1} under H_2/CO_2 conditions (Table 3).

IV.4. Discussion

IV.4.1. Constraints of microbial activity in marine surface sediment

IV.4.1.1 Bacterial community

It is hypothesized that the sources of sedimentary OM (terrigenous vs marine) can shape the microbial community and influence microbial activity in surface sediments (Fagervold et al., 2014; Heuer et al., 2014). Based on a two end-member model of δ^{13}C-TOC, where the member-end values of terrestrial and marine OM were $\delta^{13}C$ = -27.4‰ and -20.1 ‰, respectively (Harmelin-Vivien et al., 2008; Higueras et al., 2014), the proportion of terrestrial OM decreased from 84% at the river mouth site (i.e., GeoB17306 and 17307 with δ^{13}C-TOC of -26.2‰; Table IV.1) to 52% at the shelf site (i.e., GeoB17305 with δ^{13}C-TOC of -23.9‰). In the Rhône prodelta, terrestrial OM was rapidly deposited in the river mouth area and the controlled realm was within < 25 km from the river outlet (Lansard et al., 2008; 2009). During the fluvial transportation and deposition, sediments would be deposited with relatively labile riverine OM (e.g., freshwater phytoplankton) and it thus would stimulate microbial activity in surface sediment.

The decreases in bacterial $prod_{lipid}$ in the surface prodelta sediments with distance from the river mouth, when incubated under in situ SR conditions (2.99 µg lipids g_{dw}^{-1} yr^{-1} to 0.83 µg lipids g_{dw}^{-1} $yr^{-}1$; Table IV.3), is consistent with decreases in the flux of OM to the sediment. The increase in bacterial $prod_{lipid}$ in the shelf area (GeoB17305, 2.27 µg lipids g_{dw}^{-1} yr^{-1}; Table IV.3) does not follow this trend and may be a signal of increased contribution of marine-derived OM to the sediment, which is thought to be more labile (Hedge et al., 1997). Bacterial $prod_{lipid}$ may therefore be controlled by the flux of bioavailable OM in the marine sediment. As a result, the proportion of riverine OM in surface sediment decreased (Bourgeois et al., 2011), and bacterial activity subsequently decreased seaward as observed under the in situ SR conditions (Table IV.3). However, when it moved to the shelf area (i.e., GeoB17305) which was less influenced by terrestrial OM (30 km to river mouth; Table IV.1; Lansard et al., 2009),

bacterial activity increased probably due to the contribution of more labile marine OM like the phytoplankton OM.

The hypothesis that microbial activity is controlled by the proportion of labile OM in marine sediment can be supported by the investigation of other sites (Table IV.3). In the OM-lean tidal Janssand flat (TOC = 0.04-0.23 wt%), bacterial $prod_{lipid}$ ranged up to 3.58 µg g_{dw}^{-1} yr^{-1}, which was much higher than that determined in the Rhône prodelta or shelf sediments. This may be attributed to the continuous contribution of fresh and labile particulate or dissolved OM to the diffusive sediments (Beck et al., 2017), which sustain a high microbial activity when incubated in the laboratory (Chapter III). The contribution of particulate and dissolved OM was controlled by the advective movement of porewater. As a result, bacterial activity decreased with increasing depth (Table IV.3). In fjord sediments, fresh and labile OM (TOC = ~2 wt%; Bianchi et al., 2002; Reuss et al., 2005) deposited and buried due to frequent eutrophication can sustain a high bacterial activity in the surface sediments (6.38 µg g_{dw}^{-1} yr^{-1}; Table IV.3; Wegener et al., 2012). In the Rhône prodelta area, which is dominated by the terrestrially-derived OM, bacterial activity in surface sediment is likely determined by the total OM flux; however, as the OM flux weakens, bacterial activity may be stimulated by increases in the relative flux of fresh marine OM. Thus, the estimates of $prod_{lipid}$ are probably related to the bioavailability of OM in marine sediment, and can trace the activity of the entire microbial community.

Table IV.3. Summary of the estimation of microbial activity at different sites

Sites	Depth (cm)	Settings	T (°C)	TOC (wt%)	Bacteria			Archaea			SR	Ref.
					$assim_{IC}$ (µg C g_{dw}^{-1} yr^{-1})	$prod_{lipid}$ (µg lipids g_{dw}^{-1} yr^{-1})	τ_{lipid} (yr)	$assim_{IC}$ (ng C g_{dw}^{-1} yr^{-1})	$prod_{lipid}$ (ng lipids g_{dw}^{-1} yr^{-1})	τ_{lipid} (yr)		
GeoB17306	0-6	prodelta	12	1.50	0.35	2.97	10.6	0.08	0.47	88		this study
GeoB17307	0-6	prodelta	12	1.13	0.33	1.97	11.4	0.41	2.87	136		
GeoB17308	0-6	prodelta	12	0.95	0.19	0.83	21.3	0.26	2.11	120		
GeoB17305	0-6	shelf	12	0.78	0.31	2.27	7.5	0.44	4.4	95		
Himmersfjärden	0-6	fjord	4	~2[a]	1.3	6.38	3.6	0.45	0.25	277[b]		Wegener et al., 2012
Himmersfjärden	6-16	fjord	4	~2[a]	0.03	0.17	38.5	0.34	1.44	53[b]		
Janssand	0-2	intertidal	12/20	0.078	0.18	3.58	3.2					Chapter III
Janssand	2-17	intertidal	12/20	0.038	0.15	1.01	5.8					
Janssand	17-22	intertidal	12/20	0.228	0.15	1.43	10.5					
Estuary	0-5	Mud flat			12~167[c]							Boschker et al., 2014

[a] from Bianchi et al. (2002)
[b] based on total archaeal lipid-derived biphytanes with correction of a_w = 0.33 (Eq. 5)
[c] converted from 2.6–36.3 mmol C m^{-2} d^{-1} under aerobic condition by assuming 0.056 g FAs ($g_{biomass-C}$)$^{-1}$ and 1.5 g dw sediment cm^{-3}

IV.4.1.2. Archaeal community

Archaeal $prod_{lipid}$ in surface sediments from the Rhône prodelta ranged from 0.47 to 4.4 ng g_{dw}^{-1} yr^{-1} when incubated under SR conditions, which was much lower than bacterial $prod_{lipid}$. This is consistent with previous comparisons of archaeal versus bacterial activity in surface marine sediments (e.g., Lipp et al., 2008; Parkes et al., 2014). The production rate of phytane, likely derived from archaeol in the cell membrane of archaeal methanogens (Pancost et al., 2001; Lim et al., 2012; Schouten et al., 2013), was higher than that of bp-0 and bp-3, which is likely derived from uncultured archaea (Schouten et al., 2008; 2013; Elling et al., 2014), suggesting that methanogenic archaea were more active than other archaea in the prodelta and shelf sediments. The increase in archaeal $prod_{lipid}$ following addition of H_2 was mainly attributable to high production of archaeol-derived phytane, particularly at sites GeoB17306 and 17307 (Table IV.2), consistent with the stimulation of methanogens by H_2. This conclusion is supported by increased CH_4 production (Fig. IV.1) and positive values of $\delta^{13}C\text{-}CH_4$ (+400‰; Table S1) at GeoB17306 and 17307. The lower archaeal $prod_{lipid}$ rates for GeoB17308 and 17305 sediments incubated under H_2 may be attributed to detectable levels of sulfate (~ 4 mM; Fig. IV.1), which suggests that most H_2 was channeled to SR and that methanogenesis was probably still inhibited after 50 days of incubation. Furthermore, the relatively low archaeal $prod_{lipid}$ may be indicative of an archaeal community in a maintenance state rather than active growth, even though a potential high energy source (i.e., H_2) was provided. During incubation with H_2/CO_2, more IC was incorporated into CH_4 ($\Delta\delta^{13}C\text{-}CH_4$ > +400‰; Table S.IV.1) than that into archaeol-derived phytane ($\Delta\delta^{13}C$-phytane = +7‰) at GeoB17306. This difference might be related to the size of original methane and lipid pools in our incubation system, of which the former was much smaller than the latter.

Archaeal $prod_{lipid}$ at in situ SR and high energy conditions (i.e., H_2) was ca. 1000 times less than that of Bacteria. However, archaeal $prod_{lipid}$ is probably underestimated because the amount of intact polar ALDs (i.e., phytane and biphytanes) rather than the total amount of intact polar archaeal lipids was used for the estimation (see Eq. 1). The low yield of phytane and/or biphytane during the chemical cleavage of hydrocarbons (Jahn et al., 2004) would bias this estimation. In addition, the recycling of isoprenoidal hydrocarbon chains by benthic archaea, as suggested by Takano et al. (2010), could also affect the estimation of archaeal lipid production. Furthermore, the water assimilation factor (a_w, Eq. 3) is an important factor for accurate estimation of lipid production but remains poorly constrained for archaea. In the current study, $1/a_w$ = 3.3 for archaeal lipid production was much higher than that for bacteria ($1/a_w$=1.30). Therefore, further investigation of water-derived H by archaea and enhanced

recovery of GC-amenable archaeal lipid derivatives would improve the estimates of archaeal $prod_{lipid}$ in marine sediments.

IV.4.2. Turnover time (τ) of microbial lipids in surface sediment

Considering the changes in OM sources and microbial biomass in marine sediments among different sites, the turnover times of microbial lipids (τ_{lipid}) can be used to directly compare microbial production efficiency, as production rates are normalized by microbial lipid inventory (Eq. 5). When incubated under SR conditions, bacterial τ_{lipid} in Rhône prodelta ranged from 7.5 to 11.4 yr, and was longer at the river mouth (GeoB17306, 10.6 yr; Table IV.3) than that at the shelf site (GeoB17305, 7.6 yr; Table IV.3). Thus, the higher bacterial $prod_{lipid}$ values at GeoB17306 compared to GeoB17305 (Table IV.3) appear to be driven by changes in the size of the microbial community rather than the energy derived from respiration of OM. The slightly lower bacterial τ_{lipid} at the shelf site (GeoB17305) may even reflect the increased bioavailability of marine versus riverine OM. The fresh marine organic matter on the shelf appears to stimulate higher microbial activity than the terrestrial organic matter in the prodelta (Bourgeois et al., 2011; Pruski et al., 2015). This notion is supported by the much shorter bacterial τ_{lipid} (3.2 yr; Table IV.3) in the Janssand intertidal flat, where TOC was much lower, the contribution of terrestrial OM was negligible, and microbial activity was predominantly controlled by input of marine OM (Poremba et al., 1999; Wilms et al., 2006; Beck et al., 2017). In contrast, in OM-rich Himmersfjärden sediments, relatively high bacterial activity and short τ_{lipid} (3.6 year; Table IV.3; Wegener et al., 2012) was sustained by a fast sedimentation of both terrestrial and marine OM controlled (1.36 cm yr^{-1}; Bianchi et al., 2002). Therefore, bacterial τ_{lipid} probably responds to both sedimentation rate and OM sources, and fresh, labile marine OM can sustain a relatively high bacterial activity.

The conclusion that the OM source mediates high “production efficiency” (or low τ_{lipid}) is also supported by further observations during the H_2/CO_2 experiment. When the Rhone prodelta and shelf sediments were incubated with the same amount of H_2, bacterial τ_{lipid} decreased at all four sites (1.0 to 2.3 years; Table IV.3). In particular, bacterial τ_{lipid} in GeoB17307 sediment was similar to that in GeoB17305, suggesting that the bacterial community at GeoB17307 and 17305 had a similar production efficiency when H_2 was added, although the former had a higher bacterial $prod_{lipid}$ than the latter (Table IV.3). It is noticeable that bacterial τ_{lipid} at GeoB17306 and 17308 was longer than that at GeoB17305. However, τ_{lipid} for GeoB17306 might be overestimated because the initial sulfate concentration at GeoB17306 was lower (Fig. IV.1) compared to other sites, and the conditions of sulfate plus H_2 probably altered before t_{98}. As a result, real growth time for sulfate and H_2 condition may be shorter than the 50 days used

to estimate τ_{lipid} (Eq. 5). In addition, it is unclear whether this is related to the different composition of the microbial community in those sediments. The addition of H_2 probably stimulated only certain members of the microbial community, and the discrepancy of bacterial τ_{lipid} thus reflected the differences in the relative proportion of H_2-consumers. Microbial activity in anaerobic sediment is generally mediated by sequential redox reactions (Canfield and Thamdrup, 2009). In anoxic marine sediments replete with sulfate, sulfate-reducing bacteria are often the dominant members of the microbial community. After the addition of H_2, sulfate-reducing bacteria can still be stimulated but they probably shifted from heterotrophic growth to autotrophic growth. Thus, the different bacterial τ_{lipid} between river mouth (GeoB17306) and shelf sediments (GeoB17305) may reflect the differences in the predominant bacterial community, i.e., sulfate-reducing bacteria. This difference of bacterial community could be traced back to the effect of the sedimentary OM source.

In contrast, archaeal τ_{lipid} ranged from 88 to 136 years (avg. 110 yr) and was about 10 times slower than that of bacteria. This comparison suggests that the large difference in bacterial and archaeal $prod_{lipid}$ (a factor of ~ 10^3; *Section IV.4.1*) was driven predominantly by changes in population size rather than production efficiency. Both $prod_{lipid}$ and τ_{lipid} were determined for branched GDGTs and FAs to characterize microbial activity in peatland, where branched GDGTs constituted a small fraction, but shared a similar turnover time as the major FAs (Huguet et al., 2017). Archaeal τ_{lipid} (avg. 110 years) in our study sites were shorter than that in surface fjord sediment (277 years; Table IV.3; Wegener et al., 2012) when incubated under in situ SR condition; however, it is ambiguous to conclude that the archaeal community was more active in prodelta marine sediment than that in fjord sediment because different fractions of archaeal lipids were employed for estimation. In our study, the estimates of archaeal τ_{lipid} were based on polar ALDs, which are more representative of live archaea (Zink et al., 2003; Lipp et al., 2008); whereas these estimates in fjord sediment included “fossil” core lipids (e.g., GDGTs), which would dilute the hydrogen isotope measurement.

In summary, assuming that lipid and biomass turnover are similar (cf. Wegener at al., 2012), our study shows that the bacterial population in young, coastal surface sediments turnover on the scale of tens of years (Table IV.3). Moreover, the turnover times of bacterial communities in marine surface sediments were similar to those for microbes in deeper seabed with million-year-old (Braun et al., 2017) as well as those in terrestrial ecosystems like peatland and soil (Weijers et al., 2010; Huguet et al., 2017); however, the turnover times of archaeal lipids in marine surface marine sediment may have a range of hundreds of years.

IV.4.3. Inorganic carbon fixation by bacteria in coastal surface sediment

Our study reveals that, independent of high energy (i.e., H_2) or in situ SR conditions, IC was incorporated into bacterial lipids and even into the TOC pool (Fig. IV.3; Table IV.3). Because high concentrations of H_2 usually do not occur in marine surface sediments, dark IC fixation under SR conditions is more representative for natural conditions. Low IC assimilation into archaeal lipids suggests that bacteria mediated the change in $\delta^{13}C$ of TOC. When incubated under SR conditions, *assim$_{IC}$-TFAs* in surface sediments from the Rhône prodelta ranged from 0.19 to 0.35 µg C g_{dw}^{-1} yr^{-1}, which was close to the estimates in surface sediment (up 2 cm) from intertidal Janssand flat (0.18 µg C g_{dw}^{-1} yr^{-1}), but lower than Himmersfjärden (up 6 cm; 1.3 µg C g_{dw}^{-1} yr^{-1}; Table IV.3). The similar magnitude of *assim$_{IC}$-TFAs* among these different sites possibly suggests that IC fixation might be a ubiquitous phenomenon in anoxic marine surface sediments. When a plausible high energy source (H_2) was provided, *assim$_{IC}$-TFAs* in surface sediment of Rhône prodelta significantly increased by 40-fold (6.7 to 17.7 µg g_{dw}^{-1} yr^{-1}), but remained still lower than that reported for aerobic conditions (12-167 µg C g_{dw}^{-1} yr^{-1}; Table IV.3), as reported by Boschker et al. (2014). It suggests that IC fixation may be related to energy yield during OM mineralization. In general, energy from O_2 as electron donor (e.g., sulfide oxidation) is generally higher than that from anaerobic respiration (e.g., sulfate reduction; Sun et al., 1994; Harvey et al., 1995).

The increase in $\delta^{13}C$ values of TOC after incubation under SR conditions (Fig. IV.3) suggests that IC was not only fixed into lipids but also into other molecules. Assuming IC assimilation into biomass was proportional to *assim$_{IC}$-TFA* (0.056 g FAs per g biomass-C; Brinch-Iversen and King, 1990; Middelburg et al., 2000; Boschker et al., 2014), *assim$_{IC}$* into bacterial biomass (*assim$_{IC}$-bac biomass*) would thus range 2.5–4.8 µg C g_{dw}^{-1} yr^{-1} under SR conditions vs. 92–243 µg C g_{dw}^{-1} yr^{-1} under H_2/CO_2 conditions. The estimates of *assim$_{IC}$-bac biomass* account for 29–35% and 42–61% of *assim$_{IC}$-TOC* for incubation under SR and H_2/CO_2 conditions, respectively (Table S.IV.4), suggesting that non-lipid pools of biomass might be more highly labelled than lipids (Feisthauer et al., 2008), or ^{13}C-labelled metabolites have accumulated into the TOC during incubation.

IV.4.4. Implication of dark inorganic carbon fixation in marine surface sediment

Chemoautotrophic processes are generally invoked to explain dark IC fixation into microbial lipids and the TOC pool (e.g., Boschker et al., 2014; Vasquez-Cardenas et al., 2015; Dyksman et al., 2016); however, heterotrophic microorganisms my also assimilate IC (Roslev et al., 2004; Feisthauer et al., 2008; Yakimov et al., 2014). The dual SIP with D_2O and ^{13}C-bicarbonate (dissolved inorganic carbon; DIC) can reveal the dominant microbial metabolism

based on the ratio of $assim_{IC}$ into microbial lipids to $prod_{lipid}$ (*Ra/p*; ~1 and <0.3 for autotrophy vs. heterotrophy, respectively; Wegener et al., 2012).

When incubated under SR conditions, the average *Ra/p* for bacterial FAs at the four study sites were all less than 0.3 (0.12, 0.17, 0.23 and 0.14 for GeoB17306, 17307, 17308 and 17305, respectively; Table IV.3), suggesting that this dark IC fixation mainly occurred during heterotrophic processes on the basis of the above hypothesis. Similar values were also observed in the surface sediment from intertidal flat (*Ra/p* = 0.09; Wu et al., under revision) and fjord (*Ra/p* = 0.2; Wegener et al., 2012). When a plausible autotrophic condition was provided (i.e., H_2/CO_2), the *Ra/p* value for FAs significantly increased to 0.34, 0.28, 0.49 and 0.41 at GeoB17306, 17307, 17308 and 17305, respectively. Although they were not ~1, as hypothesized (Wegener et al., 2012), this shift likely parallels the stimulation of autotrophs. The production of acetate (> 1.5mM; Table S.IV.1) after the addition of H_2/CO_2 can sustain the growth of heterotrophic microbes in marine sediment (Wellsbury et al., 1997;), which may have diluted the observed Ra/p. Much higher incorporation of the ^{13}C-IC label into bulk heterotrophic biomass, compared to the FA pool due to the anapleurotic reaction during citric acid cycle (Kornberg, 1965; Gebhardt et al., 1983; Thauer, 1988), may explain the difference between $assim_{IC\text{-}biomass}$ and $assim_{IC\text{-}TOC}$.

In order to better distinguish the different bacterial community members, principal component analysis (PCA) was used to compare the results of $assim_{IC}$ and $prod_{lipid}$ for individual FAs with relative abundance of bacterial FAs from some representative cultures, including Gamma-, Dleta- and Epsilonproteobacteria (Fig. IV.6). Most of the microbial FAs were similar to the reference SR bacteria, i.e., *Desulfobulbus. sp* (Fig. IV.6), indicating that SR bacteria were active and dominant in our sediment incubations. The characteristic FAs for SR bacteria, e.g., C14, *i*C15, *a*C15, C15, *a*C17 and *i*C17 (Taylor and Parkes, 1983; Kaneda, 1991; Londry et al., 2004) were similar to those of *Desulfobulbus. Sp.* (Fig. IV.6) and also support the notion that SR bacteria were active. These FAs generally had relatively lower *Ra/p* values than other FAs under SR conditions, also supportive of heterotrophic growth by SR bacteria. The heterotrophic IC assimilation by sulfate-reducing bacteria was probably via anaplerotic (replenishing) reactions during the citrate acid cycle (Kornberg, 1965; Gebhardt et al., 1983; Thauer, 1988).

The unsaturated FAs, such as $C_{16:1\omega7}$, $C_{16:1\omega5}$, $C_{18:1\omega9c}$, $C_{18:1\omega7}$ and C_{18}, were similar to those of *Pseudomonas sp.*, *Arcobacter sp.* and *Beggiatoa* (Fig. IV.6), suggesting that they were more likely produced by Gamma- and Epsilonproteobacteria (Zhang et al., 2005; Freese et al., 2008; Lenk et al., 2011). Under SR conditions, the *Ra/p* value was relatively high, suggesting that

the above FAs were more probably derived from autotrophic production. Gamma- and Epsilonproteobacteria have been shown to fix IC via the oxidation of sulfur or ammonium (Lenk et al., 2011; Boschker et al., 2014; Vasquez-Cardenas et al., 2015; Dyksma et al., 2016). In addition, $C_{16:1\omega5}$, $C_{18:1\omega9}$, $C_{18:1\omega7}$ and C_{18} FAs had a much lower production rate compared with other FAs (Fig. IV.5), which indicates that autotrophic IC fixation play a minor role under SR conditions. Gamma- and Epsilonproteobacteria generally require O_2 to oxidize sulfur and ammonium (Boschker et al., 2014; Vasquez-Cardenas et al., 2015; Dyksma et al., 2016), and they probably had a lower activity than SR bacteria during anaerobic incubation. In summary, our results suggest that at least two bacterial functional communities exist which could fix IC in marine sediments.

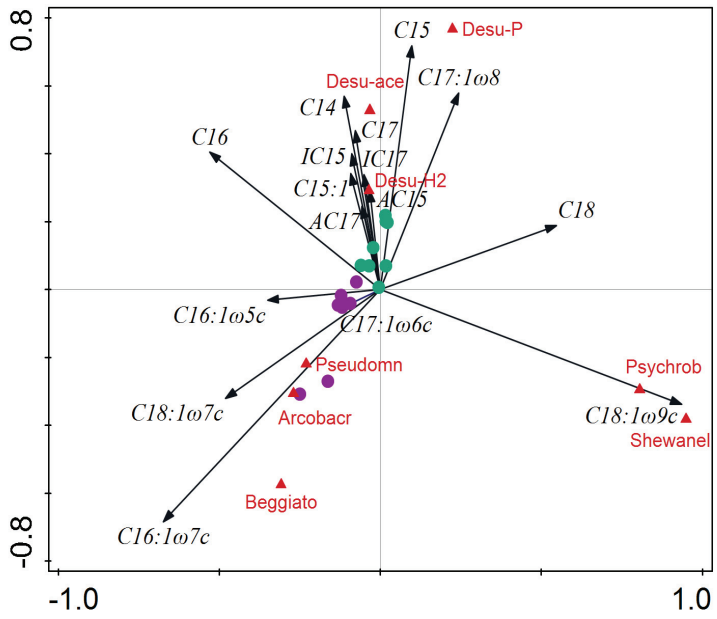

Fig. IV.6. Principal component analysis (PCA) of *assim*$_{IC}$ and *prodlipid* for individual bacterial fatty acids under SR (green dots) or H_2/CO_2 (purple dots) conditions. The relative abundance of lipids in the membranes of reference bacteria (red triangles) was also added to PCA including γ-proteobacteria *Beggiatoa*, *Pseudomonas* sp. *Psychrobacter* sp. and *Shewanella sp*. (Zhang et al., 2005; Freese et al., 2008); δ-proteobacteria *Desulfobulbus sp*. grown on H_2 or propionate (Desu-H_2 and Desu-P; Taylor and Parkes, 1983), *Desulfobacter* sp. grown on acetate (Desu-ace; Taylor and Parkes, 1983); ε-proteobacteria *Arcobacter sp.* (Freese et al., 2008). For detailed values see Table S.IV.5.

Microbial-driven OM degradation is the major process in the biogeochemical carbon cycle in marine sediments, and SR bacteria are thought to be dominant in anaerobic sulfate-rich marine sediments, which can account for 30% of OM mineralization (Jørgensen, 1982; 2016; Bowles et al., 2014). In our incubation under SR conditions, IC fixation during heterotrophic growth probably means that a part of IC should flow back to the bacterial community during degradation of organic carbon. The deuterium incorporation rates into lipids can characterize the total microbial activity, and *Ra/p* may be indicative of the ratio of carbon back flow to biomass when heterotrophic growth is dominant in sediment. The back flux would vary from 5% to 23% when combining results from other sites studied with same dual isotope labelling

methods (Table IV.3). These back fluxes of inorganic carbon were also found in environmental microbes and even pure cultures, e.g., 20% for cable bacteria during oxidation of propionate (Vasquez-Cardenas et al., 2015), 5% during the anaerobic oxidation of methane (Holler et al., 2011) and even up to 30% for sulfate-reducing bacteria (Sorokin, 1966; Wegener et al., 2012).

IV.5. Conclusion

The microbial activity in surface sediment collected from a transect off the River Rhône has been investigated by lipid-based dual stable isotope labelling incubation. The turnover times of bacterial lipids (7.5-11.4 yr) in surface sediments were much higher than those of archaeal lipids (88-136 yr), when incubated under in situ SR conditions. The activity of the bacterial community in the surface sediments was likely controlled by the contribution of labile and fresh riverine-OM during the fast sediment accumulation rate in the prodelta setting. Thus, small amounts of labile riverine OM or marine OM can still sustain a high bacterial activity, although higher degraded and modern vascular plant-derived OM is predominated in the Rhône prodelta sediment. The labelling method provides new insights and allows quantitative evaluation of the effect of OM source and bioavailability on microbial activity in marine sediment. The heterotrophic IC assimilation might be a ubiquitous phenomenon in OM-rich marine sediment, and it may be an important component in the biogeochemical carbon cycle in marine sediments.

Acknowledgements

We would thank Xavier Prieto-Mollar, Jenny Wendt, Heidi Taubner, and Martin Kölling for their support of stable isotope analyses. W. Wu was funded by Chinese Scholarship Council. We also thank the crew and scientists of RV Poseidon cruise POS450 for sampling. This study was funded by the ERC Grant Project N. 247153 (DARCLIFE; PI: K-U. Hinrichs) and by the DFG (German Research Foundation) through instrument grant 144/300-1 (LC-qTOF system). Further support was provided by GLOMAR funded by the DFG through MARUM.

Chapter V

Growth of abundant sedimentary Bathyarchaeota on lignin as an energy source

Tiantian Yu[a,b,1], Weichao Wu[c,1], Wenyue Liang[a,b], Mark Alexander Lever[d], Kai-Uwe Hinrichs[c] and Fengping Wang[a,b,2]

[a]State Key Laboratory of Microbial Metabolism, School of Life Sciences and Biotechnology, Shanghai Jiao Tong University, Shanghai, China;
[b]State Key Laboratory of Ocean Engineering, Shanghai Jiao Tong University, Shanghai, China.
[c]Organic Geochemistry Group, MARUM Center for Marine Environmental Sciences & Dept. of Geosciences, University of Bremen, 28359 Bremen, Germany.
[d]Institute of Biogeochemistry and Pollutant Dynamics, Department of Environmental Systems Sciences, Swiss Federal Institute of Technology Zurich, Zurich, Switzerland

[1]T.Y. and W.W. contributed equally to this work.
[2]To whom correspondence should be addressed. E-mail: fengpingw@sjtu.edu.cn

(***under review at Proceedings of the National Academy of Sciences of the USA***)

Abstract

Members of the archaeal phylum Bathyarchaeota are among the most abundant microorganisms on Earth. Although versatile metabolic capabilities such as acetogenesis, methanogenesis, and fermentation have been suggested for bathyarchaeotal members, no direct confirmation of these metabolic functions has been achieved through growth of Bathyarchaeota in the laboratory. Here we demonstrate, on the basis of gene copy numbers and stable isotope probing of archaeal lipids, the growth of Bathyarchaeota in enrichments of estuarine sediments with the refractory biopolymer lignin. Our culture conditions particularly selected for the bathyarchaeotal subgroup Bathy-8, which achieved estimated doubling times of ~2 to 3 months during growth on lignin. Other organic substrates (casein, oleic acid, cellulose, and phenol) did not significantly stimulate growth of Bathyarchaeota. Meanwhile, putative bathyarchaeotal tetraether lipids incorporated ^{13}C from ^{13}C-bicarbonate only when added in concert with lignin. Our results indicate organoautotrophic growth of a bathyarchaeotal group with lignin as an energy source and bicarbonate as a carbon source and shed new light into the cycling of one of Earth's most abundant biopolymers in anoxic marine sediment.

Key words: lignin degradation; Bathyarchaeota; Sedimentary carbon cycling

Significance

Marine sediment holds the largest organic carbon pool on earth, where microbial transformation of carbon is considered a key process of carbon cycling. Bathyarchaeota are one of the most abundant and active microorganisms in marine sediment. It has been suggested that Bathyarchaeota may play a globally important role in the carbon cycling in marine environment through fermentation of complex organic substances, acetogenesis, methane metabolizing based on metagenome analysis. Here for the first time, we give direct proof beyond genome information, that a group of Bathyarchaeota namely Bathy-8 could grow with lignin as an energy source and bicarbonate as a carbon source. Our work suggests that some members of the Bathyarchaeota are important, previously unrecognized degraders of lignin in marine sediments

V.1. Introduction

Bathyarchaeota (formerly referred as Miscellaneous Crenarchaeotal Group, MCG; Inagaki et al., 2003; Meng et al., 2014) are estimated to be among the most abundant microorganisms on the planet (He et al., 2016), and are particularly common in marine sediments (Inagaki et al., 2003; Jiang et al., 2011; Kubo et al., 2012; Ruff et al., 2015; Yu et al., 2017). The phylum Bathyarchaeota contains more than 19 subgroups/lineages with low intragroup similarities (Fillol et al., 2016; He et al., 2016; Kubo et al., 2012; Lazar et al., 2015) and its members have been suggested to play a globally important role in the breakdown of organic matter (Biddle et al., 2006), through fermentation (Lloyd et al., 2013), acetogenesis (He et al., 2016), and methanogenesis (Evans et al., 2015). However, due to the lack of cultures and difficulty to obtain enrichments of Bathyarchaeota (Gagen et al., 2013), the metabolic properties and capabilities of these abundant and widespread Archaea have so far mostly been inferred from single cell genomic and metagenomic analysis (Evans et al., 2015; He et al., 2016; Lazar et al., 2016; Lloyd et al., 2013; Meng et al., 2014).

The first metabolic insights into Bathyarchaeota came from organic-rich subseafloor sediments of the Peru Margin, where these Archaea were inferred to be assimilating sedimentary organic carbon based on the δ^{13}C-isotopic compositions of intact polar lipids (IPLs; Biddle et al., 2006). The organoheterotrophic physiology of Bathyarchaeota was further supported through analyses of bathyarchaeotal genomes by single-cell genome and metagenome analyses, and genes encoding enzymes for the degradation, transport, and utilization of detrital proteins, aromatic compounds and plant-derived carbohydrates were identified (Lloyd et al., 2013; Meng et al., 2014; Lazar et al., 2016). Meanwhile, stable isotope probing experiments indicated that members of two subgroups assimilated several organic substrates, including acetate, glycine, urea, lipids, and complex mixtures of organic growth substrates, while showing no significant incorporation of carbon from proteins (Seyler et al., 2014). On the other hand, hydrogenotrophic acetogenesis involving acetate synthesis from inorganic carbon (IC) has been proposed for some lineages of Bathyarchaeota (He et al., 2016). The reductive acetyl-CoA pathway, a carbon fixation pathway that is among cultured representatives exclusively present in all methanogens and acetogens, several sulfate reducers, and the facultatively denitrifying, thiosulfate-reducing, and iron-reducing archaeon *Ferroglobus placidus* (Berg et al., 2010; Lever et al., 2013, see *SI*), and that enrichment data suggest to be used also by anaerobic methanotrophic archaea (Kellermann et al., 2012), has been identified in most of the obtained bathyarchaeotal genomes (Evans et al., 2015; He et al., 2016; Lazar et al., 2016). Among these, members of the bathyarchaeotal subgroups

Bathy-3 and Bathy-8 have been suggested to be capable of methanogenesis (Evans et al., 2015). All of the above studies indicate great versatility in the metabolic potentials of Bathyarchaeota, with some lineages possibly being capable of utilizing both organic and inorganic carbon compounds for biosynthesis and energy production. However, no direct proof of carbon or energy sources has so far been obtained for Bathyarchaeota based on laboratory experiments.

Here we report our efforts to enrich the bathyarchaeotal cells from marine sediment in the laboratory by setting up a series of enrichments with diverse organic compound classes, including lipids (oleic acid), proteins (casein), aromatic monomers (phenol), aromatic polymers (lignin), and structural carbohydrates (cellulose). Stimulation of growth in Bathyarchaeota affiliated with the Bathy-8 subgroup was shown by addition of lignin. During growth on lignin, incorporation of IC into archaeal lipids was demonstrated. This study represents the first in-vitro enrichment of Bathyarchaeota, and demonstrates the organoautotrophic metabolism of members of this phylum, which likely plays an important role in the carbon cycle in marine sediments.

V.2. Results

V.2.1. Enrichments set-up

Numerous enrichment cultures from Dayangshan (DYS) estuarine sediments of northern East China Sea (Fig. S.V.1) were set up by adding diverse organic compound classes, i.e. the long-chain fatty acid oleic acid, the protein casein, the aromatic monomer phenol, the phenolic polymer lignin, and the polymeric carbohydrate cellulose (see Materials and Methods). Sediment slurries without addition of organic compounds were used as controls. Changes in the abundances of Bacteria, Archaea and Bathyarchaeota were then monitored by quantitative PCR (qPCR) using universal bacterial and archaeal 16S rRNA gene primers, and by Bathyarchaeota-specific 16S rRNA gene primers. The organic compounds were initially added at concentrations of 50 mg/L, and increased to 500 mg/L after 3.5 and 6 months incubation.

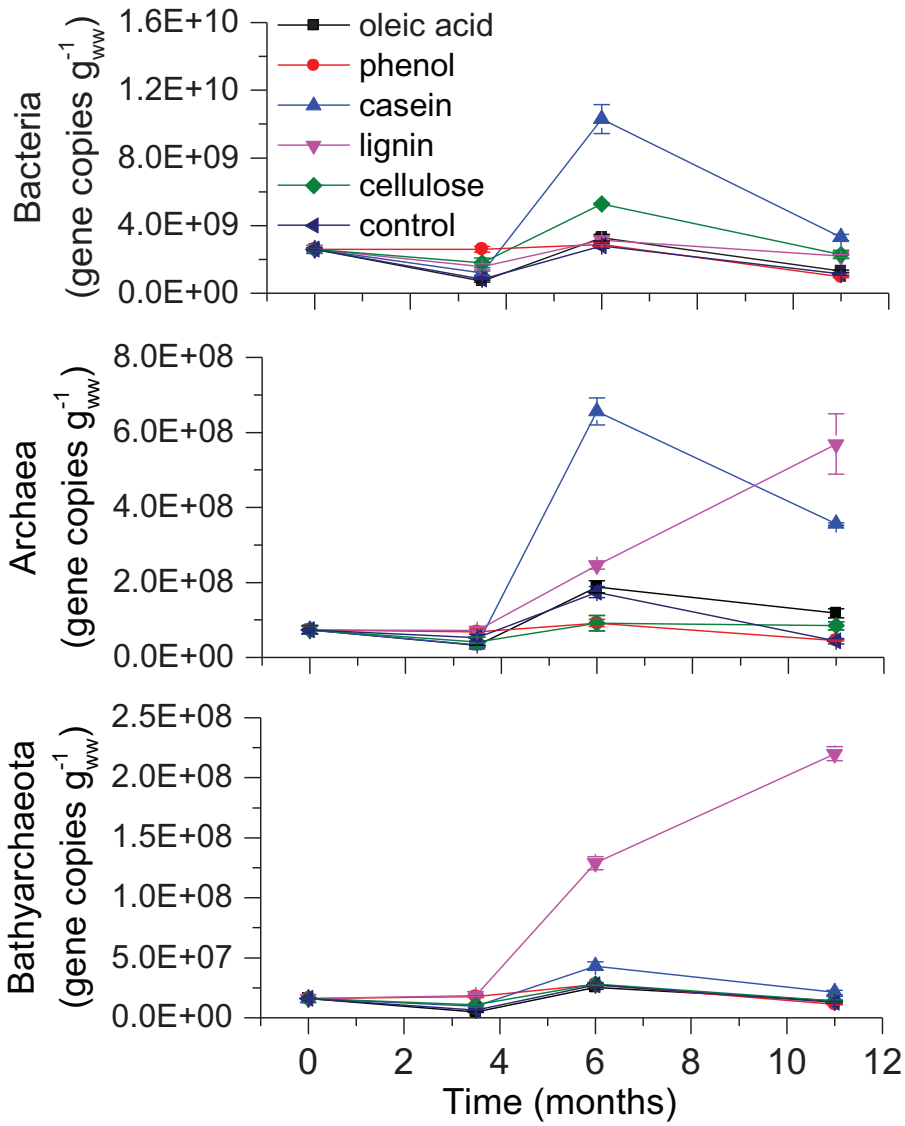

Fig. V.1. The abundance change of Bacteria, Archaea and Bathyarchaeota in sediment slurries after incubation with different organic compounds for 3.5, 6 and 11 months. The abundance (gene copies per gram wet weight of sediment; gene copies g_{ww}^{-1}) is quantified based on the respective 16s rRNA genes.

Treatment responses to substrate additions and controls are shown in Fig. V.1. In the control samples, the abundance of Bacteria, Archaea and Bathyarchaeota showed only small fluctuations over time. Casein initiated the strongest growth stimulation in total Bacteria and Archaea, with an increase in bacterial and archaeal 16S rRNA gene copies by about 3 and 9 times at t_6, respectively; bathyarchaeotal gene copies only increased slightly in response to casein. Cellulose stimulated growth of Bacteria after 3.5 months, but had no influence on archaeal or bathyarchaeotal gene copies. Phenol and oleic acid had no obvious influence on the gene copies of Bacteria, Archaea, or Bathyarchaeota. Lignin showed little influence on the growth of Bacteria, but significantly stimulated growth of Archaea, particularly Bathyarchaeota. The overall archaeal gene copy numbers increased by about 2 and 3 times at t_6 and t_{11}, while

the those of Bathyarchaeota climbed to more than 10 times at t_{11} compared to the original sample. Thus, strong growth of Bathyarchaeota was only achieved in response to lignin addition.

V.2.2. Archaeal and bathyarchaeotal community composition

Since the enrichment of Bathyarchaeota was the aim of this study, and only lignin showed significant stimulation of bathyarchaeotal growth, further detailed experiments were undertaken with the original sample, lignin enrichments, and controls. Archaeal 16S rRNA gene analyses show that Thaumarchaeota (40%) and Bathyarchaeota (33%; Fig. V.2A) were dominant archaeal groups in the original sample followed by Thermoplasmata (8%) and Parvarchaea (5%). After amendment with lignin, the relative abundance of Bathyarchaeota within the archaeal community increased to over 65% at t_{11} (Fig. V.2A), compared to a strong decrease in control samples (8-23% of total Archaea; Fig. V.2A). The percentage of methanogenic *Methanococci* reads increased both in lignin cultures and no-substrate controls, whereas the relative abundance of Thaumarchaeota decreased across lignin treatments and no-substrate controls, showing a stronger percent decrease in the former.

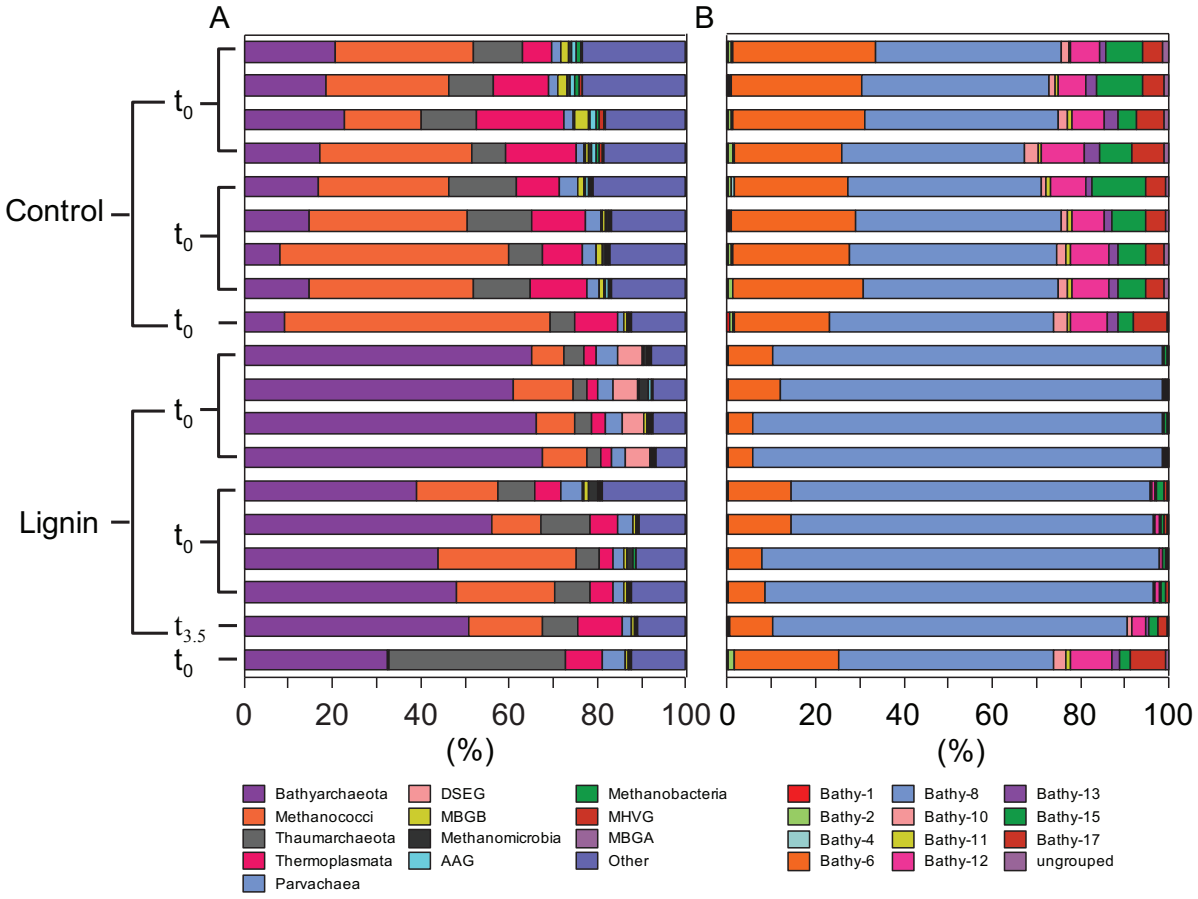

Fig.V.2. Comparison of archaeal communities at the phylum level (A) and of bathyarchaeotal communities at the subgroup-level (B) in response to lignin addition over time. t_0, $t_{3.5}$, t_6 and t_{11} indicate samples that were taken after 0, 3.5, 6, and 11 months, respectively. Only one sample from t_0 and $t_{3.5}$ was analyzed, compared to four samples at t_6 and t_{11}. Details on the phylogenetic identifications are in the Materials & Methods. DSEG, Deep Sea Euryarcheotic Group; MBGB, Marine Benthic Group B; AAG, Ancient Archaeal Group; MHVG, Marine Hydrothermal Vent Group; MBGA, Marine Benthic Group A; Other, unclassified archaea.

The bathyarchaeotal community in the original sample was dominated by the subgroups Bathy-8 (49%), Bathy-6 (24%) and Bathy-12 (10%; Fig. V.2B) based on a phylogenetic tree of bathyarchaeotal 16S rRNA genes (Fig. S.V.2). Incubation with lignin created a strong selection pressure, resulting in Bathy-8 accounting for 80-90% of the bathyarchaeotal sequences at t_6 and t_{11} (Fig. V.2B). Within the Bathy-8 subgroup, a single OTU (OTU3326) became dominant, accounting for 63-73% of all bathyarchaeotal 16S rRNA gene reads (Table S.V.1).

V.2.3. Inorganic carbon assimilation by lipid carbon isotope analysis

^{13}C-labelled sodium bicarbonate (^{13}C-IC) was provided to enrichments with and without lignin in order to test the hypothesis that members of the Bathyarchaeota assimilate IC via the reductive acetyl-CoA pathway. In the original sediment, the δ^{13}C values of the archaeal polar lipid derivatives phytane, BP-0, BP-2 and BP-3 were -35.1‰, -26.5‰, -25.8‰ and -21.9‰, respectively (Fig. V.3 and Table S.V.2). No matter whether lignin was added or not, with or without ^{13}C-IC, the δ^{13}C value of BP-3 did not change significantly at t_6 and t_{11}. However, the δ^{13}C values of phytane, BP-0, and BP-2 showed a different pattern.

In the ^{13}C-IC amended control samples, the δ^{13}C value of phytane increased by 698‰, and 1,100‰ at t_6 and t_{11}, respectively, whereas the δ^{13}C values of BP-0, BP-2 and BP-3 did not change (Fig. V.3 and Table S.V.2). When grown on lignin with ^{13}C-IC, the δ^{13}C values of phytane, BP-0 and BP-2 increased by 885‰, 137‰ and 18‰, respectively at t_6 (Fig. V.3 and Table S.V.2), vs. 1260‰, 234‰, 81‰, respectively at t_{11}.

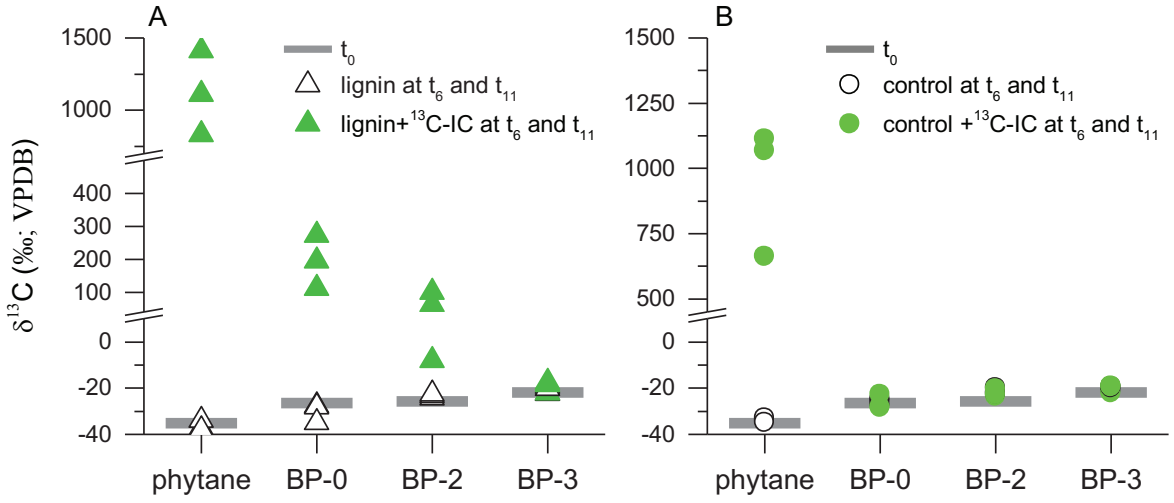

Fig. V.3. The carbon isotopic composition of archaeal polar lipid derivatives (i.e., phytane, BP-0, BP-2 and BP-3) in the lignin treatment (A) and in the control without lignin (B) samples with/-out ^{13}C-IC at t_6 and t_{11}.

V.3. Discussion

Marine sediments are one of Earth's largest organic carbon sinks. Microbial transformation of carbon is considered a key process influencing the carbon flow in sediment and ultimately atmospheric oxygen and carbon dioxide concentrations (Berner, 1989). Nevertheless, the controls on microbial organic carbon cycling are not well understood, including the biogeochemical role of Archaea, which are often abundant in marine sediments. In this study, we demonstrate that lignin addition significantly stimulated the growth of Bathyarchaeota (Fig. V.1), which are a dominant group of Archaea in marine sediments. The relative abundance of Bathyarchaeota reached up to 65% of the total archaeal community after 11 months of incubation, with a strong increase in the fraction of bathyarchaeotal subgroup Bathy-8 accounting for most of this increase (Fig. V.2). Lignin is a class of complex cross-linked phenolic polymers, and the most abundant biopolymer on Earth after cellulose. Lignin is particularly important in the formation of cell walls in vascular plants, comprising up to 25% of plant biomass (Wei et al., 2009). Structural polymers, such as cellulose, hemicellulose, and lignin, constitute the bulk of terrestrial organic matter, and can account for a significant fraction of organic carbon in marine sediments (Prahl et al., 1994). Our work suggests that members of the Bathyarchaeota are important, previously unrecognized degraders of lignin in marine sediments.

Metagenomic sequence analyses have suggested that Bathyarchaeota are capable of utilizing a variety of organic compounds including proteins (Lloyd et al., 2013), aromatic compounds

(Meng et al., 2014), and carbohydrates (He et al., 2016; Lazar et al., 2016). Yet, bathyarchaeotal 16S rRNA gene abundances increased tenfold in response to lignin addition in this study, and did not grow in response to proteins, cellulose, phenol, or oleic acid. This indicates that, at least at the study site, members of this phylum play an important role in the degradation of lignin, either directly in the depolymerization, and/or in metabolizing lignin derivatives. The fact that phenol addition did not stimulate growth of Bathyarchaeota, Archaea or Bacteria (Fig. V.1) suggests that the presence of phenolic methoxy groups in lignin could trigger the growth of Bathyarchaeota, for example via utilization of methoxy groups during acetogenesis (Lever et al., 2010).

In the enrichment with lignin, the doubling (or generation) time of Bathyarchaeota was estimated to about 2-3 months, which is similar to that of anaerobic methane oxidizing archaea (ANMEs) enriched in the laboratory (Girguis et al., 2003; Krüger et al., 2008; Zhang et al., 2010). In deep subsurface sediments, where Bathyarchaeota constitute major components of archaeal communities, bulk microbial community turnover time is estimated to range from years to decades, with even longer turnover times for subsurface archaea (Xie et al., 2013; Braun et al., 2017). Considering the extremely low carbon and energy sources present in the deep subsurface, the cell turnover time of Bathyarchaeota in the subsurface sediments are expected to be longer than that in our enrichment culture grown at high lignin concentration.

Within the Bathyarchaeota, the subgroup Bathy-8 became predominant during growth on lignin, comprising ~90% of the bathyarchaeotal community at the end of experiments (Fig. V.2B). Within the Bathy-8, OTU3326 became dominant (Table S.V.1), suggesting that this member of Bathy-8 was the main lignin degrader in the community. Members of Bathy-8 are cosmopolitan in marine sediments (Breuker et al., 2013; Lloyd et al., 2013; Lazar et al., 2015; Fillol et al., 2016; Yu et al., 2017), particularly in anoxic subsurface sediment layers (Breuker et al., 2013; Lazar et al., 2015; Yu et al., 2017). How widespread the ability to degrade lignin is within this group, and whether members of other subgroups of Bathyarchaeota are able to metabolize lignin will need to be explored through further studies using different sediments and varying cultivating conditions.

Two genomic Bins belonging to Bathy-8 (Bin-L-1 and Bin-L2) were assembled from the lignin enrichment (Table S.V.3 and Fig. S.V.3). A complete WL pathway was found in both genomes indicating the capability of these Bathy-8 to fix IC (Table S.V.4 and Table S.V.5). Physiologically characterized microorganisms which use the reductive acetyl CoA pathway typically use it for energy production and C fixation. The ability to use one metabolic pathway for energy conservation and biosynthesis has clear energetic advantages, which is why it is

perhaps not surprising that this pathway is found in anaerobic microorganisms performing low-energy catabolic reactions such as methanogenesis and acetogenesis. Members of Bathy-8 were recently suggested to be capable of methanogenesis because a metagenomic bin contained the entire methyl–coenzyme M reductase (MCR) gene cluster (Evans et al., 2015). No MCR genes were found in Bin-L-1 and Bin-L-2 (Table S.V.4 and S.V.5). No known genes for lignin degradation were found in Bin-L-1, while a gene of catalase-peroxidase and 4-oxalocrotonate tautomerase for putative lignin and aromatic compound degradation respectively, were found in Bin-L-2 (Table S.V.4 and S.V.5). No canonical genes for respiration such as dissimilatory sulfate, nitrate, or iron reduction were found in the genomes, supporting the fermenting lifestyle of Bathyarchaeota (He et al., 2016; Lazar et al., 2016). The genes and the mechanisms involved in the lignin degradation by Bathy-8 needs further exploration.

IC was incorporated into phytane as well as biphytanes with 0-2 cycloalkyl rings (Fig. V.3). This suggests that at least two different functional archaeal groups were assimilating IC for lipid biosynthesis in our experiments. The lignin-unrelated incorporation of ^{13}C-IC into phytane is presumably related to the abundance of methanogens of the dominant methanogenic class *Methanococci*. Since ^{13}C label incorporation into biphytanes was only observed in lignin treatments, it is likely that the dominant Bathyarchaeota in lignin treatments were responsible for this incorporation. Bathyarchaeota are putative producers of isoprenoidal tetraether lipids (Meador et al., 2015) and therefore a plausible source of BP-0 and BP-2. The fact that the majority of recovered bathyarchaeotal genomes from various subgroups contain genes of the reductive acetyl-CoA pathway (Wood-Ljungdahl, WL; He et al., 2016; Lazar et al., 2016) is furthermore in line with the observed ^{13}C-IC assimilation in lignin treatments.

The enrichment of Bathyarchaeota during growth on lignin indicates that members of this phylum may play an important role in the degradation of lignin in anoxic marine sediments. In accordance with previous observations in acetogenic bacteria (Drake et al., 2008), of which 88% of tested strains metabolize methoxy groups from lignin phenols, we suggest that the main bathyarchaeotal community members affiliated with Bathy-8 utilize methoxy-groups of lignin, and combine these methyl groups with CO_2 to acetyl-CoA via the carbon monoxide dehydrogenase/acetyl-CoA synthase complex (Codh/Acs). This acetyl CoA is then used as a key intermediate for biosynthesis or converted to acetate via cleavage of the cofactor to produce energy (Lever et al., 2012; He et al., 2016). Acetate production in the cultures was measured as shown in Table S.V.6. The elevated production of acetate (26.2 to 89.0 µM; Table S.V.6) at t_{11} in lignin treatments compared to non-lignin controls (3.9 to 19.9 µM; Table S.V.6) supports other lines of evidence (metagenome and the apparent importance of phenolic

methoxy groups) that are consistent with an acetogenic capability of some Bathyarchaeota. Although inorganic ^{13}C label incorporation into acetate was not specific to lignin experiments (Table S.V.6), the ^{13}C enriched acetate is clear evidence of a strong acetogenic activity in our enrichment, even though we could not demonstrate the link to lignin as substrate due to the commercial unavailability of lignin polymers with ^{13}C-labeled methoxy groups. The apparent requirement of both IC and organic lignin C for growth of Bathyarchaeota is, however, consistent with organoautotrophy, a metabolism that is widespread in acetogenic bacteria (Lever et al., 2010) and was previously observed in other subseafloor archaea (Kellermann et al., 2012).

In conclusion, we have demonstrated a organoautotrophic life strategy of selected Bathyarchaeota, which sheds new light into microbial carbon cycling and important energy substrates of microbial populations in marine sediments. The ubiquitous Bathyarchaeota may play an important, previously unrecognized role in the degradation of terrestrially derived lignin in marine sediment. Such an affinity to lignin is consistent with the high abundance of Bathyarchaeota in terrestrially influenced continental margin settings (Kubo et al., 2012). Lignocellulose material is the most abundant renewable energy resource on our planet, in which lignin depolymerization is the major barrier for bioenergy extraction. Our finding of Bathyarchaeota mediating lignin degradation may result in new strategies and enzymes for biotechnological usage of plant material for bioenergy production.

V.4. Methods

V.4.1. Sample collection

Intertidal sediments (uppermost 10 cm) were collected from Dayangshan (DYS) Island (30.592817 N, 122.083493 E) in Hangzhou Bay, northern East China Sea, China (Fig. S.V.1). Samples were stored anoxically on ice in gas-tight bags and transported to the laboratory within 3 hours, where they were kept at 4^{o}C until further treatment. The sample was dominated by silt sediment, which is mainly supplied by Yangtze River (Dai et al., 2014), and considered to be rich in terrigenous organic matter (Xu et al., 2016).

V.4.2. Cultivation conditions

About 600 g sediment was thoroughly mixed with 2 L of anaerobic artificial seawater medium (Zhang et al., 2010) without Na_2SO_4 in an anaerobic chamber (Type B Vinyl, COY). After centrifugation at 7610 g in 500 mL centrifuge bottles, the supernatant was removed and this process was repeated again to largely eliminate the original porewater. Afterwards, the

sediment was mixed again with 3 L anaerobic artificial seawater medium and dispensed into serum bottles as 100-mL sediment slurries. The following five organic growth substrates were added to different experiments at a dose of 50 mg/L: oleic acid (Sinopharm 30138518), phenol (Sinopharm 100153008), casein (Sinopharm 69006227), alkali lignin (Sigma 45-471003), and cellulose (Sinopharm 68005761). In addition, ^{13}C-$NaHCO_3$ was added to a final concentration of 0.25 μM [the percentage of ^{13}C-$NaHCO_3$ (mol/mol) to total $NaHCO_3$ was 5%] to test for assimilation of IC in archaeal lipids. The bottles were sealed with butyl rubber stoppers and aluminum crimp seals, and then the headspace was evacuated by gas pump and re-filled with 99.99% N_2 gas in the anaerobic chamber three times, after which a pressure of 200 kPa of N_2 was applied to each vial. Two replicates of each treatment were incubated, meanwhile two slurries were also incubated without addition of any organic substrates as controls. Slurries were incubated horizontally without shaking in the dark at 20°C for 3.5 months ($t_{3.5}$), after which 20 mL of slurries were sampled using a syringe with needle. The collected samples were centrifuged at 13800 g to separate the supernatant and sediments, and stored at -80°C for DNA and lipid isolation and measurement of chemical parameters.

Afterwards, higher concentrations of organic substrates (500 mg/L of each substrate) and ^{13}C-$NaHCO_3$ [final concentration is 0.5 μM; the percentage of ^{13}C-$NaHCO_3$ (mol/mol) to total $NaHCO_3$ was 10%] were added to the remaining cultures, and then incubated for another 2.5 months (t_6). Then 20 mL slurries were collected and more organic substrates (500 mg/L of each substrate) were added again, and incubated for additional 5 months (t_{11}). Thus, slurries at three time points were obtained after incubation, i.e., 3.5, 6 and 11 months.

V.4.3. DNA extraction

Total DNA was extracted from 0.2-0.3 g of wet sediment using a PowerSoil DNA Isolation Kit (MoBio, USA) according to the manufacturer's protocol. The concentration of DNA was measured by using nanodrop 2000 (Thermo) and the frozen at -80°C until processing.

V.4.4. Quantitative Polymerase Chain Reaction (Q-PCR)

Bacterial, archaeal and bathyarchaeotal 16S rRNA genes were quantified by quantitative PCR (qPCR). Archaeal, bacterial and bathyarchaeotal 16S rRNA genes were amplified using primers Uni519F/Arch908R, Bac341F/prokaryotic519R, and Bathy-442F/Bathy-644R, respectively. The reaction solution included 10 μL of SYBR_PREMIX TaqTM, 0.4 μL of ROX Reference Dye (50×; TaKaRa, China), 0.8 μM of each primer, and 1 μL of template DNA. Further details, such as primer sequences and PCR conditions are shown in Table S.V.7. Clones with archaeal, bacterial and bathyarchaeotal 16S rRNA gene (Yu et al., 2017) were

used for standard curve construction. The R^2 and efficiency of each individual qPCR assay are shown in Table S.V.7.

The mean doubling times (T) of Bathyarchaeota were calculated according to the formula: $T = (T_2 - T_1) / (\log_2 X_2 - \log_2 X_1)$ or $T = (T_2 - T_1) / [3.322 (\lg X_2 - \lg X_1)]$, which is generated from the formula $X_1 \times 2^{(T2-T1)/T} = X_2$. X_1 and X_2 are the bathyarchaeotal abundance at incubation time T_1 and T_2, respectively.

V.4.5. Illumina sequencing and data analysis

Since bathyarchaeotal growth was only observed in treatments to which lignin had been added as a growth substrate, only original sample (t_0); lignin cultures (IC+lignin ($t_{3.5}$), IC+lignin (t_6) × 2,^{13}C-IC+lignin (t_6) × 2, IC+lignin (t_{11}) × 2, ^{13}C-IC+lignin (t_{11}) × 2) and control cultures (IC ($t_{3.5}$), IC (t_6) × 2,^{13}C-IC (t_6) × 2, IC (t_{11}) × 2, ^{13}C-IC (t_{11}) × 2; a total of 19 samples) were processed for archaeal 16S rRNA genes sequencing. The hypervariable V4 regions of archaeal 16S rRNA genes were amplified using primer sets (U519F/Arch806R, Table S.V.7; Song et al., 2013) from original and enrichment samples. Each reaction solution (50 μL) contained 10×PCR buffer, dNTPs (100 μM each), 0.25 μM of each primer, 2.5 U of DNA polymerase (Ex-Taq; TaKaRa, Dalian, China) and approximately 10 ng of total DNA (measured by NanoDrop 2000). PCR products were purified using an E.Z.N.A. Gel Extraction Kit (Omega Bio-Tek, USA) according to manufacturer's instructions.

The 16S rRNA gene amplicons containing unique 8-mer barcodes used for each sample were pooled at equal concentrations, and sequenced on the Illumina Miseq platform using 2 × 250 bp cycles and the MiSeq Reagent Kit v2 (500 cycle, Illumina, USA) according to manufacturer's instructions. Raw reads were removed if they contained a 50 bp continuous fragment with an average quality score of less than 30 and/or any ambiguities. Filtered reads were merged together using FLASH (Version 1.2.6; Magoč and Salzberg. 2011). Further analysis was performed using the QIIME standard pipeline (Caporaso et al., 2010). In particular, sequence reads were first filtered to remove low-quality or ambiguous reads, and chimeric sequences were removed using the UCHIME program (Version 4.2; Edgar et al., 2011). The sequences were clustered into operational taxonomic units (OTUs) using UCLUST (Edgar et al., 2011) with a 97% sequence identity threshold. Taxonomy was assigned using the Greengenes database (version gg_13_5, http://greengenes.secondgenome.com/). The obtained archaeal sequences from each sample were randomly subsampled to generate a uniform depth of 10,372 sequences. Species richness, species diversity, and coverage were computed using QIIME's alpha diversity pipeline. Five metrics were calculated, including

observed number of species, coverage (through rarefaction analyses), Chao1, Shannon index, and Simpson index. The number of archaeal sequences in the above mentioned 19 samples (ranged from 10425 to 33848 (Table S.V.8). The number of archaeal operation taxonomic units (OTUs; cut-off, 97%) in these 19 sediment samples ranged from 423 to 869. The coverage calculation indicated that the analyzed sequences covered the diversity of archaeal populations in the investigated samples (Table S.V.8).

V.4.6. Phylogenetic analyses

From the Illumina MiSeq data set, OTUs affiliated to Bathyarchaeota which contained more than 100 sequences were selected for phylogenetic analyses, and closest phylogenetic affiliations determined by constructing a bathyarchaeotal 16S rRNA gene tree using reference sequences of the 17 bathyarchaeotal subgroups (Kubo et al., 2012) as phylogenetic anchors. For the construction of the phylogenic tree, the sequences were aligned using CLUSTALX 1.83, and the reference sequences were trimmed and retain 900bp after alignment. Neighbor-joining phylogenetic trees were constructed from pairwise comparisons with the Kimura 2-parameter distance model using the molecular evolutionary genetics analysis (MEGA) program (version 6; Tamura et al., 2013). Bootstrap values are based on 1,000 replicates for testing the robustness of the inferred topology. iTOL (http://itol.embl.de/) was used to modify the phylogenetic trees.

V.4.7. Data deposition

Sequences of Illumina sequencing raw data and sequences performed in phylogenetic analyses were submitted to GenBank under accession numbers PRJNA398600--PRJNA398689.

V.4.8. Lipid extraction and analyses

The total lipid extracts (TLEs) were extracted from lyophilized samples (~1 g) by a modified Bligh and Dyer method (Sturt et a., 2004). For the samples at t_6, a TLE aliquot of 90% was chemically treated to convert di- and tetraether lipids into their hydrocarbon derivatives phytane and several biphytanes with 0 to 3 rings via ether cleavage methods (Liu et al., 2012). For samples that had been incubated for 11 months, intact polar archaeal lipid fractions were first purified by preparative HPLC with fraction collector (Zhu et al., 2013), and then converted to hydrocarbon derivatives according to the above method (Liu et al., 2012). The $\delta^{13}C$ values of archaeal intact polar lipid derivatives were determined on a Thermo Finnigan Trace GC connected to a DELTA Plux XP isotope ratio mass spectrometer via GC combustion III

interface (both from ThermoFisher, Bremen, Germany) according to the method described by Kellermann et al. (2012)

Acknowledgements

The authors thank Karl O Stetter (Regensburg U), Hongbo Yu (Huazhong University of Science & Technology) for kind suggestions to improve the manuscript. Jiahua Wang from Shanghai Jiao Tong University helped with the metagenome analysis. This work was financially supported by the State Key R&D project of China [grant Number 2016YFA0601102], the Natural Science Foundation of China [grant numbers 41525011, 91228201, 91428308], and the Deutsche Forschungsgemeinschaft through the Gottfried Wilhelm Leibniz Program (award to K.H.; Hi 616-14-1). This study is also a contribution to the international IMBER project and the Deep Carbon Observatory.

Author contributions

T.Y., W.W., K.H., and F.W. designed experiment and analysis. T.Y., W.W., M.A.L., K.H., and F.W interpreted data. T.Y., W.W. performed experiments with the assistance of W.L.. T.Y., W.W., M.A.L., K.H., and F.W. wrote the manuscript together.

Competing financial interests

The authors declare no financial competing interests.

Chapter VI

Conclusion & Outlook

VI. Conclusion

Microbial-driven mineralization of organic matter (OM) in marine sediment is an essential cornerstone of the global carbon cycle because this process ultimately determines the short- or long-term burial of OM over geological timescales. However, the activities, metabolisms and functions of benthic microbes are poorly constrained. Generally, shallow coastal marine sediments harbor more microbes compared with the deep subseafloor due to continuous supply of terrestrially-derived OM.

Lipid-based stable isotope probing (SIP) method is conducive to investigating the microbially-deriven fluxes of biogeochemical carbon cycle, exploring microbial community and determining the potential microbial metabolisms in the marine sediments. Compared to conventional SIP methods using ^{13}C- or ^{15}N-labelled substrates, the dual SIP method with D_2O and ^{13}C-bicarbonate offers several advantages. Firstly, the addition of labelled organic substrates may distort in situ nutritional environment, whereas water and bicarbonate are plentiful in marine sediments and most natural systems. Secondly, because water is required by all organisms, regardless of their metabolism, D incorporation can estimate the total microbial activity. Lastly, the ratio of ^{13}C vs D incorporation rates into microbial lipids ($R^{13}C/D$) can distinguish predominantly heterotrophic versus autotrophic microbial metabolisms. With regard to the latter point, Wegener et al. (2012; 2016) reported $R^{13}C/D$ values of ~1 for autotrophy vs < 0.3 for heterotrophy, based on the cultivation of sulfate-reducing bacteria *Desulfosarcina variabilis*. However, the contribution of water-hydrogen to microbial lipids among species is highly variable, e.g., >90% for *Eudorina unicocca* (Zhang et al., 2009b) vs. ~60% for *E. coli* when grown on glucose (Zhang et al., 2009a). Furthermore, the investigation of water-hydrogen contribution to archaeal lipids is scarce, and only hydrogen isotope composition of archaeal lipids by *Haloarcula marismortui* has been published (Dirghangi et al., 2013) from the ongoing project "*Fractome*"[1] project by Caltech.

To investigate the implications of $R^{13}C/D$ for archaeal metabolism, the methanogic archaeon *Methanosarcina barkeri* was cultivated under autotrophic or heterotrophic conditions amended with D_2O and ^{13}C-bicarbonate (**Chapter II**). The results indicate that extent of inorganic carbon and water H incorporation into *M. barkier* cell membrane lipids varied with carbon substrate. Specifically, the contributions of inorganic carbon to lipids biosynthesis were 86.8±7.4%, 19.6±2.2% and 41.2±6.7% for growth on H_2/CO_2, acetate or methanol, respectively, and, the proportion of water-derived hydrogen to lipid biosynthesis was 35.7±4.2%, 22.6±2.3% and 39.3±2.9%. After correcting for the water fractionation factor, $R^{13}C/D$ may be used as a proxy of archaeal metabolism according to the criteria established by Wegener et al. (2012). This finding highlights the importance of determining the water-hydrogen contribution to microbial lipids for estimating microbial lipid production rates.

[1] http://fractome.caltech.edu

The dual SIP method with D_2O and ^{13}C-bicarbonate was also applied to investigate the microbial activity in shallow surface marine sediments collected from an intertidal flat Janssand (Wadden Sea, Germany; **Chapter III**) and the Rhône river prodelta (Gulf of Lions, France; **Chapter IV**). Under natural conditions with sulfate-replete artificial seawater, incorporation of D_2O and ^{13}C-IC into bacterial fatty acids was faster than into archaeal intact polar di- and tetraether-derived hydrocarbons (i.e., phytane and biphytanes). The turnover time of bacterial lipids (3.2 to 21.3 years; avg. 8.6 years) in surface sediment under in situ sulfate-reducing conditions were much shorter than those of archaeal lipids (88 to 277 years; average 110 years). This quantitative measurement is consistent with previous, indirect assessments suggesting that bacteria are more active than archaea in surface sediments. Bacterial lipid production rates ($prod_{lipid}$) and assimilation of inorganic carbon into fatty acids ($assim_{IC}$) were also quantified (Fig. VI.1; JS and RH from this study, and fjord site from Wegener et al. 2012). Bacterial $prod_{lipid}$, which is a representative parameter of the total activity of bacterial communities, was related to the bioavailability of sedimentary OM. Bacterial $prod_{lipid}$ in surface sediment ranged from 0.8 to 6.4 µg g_{dw}^{-1} yr^{-1} (Fig. VI.1). In contrast to archaeal lipids, significant incorporation of inorganic carbon was observed into bacterial fatty acids with $assim_{IC}$ of 0.15 to 1.3 µg g_{dw}^{-1} yr^{-1} (avg. 0.3 µg g_{dw}^{-1} yr^{-1}; Fig. VI.1). Furthermore, the ratio $R^{13}C/D$ into bacterial fatty acids in surface sediment ranged from 0.07 to 0.23 (Fig. VI.1) under sulfate-replete conditions, indicating that heterotrophs were predominant, and dark inorganic carbon fixation by bacteria probably resulted from anapleurotic reactions during heterotrophic growth rather than chemoautotrophic fixation, as suggested recently by Dyksma et al. (2016)

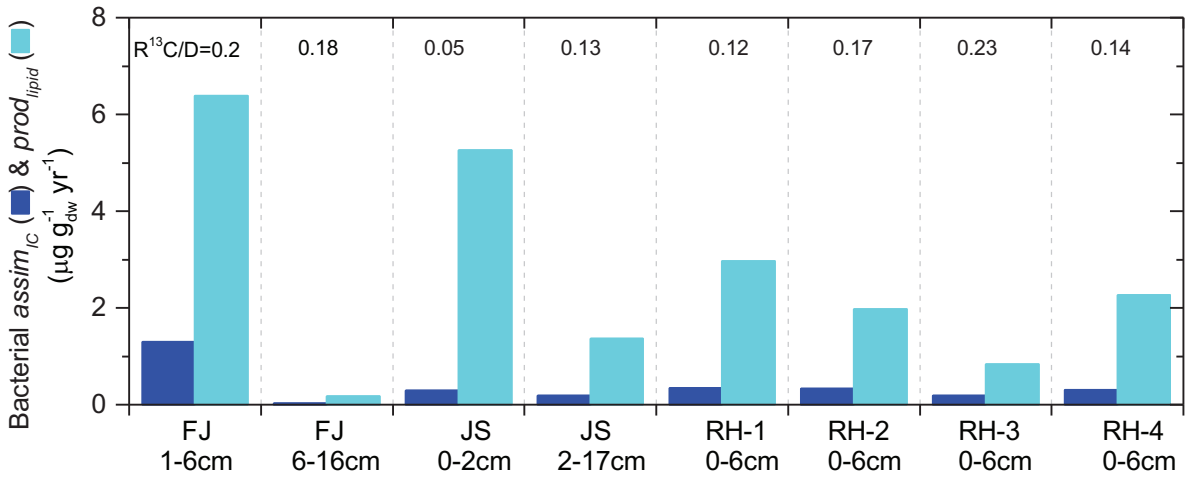

Fig. VI.1. The bacterial lipid production rates ($prod_{lipid}$; cyan) and the assimilation rates of inorganic carbon into bacterial lipids ($assim_{IC}$; blue) in the surface sediments from different sites. FJ: Himmersfjärden (Wegener et al., 2012); JS: Janssand (from **Chapter III**); RH: Rhône River prodelta (from **Chapter IV**), RH-1, RH-2, RH-3, RH-4 are sites GeoB17306, 17307, 17308 and 17305, respectively. $R^{13}C/D$ refers the ratio of $assim_{IC}$ to $prod_{lipid}$, and reveal the microbial metabolism (~ 1 for autotrophy; < 0.3 for heterotrophy).

To further explore the potential for inorganic carbon assimilation among Archaea, in particular Bathyarchaeota the most abundant microorganism in marine sediment (**Chapter IV**), diverse organic substrates (i.e., casein, oleic acid, cellulose, phenol and lignin) were added to the surface sediment collected from Hangzhou Bay (East China Sea, China). After long time incubation (i.e., 11 months), Bathyarchaeota was significantly stimulated only by the addition of lignin, with estimated doubling times of

~2 to 3 months based on gene copy numbers. Meanwhile, putative bathyarchaeotal tetraether lipids incorporated ^{13}C from ^{13}C-bicarbonate only when added in concert with lignin. This indicates that Bathyarchaeota can utilize refractory lignin as energy source and inorganic carbon as carbon source.

The inorganic carbon fixation by heterotrophic microorganisms in marine sediment may be related to anapleurotic (or replenishing) reactions during citric acid cycle (Kornberg, 1965; Thauer, 1988), acetogenesis pathways (Drake et al., 2008; Lever et al., 2010) and enzyme reversibility (Holler et al., 2011). This study emphasizes the importance of inorganic carbon fixation during heterotrophic growth for bacteria and archaea in the marine sediments, and this process therefore should be considered for constraining sedimentary carbon flux.

VI. Outlook

The contribution of water-hydrogen to microbial lipids is the main factor to constrain the application of D_2O labelling method to quantitatively assess microbial activity in environmental settings. Although the methanogen *M. barkeri* was investigated, the contribution of water-hydrogen to more diverse archaea are further required, potential candidates for example being Thaumarchaeota as representative planktonic archaea in the ocean (Könneke et al., 2005), and Bathyarchaeota as most abundant in marine sediment (He et al., 2016). In addition, defining the factors controlling water-hydrogen contribution to microbial lipids such as temperature, growth phase and metabolic process are also required. The survey of water H to microbial lipids can be further used to validate $R^{13}C/D$ as a proxy to distinguish microbial metabolisms.

By using lipid-based SIP approaches, microbial activity in surface marine sediment was investigated in this thesis. However, due to the limited study sites, the main factor controlling microbial activity such as total organic carbon, the types of sedimentary OM, bioavailability of sedimentary OM, or electron acceptors remains enigmatic. Thus, comprehensive investigations of microbial activity on surface sediment from different sites are necessary, as they would be conducive to understand the microbial role in early diagenesis of OM in marine sediment. In addition, quantitative comparison of microbial activity in between surface and subsurface sediments is also required because it is helpful to understand the effect of lability of OM on microbial activity.

Based on $R^{13}C/D$ values of lipids, it is hypothesized that dark inorganic carbon fixation is an important consequence of heterotrophic growth. However, the inorganic carbon contribution to other microbial components such as proteins and nucleic acids remains poorly understood. If inorganic carbon is also required for heterotrophic microbial biomass in marine sediment, and this contribution isn't negligible, dark inorganic carbon fixation may be an important component for OM mineralization in marine sediment, and the OM mineralization rates are required to be re-estimated. Protein- and nucleic acid-based SIP method should provide new insights into carbon utilization by microbes in marine sediments.

References

1. Adhikari, R.R. and Kallmeyer, J. (2010) Detection and quantification of microbial activity in the subsurface. Chemie der Erde - Geochemistry 70, Supplement 3, 135-143.
2. Adhikari, R.R., Glombitza, C., Nickel, J.C., Anderson, C.H., Dunlea, A.G., Spivack, A.J., Murray, R.W., D'Hondt, S. and Kallmeyer, J. (2016) Hydrogen utilization potential in subsurface sediments. Frontiers in Microbiology 7, 8.
3. Allen, M.A., Lauro, F.M., Williams, T.J., Burg, D., Siddiqui, K.S., De Francisci, D., Chong, K.W.Y., Pilak, O., Chew, H.H., De Maere, M.Z., Ting, L., Katrib, M., Ng, C., Sowers, K.R., Galperin, M.Y., Anderson, I.J., Ivanova, N., Dalin, E., Martinez, M., Lapidus, A., Hauser, L., Land, M., Thomas, T. and Cavicchioli, R. (2009) The genome sequence of the psychrophilic archaeon, *Methanococcoides burtonii*: the role of genome evolution in cold adaptation. ISME J 3, 1012-1035.
4. Antonovsky, N., Gleizer, S., Noor, E., Zohar, Y., Herz, E., Barenholz, U., Zelcbuch, L., Amram, S., Wides, A., Tepper, N., Davidi, D., Bar-On, Y., Bareia, T., Wernick, David G., Shani, I., Malitsky, S., Jona, G., Bar-Even, A. and Milo, R. (2016) Sugar synthesis from CO_2 in *Escherichia coli*. Cell 166, 115-125.
5. Baik, K.S., Park, S.C., Lim, C.H., Lee, K.H., Jeon, D.Y., Kim, C.M. and Seong, C.N. (2010) *Psychrobacter aestuarii* sp. nov., isolated from a tidal flat sediment. International Journal of Systematic and Evolutionary Microbiology 60, 1631-1636.
6. Beck, M., Köster, J., Engelen, B., Holstein, J., Gittel, A., Könneke, M., Riedel, T., Wirtz, K., Cypionka, H., Rullkötter, J. and Brumsack, H.-J. (2009) Deep pore water profiles reflect enhanced microbial activity towards tidal flat margins. Ocean Dynamics 59, 371-383.
7. Beck, M. and Brumsack, H.-J. (2012) Biogeochemical cycles in sediment and water column of the Wadden Sea: The example Spiekeroog Island in a regional context. Ocean & Coastal Management 68, 102-113.
8. Beck, M., Reckhardt, A., Amelsberg, J., Bartholomä, A., Brumsack, H.-J., Cypionka, H., Dittmar, T., Engelen, B., Greskowiak, J., Hillebrand, H., Holtappels, M., Neuholz, R., Köster, J., Kuypers, M.M.M., Massmann, G., Meier, D., Niggemann, J., Paffrath, R., Pahnke, K., Rovo, S., Striebel, M., Vandieken, V., Wehrmann, A. and Zielinski, O. (2017) The drivers of biogeochemistry in beach ecosystems: A cross-shore transect from the dunes to the low-water line. Marine Chemistry 190, 35-50.
9. Berg, I.A., Kockelkorn, D., Buckel, W. and Fuchs, G. (2007) A 3-hydroxypropionate/4-hydroxybutyrate autotrophic carbon dioxide assimilation pathway in Archaea. Science 318, 1782-1786.
10. Berg, I.A., Kockelkorn, D., Ramos-Vera, W.H., Say, R.F., Zarzycki, J., Hügler, M., Alber, B.E. and Fuchs, G. (2010a) Autotrophic carbon fixation in archaea. Nature Reviews Microbiology 8, 447-460.
11. Berg, I.A., Ramos-Vera, W.H., Petri, A., Huber, H. and Fuchs, G. (2010b) Study of the distribution of autotrophic CO_2 fixation cycles in Crenarchaeota. Microbiology 156, 256-269.
12. Berner, R.A. (1989) Biogeochemical cycles of carbon and sulfur and their effect on atmospheric oxygen over Phanerozoic time. Palaeogeography, Palaeoclimatology, Palaeoecology 75, 97-122.
13. Berry, D., Mader, E., Lee, T.K., Woebken, D., Wang, Y., Zhu, D., Palatinszky, M., Schintlmeister, A., Schmid, M.C., Hanson, B.T., Shterzer, N., Mizrahi, I., Rauch, I., Decker, T., Bocklitz, T., Popp, J., Gibson, C.M., Fowler, P.W., Huang, W.E. and Wagner, M. (2015) Tracking heavy water (D_2O) incorporation for identifying and sorting active microbial cells. Proceedings of the National Academy of Sciences of the United States of America 112, E194-E203.

14. Bianchi, T.S., Engelhaupt, E., McKee, B.A., Miles, S., Elmgren, R., Hajdu, S., Savage, C. and Baskaran, M. (2002) Do sediments from coastal sites accurately reflect time trends in water column phytoplankton? A test from Himmerfjärden Bay (Baltic Sea proper). Limnology and Oceanography 47, 1537-1544.
15. Bianchi, T.S. (2011) The role of terrestrially derived organic carbon in the coastal ocean: A changing paradigm and the priming effect. Proceedings of the National Academy of Sciences of the United States of America 108, 19473-19481.
16. Biddle, J.F., Lipp, J.S., Lever, M.A., Lloyd, K.G., Sorensen, K.B., Anderson, R., Fredricks, H.F., Elvert, M., Kelly, T.J., Schrag, D.P., Sogin, M.L., Brenchley, J.E., Teske, A., House, C.H. and Hinrichs, K.U. (2006) Heterotrophic Archaea dominate sedimentary subsurface ecosystems off Peru. Proceedings of the National Academy of Sciences of the United States of America 103, 3846-3851.
17. Billerbeck, M., Werner, U., Bosselmann, K., Walpersdorf, E. and Huettel, M. (2006a) Nutrient release from an exposed intertidal sand flat. Marine Ecology Progress Series 316, 35-51.
18. Billerbeck, M., Werner, U., Polerecky, L., Walpersdorf, E., deBeer, D. and Huettel, M. (2006b) Surficial and deep pore water circulation governs spatial and temporal scales of nutrient recylcing in intertidal sand flat sediment. Marine Ecology Progress Series 326, 61-76.
19. Blaser, M.B., Dreisbach, L.K. and Conrad, R. (2015) Carbon isotope fractionation of *Thermoanaerobacter kivui* in different growth media and at different total inorganic carbon concentration. Organic Geochemistry 81, 45-52.
20. Boschker, H.T.S., Nold, S.C., Wellsbury, P., Bos, D., der Graaf, W., Pel, R., Parkes, R.J. and Cappenberg, T.E. (1998) Direct linking of microbial populations to specific biogeochemical processess by ^{13}C-labelling of biomarkers. Nature 392, 801-805.
21. Boschker, H.T.S. and Middelburg, J.J. (2002) Stable isotopes and biomarkers in microbial ecology. FEMS Microbiology Ecology 40, 85-95.
22. Boschker, H.T.S., Vasquez-Cardenas, D., Bolhuis, H., Moerdijk-Poortvliet, T.W.C. and Moodley, L. (2014) Chemoautotrophic carbon fixation rates and active acterial communities in intertidal marine sediments. PLoS ONE 9, e101443.
23. Bourgeois, S., Pruski, A.M., Sun, M.Y., Buscail, R., Lantoine, F., Kerhervé, P., Vétion, G., Rivière, B. and Charles, F. (2011) Distribution and lability of land-derived organic matter in the surface sediments of the Rhône prodelta and the adjacent shelf (Mediterranean Sea, France): a multi proxy study. Biogeosciences 8, 3107-3125.
24. Bowles, M.W., Mogollón, J.M., Kasten, S., Zabel, M. and Hinrichs, K.-U. (2014) Global rates of marine sulfate reduction and implications for sub–sea-floor metabolic activities. Science 344, 889-891.
25. Braun, S., Mhatre, S.S., Jaussi, M., Røy, H., Kjeldsen, K.U., Pearce, C., Seidenkrantz, M.-S., Jørgensen, B.B. and Lomstein, B.A. (2017) Microbial turnover times in the deep seabed studied by amino acid racemization modelling. Scientific Reports 7, 5680.
26. Breuker, A., Stadler, S. and Schippers, A. (2013) Microbial community analysis of deeply buried marine sediments of the New Jersey shallow shelf (IODP Expedition 313). FEMS Microbiology Ecology 85, 578-592.
27. Brinch-Iversen, J. and King, G.M. (1990) Effects of substrate concentration, growth state, and oxygen availability on relationships among bacterial carbon, nitrogen and phospholipid phosphorus content. FEMS Microbiology Letters 74, 345-355.
28. Brochier-Armanet, C., Boussau, B., Gribaldo, S. and Forterre, P. (2008) Mesophilic crenarchaeota: proposal for a third archaeal phylum, the Thaumarchaeota. Nature Reviews Microbiology 6, 245-252.
29. Buckel, W. and Thauer, R.K. (2013) Energy conservation via electron bifurcating ferredoxin reduction and proton/Na^+ translocating ferredoxin oxidation. Biochimica et Biophysica Acta (BBA) - Bioenergetics 1827, 94-113.
30. Canfield, D.E. (1989) Sulfate reduction and oxic respiration in marine sediments: implications for organic carbon preservation in euxinic environments. Deep Sea Research Part A. Oceanographic Research Papers 36, 121-138.

31. Canfield, D.E., Jørgensen, B.B., Fossing, H., Glud, R., Gundersen, J., Ramsing, N.B., Thamdrup, B., Hansen, J.W., Nielsen, L.P. and Hall, P.O.J. (1993) Pathways of organic carbon oxidation in three continental margin sediments. Marine Geology 113, 27-40.
32. Canfield, D.E. and Thamdrup, B. (2009) Towards a consistent classification scheme for geochemical environments, or, why we wish the term 'suboxic' would go away. Geobiology 7, 385-392.
33. Caporaso, J.G., Kuczynski, J., Stombaugh, J., Bittinger, K., Bushman, F.D., Costello, E.K., Fierer, N., Pena, A.G., Goodrich, J.K., Gordon, J.I., Huttley, G.A., Kelley, S.T., Knights, D., Koenig, J.E., Ley, R.E., Lozupone, C.A., McDonald, D., Muegge, B.D., Pirrung, M., Reeder, J., Sevinsky, J.R., Turnbaugh, P.J., Walters, W.A., Widmann, J., Yatsunenko, T., Zaneveld, J. and Knight, R. (2010) QIIME allows analysis of high-throughput community sequencing data. Nature Methods 7, 335-336.
34. Cathalot, C., Rabouille, C., Pastor, L., Deflandre, B., Viollier, E., Buscail, R., Grémare, A., Treignier, C. and Pruski, A. (2010) Temporal variability of carbon recycling in coastal sediments influenced by rivers: assessing the impact of flood inputs in the Rhône River prodelta. Biogeosciences 7, 1187-1205.
35. Cathalot, C., Rabouille, C., Tisnérat-Laborde, N., Toussaint, F., Kerhervé, P., Buscail, R., Loftis, K., Sun, M.Y., Tronczynski, J., Azoury, S., Lansard, B., Treignier, C., Pastor, L. and Tesi, T. (2013) The fate of river organic carbon in coastal areas: A study in the Rhône River delta using multiple isotopic ($\delta^{13}C$, $\Delta^{14}C$) and organic tracers. Geochimica et Cosmochimica Acta 118, 33-55.
36. Chan, M., Himes, R.H. and Akagi, J.M. (1971) Fatty Acid Composition of Thermophilic, Mesophilic, and Psychrophilic Clostridia. Journal of Bacteriology 106, 876-881.
37. D'Hondt, S., Jørgensen, B.B., Miller, D.J., Batzke, A., Blake, R., Cragg, B.A., Cypionka, H., Dickens, G.R., Ferdelman, T., Hinrichs, K.U., Holm, N.G., Mitterer, R., Spivack, A., Wang, G., Bekins, B., Engelen, B., Ford, K., Gettemy, G., Rutherford, S.D., Sass, H., Skilbeck, C.G., Aiello, I.W., Guerin, G., House, C.H., Inagaki, F., Meister, P., Naehr, T., Niitsuma, S., Parkes, R.J., Schippers, A., Smith, D.C., Teske, A., Wiegel, J., Padilla, C.N. and Acosta, J.L. (2004) Distributions of microbial activities in deep subseafloor sediments. Science 306, 2216-2221.
38. D'Hondt, S., Spivack, A.J., Pockalny, R., Ferdelman, T.G., Fischer, J.P., Kallmeyer, J., Abrams, L.J., Smith, D.C., Graham, D., Hasiuk, F., Schrum, H. and Stancin, A.M. (2009) Subseafloor sedimentary life in the South Pacific Gyre. Proceedings of the National Academy of Sciences of the United States of America 106, 11651-11656.
39. Dai, Z.-J., Liu, J.T., Xie, H.-L. and Shi, W.-Y. (2014) Sedimentation in the outer Hangzhou Bay, China: The influence of Changjiang sediment load. Journal of Coastal Research, 1218-1225.
40. Damare, S., Raghukumar, C. and Raghukumar, S. (2006) Fungi in deep-sea sediments of the central Indian Basin. Deep Sea Research Part I: Oceanographic Research Papers 53, 14-27.
41. Dick, G.J., Andersson, A.F., Baker, B.J., Simmons, S.L., Thomas, B.C., Yelton, A.P. and Banfield, J.F. (2009) Community-wide analysis of microbial genome sequence signatures. Genome Biology 10, R85.
42. Dirghangi, S.S. and Pagani, M. (2013) Hydrogen isotope fractionation during lipid biosynthesis by *Haloarcula marismortui*. Geochimica et Cosmochimica Acta 119, 381-390.
43. Drake, H.L., Gossner, A.S. and Daniel, S.L. (2008) Old acetogens, new light. Annals of the New York Academy of Sciences 1125, 100-128.
44. Dumont, M.G. and Murrell, J.C. (2005) Stable isotope probing -- linking microbial identity to function. Nature Reviews Microbiology 3, 499-504.
45. Dyksma, S., Bischof, K., Fuchs, B.M., Hoffmann, K., Meier, D., Meyerdierks, A., Pjevac, P., Probandt, D., Richter, M., Stepanauskas, R. and Mußmann, M. (2016) Ubiquitous *Gammaproteobacteria* dominate dark carbon fixation in coastal sediments. The ISME Journal 10, 1939-1953.

46. Edgar, R.C., Haas, B.J., Clemente, J.C., Quince, C. and Knight, R. (2011) UCHIME improves sensitivity and speed of chimera detection. Bioinformatics 27, 2194-2200.
47. Edgcomb, V.P., Beaudoin, D., Gast, R., Biddle, J.F. and Teske, A. (2011) Marine subsurface eukaryotes: the fungal majority. Environmental Microbiology 13, 172-183.
48. Eikmanns, B. and Thauer, R. (1984) Catalysis of an isotopic exchange between CO_2 and the carboxyl group of acetate by *Methanosarcina barkeri* grown on acetate. Archives of Microbiology 138, 365-370.
49. Ekiel, I., Smith, I. and Sprott, G.D. (1983) Biosynthetic pathways in *Methanospirillum hungatei* as determined by ^{13}C nuclear magnetic resonance. Journal of Bacteriology 156, 316-326.
50. Elling, F.J., Könneke, M., Lipp, J.S., Becker, K.W., Gagen, E.J. and Hinrichs, K.-U. (2014) Effects of growth phase on the membrane lipid composition of the thaumarchaeon *Nitrosopumilus maritimus* and their implications for archaeal lipid distributions in the marine environment. Geochimica et Cosmochimica Acta 141, 579-597.
51. Elvert, M., Suess, E., Greinert, J. and Whiticar, M.J. (2000) Archaea mediating anaerobic methane oxidation in deep-sea sediments at cold seeps of the eastern Aleutian subduction zone. Organic Geochemistry 31, 1175-1187.
52. Elvert, M., Boetius, A., Knittel, K. and Jørgensen, B.B. (2003) Characterization of specific membrane fatty acids as chemotaxonomic markers for sulfate-reducing bacteria Involved in anaerobic oxidation of methane. Geomicrobiology Journal 20, 403-419.
53. Engelhardt, T., Sahlberg, M., Cypionka, H. and Engelen, B. (2013) Biogeography of *Rhizobium radiobacter* and distribution of associated temperate phages in deep subseafloor sediments. ISME J 7, 199-209.
54. Englebrecht, A.C. and Sachs, J.P. (2005) Determination of sediment provenance at drift sites using hydrogen isotopes and unsaturation ratios in alkenones. Geochimica et Cosmochimica Acta 69, 4253-4265.
55. Evans, P.N., Parks, D.H., Chadwick, G.L., Robbins, S.J., Orphan, V.J., Golding, S.D. and Tyson, G.W. (2015) Methane metabolism in the archaeal phylum Bathyarchaeota revealed by genome-centric metagenomics. Science 350, 434-438.
56. Fagervold, S.K., Bourgeois, S., Pruski, A.M., Charles, F., Kerherve, P., Vetion, G. and Galand, P.E. (2014) River organic matter shapes microbial communities in the sediment of the Rhone prodelta. ISME J 8, 2327-2338.
57. Feisthauer, S., Wick, L.Y., Kästner, M., Kaschabek, S.R., Schlömann, M. and Richnow, H.H. (2008) Differences of heterotrophic $^{13}CO_2$ assimilation by *Pseudomonas knackmussii* strain B13 and *Rhodococcus opacus* 1CP and potential impact on biomarker stable isotope probing. Environmental Microbiology 10, 1641-1651.
58. Ferry, J.G. and Lessner, D.J. (2008) Methanogenesis in marine sediments. Annals of the New York Academy of Sciences 1125, 147-157.
59. Fillol, M., Auguet, J.-C., Casamayor, E.O. and Borrego, C.M. (2016) Insights in the ecology and evolutionary history of the *Miscellaneous Crenarchaeotic Group* lineage. ISME J 10, 665-677.
60. Freese, E., Sass, H., Rütters, H., Schledjewski, R. and Rullkötter, J. (2008) Variable temperature-related changes in fatty acid composition of bacterial isolates from German Wadden sea sediments representing different bacterial phyla. Organic Geochemistry 39, 1427-1438.
61. Froelich, P.N., Klinkhammer, G.P., Bender, M.L., Luedtke, N.A., Heath, G.R., Cullen, D., Dauphin, P., Hammond, D., Hartman, B. and Maynard, V. (1979) Early oxidation of organic matter in pelagic sediments of the eastern equatorial Atlantic: suboxic diagenesis. Geochimica et Cosmochimica Acta 43, 1075-1090.
62. Gagen, E.J., Huber, H., Meador, T., Hinrichs, K.U. and Thomm, M. (2013) Novel cultivation-based approach to understanding the miscellaneous crenarchaeotic group (MCG) archaea from sedimentary ecosystems. Applied and Environmental Microbiology 79, 6400-6406.

63. Gebhardt, N.A., Linder, D. and Thauer, R.K. (1983) Anaerobic acetate oxidation to CO_2 by *Desulfobacter postgatei*. Archives of Microbiology 136, 230-233.
64. Gill, I. and Valivety, R. (1997) Polyunsaturated fatty acids, part 1: Occurrence, biological activities and applications. Trends in Biotechnology 15, 401-409.
65. Girguis, P.R., Orphan, V.J., Hallam, S.J. and DeLong, E.F. (2003) Growth and methane oxidation rates of anaerobic methanotrophic Archaea in a continuous-flow bioreactor. Applied and Environmental Microbiology 69, 5472-5482.
66. Goldhammer, T., Brunner, B., Bernasconi, S.M., Ferdelman, T.G. and Zabel, M. (2011) Phosphate oxygen isotopes: Insights into sedimentary phosphorus cycling from the Benguela upwelling system. Geochimica et Cosmochimica Acta 75, 3741-3756.
67. Harmelin-Vivien, M., Loizeau, V., Mellon, C., Beker, B., Arlhac, D., Bodiguel, X., Ferraton, F., Hermand, R., Philippon, X. and Salen-Picard, C. (2008) Comparison of C and N stable isotope ratios between surface particulate organic matter and microphytoplankton in the Gulf of Lions (NW Mediterranean). Continental Shelf Research 28, 1911-1919.
68. Harmelin-Vivien, M., Dierking, J., Bănaru, D., Fontaine, M.F. and Arlhac, D. (2010) Seasonal variation in stable C and N isotope ratios of the Rhone River inputs to the Mediterranean Sea (2004–2005). Biogeochemistry 100, 139-150.
69. Harvey, H.R., Fallon, R.D. and Patton, J.S. (1986) The effect of organic matter and oxygen on the degradation of bacterial membrane lipids in marine sediments. Geochimica et Cosmochimica Acta 50, 795-804.
70. Harvey, R.H., Tuttle, J.H. and Bell, T.J. (1995) Kinetics of phytoplankton decay during simulated sedimentation: Changes in biochemical composition and microbial activity under oxic and anoxic conditions. Geochimica et Cosmochimica Acta 59, 3367-3377.
71. Hayes, J. (1993) Factors controlling ^{13}C contents of sedimentary organic compounds: Principles and evidence. Marine Geology 113, 111-125.
72. Hayes, J. (2001) Fractionation of carbon and hydrogen isotopes in biosynthetic processes. Reviews in Mineralogy and Geochemistry 43, 225-277.
73. He, Y., Li, M., Perumal, V., Feng, X., Fang, J., Xie, J., Sievert, S. and Wang, F. (2016) Genomic and enzymatic evidence for acetogenesis among multiple lineages of the archaeal phylum Bathyarchaeota widespread in marine sediments. Nature Microbiology 1, 16035.
74. Hedges, J., Keil, R. and Benner, R. (1997) What happens to terrestrial organic matter in the ocean? Organic Geochemistry 27, 195-212.
75. Hedges, J.I. and Keil, R.G. (1995) Sedimentary organic matter preservation: an assessment and speculative synthesis. Marine Chemistry 49, 81-115.
76. Heinzelmann, S.M., Villanueva, L., Sinke-Schoen, D., Damsté, J.S.S., Schouten, S. and Van der Meer, M.T. (2015) Impact of metabolism and growth phase on the hydrogen isotopic composition of microbial fatty acids. Frontiers in Microbiology 6, 408.
77. Heuer, V., Elvert, M., Tille, S., Krummen, M., Mollar, X.P., Hmelo, L.R. and Hinrichs, K.U. (2006) Online $\delta^{13}C$ analysis of volatile fatty acids in sediment/porewater systems by liquid chromatography-isotope ratio mass spectrometry. Limnology and Oceanography: Methods 4, 346-357.
78. Heuer, V., Aiello, I., Elvert, M., Goldenstein, N., Goldhammer, T., Könneke, M., Liu, X., Pape, S., Schmidt, F., Wendt, J. and Zhuang, G. (2014) Report and preliminary results of R/V POSEIDON cruise POS450, DARCSEAS II - Deep suseafloor Archaea in the Western Mediterranean sea: Carbon Cycle, Life Strategies, and Role in Sedimentary Ecosystem, Barcelona (Spain) - Malaga (Spain), April 2 - 13, 2013. Berichte, MARUM - Zentrum für Marine Unweltwissenschaften, Fachbereich Geowissenschaften, Universität Bremen No. 305, 42.
79. Heuer, V.B., Pohlman, J.W., Torres, M.E., Elvert, M. and Hinrichs, K.-U. (2009) The stable carbon isotope biogeochemistry of acetate and other dissolved carbon species in deep subseafloor sediments at the northern Cascadia Margin. Geochimica et Cosmochimica Acta 73, 3323-3336.

80. Higueras, M., Kerhervé, P., Sanchez-Vidal, A., Calafat, A., Ludwig, W., Verdoit-Jarraya, M., Heussner, S. and Canals, M. (2014) Biogeochemical characterization of the riverine particulate organic matter transferred to the NW Mediterranean Sea. Biogeosciences 11, 157-172.
81. Hinrichs, K.U., Hayes, J.M., Sylva, S.P., Brewer, P.G. and Delong, E.F. (1999) Methane-consuming archaebacteria in marine sediment. Science 398, 802-805.
82. Hoehler, T.M. and Jørgensen, B.B. (2013) Microbial life under extreme energy limitation. Nature Reviews Microbiology 11, 83-94.
83. Holler, T., Wegener, G., Niemann, H., Deusner, C., Ferdelman, T.G., Boetius, A., Brunner, B. and Widdel, F. (2011) Carbon and sulfur back flux during anaerobic microbial oxidation of methane and coupled sulfate reduction. Proceedings of the National Academy of Sciences of the United States of America 108, E1484–E1490.
84. Huang, H., Wang, S., Moll, J. and Thauer, R.K. (2012) Electron bifurcation involved in the energy metabolism of the acetogenic bacterium *Moorella thermoacetica* growing on glucose or H_2 plus CO_2. Journal of Bacteriology 194, 3689-3699.
85. Huber, H., Gallenberger, M., Jahn, U., Eylert, E., Berg, I.A., Kockelkorn, D., Eisenreich, W. and Fuchs, G. (2008) A dicarboxylate/4-hydroxybutyrate autotrophic carbon assimilation cycle in the hyperthermophilic Archaeum *Ignicoccus hospitalis*. Proceedings of the National Academy of Sciences of the United States of America 105, 7851-7856.
86. Hugler, M. and Sievert, S.M. (2011) Beyond the Calvin cycle: autotrophic carbon fixation in the ocean. Annual Review of Marine Science 3, 261-289.
87. Huguet, A., Meador, T.B., Laggoun-Défarge, F., Könneke, M., Wu, W., Derenne, S. and Hinrichs, K.-U. (2017) Production rates of bacterial tetraether lipids and fatty acids in peatland under varying oxygen concentrations. Geochimica et Cosmochimica Acta 203, 103-116.
88. Inagaki, F., Suzuki, M., Takai, K., Oida, H., Sakamoto, T., Aoki, K., Nealson, K.H. and Horikoshi, K. (2003) Microbial communities associated with geological horizons in coastal subseafloor sediments from the Sea of Okhotsk. Applied and Environmental Microbiology 69, 7224-7235.
89. Inagaki, F., Hinrichs, K.-U., Kubo, Y., Bowles, M.W., Heuer, V.B., Hong, W.-L., Hoshino, T., Ijiri, A., Imachi, H., Ito, M., Kaneko, M., Lever, M.A., Lin, Y.-S., Methé, B.A., Morita, S., Morono, Y., Tanikawa, W., Bihan, M., Bowden, S.A., Elvert, M., Glombitza, C., Gross, D., Harrington, G.J., Hori, T., Li, K., Limmer, D., Liu, C.-H., Murayama, M., Ohkouchi, N., Ono, S., Park, Y.-S., Phillips, S.C., Prieto-Mollar, X., Purkey, M., Riedinger, N., Sanada, Y., Sauvage, J., Snyder, G., Susilawati, R., Takano, Y., Tasumi, E., Terada, T., Tomaru, H., Trembath-Reichert, E., Wang, D.T. and Yamada, Y. (2015) Exploring deep microbial life in coal-bearing sediment down to ~2.5 km below the ocean floor. Science 349, 420-424.
90. Jahn, U., Summons, R., Sturt, H., Grosjean, E. and Huber, H. (2004) Composition of the lipids of *Nanoarchaeum equitans* and their origin from its host *Ignicoccus* sp. strain KIN4/I. Archives of Microbiology 182, 404-413.
91. Jain, S., Caforio, A. and Driessen, A.J.M. (2014) Biosynthesis of archaeal membrane ether lipids. Frontiers in Microbiology 5, 641.
92. Jehmlich, N., Vogt, C., Lünsmann, V., Richnow, H.H. and von Bergen, M. (2016) Protein-SIP in environmental studies. Current Opinion in Biotechnology 41, 26-33.
93. Jiang, L., Zheng, Y., Chen, J., Xiao, X. and Wang, F. (2011) Stratification of achaeal communities in shallow sediments of the Pearl River Estuary, Southern China. Antonie Van Leeuwenhoek 99, 739-751.
94. Johnson, M.S., Zhulin, I.B., Gapuzan, M.E. and Taylor, B.L. (1997) Oxygen-dependent growth of the obligate anaerobe *Desulfovibrio vulgaris* Hildenborough. Journal of Bacteriology 179, 5598-5601.
95. Jørgensen, B.B. (1978) A comparison of methods for the quantification of bacterial sulfate reduction in coastal marine sediments. Geomicrobiology Journal 1, 11-27.

96. Jørgensen, B.B. (1982) Mineralization of organic matter in the sea bed—the role of sulphate reduction. Nature 296, 643-645.
97. Jørgensen, B.B. and Marshall, I.P.G. (2016) Slow microbial life in the seabed. Annual Review of Marine Science 8, 311-332.
98. Jorgensen, S.L., Hannisdal, B., Lanzén, A., Baumberger, T., Flesland, K., Fonseca, R., Øvreås, L., Steen, I.H., Thorseth, I.H., Pedersen, R.B. and Schleper, C. (2012) Correlating microbial community profiles with geochemical data in highly stratified sediments from the Arctic Mid-Ocean Ridge. Proceedings of the National Academy of Sciences of the United States of America 109, E2846–E2855.
99. Kallmeyer, J., Pockalny, R., Adhikari, R.R., Smith, D.C. and D'Hondt, S. (2012) Global distribution of microbial abundance and biomass in subseafloor sediment. Proceedings of the National Academy of Sciences of the United States of America 109, 16213-16216.
100. Kaneda, T. (1991) Iso- and anteiso-fatty acids in bacteria: biosynthesis, function, and taxonomic significance. Microbiological Reviews 55, 288-302.
101. Kaneko, M., Kitajima, F. and Naraoka, H. (2011) Stable hydrogen isotope measurement of archaeal ether-bound hydrocarbons. Organic Geochemistry 42, 166-172.
102. Kellermann, M.Y., Wegener, G., Elvert, M., Yoshinaga, M.Y., Lin, Y.S., Holler, T., Mollar, X.P., Knittel, K. and Hinrichs, K.U. (2012) Autotrophy as a predominant mode of carbon fixation in anaerobic methane-oxidizing microbial communities. Proceedings of the National Academy of Sciences of the United States of America 109, 19321-19326.
103. Kellermann, M.Y., Yoshinaga, M.Y., Wegener, G., Krukenberg, V. and Hinrichs, K.-U. (2016) Tracing the production and fate of individual archaeal intact polar lipids using stable isotope probing. Organic Geochemistry 95, 13-20.
104. Kenealy, W.R. and Zeikus, J.G. (1982) One-carbon metabolism in methanogens: evidence for synthesis of a two-carbon cellular intermediate and unification of catabolism and anabolism in *Methanosarcina barkeri*. Journal of Bacteriology 151, 932-941.
105. Koga, Y. and Morii, H. (2007) Biosynthesis of ether-type polar lipids in archaea and evolutionary considerations. Microbiology and Molecular Biology Reviews 71, 97-120.
106. Koho, K., Nierop, K., Moodley, L., Middelburg, J., Pozzato, L., Soetaert, K., Van der Plicht, J. and Reichart, G.-J. (2013) Microbial bioavailability regulates organic matter preservation in marine sediments. Biogeosciences 10, 1131-1141.
107. Könneke, M., Schubert, D.M., Brown, P.C., Hugler, M., Standfest, S., Schwander, T., Schada von Borzyskowski, L., Erb, T.J., Stahl, D.A. and Berg, I.A. (2014) Ammonia-oxidizing archaea use the most energy-efficient aerobic pathway for CO_2 fixation. Proceedings of the National Academy of Sciences of the United States of America 111: 8239-8244.
108. Könneke, M., Lipp, J.S. and Hinrichs, K.-U. (2012) Carbon isotope fractionation by the marine ammonia-oxidizing archaeon Nitrosopumilus maritimus. Organic Geochemistry 48, 21-24.
109. Kopf, S.H., McGlynn, S.E., Green-Saxena, A., Guan, Y., Newman, D.K. and Orphan, V.J. (2015) Heavy water and ^{15}N labeling with NanoSIMS analysis reveals growth-rate dependent metabolic heterogeneity in chemostats. Environmental Microbiology 17, 2542-2556.
110. Kopf, S.H., Sessions, A.L., Cowley, E.S., Reyes, C., Van Sambeek, L., Hu, Y., Orphan, V.J., Kato, R. and Newman, D.K. (2016) Trace incorporation of heavy water reveals slow and heterogeneous pathogen growth rates in cystic fibrosis sputum. Proceedings of the National Academy of Sciences of the United States of America 113, E110-E116.
111. Kornberg, H.L. (1965) Anaplerotic sequences in microbial metabolism. Angewandte Chemie International Edition 4, 558-565.

112. Kreuzer-Martin, H.W., Lott, M.J., Ehleringer, J.R. and Hegg, E.L. (2006) Metabolic processes account for the majority of the intracellular water in log-phase *Escherichia coli* Cells as revealed by hydrogen Isotopes. Biochemistry 45, 13622-13630.
113. Kreuzer-Martin, H.W. (2007) Stable isotope probing: linking functional activity to specific members of microbial communities. Soil Science Society of America Journal 71, 611-619.
114. Krüger, M., Wolters, H., Gehre, M., Joye, S.B. and Richnow, H.-H. (2008) Tracing the slow growth of anaerobic methane-oxidizing communities by ^{15}N-labelling techniques. FEMS Microbiology Ecology 63, 401-411.
115. Krummen, M., Hilkert, A.W., Juchelka, D., Duhr, A., Schlüter, H. and Pesch, R. (2004) A new concept for isotope ratio monitoring liquid chromatography/mass spectrometry. Rapid Communications in Mass Spectrometry 18, 2260~2266.
116. Kubo, K., Lloyd, K.G., J, F.B., Amann, R., Teske, A. and Knittel, K. (2012) Archaea of the Miscellaneous Crenarchaeotal Group are abundant, diverse and widespread in marine sediments. ISME J 6, 1949-1965.
117. Lagesen, K., Hallin, P., Rodland, E.A., Staerfeldt, H.H., Rognes, T. and Ussery, D.W. (2007) RNAmmer: consistent and rapid annotation of ribosomal RNA genes. Nucleic Acids Research 35, 3100-3108.
118. Langerhuus, A.T., Røy, H., Lever, M.A., Morono, Y., Inagaki, F., Jørgensen, B.B. and Lomstein, B.A. (2012) Endospore abundance and D:L-amino acid modeling of bacterial turnover in holocene marine sediment (Aarhus Bay). Geochimica et Cosmochimica Acta 99, 87-99.
119. Lansard, B., Rabouille, C., Denis, L. and Grenz, C. (2008) In situ oxygen uptake rates by coastal sediments under the influence of the Rhône River (NW Mediterranean Sea). Continental Shelf Research 28, 1501-1510.
120. Lansard, B., Rabouille, C., Denis, L. and Grenz, C. (2009) Benthic remineralization at the land–ocean interface: A case study of the Rhône River (NW Mediterranean Sea). Estuarine, Coastal and Shelf Science 81, 544-554.
121. Larkin, M.A., Blackshields, G., Brown, N.P., Chenna, R., McGettigan, P.A., McWilliam, H., Valentin, F., Wallace, I.M., Wilm, A., Lopez, R., Thompson, J.D., Gibson, T.J. and Higgins, D.G. (2007) Clustal W and Clustal X version 2.0. Bioinformatics 23, 2947-2948.
122. Laso-Pérez, R., Wegener, G., Knittel, K., Widdel, F., Harding, K.J., Krukenberg, V., Meier, D.V., Richter, M., Tegetmeyer, H.E., Riedel, D., Richnow, H.H., Adrian, L., Reemtsma, T., Lechtenfeld, O.J. and Musat, F. (2016) Thermophilic archaea activate butane via alkyl-coenzyme M formation. Nature 539, 396-401.
123. Lazar, C.S., Biddle, J.F., Meador, T.B., Blair, N., Hinrichs, K.U. and Teske, A.P. (2015) Environmental controls on intragroup diversity of the uncultured benthic archaea of the miscellaneous Crenarchaeotal group lineage naturally enriched in anoxic sediments of the White Oak River estuary (North Carolina, USA). Environmental Microbiology 17, 2228-2238.
124. Lazar, C.S., Baker, B.J., Seitz, K., Hyde, A.S., Dick, G.J., Hinrichs, K.-U. and Teske, A.P. (2016) Genomic evidence for distinct carbon substrate preferences and ecological niches of Bathyarchaeota in estuarine sediments. Environmental Microbiology 18, 1200-1211.
125. Leavitt, W.D., Flynn, T.M., Suess, M.K. and Bradley, A.S. (2016) Transhydrogenase and growth substrate influence lipid hydrogen isotope ratios in *Desulfovibrio alaskensis* G20. Frontiers in Microbiology 7.
126. Lenk, S., Arnds, J., Zerjatke, K., Musat, N., Amann, R. and Mussmann, M. (2011) Novel groups of *Gammaproteobacteria* catalyse sulfur oxidation and carbon fixation in a coastal, intertidal sediment. Environmental Microbiology 13, 758-774.
127. Lever, M. (2012) Acetogenesis in the energy-starved deep biosphere – a paradox? Frontiers in Microbiology 2, 1-14.
128. Lever, M.A., Heuer, V.B., Morono, Y., Masui, N., Schmidt, F., Alperin, M.J., Inagaki, F., Hinrichs, K.-U. and Teske, A. (2010) Acetogenesis in deep subseafloor sediments of

the Juan de Fuca Ridge Flank: a synthesis of geochemical, thermodynamic, and gene-based evidence. Geomicrobiology Journal 27, 183-211.
129. Lever, M.A., Rouxel, O., Alt, J.C., Shimizu, N., Ono, S., Coggon, R.M., Shanks, W.C., Lapham, L., Elvert, M. and Prieto-Mollar, X. (2013) Evidence for microbial carbon and sulfur cycling in deeply buried ridge flank basalt. Science 339, 1305-1308.
130. Li, D., Liu, C.M., Luo, R., Sadakane, K. and Lam, T.W. (2015) MEGAHIT: an ultra-fast single-node solution for large and complex metagenomics assembly via succinct de Bruijn graph. Bioinformatics 31, 1674-1676.
131. Li, H. and Durbin, R. (2009) Fast and accurate short read alignment with Burrows-Wheeler transform. Bioinformatics 25, 1754-1760.
132. Li, H., Yu, C., Wang, F., Chang, S.J., Yao, J. and Blake, R.E. (2016) Probing the metabolic water contribution to intracellular water using oxygen isotope ratios of PO4. Proceedings of Lunar and Planetary Science 113, 5862-5867.
133. Lim, K.L., Pancost, R.D., Hornibrook, E.R., Maxfield, P.J. and Evershed, R.P. (2012) Archaeol: an indicator of methanogenesis in water-saturated soils. Archaea 2012, 9.
134. Lin, Y.S., Lipp, J.S., Elvert, M., Holler, T. and Hinrichs, K.U. (2012) Assessing production of the ubiquitous archaeal diglycosyl tetraether lipids in marine subsurface sediment using intramolecular stable isotope probing. Environmental Microbiology 15, 1634-1646.
135. Lipp, J.S., Morono, Y., Inagaki, F. and Hinrichs, K.U. (2008) Significant contribution of Archaea to extant biomass in marine subsurface sediments. Nature 454, 991-994.
136. Liu, X.-L., Lipp, J.S., Simpson, J.H., Lin, Y.-S., Summons, R.E. and Hinrichs, K.-U. (2012) Mono- and dihydroxyl glycerol dibiphytanyl glycerol tetraethers in marine sediments: Identification of both core and intact polar lipid forms. Geochimica et Cosmochimica Acta 89, 102-115.
137. Lloyd, K.G., Schreiber, L., Petersen, D.G., Kjeldsen, K.U., Lever, M.A., Steen, A.D., Stepanauskas, R., Richter, M., Kleindienst, S., Lenk, S., Schramm, A. and Jørgensen, B.B. (2013) Predominant archaea in marine sediments degrade detrital proteins. Nature 496, 215-218.
138. Logemann, J., Graue, J., Koester, J., Engelen, B., Rullkoetter, J. and Cypionka, H. (2011) A laboratory experiment of intact polar lipid degradation in sandy sediments. Biogeosciences 8, 2547-2560.
139. Lomstein, B.A., Langerhuus, A.T., D'Hondt, S., Jorgensen, B.B. and Spivack, A.J. (2012) Endospore abundance, microbial growth and necromass turnover in deep sub-seafloor sediment. Nature 484, 101-104.
140. Londry, K.L., Jahnke, L.L. and Des Marais, D.J. (2004) Stable carbon isotope ratios of lipid biomarkers of sulfate-reducing bacteria. Applied and Environmental Microbiology 70, 745-751.
141. Londry, K.L., Dawson, K.G., Grover, H.D., Summons, R.E. and Bradley, A.S. (2008) Stable carbon isotope fractionation between substrates and products of *Methanosarcina barkeri*. Organic Geochemistry 39, 608-621.
142. Ludwig, W., Meybeck, M. and Abousamra, F. (2003) Riverine transport of water, sediment, and pollutants to the Mediterranean Sea, UNEP MAP Technical Report Series No. 141. UNEP/MAP, Athens.
143. Madigan, M.T., Martinko, J.M., Bender, K.S., Buckley, D.H. and Stahl, D.A. (2015) Brock biology of microorganisms, 14th ed. Prentice Hall Upper Saddle River, NJ.
144. Magoč, T. and Salzberg, S.L. (2011) FLASH: fast length adjustment of short reads to improve genome assemblies. Bioinformatics 27, 2957-2963.
145. Matsuyama, H., Minami, H., Sakaki, T., Kasahara, H., Watanabe, A., Onoda, T., Hirota, K. and Yumoto, I. (2015) *Psychrobacter oceani* sp. nov., isolated from marine sediment. International Journal of Systematic and Evolutionary Microbiology 65, 1450-1455.
146. Meador, T.B., Bowles, M., Lazar, C.S., Zhu, C., Teske, A. and Hinrichs, K.-U. (2015) The archaeal lipidome in estuarine sediment dominated by members of the Miscellaneous Crenarchaeotal Group. Environmental Microbiology 17, 2441-2458.

147. Meng, J., Xu, J., Qin, D., He, Y., Xiao, X. and Wang, F. (2014) Genetic and functional properties of uncultivated MCG archaea assessed by metagenome and gene expression analyses. ISME J 8, 650-659.
148. Middelboe, M., Glud, R.N. and Filippini, M. (2011) Viral abundance and activity in the deep sub-seafloor biosphere. Aquatic Microbial Ecology 63, 1-8.
149. Middelburg, J.J., Vlug, T., Jaco, F. and van der Nat, W.A. (1993) Organic matter mineralization in marine systems. Global and Planetary Change 8, 47-58.
150. Middelburg, J.J., Barranguet, C., Boschker, H.T., Herman, P.M., Moens, T. and Heip, C.H. (2000) The fate of intertidal microphytobenthos carbon: An in situ ^{13}C-labeling study. Limnology and Oceanography 45, 1224-1234.
151. Mitterer, R.M. (2010) Methanogenesis and sulfate reduction in marine sediments: A new model. Earth and Planetary Science Letters 295, 358-366.
152. Moeslundi, L., Thamdrup, B. and Jørgensen, B.B. (1994) Sulfur and iron cycling in a coastal sediment: radiotracer studies and seasonal dynamics. Biogeochemistry 27, 129-152.
153. Mußmann, M., Ishii, K., Rabus, R. and Amann, R. (2005) Diversity and vertical distribution of cultured and uncultured *Deltaproteobacteria* in an intertidal mud flat of the Wadden Sea. Environmental Microbiology 7, 405-418.
154. Nichols, P.D., Guckert, J.B. and White, D.C. (1986) Determination of monosaturated fatty acid double-bond position and geometry for microbial monocultures and complex consortia by capillary GC-MS of their dimethyl disulphide adducts. Journal of Microbiological Methods 5, 49-55.
155. Noguchi, H., Park, J. and Takagi, T. (2006) MetaGene: prokaryotic gene finding from environmental genome shotgun sequences. Nucleic Acids Research 34, 5623-5630.
156. Osburn, M.R., Sessions, A.L., Pepe-Ranney, C. and Spear, J.R. (2011) Hydrogen-isotopic variability in fatty acids from Yellowstone National Park hot spring microbial communities. Geochimica et Cosmochimica Acta 75, 4830-4845.
157. Osburn, M.R., Dawson, K.S., Fogel, M.L. and Sessions, A.L. (2016) Fractionation of hydrogen isotopes by sulfate- and nitrate-reducing Bacteria. Frontiers in Microbiology 7.
158. Øvreås, L., Forney, L., Daae, F.L. and Torsvik, V. (1997) Distribution of bacterioplankton in meromictic Lake Saelenvannet, as determined by denaturing gradient gel electrophoresis of PCR-amplified gene fragments coding for 16S rRNA. Applied and Environmental Microbiology 63, 3367-3373.
159. Owen, O.E., Kalhan, S.C. and Hanson, R.W. (2002) The key role of anaplerosis and cataplerosis for citric acid cycle function. Journal of Biological Chemistry 277, 30409-30412.
160. Pancost, R.D., Hopmans, E.C. and Sinninghe Damsté, J.S. (2001) Archaeal lipids in Mediterranean cold seeps: molecular proxies for anaerobic methane oxidation. Geochimica et Cosmochimica Acta 65, 1611-1627.
161. Parkes, R.J., Cragg, B., Roussel, E., Webster, G., Weightman, A. and Sass, H. (2014) A review of prokaryotic populations and processes in sub-seafloor sediments, including biosphere:geosphere interactions. Marine Geology 352, 409-425.
162. Parks, D.H., Imelfort, M., Skennerton, C.T., Hugenholtz, P. and Tyson, G.W. (2015) CheckM: assessing the quality of microbial genomes recovered from isolates, single cells, and metagenomes. Genome Research 25, 1043-1055.
163. Pastor, L., Deflandre, B., Viollier, E., Cathalot, C., Metzger, E., Rabouille, C., Escoubeyrou, K., Lloret, E., Pruski, A.M., Vétion, G., Desmalades, M., Buscail, R. and Grémare, A. (2011) Influence of the organic matter composition on benthic oxygen demand in the Rhône River prodelta (NW Mediterranean Sea). Continental Shelf Research 31, 1008-1019.
164. Penger, J., Conrad, R. and Blaser, M. (2014) Stable carbon isotope fractionation of six strongly fractionating microorganisms is not affected by growth temperature under laboratory conditions. Geochimica et Cosmochimica Acta 140, 95-105.

165. Poremba, K., Tillmann, U. and Hesse, K.-J. (1999) Tidal impact on planktonic primary and bacterial production in the German Wadden Sea. Helgoland marine research 53, 19-27.
166. Prahl, F.G., Ertel, J.R., Goni, M.A., Sparrow, M.A. and Eversmeyer, B. (1994) Terrestrial organic carbon contributions to sediments on the Washington margin. Geochimica et Cosmochimica Acta 58, 3035-3048.
167. Price, M.N., Dehal, P.S. and Arkin, A.P. (2010) FastTree 2--approximately maximum-likelihood trees for large alignments. PLoS ONE 5, e9490.
168. Pruski, A.M., Buscail, R., Bourgeois, S., Vétion, G., Coston-Guarini, J. and Rabouille, C. (2015) Biogeochemistry of fatty acids in a river-dominated Mediterranean ecosystem (Rhône River prodelta, Gulf of Lions, France): Origins and diagenesis. Organic Geochemistry 83–84, 227-240.
169. Puigbò, P., Wolf, Y.I. and Koonin, E.V. (2009) Search for a 'Tree of Life' in the thicket of the phylogenetic forest. Journal of Biology 8, 59.
170. Ragsdale, S.W. and Pierce, E. (2008) Acetogenesis and the Wood–Ljungdahl pathway of CO_2 fixation. Biochimica et Biophysica Acta (BBA) - Proteins and Proteomics 1784, 1873-1898.
171. Ramos-Vera, W.H., Berg, I.A. and Fuchs, G. (2009) Autotrophic carbon dioxide assimilation in *Thermoproteales* revisited. Journal of Bacteriology 191, 4286-4297.
172. Reuss, N., Conley, D.J. and Bianchi, T.S. (2005) Preservation conditions and the use of sediment pigments as a tool for recent ecological reconstruction in four Northern European estuaries. Marine Chemistry 95, 283-302.
173. Rosa, M.D. and Gambacorta, A. (1986) Lipid biogenesis in archaebacteria. Systematic and Applied Microbiology 7, 278-285.
174. Roslev, P., Larsen, M.B., Jørgensen, D. and Hesselsoe, M. (2004) Use of heterotrophic CO_2 assimilation as a measure of metabolic activity in planktonic and sessile bacteria. Journal of Microbiological Methods 59, 381-393.
175. Røy, H., Lee, J.S., Jansen, S. and de Beer, D. (2008) Tide-driven deep pore-water flow in intertidal sand flats. Limnology and Oceanography 53, 1521-1530.
176. Ruff, S.E., Biddle, J.F., Teske, A.P., Knittel, K., Boetius, A. and Ramette, A. (2015) Global dispersion and local diversification of the methane seep microbiome. Proceedings of the National Academy of Sciences of the United States of America 112, 4015-4020.
177. Rusch, A., Forster, S. and Huettel, M. (2001) Bacteria, diatoms and detritus in an intertidal sandflat subject to advective transport across the water-sediment interface. Biogeochemistry 55, 1-27.
178. Rütters, H., Sass, H., Cypionka, H. and Rullkötter, J. (2002) Microbial communities in a Wadden Sea sediment core—clues from analyses of intact glyceride lipids, and released fatty acids. Organic Geochemistry 33, 803-816.
179. Sachs, J.P. and Schwab, V.F. (2011) Hydrogen isotopes in dinosterol from the Chesapeake Bay estuary. Geochimica et Cosmochimica Acta 75, 444-459.
180. Sachs, J.P. and Kawka, O.E. (2015) The influence of growth rate on $^{2}H/^{1}H$ fractionation in continuous cultures of the coccolithophorid *Emiliania huxleyi* and the diatom *Thalassiosira pseudonana*. PLoS ONE 10, e0141643.
181. Sachse, D., Billault, I., Bowen, G.J., Chikaraishi, Y., Dawson, T.E., Feakins, S.J., Freeman, K.H., Magill, C.R., McInerney, F.A., van der Meer, M.T.J., Polissar, P., Robins, R.J., Sachs, J.P., Schmidt, H.-L., Sessions, A.L., White, J.W.C., West, J.B. and Kahmen, A. (2012) Molecular paleohydrology: interpreting the hydrogen-isotopic composition of lipid biomarkers from photosynthesizing organisms. Annual Review of Earth and Planetary Sciences 40, 221-249.
182. Sakai, S., Takaki, Y., Shimamura, S., Sekine, M., Tajima, T., Kosugi, H., Ichikawa, N., Tasumi, E., Hiraki, A.T., Shimizu, A., Kato, Y., Nishiko, R., Mori, K., Fujita, N., Imachi, H. and Takai, K. (2011) Genome sequence of a mesophilic hydrogenotrophic *methanogen Methanocella paludicola*, the first cultivated representative of the order *Methanocellales*. PLoS ONE 6, e22898.

183. Schimmelmann, A., Sessions, A.L. and Mastalerz, M. (2006) Hydrogen isotopic composition of organic matter during diagenesis and thermal maturation. Annual Review of Earth and Planetary Sciences 34, 501-533.
184. Schmidt, F., Koch, B.P., Goldhammer, T., Elvert, M., Witt, M., Lin, Y.-S., Wendt, J., Zabel, M., Heuer, V.B. and Hinrichs, K.-U. (2017) Unraveling signatures of biogeochemical processes and the depositional setting in the molecular composition of pore water DOM across different marine environments. Geochimica et Cosmochimica Acta 207, 57-80.
185. Schouten, S., Ossebaar, J., Schreiber, K., Kienhuis, M.V.M., Langer, G., Benthien, A. and Bijma, J. (2006) The effect of temperature, salinity and growth rate on the stable hydrogen isotopic composition of long chain alkenones produced by *Emiliania huxleyi* and *Gephyrocapsa oceanica*. Biogeosciences 3, 113-119.
186. Schouten, S., Hopmans, E.C., Baas, M., Boumann, H., Standfest, S., Konneke, M., Stahl, D.A. and Sinninghe Damsté, J.S. (2008) Intact membrane lipids of "*Candidatus* Nitrosopumilus maritimus," a cultivated representative of the cosmopolitan mesophilic group I crenarchaeota. Applied and Environmental Microbiology 74, 2433-2440.
187. Schouten, S., Hopmans, E.C. and Sinninghe Damsté, J.S. (2013) The organic geochemistry of glycerol dialkyl glycerol tetraether lipids: A review. Organic Geochemistry 54, 19-61.
188. Seidel, M., Graue, J., Engelen, B., Köster, J., Sass, H. and Rullkötter, J. (2012) Advection and diffusion determine vertical distribution of microbial communities in intertidal sediments as revealed by combined biogeochemical and molecular biological analysis. Organic Geochemistry 52, 114-129.
189. Seidel, M., Rütters, H., Rullkötter, J. and Sass, H. (2013) Phosphate-free ornithine lipid contents in *Desulfovibrio* spp. respond to growth temperature. Organic Geochemistry 59, 133-142.
190. Sessions, A., Burgoyne, T., Schimmelmann, A. and Hayes, J. (1999) Fractionation of hydrogen isotopes in lipid biosynthesis. Organic Geochemistry 30, 1193-1200.
191. Sessions, A.L., Jahnke, L.L., Schimmelmann, A. and Hayes, J.M. (2002) Hydrogen isotope fractionation in lipids of the methane-oxidizing bacterium *Methylococcus capsulatus*. Geochimica et Cosmochimica Acta 66, 3955-3969.
192. Sessions, A.L. and Hayes, J.M. (2005) Calculation of hydrogen isotopic fractionations in biogeochemical systems. Geochimica et Cosmochimica Acta 69, 593-597.
193. Sessions, A.L. (2016) Factors controlling the deuterium contents of sedimentary hydrocarbons. Organic Geochemistry 96, 43-64.
194. Seyler, L.M., McGuinness, L.M. and Kerkhof, L.J. (2014) Crenarchaeal heterotrophy in salt marsh sediments. ISME J, 1-10.
195. Song, Z.-Q., Wang, F.-P., Zhi, X.-Y., Chen, J.-Q., Zhou, E.-M., Liang, F., Xiao, X., Tang, S.-K., Jiang, H.-C., Zhang, C.L., Dong, H. and Li, W.-J. (2013) Bacterial and archaeal diversities in Yunnan and Tibetan hot springs, China. Environmental Microbiology 15, 1160-1175.
196. Sorokin, Y.I. (1966) Role of carbon dioxide and acetate in biosynthesis by sulphate-reducing bacteria. Nature 210, 551-552.
197. Spaans, S., Weusthuis, R., Van Der Oost, J. and Kengen, S. (2015) NADPH-generating systems in bacteria and archaea. Frontiers in Microbiology 6.
198. Sturt, H.F., Summons, R.E., Smith, K., Elvert, M. and Hinrichs, K.U. (2004) Intact polar membrane lipids in prokaryotes and sediments deciphered by high-performance liquid chromatography/electrospray ionization multistage mass spectrometry-new biomarkers for biogeochemistry and microbial ecology. Rapid Communications in Mass Spectrometry 18, 617-628.
199. Summons, R.E., Franzmann, P.D. and Nichols, P.D. (1998) Carbon isotopic fractionation associated with methylotrophic methanogenesis. Organic Geochemistry 28, 465-475.

200. Sun, M.-Y. and Wakeham, S.G. (1994) Molecular evidence for degradation and preservation of organic matter in the anoxic Black Sea Basin. Geochimica et Cosmochimica Acta 58, 3395-3406.
201. Sun, M.-Y., Wakeham, S.G. and Lee, C. (1997) Rates and mechanisms of fatty acid degradation in oxic and anoxic coastal marine sediments of Long Island Sound, New York, USA. Geochimica et Cosmochimica Acta 61, 341-355.
202. Takano, Y., Chikaraishi, Y., Ogawa, N.O., Nomaki, H., Morono, Y., Inagaki, F., Kitazato, H., Hinrichs, K.-U. and Ohkouchi, N. (2010) Sedimentary membrane lipids recycled by deep-sea benthic archaea. Nature Geoscience 3, 858-861.
203. Tamura, K., Stecher, G., Peterson, D., Filipski, A. and Kumar, S. (2013) MEGA6: molecular evolutionary genetics analysis version 6.0. Molecular Biology and Evolution 30, 2725-2729.
204. Taylor, J. and Parkes, R.J. (1983) The cellular fatty acids of the sulphate-reducing bacteria, *Desulfobacter sp., Desulfobulbus sp.* and *Desulfovibrio desulfuricans*. Journal of General Microbiology 129, 3303-3309.
205. ter Braak, C. and Šmilauer, P. (2012) Canoco reference manual and user's guide: software for ordination (version 5.0), Ithaca, NY, USA.
206. Thauer, R.K. (1988) Citric-acid cycle, 50 years on modifications and an alternative pathway in anaerobic bacteria. The FEBS Journal 176, 497-508.
207. Thauer, R.K. (1998) Biochemistry of methanogenesis: a tribute to Marjory Stephenson:1998 Marjory Stephenson Prize Lecture. Microbiology 144, 2377-2406.
208. Thauer, R.K., Kaster, A.-K., Seedorf, H., Buckel, W. and Hedderich, R. (2008) Methanogenic archaea: ecologically relevant differences in energy conservation. Nature Reviews Microbiology 6, 579-591.
209. Thomsen, U. and Kristensen, E. (1997) Dynamics of $\sum CO_2$ in a surficial sandy marine sediment: the role of chemoautotrophy. Aquatic Microbial Ecology 12, 165-176.
210. Valentine, D.L., Chidthaisong, A., Rice, A., Reeburgh, W.S. and Tyler, S.C. (2004a) Carbon and hydrogen isotope fractionation by moderately thermophilic methanogens. Geochimica et Cosmochimica Acta 68, 1571-1590.
211. Valentine, D.L., Sessions, A.L., Tyler, S.C. and Chidthaisong, A. (2004b) Hydrogen isotope fractionation during H_2/CO_2 acetogenesis: hydrogen utilization efficiency and the origin of lipid-bound hydrogen. Geobiology 2, 179-188.
212. Valentine, D.L. (2007) Adaptations to energy stress dictate the ecology and evolution of the Archaea. Nature Reviews Microbiology 5, 316-323.
213. Valentine, D.L. (2009) Isotopic remembrance of metabolism past. Proceedings of the National Academy of Sciences of the United States of America 106, 12565-12566.
214. van der Meer, M.T.J., Benthien, A., French, K.L., Epping, E., Zondervan, I., Reichart, G.-J., Bijma, J., Sinninghe Damsté, J.S. and Schouten, S. (2015) Large effect of irradiance on hydrogen isotope fractionation of alkenones in *Emiliania huxleyi*. Geochimica et Cosmochimica Acta 160, 16-24.
215. Vasquez-Cardenas, D., van de Vossenberg, J., Polerecky, L., Malkin, S.Y., Schauer, R., Hidalgo-Martinez, S., Confurius, V., Middelburg, J.J., Meysman, F.J. and Boschker, H.T.S. (2015) Microbial carbon metabolism associated with electrogenic sulphur oxidation in coastal sediments. ISME J 9, 1966-1978.
216. Vignais, P.M. (2008) Hydrogenases and H+-reduction in primary energy conservation, in: Schäfer, G., Penefsky, H.S. (Eds.), Bioenergetics: energy conservation and conversion. Springer Berlin Heidelberg, Berlin, Heidelberg, pp. 223-252.
217. Villanueva, L., Damste, J.S. and Schouten, S. (2014) A re-evaluation of the archaeal membrane lipid biosynthetic pathway. Nature Reviews Microbiology.
218. Volkman, J.K., Rohjans, D., Rullkötter, J., Scholz-Böttcher, B.M. and Liebezeit, G. (2000) Sources and diagenesis of organic matter in tidal flat sediments from the German Wadden Sea. Continental Shelf Research 20, 1139-1158.
219. Wang, Y. and Sessions, A.L. (2008) Memory effects in compound-specific D/H analysis by gas chromatography/pyrolysis/isotope-ratio mass spectrometry. Analytical Chemistry 80, 9162-9170.

220. Wegener, G., Bausch, M., Holler, T., Nguyen Manh, T., Mollar, X.P., Kellermann, M.Y., Hinrichs, K.-U. and Boetius, A. (2012) Assessing sub-seafloor microbial activity by combined stable isotope probing with deuterated water and ^{13}C-bicarbonate. Environmental Microbiology 14, 1517-1527.
221. Wegener, G., Kellermann, M.Y. and Elvert, M. (2016) Tracking activity and function of microorganisms by stable isotope probing of membrane lipids. Current Opinion in Biotechnology 41, 43-52.
222. Wei, H., Xu, Q., Taylor, L.E., Baker, J.O., Tucker, M.P. and Ding, S.-Y. (2009) Natural paradigms of plant cell wall degradation. Current Opinion in Biotechnology 20, 330-338.
223. Weijers, J.W.H., Wiesenberg, G.L.B., Bol, R., Hopmans, E.C. and Pancost, R.D. (2010) Carbon isotopic composition of branched tetraether membrane lipids in soils suggest a rapid turnover and a heterotrophic life style of their source organism(s). Biogeosciences 7, 2959-2973.
224. Weimer, P.J. and Zeikus, J.G. (1978) Acetate metabolism in *Methanosarcina barkeri*. Archives of Microbiology 119, 175-182.
225. Wellsbury, P., Goodman, K., Barth, T., Cragg, B.A., Barnes, S.P. and Parkes, R.J. (1997) Deep marine biosphere fuelled by increasing organic matter availability during burial and heating. Nature 388, 573-576.
226. Whitman, W.B., Coleman, D.C. and Wiebe, W.J. (1998) Prokaryotes: The unseen majority. Proceedings of the National Academy of Sciences of the United States of America 95, 6578-6583.
227. Widdel, F. and Pfennig, N. (1981) Studies on dissimilatory sulfate-reducing bacteria that decompose fatty acids. Archives of Microbiology 129, 395-400.
228. Wilms, R., Köpke, B., Sass, H., Chang, T.S., Cypionka, H. and Engelen, B. (2006a) Deep biosphere-related bacteria within the subsurface of tidal flat sediments. Environmental Microbiology 8, 709-719.
229. Wilms, R., Sass, H., Köpke, B., Köster, J., Cypionka, H. and Engelen, B. (2006b) Specific bacterial, archaeal, and eukaryotic communities in tidal-flat sediments along a vertical profile of several meters. Applied and Environmental Microbiology 72, 2756-2764.
230. Wrighton, K.C., Thomas, B.C., Sharon, I., Miller, C.S., Castelle, C.J., VerBerkmoes, N.C., Wilkins, M.J., Hettich, R.L., Lipton, M.S., Williams, K.H., Long, P.E. and Banfield, J.F. (2012) Fermentation, hydrogen, and sulfur metabolism in multiple uncultivated bacterial phyla. Science 337, 1661-1665.
231. Xie, S., Lipp, J.S., Wegener, G., Ferdelman, T.G. and Hinrichs, K.U. (2013) Turnover of microbial lipids in the deep biosphere and growth of benthic archaeal populations. Proceedings of the National Academy of Sciences of the United States of America 110, 6010-6014.
232. Xu, F., Ji, Z., Wang, K., Jin, H. and Loh, P.S. (2016) The distribution of sedimentary organic matter and implication of its transfer from Changjiang Estuary to Hangzhou Bay, China. Open Journal of Marine Science 6, 103.
233. Yakimov, M.M., La Cono, V., Smedile, F., Crisafi, F., Arcadi, E., Leonardi, M., Decembrini, F., Catalfamo, M., Bargiela, R., Ferrer, M., Golyshin, P.N. and Giuliano, L. (2014) Heterotrophic bicarbonate assimilation is the main process of de novo organic carbon synthesis in hadal zone of the Hellenic Trench, the deepest part of Mediterranean Sea. Environmental Microbiology Reports 6, 709-722.
234. Yu, T., Liang, Q., Niu, M. and Wang, F. (2017) High occurrence of Bathyarchaeota (MCG) in the deep-sea sediments of South China Sea quantified using newly designed PCR primers. Environmental Microbiology Reports 9, 374-382.
235. Zhang, C.L., Huang, Z., Cantu, J., Pancost, R.D., Brigmon, R.L., Lyons, T.W. and Sassen, R. (2005) Lipid Biomarkers and Carbon Isotope Signatures of a Microbial (*Beggiatoa*) Mat Associated with Gas Hydrates in the Gulf of Mexico. Applied and Environmental Microbiology 71, 2106-2112.

236. Zhang, X., Gillespie, A.L. and Sessions, A.L. (2009a) Large D/H variations in bacterial lipids reflect central metabolic pathways. Proceedings of the National Academy of Sciences of the United States of America 106, 12580-12586.
237. Zhang, Y., Henriet, J.-P., Bursens, J. and Boon, N. (2010) Stimulation of in vitro anaerobic oxidation of methane rate in a continuous high-pressure bioreactor. Bioresource Technology 101, 3132-3138.
238. Zhang, Z. and Sachs, J.P. (2007) Hydrogen isotope fractionation in freshwater algae: I. Variations among lipids and species. Organic Geochemistry 38, 582-608.
239. Zhang, Z., Sachs, J.P. and Marchetti, A. (2009b) Hydrogen isotope fractionation in freshwater and marine algae: II. Temperature and nitrogen limited growth rate effects. Organic Geochemistry 40, 428-439.
240. Zhu, C., Lipp, J.S., Wörmer, L., Becker, K.W., Schröder, J. and Hinrichs, K.-U. (2013) Comprehensive glycerol ether lipid fingerprints through a novel reversed phase liquid chromatography–mass spectrometry protocol. Organic Geochemistry 65, 53-62.
241. Zink, K.-G., Wilkes, H., Disko, U., Elvert, M. and Horsfield, B. (2003) Intact phospholipids—microbial “life markers” in marine deep subsurface sediments. Organic Geochemistry 34, 755-769.

Author contributions

Chapter II **Substrate-dependent utilization of carbon and hydrogen for lipid biosynthesis by *Methanosarcina barkeri***

(In preparation for *Geochimica et Cosmochimica Acta*)

Weichao Wu, Travis Meador, Marcus Elvert, Gunter Wegener, Martin Könneke, Kai-Uwe Hinrichs

W. Wu, T. Meador and K.-U. Hinrichs designed this study; W. Wu performed this study; ***W. Wu,*** T. Meador, M. Elvert, G. Wegener, M. Könneke and K.-U. Hinrichs analyzed data; W. Wu wrote the paper with contributions from all co-authors

Chapter III **Production and turnover of microbial organic matter in surface sandy sediments**

(In revision for *Organic Geochemistry*)

Weichao Wu, Travis Meador, Kai-Uwe Hinrichs

T. Meador and K.-U. Hinrichs designed this study; ***W. Wu*** and T. Meador performed this study; ***W. Wu*** wrote the paper with contributions from all co-authors.

Chapter IV **Microbial activity in marine surface sediment controlled by the proportion of terrestrial organic matter**

(In preparation for *Geochimica et Cosmochimica Acta*)

Weichao Wu, Travis Meador, Julius Lipp, Marcus Elvert, Verena Heuer, Kai-Uwe Hinrichs

W. Wu, K.-U. Hinrichs and V. Heuer designed this study; ***W. Wu*** performed this study; ***W. Wu***, T. Meador, J. Lipp, M. Elvert, V. Heuer and K.-U. Hinrichs analyzed data; ***W. Wu*** wrote the paper with contributions from all co-authors.

Chapter V **Growth of abundant sedimentary Bathyarchaeota on lignin as an energy source**

(under review at *Proceedings of the National Academy of Sciences of the USA*)

Tiantian Yu, ***Weichao Wu*** **(co-first author)**, Wenyue Liang, Mark Alexander Lever, Kai-Uwe Hinrichs and Fengping Wang

T. Yu and F. Wang design this study. T. Yu, ***W. Wu*** and W. Liang performed this study. T. Yu and ***W. Wu*** wrote the paper with contributions from all co-authors.

Supplementary materials

Chapter I
Table S.I.1

Chapter II
Table S.II.1
Fig. S.II.1
Fig. S.II.2

Chapter III
No

Chapter IV
Table S.IV.1
Table S.IV.2
Table S.IV.3
Table S.IV.4
Table S.IV.5

Chapter V
SI Text
SI Fig. S1
SI Fig. S2
SI Fig. S3
SI Tables S1
SI Tables S2
SI Tables S3
SI Tables S4
SI Tables S5
SI Tables S6
SI Tables S7
SI Tables S8

Supplementary materials for Chapter I

Table S.I.1. Summary of the water H assimilation constant (a_w) to different lipids by Eukaryote, Bacteria and Archaea. FA, fatty acid; LB, Lysogeny broth.

Domains	Cultures	Energy	Lipids	a_w	References
Eukaryote	*Eudorina unicocca*	light	C16 FA	0.92	Zhang et al., 2009b
			C16 FA	0.89	
	Volvox aureus	light	C16 FA	0.92	
			C16 FA	0.87	
	Botryococcus braunni	light	C18:1 FA	0.78	Zhang et al., 2014
			C29:2 alkadiene	0.71	
	Emiliania huxleyi	light	C37 alkenones	0.73	Englebrecht and Sachs, 2005
			C38 alkenones	0.75	
			C37 alkenones	0.79	Schouten et al., 2006
	Gephyrocapsa oceanica	light	C37 alkenones	0.77	
	Thalassiosira pseudonana	light	C14 FA	0.82	Maloney et al., 2016
			C16 FA	0.82	
			C16:1 FA	0.84	
			sterols	0.67	
	Tetrahymena thermophila	dextrose	tetrahymanol	0.95	Dirghangi and Pagani, 2013b
			tetrahymanol	0.96	
			tetrahymanol	1.04	
			C14 FA	1.09	
			C14 FA	1.15	
			C14 FA	1.15	
Bacteria	*cupriavidus oxalaticus*	oxalate	C16:1 FA	0.64	Zhang et al., 2009a
			C16 FA	0.69	
			C18:1 FA	0.7	
		formate	C16:1 FA	0.64	
			C16 FA	0.73	
			C18:1 FA	0.72	
			C16:1 FA	0.69	
			C16 FA	0.69	
			C18:1 FA	0.70	
		acetate	C16:1 FA	0.52	
			C16 FA	0.58	
			C18:1 FA	0.54	
		succinate	C16:1 FA	0.83	
			C16 FA	0.8	
			C18:1 FA	0.89	
			C16:1 FA	0.76	
			C16 FA	0.79	
			C18:1 FA	0.75	

Bacteria	*E. coli*	glucose	C16:1 FA	0.6	Zhang et al., 2009a
			C16 FA	0.65	
			C18:1 FA	0.63	
		LB	C16:1 FA	0.44	
			C16 FA	0.52	
			C18:1 FA	0.48	
	Sporomusa sp.	H_2/CO_2	total lipids	0.59	Valentine et al., 2004a
	Paracoccus denitrificans	acetate	total lipids	0.61	Osburn et al., 2016
		succinate	total lipids	0.67	
			total lipids	0.55	
		thiosulfate-O_2	total lipids	0.75	
		H_2-O_2	total lipids	0.62	
		H_2-NO_3^-	total lipids	0.61	
	Desulfobulbus alaskensis	pyruvate-SO_4^{2-}	total lipids	0.48	
			total lipids	0.51	
Archaea	*Haloarcula marismortui*	pyruvate	archaeol	0.77	Dirghangi and Pagani, 2013a
		succinate	archaeol	0.60	
		glycerol	archaeol	0.55	
	Methanosarcina barkeri	H_2/CO_2	archaeol	0.33	Chapter II
		acetate	archaeol	0.22	
		methanol	archaeol	0.37	
		H_2/CO_2	hydroxyarchaeol	0.33	
		acetate	hydroxyarchaeol	0.23	
		methanol	hydroxyarchaeol	0.39	

Supplementary materials for Chapter II

Table S.II.1. Summary of the regressions of F_{lipid} (PMI, unsPMIs, AR and OH-AR) on F_{water} of by *M. barkeri* grown on H_2/CO_2, acetate and methanol. The unit of intercept and its standard error is 10^3 ppm. (n.a., not analyzed due to no detection of this compound).

Lipids	Regression	H_2/CO_2	Acetate	Methanol
PMI	slope	0.405±0.020	0.230±0.008	0.065±0.065
	intercept	0.138±0.106	0.123±0.050	0.282±0.535
	R^2	0.990	0.994	0.350
unsPMIs	slope	n.a.	n.a.	0.425±0.015
	intercept	n.a.	n.a.	-0.076±0.106
	R^2	n.a.	n.a.	0.99
AR	slope	0.332±0.032	0.223±0.007	0.369±0.013
	intercept	0.100±0.163	0.055±0.051	0.023±0.096
	R^2	0.960	0.995	0.99
OH-AR	slope	0.334±0.031	0.229±0.009	0.385±0.014
	intercept	0.068±0.155	0.021±0.067	-0.004±0.099
	R^2	0.970	0.992	0.993

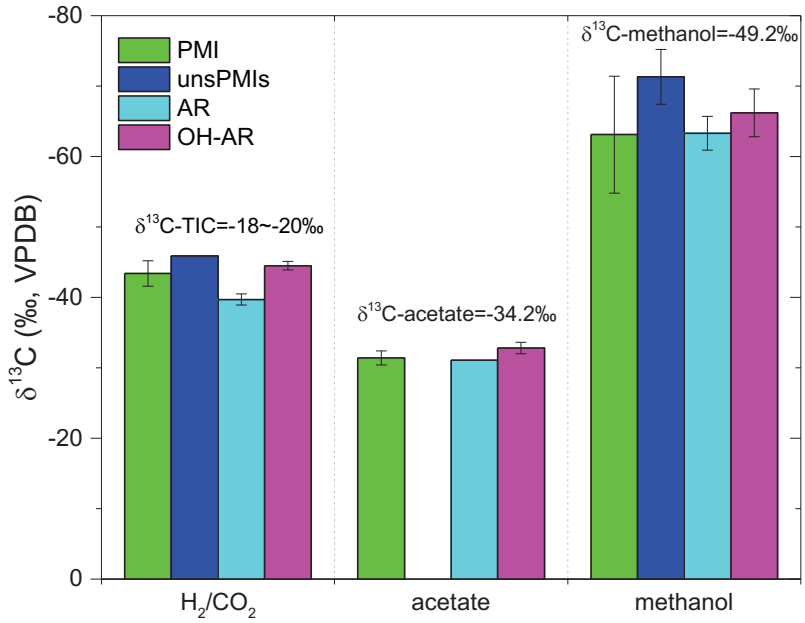

Fig. S.II.1. The carbon isotopic composition of lipid produced by *M. barkeri* grown on non-labeled H_2/CO_2, acetate and methanol

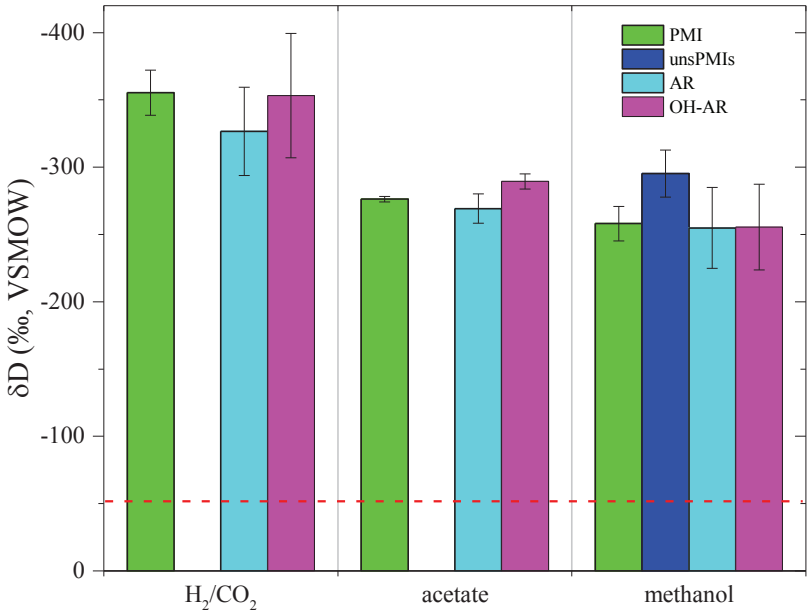

Fig. S.II.2. The hydrogen isotopic composition of lipids produced by *M. barkeri* when grown on different substrates in natural water medium (δD=-50.6‰; red dash line).

Supplementary materials for chapter IV

Table S.IV.1. The production of methane and acetate after incubation for 100 days. The data are shown as average ± standard deviation (n=2).

Sites	CH_4	acetate	
	$\delta^{13}C$ (‰)	$\delta^{13}C$ (‰)	concentration (mM)
GeoB17306	345±39	400±14	36.0±4.1
GeoB17307	416±82	483±91	16.4±2.7
GeoB17308	212±61*	366±28	1.5±0.0
GeoB17305	96*	395±5	9.1±0.4

* for reference due to limited amount for reliable analysis

Table S.IV.2. The $\delta^{13}C$ values of bacterial fatty acids and intact archaeal lipid derivatives (μg g_{dw}^{-1}) in surface sediment after incubation at t_0, t_{50} and t_{100}. n.d.: not determined

	Lipids	GeoB17306			GeoB17307			GeoB17308			GeoB17305		
		t_0	t_{50}	t_{100}	t_0	t_{50}	t_{100}	t_0	t_{50}	t_{100}	t_0	t_{50}	t_{100}
Bacteria	*i*C_{14}	-29.8	-22.0	-17.2	-31.3	-15.1	8.2	-26.1	-11.4	-2.3	-25.2	-0.1	4.3
	C_{14}	-30.8	-26.7	2.0	-31.0	-21.9	23.4	-27.0	-17.5	15.5	-26.0	-4.4	15.3
	iC_{15}	-29.5	-24.0	-4.5	-29.3	-19.9	25.1	-25.3	-21.5	10.6	-23.7	-17.0	3.9
	aC_{15}	-31.1	-17.2	0.0	-31.5	-9.8	28.6	-26.7	-11.37	2.8	-25.4	-1.9	9.2
	$C_{15:1}$	-29.7[a]	-29.7[a]	94.8	-30.1[a]	-30.1[a]	100.9	-25.5[a]	-25.5[a]	187.6	-24.4[a]	-24.4[a]	223
	C_{15}	-28.6	-24.2	64.7	-29.5	-18.8	58.2	-24.4	-15.7	99.7	-23.9	3.0	87.8
	iC_{16}	-30.3	-24.7	-17.2	-29.2	-20.4	-6.8	-26.6	-16.9	1.0	-23.7	-10.5	-4.5
	$C_{16:1\omega7}$	-32.6	-19.5	84.5	-29.9	-8.5	225.3	-26.6	-7.4	150.5	-24.7	13.4	116.3
	$C_{16:1\omega5}$	-38.0	-18.2	98.5	-34.0	-10.2	169.3	-33.2	-7.7	190.8	-28.3	77.6	189.4
	C_{16}	-32.0	-28.0	2.9	-31.8	-22.3	74.0	-28.4	-17.7	72.8	-26.9	-2.6	44.4
	iC_{17}	-35.8	-23.6	-24.9	-29.1	-22.2	-34.6	-25.8	-21.5	-31.1	-24.9	-14.8	-23.8
	aC_{17}	-34.0	-17.7	-10.3	-27.7	-14.5	-23.0	-24.3	-12.5	-21.7	-22.9	-5.2	-28.7
	$C_{17:1\omega8}$	-39.6	-24.8	58.2	-32.1	-20.9	18.1	-29.0	-21.6	102.1	-28.5	-11.1	140
	$C_{17:1\omega6}$	-39.2	-23.3	179.3	-31.9	-22.0	166.7	-27.6	-20.7	262.4	-26.7	28.8	248
	C_{17}	-32.3	-25.7	72.2	-29.3	-21.1	25.1	-27.1	-14.9	144.2	-28.2	5.1	97
	$C_{18:2}$	-25.3	-26.9	-27.9	-27.5	-22.5	-22.2	-19.9	-17.4	-20.1	-19.9	-19.1	-25.9
	$C_{18:1\omega9}$	-26.8	-24.4	-21.6	-29.9	-20.8	-5.5	-24.8	-17.0	-7.6	-22.8	-11.0	-10.2
	$C_{18:1\omega7}$	-31.0	-29.2	-4.2	-35.1	-22.4	132.5	-28.8	-20.1	59.7	-27.7	-9.6	36.9
	C_{18}	-28.9	-29.3	-24.9	-32.4	-26.7	-19.4	-28.1	-20.5	-12.5	-28.2	-18.0	-18
Archaea	phytane	-29.6	-30.9	-23.5	-29.1	-29.7	-29.6	-26.6	-27.2	-29.2	-23.6	-27.1	-27.7
	bp-0	-28.6	-28.7	-28.5	-29.8	-28.2	-27.9	-25.8	-24.6	-24.5	-24.9	-21.7	-22.6
	bp-1	-25.7	n.d.	n.d.	n.d.	n.d.	-31.7	-22.7	-20.6	-20.9	-19.5	-20.1	-18.2
	bp-2	-36.5	-36.0	-38.7	-38.4	-35.7	-35.5	-23.7	-23.6	-23.4	-19.5	-19.5	-21.0
	bp-3	-22.9	-22.4	-22.9	-21.5	n.d.	-23.9	-20.6	-19.7	-19.2	-18.8	-18.9	-18.7

a: this value is gained from the average of *i*C_{15}, *a*C_{15} and C_{15} due to the need of further calculation

Table S.IV.3. The hydrogen isotope composition (δD, ‰) of bacterial fatty acids and intact archaeal lipid derivates (μg g_{dw}^{-1}) in surface sediment after incubation at t_0, t_{50} and t_{100}. (n.d.: not determined)

	Lipids	GeoB17306			GeoB17307			GeoB17308			GeoB17305		
		t_0	t_{50}	t_{100}	t_0	t_{50}	t_{100}	t_0	t_{50}	t_{100}	t_0	t_{50}	t_{100}
Bacteria	*i*C_{14}	-150	2202	4188	n.d.	2019	0	n.d.	n.d.	n.d.	n.d.	n.d.	n.d.
	C_{14}	-150	1432	5592	-151	1294	6878	-140	518	4072	-140	1263	4573
	iC_{15}	-81	2482	7220	-90	1835	7873	1	590	6120	-68	1409	6661
	aC_{15}	-170	3387	7853	-174	2286	7975	-132	747	3876	-160	1500	3840
	$C_{15:1}$	-125	2531	17443	-132	1857	9654	-78	731	10477	-115	1620	31285
	C_{15}	-123	1723	14536	-132	1448	11044	-103	856	13638	-118	1951	18533
	iC_{16}	n.d.	n.d.	n.d	n.d.	n.d.	n.d.	n.d.	n.d.	n.d.	nd	n.d.	n.d.
	$C_{16:1\omega7}$ / $C_{16:1\omega5}$	-129	1362	16505	-147	1081	32345	-127	407	18260	-112	2355	22613
	C_{16}	-141	614	6985	-159	606	17164	-132	417	11390	-136	1817	10290
	iC_{17}	-100	1319	4600	-100	1075	10240	-100	411		-100	1415	5138
	aC_{17}			5576			7909			7345			3112
	$C_{17:1\omega8}$			11065			14236						18585
	$C_{17:1\omega6}$			25634			26257			29174			38596
	C_{17}			20800			15337			26800			26583
	$C_{18:2}$ / $C_{18:1\omega9}$ / $C_{18:1\omega7}$	-135	350	3915	-161	328	20948	-143	181	6509	-120	696	7191
	C_{18}	-129	285	1889	-119	257	6438	-121	327	3366	-120	899	2665
Archaea	phytane	-276	-198	978	-220	-201	48	-205	-193	37	-245	-121	7
	bp-0	-200	-157	-82	-211	-121	-124	-226	-178	-152	-210	-184	-162
	bp-1	n.d.	n.d.	n.d.	n.d.	n.d.	n.d.	n.d.	n.d.	n.d.	n.d.	n.d.	n.d.
	bp-2	n.d.	n.d.	n.d.	n.d.	n.d.	n.d.	-231	-155	n.d.	-158	-122	-172
	bp-3	n.d.	n.d.	n.d.	n.d.	n.d.	n.d.	-138	-111	n.d.	-166	-116	-131

Table S.IV.4. The comparison of inorganic carbon incorporation ($assim_{IC}$) into bacterial lipids, biomass and TOC. S1 and S2 refer duplicate samples; SR and H2 refer the incubation conditions with sulfate-reducing and H_2/CO_2, respectively.

Sites	Samples	$assim_{IC}$ ($\mu g\ g_{dw}^{-1}\ yr^{-1}$)			$assim_{IC\text{-}bac\ lipids}$ to $assim_{IC\text{-}TOC}$	$assim_{IC\text{-}bac\ biomass}$ to $assim_{IC\text{-}TOC}$
		Bac lipids	*Bac biomass*	*TOC*		
GeoB17306	SR-S_1	0.36	4.9	10.4±2.4	3.4%	47%
	SR-S_2	0.33	4.6	11.3±2.6	2.9%	41%
	H_2-S_1	9.56	131	230±25	4.2%	57%
	H_2-S_2	8.58	118	205±30	4.2%	58%
GeoB17307	SR-S_1	0.32	4.4	15.3±7.3	2.1%	29%
	SR-S_2	0.33	4.6	15.6±7.4	2.1%	29%
	H_2-S_1	9.45	130	315±25	3.0%	41%
	H_2-S_2	25.94	356	444±39	5.8%	80%
GeoB17308	SR-S_1	0.25	3.40	6.9±2.2	3.6%	49%
	SR-S_2	0.12	1.67	6.6±2.1	1.8%	25%
	H_2-S_1	14.25	196	302±21	4.7%	65%
	H_2-S_2	11.16	153	235±17	4.8%	65%
GeoB17305	SR-S_1	0.34	4.63	9.9±0.8	3.4%	47%
	SR-S_2	0.28	3.82	10.2±0.9	2.7%	37%
	H_2-S_1	6.3	87	187±14	3.4%	46%
	H_2-S_2	7.1	97	220±15	3.2%	44%

Table S.IV.5. Percentages (%) of fatty acids in reference cultures used for PCA analysis.

Cultures	*Desulfob*-pro[a]	*Desulfob*-H_2[b]	*Desulfobac*-ace[c]	*Beggiatoa*[d]	*Pseudomonas*[e]	*Psychrobacter*[e]	*Shewanella*[e]	*Arcobacer*[f]
C14	4.6	9.5	22.5	1.3	3.5	0.5	0.4	5.4
*i*C15	0.0	0.1	4.3	0.7	0.0	0.0	0.0	0.0
*a*C15	0.9	0.2	0.2	0.7	0.0	0.1	0.3	0.1
C15:1	5.4	0.6	0.0	0.1	0.0	0.0	0.0	0.0
C15	6.5	5.2	0.7	0.4	0.4	0.5	0.1	0.2
C16:1ω7	3.8	8.0	3.8	66.4	27.0	8.1	3.6	50.0
C16:1ω5	0.0	0.0	0.0	0.0	0.0	0.0	0.0	3.4
C16	11.5	20.3	44.3	8.3	18.0	3.8	2.1	23.0
*i*C17	0.0	0.0	0.5	0.1	0.0	0.0	0.0	0.0
*a*C17	0.0	0.0	0.1	0.2	0.0	0.0	0.0	0.0
C17:1ω8	39.7	11.0	0.0	0.0	0.3	6.1	1.3	0.0
C17:1ω6	0.4	0.0	0.0	0.0	0.0	2.3	2.1	0.0
C17	0.7	0.7	0.3	0.0	0.1	0.5	0.2	0.1
C18:1ω9	1.3	0.9	0.8	0.3	0.0	68.0	84.0	0.3
C18:1ω7	6.3	22.6	2.0	16.6	48.0	0.0	0.5	17.0
C18	2.3	4.5	2.9	0.0	1.0	8.8	3.7	0.5

a: Sulfate-reducing bacteria *Desulfobulbus* grown on propionate from Taylor and Parkes (1983)
b: Sulfate-reducing bacteria *Desulfobulbus sp* grown on H_2 from Taylor and Parkes (1983)
c: Sulfate-reducing bacteria *Desulfobacter sp* grown on acetate from Taylor and Parkes (1983)
d: Sulfur-oxidizing Gammaproteobacteria *Beggiatoa* ubiquitous in gas hydrates and cold seep in Gulf of Mexico from Zhang et al. (2005)
e: *Gammaproteobacteria Pseudomonas sp.* NA101, *Psychrobacter sp.* NC201 and *Shewanella sp.* NA042 isolated from German Wadden sea sediment from Freese et al. (2008)
f: *Epsilonproteobacteria Arcobacter sp.* NA105 isolated from German Wadden sea sediment from Freese et al. (2008)

Supplementary materials for Chapter V

Method

Acetate measurement: Concentrations and carbon isotope composition of acetate in the supernatant of slurries were performed on LC-IRMS according to the method by Heuer et al. (2006) prior to analysis, DIC in each water sample was removed by adding 85% H_3PO_4 as the volume ratio of 1:9 relative to sample volume, and then purging with 40 mL N_2. The concentrations of acetate were quantified based on the relationship between the peak area and external acetate of known amount. The $\delta^{13}C$ values of acetate were dealt on ISODAT NT 2.0 software and calibrated by reference CO_2 gas.

DNA isolation for metagenomic sequencing: The DNA for metagenomic sequencing was isolated from lignin culture by using SDS-based DNA extraction (He et al., 2016).

Metagenome library construction and sequencing. 2.5-5 μg of DNA were initially fragmented by Covaris and then tested by electrophoresis using 1% agarose gel. Fragmented DNA was combined with an end repair mix and incubated at 20 °C for 30 min. The end-repaired DNA was then purified with a QIAquick PCR Purification Kit (Qiagen). Subsequently, the A-tailing mix was added and the mixture was incubated at 37 °C for 30 min. The purified 3′ ends adenylate DNA were incubated in the adapter ligation reaction at 20 °C for 15 min. After this process, the adapter-ligated DNA was selected by running a 2% agarose gel to recover the target fragments. The gel was purified with a QIAquick Gel Extraction kit (Qiagen), and several rounds of PCR amplification with a PCR primer cocktail and PCR master mix were performed to enrich the adapter-ligated DNA fragments. The PCR products were then selected by running another 2% agarose gel to recover the target fragments. Gel purification was achieved using a QIAquick Gel Extraction kit (Qiagen) and the final libraries were validated by the average molecule length on an Agilent 2100 Bioanalyzer instrument (Agilent DNA 1000 Reagents) and by real-time q-PCR (TaqMan Probe). The qualified libraries (with a 350 bp insert size) were amplified on cBot to generate a cluster on the flow cell (TruSeq PE Cluster Kit V3-cBot-HS, Illumina). Pair-end sequencing of the amplified flow cell was performed using a HiSeq X System (Illumina, at BGI-Shenzhen).

De novo assembly and binning of metagenomic sequences. Sickle (https://github.com/najoshi/sickle) was used to dereplicate and trim the raw shotgun sequencing metagenomic reads with the 'pe' option and default setting. The dereplicated, trimmed and paired-end DNA reads were assembled using MEGAHIT (Li et al., 2015) with the following parameters: k-min 31, k-max 127, step 4 (Dick et al., 2009). Assembled contigs were binned into putative taxonomic groups using Databionics ESOM Tools (http://databionic-

esom.sourceforge.net). Only contigs longer than 3kb were considered for ESOM binning, and longer contigs were chopped into 8kb windows for this analysis. The tetranucleotide frequencies of each DNA fragment of assembled contig and reference genomes were determined using a custom Perl script. DNA fragments were then clustered by tetranucleotide frequency using Data bionics ESOM tools. An assembled contig was designed in a specific genomic bin if all fragments of the assembled sequence were placed into this genomic bin during the ESOM binning process. Initially, one Bathyarchaeota genomic bin were identified from ESOM binning. The completeness of the genomic bin was then estimated by counting universal single-copy genes (Lloyd et al., 2013). One initial Bathyarchaeota genomic bin (Bin-L) was shown to contain a least two closely related genomes based on the number of single copy genes. These contigs were further separated by plotting the differential guanine and cytosine content and assembled sequence coverage within the bin. Read coverage was generated by mapping paired end reads to the assembled contigs using the Burrows-Wheeler Aligner (Li and Durbin, 2009). After this step, Bin-L was divided into two bins (Bin-L-1 and Bin-L-2). To rule out contamination, all identified genomic bins were rebinned with the method described by Wrighton and colleagues (Wrighton et al., 2012) a binning method considering both sequence composition and sequencing coverage. After this step, some contigs were identified as potential contamination from bacteria and other archaea and thus removed from identified Bathyarchaeota. Detailed estimates of genome contamination and completeness (shown as 'Completeness' and 'Contamination' in Table S.V.3) were assessed based on lineage-specific marker sets with CheckM (Parkes et al., 2015).

Metagenome annotation. Protein coding sequences (CDS) were determined using MetaGene (Noguchi et al., 2006) with the default settings. Ribosomal RNA (rRNA) genes were called with RNAmmer (Lagesen et al., 2007), and the archaeal model was used to identify all three rRNA subunits. The sequences with reliable hits in the NR database were also compared against KEGG with E-values $<1\times10^{-5}$. For each predicted CDS, functional information was collected by a sequence-similarity search against the NCBI NR database using BLASTP with E-values of $<1\times10^{-5}$. In order to reveal how the bathyarchaeotal groups take part in the process of lignin degradation, a best reciprocal BLASTP approach was used with protein coding sequences (CDS) of these two bins and reference protein sequences involving lignin degradation which collected from NCBI NR database. To determine the existence of methyl–coenzyme M reductase (MCR) complex, the protein sequences of *mcrA* (Laso-Peréz et al., 2016) were also used as reference for BLASTP.

Phylogenetic tree construction for functional genes: All publicly available Bathyarchaeota genomic bins and some partial/uncultured archaeal genomes (Thaumachaeota and

Aigarchaeota), were included in the phylogenetic analysis. Archaea conserved single copy genes (CSCGs) were used to infer the phylogenetic affiliation of inspected Bathyarchaeota genomic bins. Previously, 58 prokaryotic genes were considered to undergo no horizontal gene transfer events (Puigbò et al., 2009). A total of 32 of 58 archaeal CSCGs were found to be present in most of the archaeal genomes, and in both Bathyarchaeota genomic bins. Homologue sequences were individually aligned with ClustalW (Larkin et al., 2007). For the phylogenetic analysis, deletions and highly variable regions were removed using a 30% positional conservatory filter, and alignments were concatenated for the final alignment whenever required. Short alignments containing fewer than 20 amino-acid residues were discarded. The individual alignments of proteins were concatenated to a 'supermatrix' alignment for phylogenetic inference. A maximum-likelihood-based approach with FastTree (Price et al., 2010) was performed using the Jones–Taylor–Thornton (JTT) model with the CAT approximation.

Text

Overview of bathyarchaeotal genomic bins

De novo assembly of metagenomic reads and binning by tetranucleotide signatures (for details see Methods) revealed that there were two Bathyarchaeota genomic bins named Bin-L-1 and Bin-L-2 (Table S.V.3). These two bins were 2.19Mb and 2.28Mb, and genome completeness were 82.7% and 71.0% based on the presence of single-copy genes. The phylogeny based on 32 concatenated conserved single-copy genes (Lloyd et al., 2013; Puigbò et al., 2009) from Bathyarchaeota and its relative archaeal groups (Thaumarchaeota and Aigarchaeota) revealed that both bins belonged to Bathy-8 (Fig. S.V.3). This result consisted of the 16S rRNA gene diversity data showed that Bathy-8 were enriched in the lignin cultures (Fig. V.2).

Genes of catalase-peroxidase and 4-oxalocrotonate tautomerase putatively involved in lignin degradation and aromatic compound degradation respectively, were only found in the genomic bin Bin-L-2 (Table S.V.4 and Table S.V.4). Genes of all five subunits of the carbon monoxide dehydrogenase/acetyl-CoA synthase complex (Codh/Acs), and the key enzymes for the WL pathway were found in both of the genomic bins (Table S.V.4 and Table S.V.5). In addition, most of the genes that encode enzymes for the methyl branch of the WL pathway in archaea, through which CO_2 is reduced to methyltetrahydromethanopterin, were also found. Except methylenetetrahydromethanopterin dehydrogenase (Mtd), formylmethanofuran dehydrogenase (FwdA-F), formylmethanofuran:tetrahydromethanopterin formyltransferase (Ftr), N_5,N_{10}-methenyltetrahydromethanopterin cyclohydrolase (Mch), and N_5,N_{10}-methylenetetrahydromethanopterin reductase (Mer) were all identified in these two genomic bins (Table S.V.5). Neither of these two Bathyarchaeota genomic bins contains genes coding the key gene for methane metabolism, i.e., methyl–coenzyme M reductase (MCR) or *mcr* (Table S.V.4 and Table S.V.5), although their closely related genomic bin BA2 was found containing the genes of MCR complex (Evans et al., 2015). For the ability to metabolize acetate, the phosphate acetyltransferase (Pta) and acetate kinase (Ack) were not found in these two genomic bins, but the acetyl-CoA synthetase (Acss) can be found in the genomic bin Bin-L-2 (Table S.V.5). In addition, the partial tricarboxylic acid (TCA) cycle and complete glycolysis pathway was identified in genomic bins (Table S.V.4 and Table S.V.5).

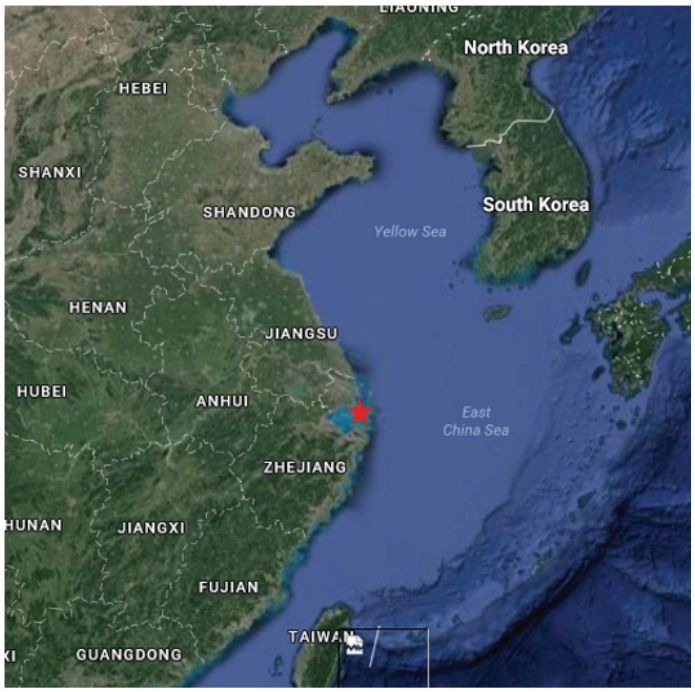

Fig. S.V.1. Location of the sediment samples for enrichment: DaYangShan (DYS) Island, Hanzhou Bay, China East Sea, China (30.592817 N, 122.083493 E).

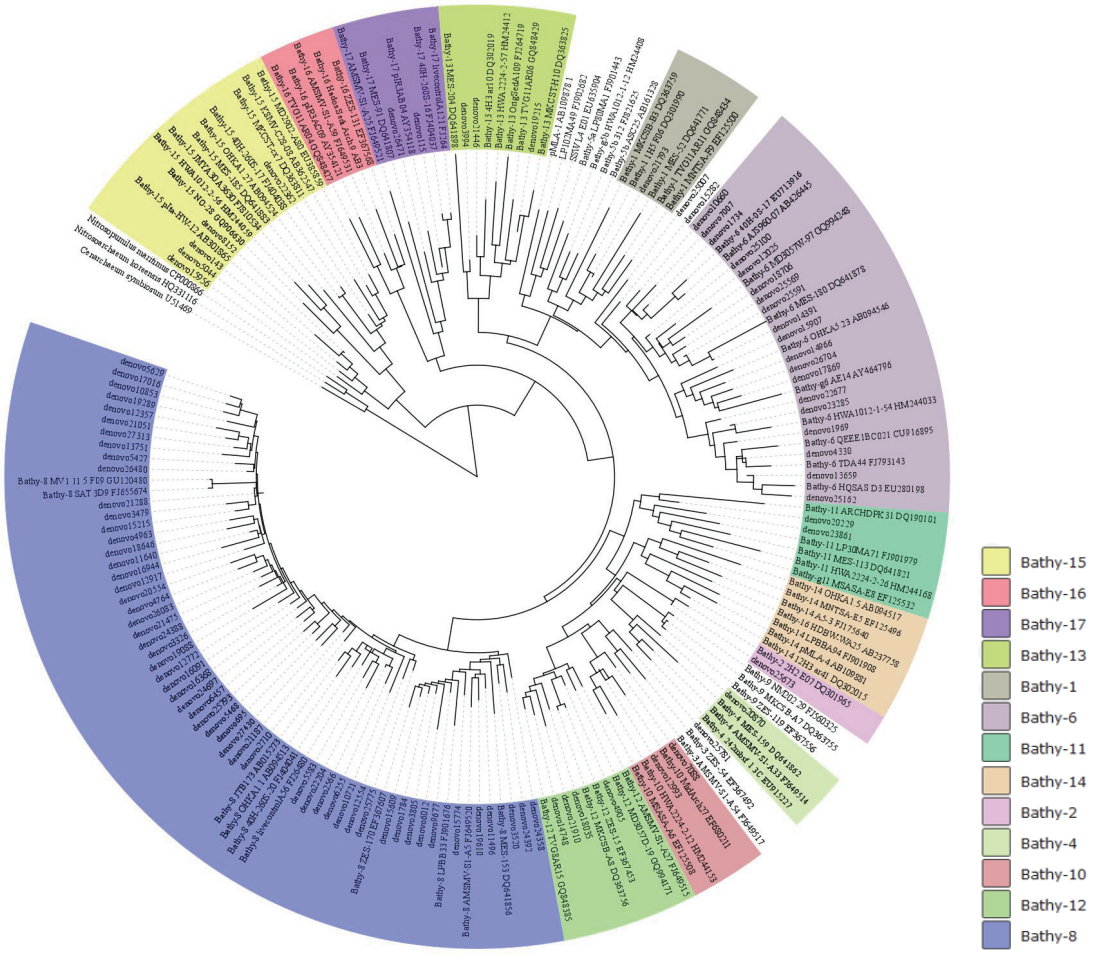

Fig. S.V.2. Neighbour-joining (NJ) phylogenetic tree based on bathyarchaeaotal 16S rRNA gene sequences obtained from illumina sequencing data. The 16S rRNA gene of *Cenarchaeum symbiosum* (U51469), *Nitrosopumilus maritimus* (CP000866) and *Nitrosoarchaeum koreensis* (HQ331116) were used as outgroup. Bootstrap values are based on 1,000 replicates. Bar, 0.02 substitutions per nucleotide position.

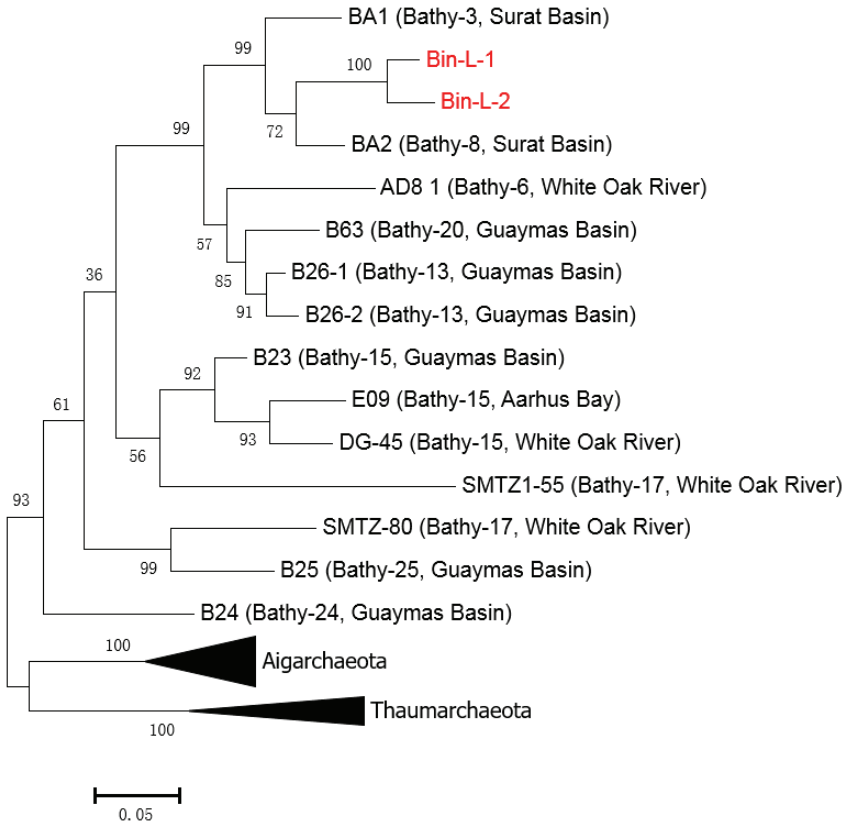

Fig. S.V.3. Maximum-likelihood Phylogenetic trees of concatenated alignments constituting 32 conserved archaeal single-copy genes (Puigbò et al., 2009). Bin-L-1 and Bin-L2 retrieved from this study were marked in red.

Table S.V.1. Ten dominant OUT of Bathyarchaeota after treatment with-/out lignin

OTU	subgroup	t_0	Lignin									control								
			$t_{3.5}$	t_6				t_{11}				$t_{3.5}$	t_6				t_{11}			
			N[a]	N	N	Y[b]	Y	N	N	Y	Y	N	N	N	Y	Y	N	N	Y	Y
denovo3326	Bathy-8	191	2692	5069	9636	12659	7274	16707	11592	8750	9941	53	103	161	106	144	108	106	172	151
denovo3805	Bathy-8	1002	381	180	206	576	225	148	141	132	126	312	373	678	360	481	732	666	532	492
denovo25775	Bathy-8	461	394	225	238	550	221	826	605	733	852	129	155	311	134	234	229	282	264	257
denovo13659	Bathy-6	4	17	267	615	1643	1075	545	325	906	766	0	3	7	5	10	2	2	6	11
denovo25100	Bathy-6	465	192	95	92	309	147	91	77	57	86	135	263	414	233	323	424	375	394	421
denovo1734	Bathy-6	280	174	115	111	395	143	141	105	67	73	74	165	254	145	230	155	392	339	353
denovo5583	Bathy-8	181	173	72	111	134	106	538	285	260	339	62	59	130	73	99	72	101	139	130
denovo21051	Bathy-8	3	174	200	335	540	278	307	304	189	221	0	4	1	3	3	3	3	4	3
denovo14748	Bathy-12	220	67	38	36	125	48	32	20	19	13	43	91	174	70	122	164	143	109	105
denovo26471	Bathy-17	255	84	26	37	117	45	42	33	23	26	69	50	102	62	91	171	145	122	114

N: no use of labeled substrate of ^{13}C-$NaHCO_3$; Y: use of labeled substrate of ^{13}C-$NaHCO_3$.

Table S.V.2. The $\delta^{13}C$ values (‰; VPDB; mean ± standard error, n = 2) of archaeal lipid derivatives in original sample, lignin and control samples after incubation for 6 months and 11 months.

Lipids	original sample	Lignin						Control					
		t_6		t_{11}				t_6		t_{11}			
		N[a*]	Y[b*]	N	N	Y	Y	N*	Y*	N	N	Y	Y
phytane	-35.1	-37.4	830	-34.0±0.6	-38.0±0.7	1410±79	1109±50	-34.0	663±34	-33.0±0.2	-34.8±0.9	1067±91	1113±132
BP-0	-26.5±2.4	-27.7±2.3	111±0.9	-28.1±2.2	-34.9±0.8	273±28	194.7±20	25.5±0.3	28.0±1.4	-24.7±0.5	-27.1±2.3	-22.7±0.9	-28.3±6.1
BP-2	-25.8±1.9	-24.3±2.7	-8.1±0.5	-23.2±0.4	-22.6±0.4	99.1±0.9	62.2±2.0	-21.9	23.5±0.1	-22.5±2.1	-19.9±0.1	-22.9±0.3	-20.5±0.3
BP-3	-21.9±1.1	-22.3±1.8	-22.0±1.1	-19.3±0.1	-20.2±3.0	-18.4±0.7	-17.5±0.2	-21.2	22.0±1.3	-19.4±0.1	-19.9±0.7	-19.4±0.2	-19.1±0.0

*Before extracting the archaeal lipids, duplicate cultivation sediments were combined because of the limited samples.
N: no use of labeled substrate of ^{13}C-$NaHCO_3$; Y: use of labeled substrate of ^{13}C-$NaHCO_3$

Table S.V.3. Overview of bathyarchaeotal genomic bins.

	Bin-L-1	Bin-L-2
Completeness (%)	82.47%	71.03%
Contamination (%)	2.34%	1.32%
Genome size (Mb)	2.19	2.28
Number of contigs	253	425
N50 value (bp)	12870	5778
Mean contig length (bp)	8876	5491
GC content (%)	41.66	43.5
predicted genes	2389	2712

Table S.V.4. Overview of bathyarchaeotal genomic bins.

Gene name	Genomic Bin	
	Bin-L-1	Bin-L-2
catalase-peroxidase (putative lignin degradation)	-	+
4-oxalocrotonate tautomerase (Degradation of aromatic compounds)	-	+
reductive acetyl-CoA，Wood–Ljungdahl, WL pathway	+	+
methyl–coenzyme M reductase, MCR (Methane metabolism)	-	-
Pta-Ack pathway (acetogenesis)	-	-
TCA cycle	partial	partial
Glycolysis	complete	complete
Fatty acid metabolism	-	-
protease or peptidase	+	+

Table S.V.5. List of genes in bathyarchaeotal subgroup 8: Bin-L-1 and Bin-L-2.

Gene name	Abbrev.	Genomic Bin	
		Bin-L-1	Bin-L-2
Degradation of lignin and aromatic compounds			
catalase-peroxidase	*katG*	0	1
4-oxalocrotonate tautomerase	*praC, xylH*	0	1
Methane metabolism and WL pathway			
acetyl-CoA synthetase	*Acss, acs*	0	1
2,3-bisphosphoglycerate-independent phosphoglycerate mutase	*apgM*	0	1
acetyl-CoA decarbonylase/synthase complex subunit alpha	*codhA*	2	2
acetyl-CoA decarbonylase/synthase complex subunit epsilon	*codhB*	2	1
acetyl-CoA decarbonylase/synthase complex subunit beta	*codhC*	2	1
acetyl-CoA decarbonylase/synthase complex subunit delta	*codhD, acsD*	1	1
acetyl-CoA decarbonylase/synthase complex subunit gamma	*codhE, acsC*	1	1
coenzyme F420-0:L-glutamate ligase / coenzyme F420-1:gamma-L-glutamate ligase	*cofE, fbiB*	1	1
sulfopyruvate decarboxylase subunit beta	*comE*	1	0
carbon-monoxide dehydrogenase iron sulfur subunit	*cooF*	1	1
enolase	*ENO, eno*	1	1
bifunctional enzyme Fae/Hps	*fae-hps*	1	2
fructose-bisphosphate aldolase, class II	*FBA, fbaA*	1	0
coenzyme F420 hydrogenase subunit beta	*frhB*	2	1
formylmethanofuran--tetrahydromethanopterin N-formyltransferase	*ftr*	3	3
formylmethanofuran dehydrogenase subunit A	*fwdA, fmdA*	2	1
formylmethanofuran dehydrogenase subunit B	*fwdB, fmdB*	2	1
formylmethanofuran dehydrogenase subunit C	*fwdC, fmdC*	2	2
formylmethanofuran dehydrogenase subunit D	*fwdD, fmdD*	1	0
4Fe-4S ferredoxin	*fwdF, fmdF*	1	0
fructose-1,6-bisphosphatase II	*glpX*	1	1
glycine hydroxymethyltransferase	*glyA, SHMT*	1	2
heterodisulfide reductase subunit A	*hdrA*	3	2
heterodisulfide reductase subunit B	*hdrB*	3	2
heterodisulfide reductase subunit C	*hdrC*	3	1
6-phospho-3-hexuloisomerase	*hxlB*	1	0
fructose-bisphosphate aldolase / 2-amino-3,7-dideoxy-D-threo-hept-6-ulosonate synthase	*K16306*	1	2
methenyltetrahydromethanopterin cyclohydrolase	*mch*	1	2
malate dehydrogenase	*mdh*	1	1
5,10-methylenetetrahydromethanopterin reductase	*mer*	1	1
tyrosine decarboxylase / aspartate 1-decarboxylase	*mfnA, adc*	2	0
(5-formylfuran-3-yl)methyl phosphate synthase	*mfnB*	0	1
tyramine---L-glutamate ligase	*mfnD*	1	0
5-(aminomethyl)-3-furanmethanol phosphate kinase	*mfnE*	0	1
(4-(4-[2-(gamma-L-glutamylamino)ethyl]phenoxymethyl)furan-2-yl)methanamine synthase	*mfnF*	0	1
methylene-tetrahydromethanopterin dehydrogenase	*mtdB*	1	1
tetrahydromethanopterin S-methyltransferase subunit H	*mtrH*	1	1
6-phosphofructokinase	*pfkA, PFK*	1	0
pyruvate ferredoxin oxidoreductase alpha subunit	*porA*	1	1
pyruvate ferredoxin oxidoreductase beta subunit	*porB*	1	2
pyruvate ferredoxin oxidoreductase delta subunit	*porD*	1	1
pyruvate ferredoxin oxidoreductase gamma subunit	*porG*	1	0

phosphoenolpyruvate carboxylase	*ppc*	2	1
pyruvate, water dikinase	*pps, ppsA*	1	2
D-3-phosphoglycerate dehydrogenase	*serA, PHGDH*	1	1
phosphoserine phosphatase	*serB, PSPH*	3	2
TCA cycle			
citrate synthase	*CS, gltA*	1	1
isocitrate dehydrogenase (NAD+)	*IDH3*	1	0
malate dehydrogenase	*mdh*	1	1
pyruvate ferredoxin oxidoreductase alpha subunit	*porA*	1	1
pyruvate ferredoxin oxidoreductase beta subunit	*porB*	1	2
pyruvate ferredoxin oxidoreductase delta subunit	*porD*	1	1
pyruvate ferredoxin oxidoreductase gamma subunit	*porG*	1	0
fumarate hydratase subunit alpha	*fumA*	1	0
fumarate hydratase subunit beta	*fumB*	1	0
Glycolysis			
2,3-bisphosphoglycerate-independent phosphoglycerate mutase	*apgM*	2	1
enolase	*ENO, eno*	1	1
fructose-bisphosphate aldolase, class II	*FBA, fbaA*	1	0
glyceraldehyde 3-phosphate dehydrogenase	*GAPDH, gapA*	1	1
glucokinase	*glk*	1	2
6-phosphofructokinase 1	*pfkA, PFK*	1	0
glucose/mannose-6-phosphate isomerase	*pgi-pmi*	1	0
phosphoglycerate kinase	*PGK, pgk*	1	1
pyruvate kinase	*PK, pyk*	1	0
triosephosphate isomerase (TIM)	*TPI, tpiA*	1	1
Fatty acid metabolism			
acetyl-CoA C-acetyltransferase	*atoB*	0	1
protease and peptidase			
serine protease		2	0
LysW-gamma-L-lysine/LysW-L-ornithine carboxypeptidase	*lysK, argE*	1	0
signal peptidase, endoplasmic reticulum-type	*SEC11 sipW*	2	1
peptide chain release factor subunit 1	*ETF1, ERF1;*	0	1
LysW-gamma-L-lysine/LysW-L-ornithine carboxypeptidase	*lysK, argE*	0	2
transport system			
iron complex transport system ATP-binding protein	*ABC.FEV.A*	4	4
iron complex transport system permease protein	*ABC.FEV.P*	4	6
iron complex transport system substrate-binding protein	*ABC.FEV.S*	6	7
ABC transporters：			
cobalt/nickel transport system permease protein	*cbiM*	1	0
cobalt/nickel transport protein	*cbiN*	1	0
cobalt/nickel transport system ATP-binding protein	*cbiO*	1	0
cobalt/nickel transport system permease protein	*cbiQ*	1	0
energy-coupling factor transport system ATP-binding protein	*ecfA1*	1	2
energy-coupling factor transport system ATP-binding protein	*ecfA2*	1	1
energy-coupling factor transport system permease protein	*ecfT*	1	2
lipooligosaccharide transport system ATP-binding protein	*nodI*	0	1
phosphate transport system permease protein	*pstA*	1	2
phosphate transport system ATP-binding protein	*pstB*	1	3
phosphate transport system permease protein	*pstC*	2	2
phosphate transport system substrate-binding protein	*pstS*	2	1

molybdate/tungstate transport system substrate-binding protein	*wtpA*	3	2
molybdate/tungstate transport system permease protein	*wtpB*	2	2
zinc transport system substrate-binding protein	*znuA*	1	0
zinc transport system permease protein	*znuB*	1	1
zinc transport system ATP-binding protein	*znuC*	1	1

Table S.V.6. The carbon isotope composition ($\delta^{13}C$) and concentration of acetate in water medium after incubation with-/out lignin and ^{13}C-bicarbonate

Conditions	^{13}C-IC	Time	Sample	$\delta^{13}C$ (‰; VPDB)	Concentration (µM)
lignin	NO	t_6	5-1-6	-14.5[a]	4.7±1.9
		t_6	5-2-6	-19.9[a]	5.6±1.5
	YES	t_6	5-3-6	531±10	33.6±1.1
		t_6	5-4-6	1990±228	5.4±1.7
	NO	t_{11}	5-1-11	-15.9	26.2
		t_{11}	5-2-11	-17.2	44.3
	YES	t_{11}	5-3-11	513±79	89.0
		t_{11}	5-4-11	1040±43	35.8
control	NO	t_6	7-1-6	-8.2[a]	6.4
		t_6	7-2-6	-10.8[a]	5.0
	YES	t_6	7-3-6	1735	6.5
		t_6	7-4-6	1531±400	5.7±3.7
	NO	t_{11}	7-1-11	-28.1	19.9
		t_{11}	7-2-11	-21.6	11.0
	YES	t_{11}	7-3-11	132	3.9
		t_{11}	7-4-11	n.d.	n.d.

a: those values are not reliable and just for reference due to not sufficient amount (< 10 µM) for $\delta^{13}C$ measurement. n.d.: not detected.

Table S.V.7. Primers and conditions used for pyrosequencing, cloning and Q-PCR.

Target description	Primer name	Sequence (5'-3')	PCR Type	Annealing temperature	Product length (bp)	References	R^2	Efficiency (%)
Bacteria	Bac520F Bac802R	AYTGGGYDTAAAGNG TACNVGGGTATCTAATCC	Illumina sequencing	55ºC	282	Song et al., 2013		
Archaea	U519F Arch806R	YMGCCRCGGKAAHACC GGACTACNSGGGTMTCTAAT	Illumina sequencing	55ºC	287	Song et al., 2013		
Bacteria	Bac 341F prokaryotic 519R	CCTACGGGWGGCWGCA TTACCGCGGCKGCTG	Q-PCR	56ºC	389	Jorgensen et al., 2012 Ovreås et al., 1997	0.993-0.995	96%
Archaea	Uni519F Arch 908R	CAGCMGCCGCGGTAA CCCGCCAATTCCTTTAAGTT	Q-PCR	60ºC	178	Jorgense et al., 2012	0.993-0.995	86-87%
Bathyarchaeota	Bathy-442F Bathy-644R	AGACTGGTGTCAGCCGCC TCGCCACTGGTGGTCCTC	Q-PCR	58ºC	202	Yu et al., 2017	0.993-0.996	84-86%

Table S.V.8. Observed archaeal richness and diversity estimates based on 97% OTU clusters.

			Quality Reads	species	species*	chao1*	simpson*	shannon*	coverage*
original sample			14920	523	478	601	0.94	5.69	0.99
lignin	$t_{3.5}$	N	10425	477	476	671	0.89	4.98	0.98
	t_6	N	14672	615	569	887	0.82	4.45	0.98
		N	29211	783	510	855	0.78	3.91	0.98
		Y	33848	869	560	865	0.84	4.68	0.98
		Y	25447	835	601	886	0.87	4.92	0.98
	t_{11}	N	32768	699	432	729	0.72	3.8	0.98
		N	23092	617	446	733	0.74	3.94	0.98
		Y	20824	614	460	745	0.8	4.18	0.98
		Y	22331	656	476	772	0.79	4.29	0.98
control	$t_{3.5}$	N	14539	423	376	524	0.56	3.03	0.99
	t_6	N	13456	616	552	853	0.81	4.7	0.98
		N	42448	819	499	757	0.65	3.75	0.98
		Y	13062	655	599	856	0.82	4.78	0.98
		Y	15869	724	627	879	0.86	5.18	0.98
	t_{11}	N	18658	642	523	739	0.83	4.89	0.98
		N	13898	597	541	745	0.94	5.79	0.98
		Y	17282	730	612	834	0.87	5.34	0.98
		Y	14324	661	588	798	0.84	5.09	0.98

N: no use of labeled substrate of ^{13}C-$NaHCO_3$; Y: use of labeled substrate of ^{13}C-$NaHCO_3$.

*standardized numbers based on subsampling of 10372 sequences.

Acknowledgments

First of all, I would like to thank Prof. Dr. Kai-Uwe Hinrichs who gave me the chance to work on my PhD study in such an international community in Organic Geochemistry Lab at MARUM and gave me critical comments and extremely constructive advices on my PhD work.

Sincerely thanks to Prof. Dr. Volker Thiel for his willingness to review my thesis and I will look forward to his comments.

I am deeply grateful to Dr. Travis Meador who sacrificed lots of time for guiding my work, and discussing and answering my questions. Thanks for your valuable and constructive comments on all my manuscripts, which is crucial for finishing my PhD study in time.

I am sincerely thankful to Drs. Marcus Elvert, Martin Könneke and Gunter Wegener who gave up their time to attend my thesis committee meetings with critical discussion and helpful advices.

Many thanks to our technician group Heidi Taubner, Xavier Prieto Mollar, Julius Lipp, Jenny Wendt and Jessica Arndt who helped me a lot on my sample preparation and measuring. I have learned a lot about analytical techniques. Without your help, I don't think I can harvest high quality and reliable data. Thanks to all my friends and colleagues, Bernhard, Birgit, Chun (Charli), Evert, Florence, Frauke, Friederik, Guangchao, Jinpeng, Jinxiang, Lars, Marcos, Min, Nadine, Oliver, Qingzeng, Rebecca, Rishi, Sarah, Shuchai, Sitan, Susanne, Thomas, Verena, Weihua, Xiuran and Xiaolei. Thank you for all your help. It was really great to work with you. I would like to thank GLOMAR and its team for the funding which gave me the opportunities to attend several international conferences.

Lastly, I was funded by China Scholarship Council (CSC) for living costs in Germany, and I also thank my Chinese government. Furthermore, I very appreciated for the support from my wife. Without your encouragement and accompany, I don't think I can survive to finish this thesis. Meanwhile, I also thank my little daughter Xixi, and your smile always makes Papa relieve stress and makes me stronger. I should thank my family in China during all my life with permanent understanding and encouragement.

November 20, 2017
Bremen